Biological and Chemical Investigation of Cultured Cyanobacteria

By

HYUNJUNG KIM

B.S., Chung-Ang University, South Korea, 2003

M.S., Chung-Ang University, South Korea, 2005

DISSERTATION

Submitted as partial fulfillment of the requirements
for the degree of Doctor of Philosophy in Pharmacognosy
in the Graduate College of the
University of Illinois at Chicago, 2012

Chicago, Illinois

Doctoral Committee:
Dr. Jimmy Orjala, Chair/Advisor
Dr. Steven M. Swanson
Dr. Michael J. Federle
Dr. Brian T. Murphy
Dr. Yee-Kin Ho, Department of Biochemistry and Molecular Genetics

DEDICATION

I dedicate this dissertation to my mother

Haengkeum Yu

Who has given me strength to persevere beyond all the challenges I have faced throughout my life.

Without her presence, support, and love, I could not have completed this dissertaion.

I love you.

TABLE OF CONTENTS

Chapter Page

TABLE OF CONTENTS (Continued)

Chapter Page

TABLE OF CONTENTS (Continued)

Chapter Page

LIST OF TABLES

LIST OF FIGURES

LIST OF FIGURES (Continued)

LIST OF FIGURES (Continued)

LIST OF FIGURES (Continued)

LIST OF FIGURES (Continued)

LIST OF ABBREVIATIONS

$[\alpha]_D$	Specific optical rotation
A498	Human renal cancer cell
Ac	Acetyl
Ala	Alanine
Aound	3-amino-2,7,8-trihydroxy-10-methyl-5-oxyundecanoyl
Atpoa	3-amino-2,5,7-trihydroxy-8-phenyloctanoic acid
aq	Aqueous
ax	Axial
B16	Human melanoma cancer cell
c	Concentration
Calcd	Calculated
Caco-2	Human intestinal cancer cell
C_{18}	Octadecasilyl
C_8	Octasilyl
CCALA	Culture Collection of Autotrophic Organisms at the Academy of Sciences of the Czech Republic
CCMP	Provasoli-Guillard National Center for Culture of Marine Phytoplankton
$CDCl_3$	Deuterated chloroform
CEM	Human lymphocytic leukemia
CH_2Cl_2	Dichloromethane
COSY	Homonuclear correlation spectroscopy
^{13}C NMR	Carbon-13 nuclear magnetic resonance
CX-1	Human colon adenocarcinoma cell
1D, 2D	One-, Two-Dimension
δ_H	Proton chemical shift
δ_C	Carbon-13 chemical shift
DEPTQ	Distortionless enhancement by polarization transfer, quaternary carbon sensitive spectroscopy (NMR)
Dhb	Dehydrobutyrine
DMSO-d_6	Deuterated dimethylsulfoxide
ED_{50}	Dose that results in half of the maximal effect
EM9	Chinese hamster ovary cancer cell
ESI	Electrospray ionization
FDA	United States Food and Drug Administration
FI	Factor-independent cell
Gln	Glutamine
Gly	Glycine
NCI-H460	Human large lung carcinoma cell line
NSF-60	Human myeloblastic cell
HeLa	Human cervical cancer cell
HMBC	Heteronuclear Multiple-Bond Correlation
^1H NMR	Proton Nuclear Magnetic Resonance
HCT-116	Human colorectal carcinoma
HL-60	Human promyelocytic leukemia cell
Hphe	Homophenylalanine
HPLC	High performance liquid chromatography
HRESI-MS	High resolution mass spectrometry using electrospray ionization
HSQC	Heteronuclear Single Quantum Correlation
HT-29	Human colon adenocarcinoma cell line
Hz	Hertz
IC_{50}	Half of the maximal inhibitory concentration
Ile	Isoleucine
IT-TOF	Hybrid ion trap and time of flight mass spectrometer
IR	Infrared spectroscopy
KB	Human Carcinoma Cells of the Nasopharynx

klx	Kilolux
L	Liter
L1210	Mouse lymphocytic leukemia cell
LoVo	Human colon carcinoma cell line
λ (nm)	Wavelength in nanometers
LC	Liquid column chromatography
LD_{50}	Half of the maximal lethal concentration
LOXIMVI	Human melanoma cancer cell
$[M+H]^+$	Protonated Molecular Ion
$[M-H]^-$	Deprotonated Molecular Ion
$[M+Na]^+$	Sodiated Molecular Ion
MeOH	Methanol
MCF-7	Human breast adenocarcinoma
MCF-7/ADR	Adriamycin-resistant breast caner cell
MDA-MB-435	Human melanoma cancer cell
MDA-MB-231	Human breast cancer cell
MS	Mass spectrometry
MHz	Megahertz
MIC	Minimum inhibition concentration
mL	Milliliter
mM	Millimolar
Molt-4	Human acute lymphoblastic leukemia cell
MTS	3-(4,5-dimethylthiazol-2-yl)-5-(3-carboxymethoxyphenyl)-2-(4-sulfophenyl)-2H-tetrazolium, inner salt
m/z	Mass-to-charge ratio
v (cm^{-1})	Infrared absorption frequency in reciprocal centimeters
neuro-2a	Mouse neuroblastoma cell
nM	Nanomolar
NMe	*N*-methyl
NH_3	Ammonia
NMR	Nuclear Magnetic Resonance
NOESY	Nuclear Overhauser Effect Spectroscopy
OMe	*O*-Methyl
P-388	Human leukemia cell
PCR	Polymerase chain reaction
Phe	Phenylalanine
Pro	Proline
qC	Quaternary carbon
rDNA	Ribosomal DNA
ROESY	Rotatin-frame nuclear overhauser spectroscopy
SAG	Culture Collection of Algae at the University of Göttingen, Germany
SF268	Human glioblastoma cell line
SKBR3	Human breast
SKMEL28	Human melanoma
SKOV3	Human ovarian
SKVLB-1	Multidrug-resistant cell overexpressing P-glycoprotein
SNB-75	Human astrocytoma cell
Thr	Threonine
t_R	Retention time
Trp	Tryptophan
TOCSY	Total correlation spectroscopy
U251	Human glioblastoma
UIC	University of Illinois at Chicago
UTEX	Culture Collection of Algae at the University of Texas at Austin
UV	Ultraviolet light

UV20	Chinese hamster ovary cell
µg/mL	Micrograms per milliliter
µL	Microliter
µM	Micromolar
Val	Valine
XRS-6	Chinese hamster ovary cancer

SUMMARY

Cyanobacteria have been used as a source of natural products for drug development. Previous studies have demonstrated that compounds with cytotoxic activity are widely distributed in cyanobacteria and that the chemical classes of the cytotoxic compounds are diverse. Several compounds derived from cyanobacteria are approved by FDA or under clinical evaluations for cancer treatment, further validating that these organisms have great potential as a source for anticancer drugs. These cytotoxic compounds from both marine and freshwater/terrestrial cyanobacteria are comprehensively reviewed in chapter 2.

In this study, an extract library from cultured cyanobacteria was established and evaluated for biological activities. A total of 306 strains of cultured cyanobacteria were evaluated for cytotoxicity using a set of cancer cells (HT-29, MCF-7, NCI-H460, and SF268 as well as a cancer cell panel consisting of 12 different cancer cells) and for 20S proteasome inhibition. Eleven strains showed significant cytotoxicity and/or inhibition of 20S proteasome. The results of the biological screening are described in the chapter 3.

Five strains of cyanobacteria, *Fischerella* sp. (SAG 46.79), *Westiellopsis* sp. (SAG 20.93), *Fischerella muscicola* (UTEX LB1829), *Nostoc* sp. (UIC 10047), and *Oscillatoria* sp. (UIC 10109), were cultured for chemical investigation. Activity-guided isolation led to the identification of four new fischerindole-type alkaloids, 12-*epi*-fischerindole I and W nitriles (**217** and **219**) and deschloro 12-*epi*-fischerindole I and W nitriles (**218** and **220**), along with a known compound hapalosin (**221**). All four compounds contained a nitrile moiety, and 12-*epi*-fischerindole W nitrile (**219**) and deschloro 12-epi-fischerindole W nitrile (**220**) represented a new carbon skeleton for the fischerindole class of compounds. Three new hapalindole-type alkaloids, hapalindole X (**294**), deschloro hapalindole I (**295**), and 13-hydroxy dechlorofontonamide (**296**), were isolated from both *Westiellopsis* sp. (SAG 20.93) and *Fischerella muscicola* (UTEX LB1829). Hapalindole X (**294**) represented the first example of a tetracyclic hapalindole with an exocyclic methylene moiety. One previously described boron-containing polyketide, borophycin (**162**), was isolated as the major active compound from *Nostoc* sp. (UIC 10047), obtained from a sample collected in Illinois, USA. Investigation of *Oscillatoria* sp. (UIC 10109), obtained from a sample collected in Puerto Rico, led to the isolation of two new dodecapeptides, verdeamides A (**332**) and B (**333**), both containing an unusual β-amino moiety (3-amino-2,5,7,8-tetrahydroxy-10-methylundecanoic acid, Aound).

Most of the compounds obtained in this study exhibited moderate to strong cytotoxicity and/or 20S proteasome inhibition. Verdeamides A (**332**) and B (**333**) from *Oscillatoria* sp. (UIC 10109) showed the most potent activity for both cytotoxicity and inhibition of 20S proteasome in SW-620, NCI-H23, and MDA-MB-435 cells (ED_{50} values ranging from 0.7 to 4.4 μM), indicating the level of activity to be comparable for both the phenotypic and the target-based assays. These results indicated the 20S proteasome inhibition to be a potential mechanism of action for these compounds. Borophycin (**162**) from *Nostoc* sp. also showed cytotoxicity against HT-29, NCI-H460, MCF-7, SF268, and IMR90 cells (ED_{50} values ranging from 0.49 to 1.5 μM). Three hapalindole-type alkaloids, hapalindole X (**294**) and deschloro hapalindole I (**295**) from *Westiellopsis* sp. (SAG 20.93), and 13-hydroxy dechlrofontonamide (**296**) from *Fischerella muscicola* (UTEX LB1829) did not display any significant cytotoxicity. However, hapalindole X (**294**) showed inhibitory activity against *M. tuberculosis* and *C. albicans* (IC_{50} values of 2.5 μM) with moderate Vero cell cytotoxicity (IC_{50} value of 35.2 μM). The four new nitrile-containing fischerindoles (**217**-**220**) did not exhibit strong bioactivities, except deschloro 12-*epi*-fischerindole I nitrile (**218**) which was found to be weakly cytotoxic against HT-29 cells (ED_{50} value of 23 μM). The isolation, structural elucidation, and evaluation of biological activity of these compounds are described in the chapter 4.

In summary, cyanobacteria have shown a great potential as a source for discovery of anticancer lead compounds, and the results of our study also support this. We believe that continued efforts on the chemical and biological evaluation of these organisms will provide a great opportunity for the discovery of new anticancer lead compounds.

Chapter 1. INTRODUCTION

1 Introduction

1.1 Impact of cancer

Cancer is a major cause of death worldwide. In the United States, cancer accounts for nearly one in every four deaths, and is a major public concern. The American Cancer Society estimates approximately 1.64 million new cases, and 577,190 deaths, or more than 1,500 deaths a day related to cancer in 2012 [1]. Prostate and breast cancers are the most frequently diagnosed cancers in men and women, respectively. In 2011, approximately 28,170 and 39,920 deaths are estimated for prostate and breast cancers, respectively. Lung cancer accounts for more death than any other cancer in both men and women, and approximately 160,340 deaths, accounting for 28% of all cancer deaths, are expected to occur in 2012 [1]. The National Institutes of Health estimated overall costs of cancer in 2010 at 263.8 billion dollars (102.8 billion dollars for total of all health expenditures, 20.9 billion dollars for cost of lost productivity due to illness, and 140.1 billion dollars for cost of lost productivity due to premature death) [2].

Numerous efforts have been made to understand and treat cancer. Cancer chemotherapy has been used as an important complement to surgery and radiation to treat many types of solid tumors, lymphomas, and leukemia [3]. However, tumor cells are developing resistance against currently available drugs, such as vinca alkaloids and taxanes, and this is thought to be a major cause of failure in the chemotherapeutic treatment of cancer [4]. Moreover, the incidence of new types of cancer such as glioblastoma is rapidly increasing, accelerating the urgency for new anticancer drugs.

1.2 Natural products and the discovery of anticancer drugs

Natural products have served as a source of drugs over the past two centuries [5-14]. In particular, the study of natural products has led to the discovery of several anticancer drugs, e.g. Taxol, vinblastine and vincristine, topotecan, etoposide, doxorubicin, combrestatin A4, and ecteinascidin 743, calicheamicin, and brentuximab vedotin (**6**, Figure 4) [15-21].

During the period of 01/1981-06/2006, 100 new chemical entities were introduced for the treatment of cancer, more than 60% of which were classified as natural products or derivatives based on natural products [19]. Despite the success of natural products as a source for the development of anticancer drugs, many large pharmaceutical companies have decreased the screening of natural

products for drug discovery in favor of combinatorial and synthetic chemistry libraries [22-24]. This shift is mostly due to the inherent limitations of natural products drug discovery programs: *1)* to build and maintain a high-quality natural product library takes a relatively long time and requires a specific skill set, *2)* purifying procedures are labor-intensive and time-consuming, *3)* known compounds are repeatedly isolated, and *4)* structure elucidation of often structurally complex compounds takes long periods of time [23]. However, it has been shown that natural products have characteristics that are not frequently observed in molecules from combinatorial or synthetic chemistry, such as a high number of chiral centers, a high degree of structural rigidity, and a high number of oxygen and a low number of nitrogen in the molecules [22, 24]. These properties allow natural products to uniquely fit into biological receptors, and natural products are well suited to bind to the complex protein targets associated with diseases such as cancer [25, 26]. Moreover, natural products have the advantage of high molecular diversity. Bioactive natural products often occur as part of a family or related molecules, which makes it possible to isolate a number of homologues and to obtain structure activity information [27]. Natural products have not only yielded new and effective drugs, but have also provided insight into new mechanisms of action for the development of anticancer agents.

Given all of these advantages offered by natural products, it is necessary to continue to explore new types of natural products to facilitate anticancer drug discovery, and to add small molecules to drug pipelines. We can assume that we have barely accessed nature's vast compound library based on the fact that a wide range of novel, bioactive secondary metabolites are continually discovered. It is believed that natural products will continue to provide a source of unmatched structural diversity for drug discovery, particularly for new anticancer agents.

1.3 Aims of the present study

This study is part of an ongoing collaborative multidisciplinary research project, in which a diverse group of organisms such as tropical plants, aquatic/terrestrial cyanobacteria, and filamentous fungi are studied to discover new anticancer drug leads [3]. There has been growing interest in the detailed investigation of cyanobacteria. Still, the drug potential of metabolites from cyanobacteria remains relatively unexplored.

The main scope of this study was to isolate the biologically active secondary metabolites from cell material of the cultured cyanobacteria, to determine the chemical structures, and to evaluate the biological activities of these isolates.

Aim 1. To evaluate cultured cyanobacteria metabolites for biological activity

Cyanobacteria strains were obtained from various culture collections or isolated from samples collected in the field. Unialgal strains were cultured, harvested, and extracted. An extract library of the cultured cyanobacteria was established and used to evaluate their biological activities such as cytotoxicity against a set of human cancer cell lines, i.e. HT-29, NCI-H460, MCF-7, and SF268, as well as for inhibition of the 20S proteasome, an established target for cancer treatment.

Aim 2. To isolate bioactive secondary metabolites from cultured cyanobacteria

Bioactive cyanobacteria strains were prepared in large-scale and the biomass of these strains was extracted and fractionated. Bioassay-guided isolation was used to obtain bioactive secondary metabolites. Biological activities of these isolated metabolites were evaluated.

Aim 3. To elucidate the structure of isolated secondary metabolites using a combination of spectroscopic analyses

The structures of isolated secondary metabolites were determined by a combination of spectroscopic analyses mainly based on 1D and 2D NMR and HRESIMS data.

Five cyanobacteria strains, *Fischerella* sp. (SAG 46.79), *Westiellopsis* sp. (SAG 20.93), *Fischerella muscicola* (UTEX LB1829), *Nostoc* sp. (UIC 10047), and *Oscillatoria* sp. (UIC 10109), were selected for further study based on the results of initial biological evaluations. The isolation, structure elucidation, and bioactivity evaluation of the secondary metabolites isolated from these strains are presented herein.

Chapter 2. CYANOBACTERIA: POTENTIAL SOURCE FOR NEW ANTICANCER DRUG LEADS

2 Cyanobacteria: Potential Source for New Anticancer Drug Leads

2.1 Introduction

Cyanobacteria (blue-green algae) are Gram-negative photoautotrophic, and among the most successful and oldest life forms present on earth [28]. These organisms are both morphologically and physiologically diverse and can be found in a variety of habitats such as freshwater lakes, oceans, and deserts. Morphological groups of cyanobacteria include unicellular or colonial coccoid, non-heterocystous or heterocystous filament, and branched filament [29]. Heterocysts are specialized cells that can convert atmospheric nitrogen (N_2) to a biologically useful form (NH_3) by a process known as nitrogen fixation [30]. All heterocystous and some coccoid/filamentous cyanobacteria have the ability to perform nitrogen fixation. This has enabled these organisms to exploit environments such as polar, open ocean, and desert regions. In addition, cyanobacteria exhibit remarkable ecophysiological adaptations and can tolerate dessication, hypersalinity, hyperthermal, and high ultraviolet light conditions for many years [29, 30].

The medicinal features of cyanobacteria were first recognized in 1500 BC when *Nostoc* sp. were used to treat some diseases [31]. The first scientific report on cyanobacteria was made in 1878, describing the death of livestock in South Australia due to cyanobacterial toxins [32]. Since then, cyanobacteria have been studied for their production of toxins that threatens the health of both humans and livestock. In recent decades, however, cyanobacteria have emerged as a source for searching new compounds as new drugs or drug leads [16, 29, 33, 34].

The most extensive work on cyanobacteria started in the 1970s by Professor Richard Moore. Currently, more than 4,000 strains of freshwater/terrestrial and marine cyanobacteria have been screened in various assays and approximately 1,000 molecules isolated [35]. It has been shown that cyanobacteria produce secondary metabolites with a variety of biological activities, such as antibiotic, algicidal, cytotoxic, immunosuppressive, and enzyme inhibiting activities [36-41]. The expected rate of rediscovery of known compounds from cyanobacteria is far lower than that from most other other natural product sources [29]. In addition, several compounds derived from cyanobacteria and their synthetic analogues, e.g. dolastatin 10 (**1**), bentuximab vedotin (**6**), glembatumumab vedotin, SGN-75, ASG-5ME, curacin A (**23**), and apratoxin S4 (**47**), have already been approved by FDA or entered pre-clinical or clinical trials for cancer treatment. Thus, it is believed that cyanobacteria will continue to provide active metabolites, in particular for cancer

chemotherapeutics, and that these biologically active metabolites will have the potential to become new leads for the development of anticancer drugs.

The spectrum of bioactive secondary metabolites produced by cyanobacteria is diverse. Mixed PKS-NRPS hybrid biosynthetic pathways (polyketide non-ribosomal peptide synthetase) afford the most prominent structural class of cyanobacterial secondary metabolites [42]. Of the mixed PKS-NRPS secondary metabolites, approximately 60% are cyclic and 36% are halogenated. Secondly, there are pure peptides, roughly 70% of which are cyclic and only about 9% are halogenated. Polyketides, unlike mixed PKS-NRPS and pure peptides, show a more equal distribution of linear, cyclic, and polycyclic structures. Another class of cyanobacterial secondary metabolites is alkaloids. More than 70% of the alkaloids isolated from cyanobacteria have fused polycyclic structures and over 40% are halogenated [16, 42]. Other classes of secondary metabolites such as terpenes, fatty acids, and depsides are also produced by cyanobacteria.

More than 200 cytotoxic secondary metabolites have been reported from cyanobacteria and used to discover new anticancer drugs or drug leads. Chapter 2 aims to comprehensively review cytotoxic compounds isolated from cyanobacteria and over 200 compounds are reviewed. The compounds are grouped based on chemical structures (Figure 1) and the origin of source cyanobacteria (Figures 2 and 3). Out of 115 cytotoxic compounds derived from marine cyanobacteria, 69.6% are mixed PKS-NRPS (Figure 1). The majority of these compounds were obtained from the order Oscillatoriales, while only a few were obtained from the order Nostocales (Figure 2). The genus *Lyngbya* produced the majority of cytotoxic compounds from the order Oscillatoriales (Figure 2).

On the other hand, a variety of compound classes such as peptides, polyketides, mixed PKS-NRPS, alkaloids, terpenoids, and nucleosides have been reported from freshwater/terrestrial cyanobacteria (Figure 1). Filamentous cyanobacteria of the orders Oscillatoriales, Nostocales, and Stigonematales all produce cytotoxic compounds. The majority of the compounds were obtained from the order Nostocales, and the genus, *Nostoc*, that produced more than 30% of the cytotoxic compounds (Figure 3). Some cytotoxic compounds were produced from non-filamentous cyanobacteria belonging to the order Chroococcales, while no cytotoxic metabolites have been found in the order Pleurocapsales (Figure 3). All compounds covered in this review chapter are summarized in Table 1 and 2 for marine-derived and freshwater/terrestrial cyanobacteria, respectively.

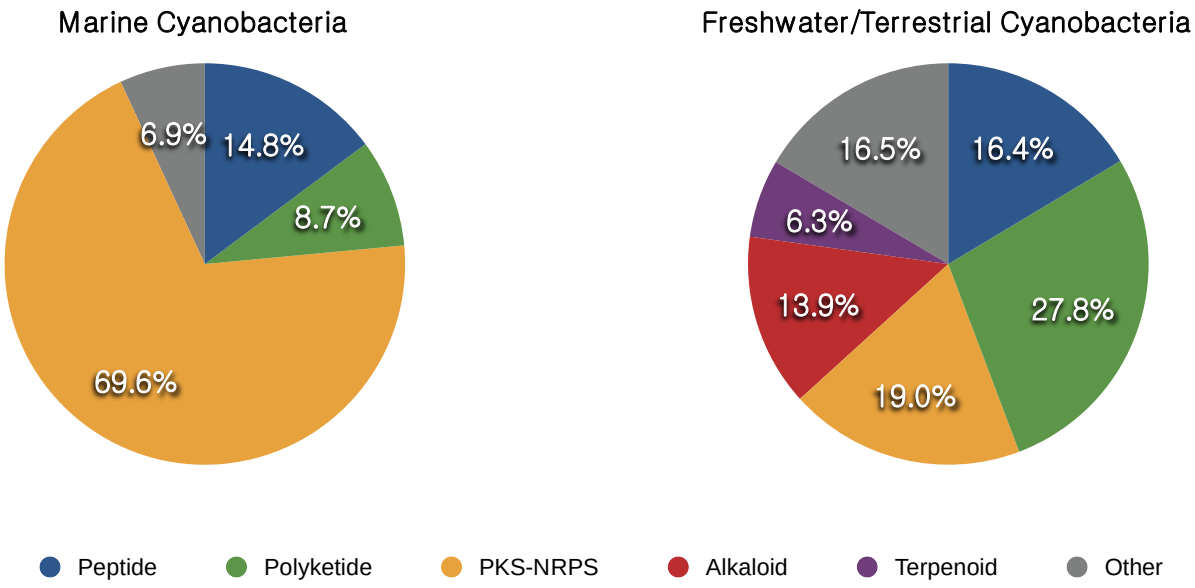

Figure 1. The chemical classes of cytotoxic compounds from marine-derived and freshwater/terrestrial cyanobacteria

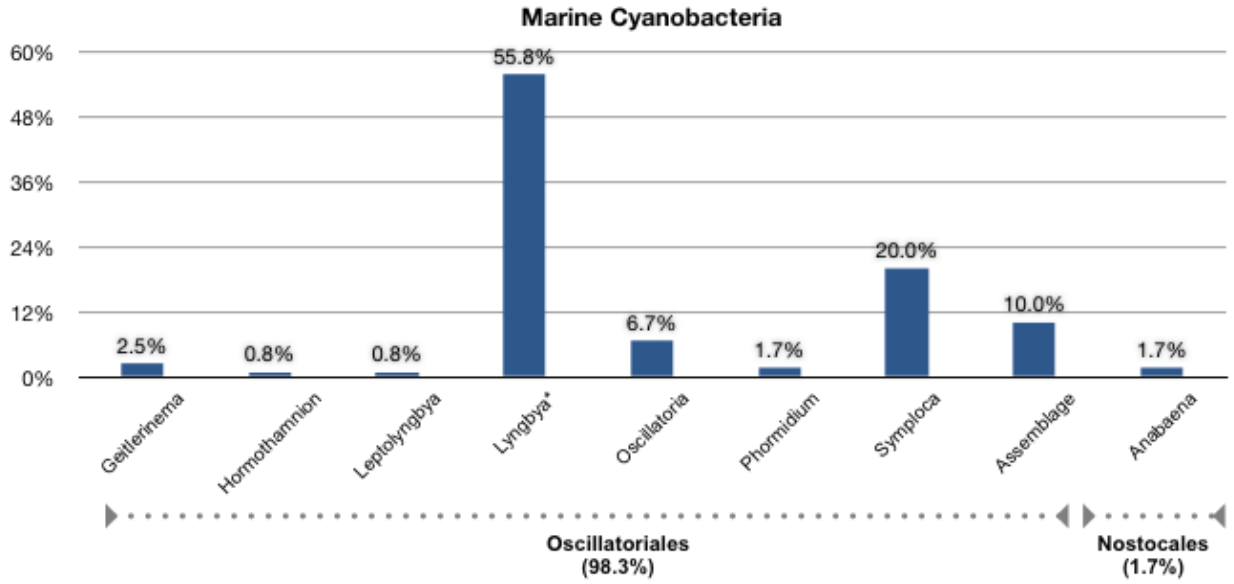

Figure 2. Sources of cytotoxic compounds from marine-derived cyanobacteria

*Due to similar morphology, the genus *Moorea* has been incorrectly classified as the genus *Lyngbya*. Many members of the genus *Lyngbya* are now described as *Moorea*, a genus named in memory of Professor Richard E. Moore [43, 44].

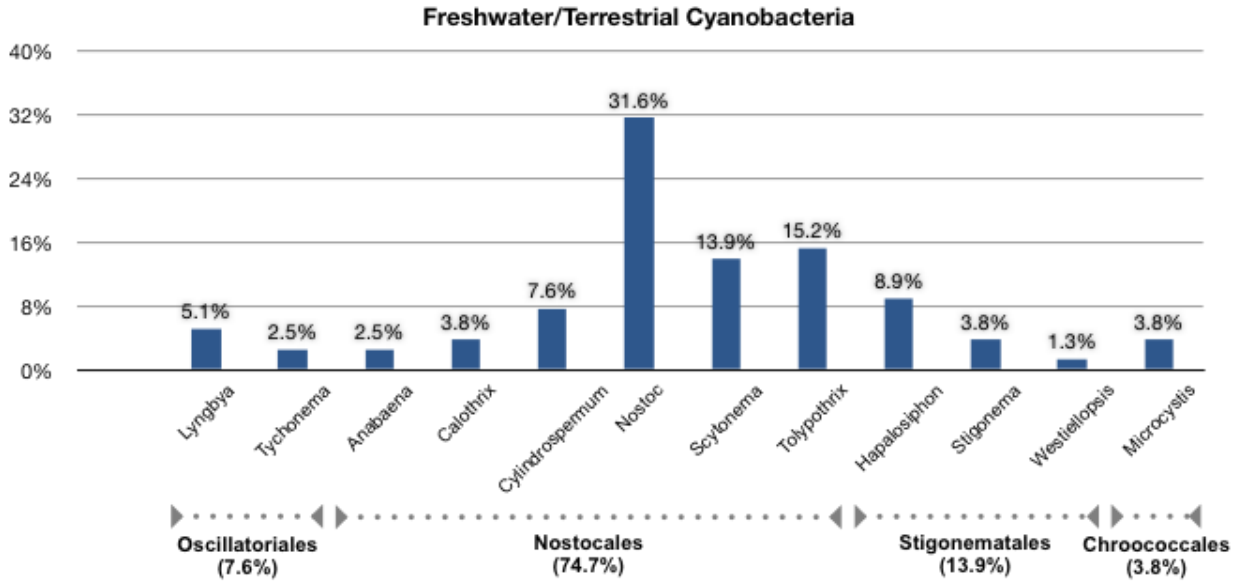

Figure 3. Sources of cytotoxic compounds from freshwater/terrestrial cyanobacteria

TABLE 1. CYTOTOXIC COMPOUNDS FROM MARINE CYANOBACTERIA

Source	Compound	Class	Collection Site	Reference
Anabaena torulosa	laxaphycins A (**109**) and B (**110**)	cyclic peptide	French Polynesia	[45]
Geitlerinema sp.	mitsoamide (**119**)	linear lipopeptide	Madagascar	[46]
	ankaraholides A (**116**) and B (**117**)	polyketide	Madagascar	[47]
Hormothamnion enteromorphoides	hormothamnin (**111**)	cyclic undecapeptide	Puerto Rico	[48]
Leptolyngbya sp.	coibamide A (**120**)	cyclic depsipeptide	Panama	[49]
	grassypeptolides D (**121**) and E (**122**)	cyclic depsipeptide	Red Sea	[50]
Lyngbya bouillonii	apratoxin E (**40**)	cyclic depsipeptide	Guam	[51]
	apratoxins F (**41**) and G (**42**)	cyclic depsipeptide	Palmyra Atoll	[52]
Lyngbya confervoides	grassypeptolide A-C (**84**-**86**)	cyclic depsipeptide	Florida	[53]
	obyanamide (**47**)	cyclic depsipeptide	Saipan	[54]
Lyngbya majuscula	caylobolide A (**64**)	macrolactone	Bahamas	[55]
	curacin A (**23**)	linear lipopeptide	Curaçao	[56]
	desmethoxymajusculamide C (**93**)	cyclic depsipeptide	Curaçao	[57]
	apratoxins A-C (**36**-**38**)	cyclic depsipeptide	Guam	[58, 59]
	cocosamides A (**107**) and B (**108**)	cyclic depsipeptide	Guam	[60]
	grassypeptolides F (**87**) and G (**88**)	cyclic depsipeptide	Palau	[61]
	lyngbyabellins A (**25**) and B (**26**)	cyclic depsipeptide	Guam and Florida	[62, 63]
	pitipeptolides A (**45**) and B (**46**)	cyclic depsipeptide	Guam	[64]
	pitiprolamide (**102**)	cyclic depsipeptide	Guam	[65]
	hectochlorin (**35**)	cyclic depsipeptide	Jamaica and Panama	[66, 67]
	jamaicamides A-C (**73**-**75**)	linear lipopeptide	Jamaica	[68]
	tanikolide dimer (**93**)	cyclic depside	Madagascar	[69]
	palmyramide A (**106**)	cyclic depsipeptide	Palmyra Atoll	[70]
	malyngolide dimer (**92**)	cyclic depside	Panama	[71]
	aurilides B (**76**) and C (**77**)	cyclic depsipeptide	Papua New Guinea	[72]
	dolabellin (**34**)	linear depsipeptide	Papua New Guinea	[73, 74]
	guineamides A-F (**48**-**53**)	cyclic depsipeptide	Papua New Guinea	[75]
	lyngbyabellins E-I (**28**, **30**-**33**)	depsipeptide	Papua New Guinea	[76]
Lyngbya majuscula and *Lyngbya sordia*	apratoxin D (**39**)	cyclic depsipeptide	Papua New Guinea	[77]

TABLE 1 (continued). CYTOTOXIC COMPOUNDS FROM MARINE CYANOBACTERIA

Source	Compound	Class	Collection Site	Reference
Lyngbya semiplena	semiplenamides A-G (**66**-**72**)	N-containing lipid	Papua New Guinea	[78]
	wewakpeptins A-D (**80**-**83**)	cyclic depsipeptide	Papua New Guinea	[79]
Lyngbya sp.	palau'imide (**61**)	N-acylpyrrolinone	Guam	[80]
	bisebromoamide (**101**)	linear peptide	Okinawa	[81]
	lyngbyacyclamides A (**104**) and B (**105**)	cyclic peptide	Okinawa	[82]
	lyngbyabellins C (**27**) and D (**29**)	cyclic depsipeptide	Palau	[80, 83]
	palau'amide (**62**)	cyclic depsipeptide	Palau	[84, 85]
	ulongamides A-F (**54**-**59**)	cyclic depsipeptide	Palau	[86]
	ulongapeptin (**63**)	cyclic depsipeptide	Palau	[87]
Assemblage of *Lyngbya majuscula* and *Schizothrix* sp.	somocystinamide A (**137**)	linear lipopeptide	Fiji	[88]
cf. *Oscillatoria margaritifera*	veraguamides A-C (**123**-**125**) and H-L (**130**-**134**)	cyclic depsipeptide	Panama	[89]
Phormidium spp.	caylobolide B (**65**)	macrolactone	Florida	[90]
Symploca cf. *hydnoides*	veraguamides D-G (**126**-**129**)	cyclic depsipeptide	Guam	[91]
Symploca cf. sp.	swinholide A (**118**)	polyketide	Fiji	[47, 92]
Symploca hydnoides	symplostatin 1 (**7**)	linear peptide	Guam	[93]
	malevamide D (**10**)	depsipeptide ester	Hawaii	[94]
Symploca sp.	largazole (**22**)	cyclic depsipeptide	Florida	[95]
	guamamide (**17**)	N-containing lipid	Guam	[96]
	micromide (**16**)	linear peptide	Guam	[96]
	apramides A (**18**), B (**19**), and G (**20**)	linear peptide	Guam	
	dolastatin 10 (**1**)	linear peptide	Palau	[97, 98]
	belamide A (**21**)	linear peptide	Panama	[99]
	symplostatin 3 (**8**)	linear depsipeptide	Hawaii	[100]
	tasiamide (**11**) and tasiamide B (**12**)	linear peptide	Palau	[101, 102]
	tasipeptins A (**14**) and B (**15**)	cyclic depsipeptide	Palau	[101]
Synechocystis sp.	nakienones A-C (**112**-**114**)	polyketide	Okinawa	[103]
	nakitriol (**115**)	polyketide	Okinawa	[103]

TABLE 2. CYTOTOXIC COMPOUNDS FROM FRESHWATER/TERRESTRIAL CYANOBACTERIA

Source	Compound	Class	Reference
Order Nostocales			
Anabaena affinis (VS-1)	nucleosides (**136** and **137**)	nucleoside	[104]
Anabaena laxa	laxaphycins A (**109**) and B (**110**)	lipopeptide	[105, 106]
Calothrix fusca	calophycin (**187**)	lipopeptide	[107]
Calothrix sp.	calothrixins A (**188**) and B (**189**)	pentacyclic indole	[108]
Cylindrospermum lichenforme	cylindrocyclophanes A-F (**149**-**154**)	paracyclophane	[109]
Nostoc commune	comnostins A-E (**165**-**169**)	diterpenoid	[110]
	nostofungicidine (**163**)	lipopeptide	[111]
Nostoc linckia UTEX B1932	nostocyclophanes A-D (**156**-**159**)	paracyclophane	[112]
Nostoc linckia *Nostoc spongiaeforme*	borophycin (**162**)	polyketide	[113, 114]
Nostoc sp. 152	nostophycin (**164**)	cyclic peptide	[115]
Nostoc sp. ATCC53789	cryptophycin (**150**)	depsipeptide	[116]
	nostocyclopeptides A1 (**170**) and A2 (**171**)	cyclic peptide	[117]
Nostoc sp. CAVN10	carbamidocyclophanes A-E (**172**-**176**)	paracyclophane	[118]
Nostoc sp. GSV224	cryptophycins	peptide	[119]
Nostoc sp. UIC 10022A	cylindrocyclophanes A_1-A_4 (**177**-**180**), C_1-C_4 (**181**-**184**), F_4 (**185**), A (**149**), C (**15`**), and F (**154**)	paracyclophane	[120]
Nostoc sphaericum	indolocarbazole (**155**)	alkaloid	[121]
Scytonema mirabile	mirabimides A-E (**139**-**143**)	lipopeptide	[122]
Scytonema sp.	scytonemin (**138**)	alkaloid	[123]
Scytonema spp. *Scytonema pseudohomanni* *Cylindrospermum muscicola*	scytophycins A-E (**144**-**148**)	polyketide	[124]
Tolypothrix conglutinata var. *colorata*	tolytoxin (**190**)	polyketide	[125]
Tolypothrix nodosa Bharadwaja (UH HT-58-2)	tolyporphins A-K (**191**-**201**)	porphinoid	[126-128]
Order Oscillatoriales			
Lyngbya sp.	pahayokolides A (**210**) and B **(211**)	lipopeptide	[129, 130]
Tychonema sp.	tychonamides A (**212**) and B (**213**)	lipopeptide	[131]
Order Stigonematales			
Hapalosiphon welwitschii *Westiella intricate*	welwitindolinones (**203**-**209**)	alkaloid	[132]
Westiellopsis prolifica	westiellamide (**202**)	cyclic peptide	[133]
Order Chroococcales			
Microcystis sp.	microcyclamide MZ568 (**214**)	cyclic peptide	[134]
Microcystis aeruginosa (NIES-298)	microcyclamide (**215**)	cyclic peptide	[135]
Microcystis aeruginosa (NO-15-1840)	microcystilide A (**216**)	peptide	[136]

2.2 Cytotoxic secondary metabolites from marine cyanobacteria sorted by genera

2.2.1 *Symploca*

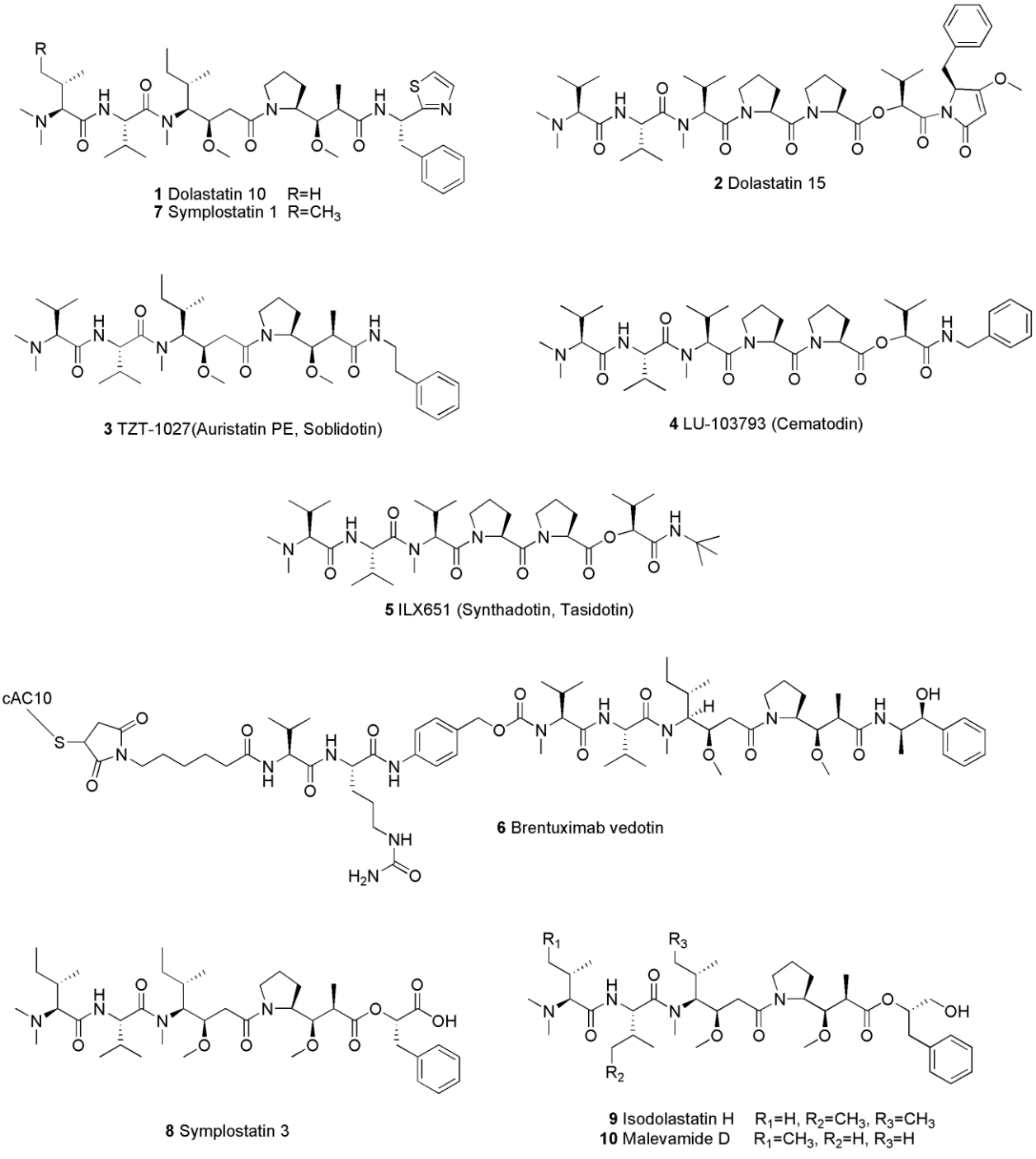

Figure 4. Structures of dolastatins, symplostatins, and synthetic analogues

Dolastatin 10 (**1**, Figure 4), a linear pentapeptide, was originally isolated from *Dolabella auricularia*, a sea hare, from the Indian Ocean [97]. The structure of dolastatin 10 contained a terminal *N*,*N*-dimethylvaline, which also has been found in other bioactive cyanobacterial peptides [49]. Furthermore, the C-terminal of the molecule had a dolaphenine unit comprised of condensed phenylalanine and cysteine residues, in which the thiazoline ring was oxidatively decarboxylated to the mono-substituted thiazole ring [42, 97]. Fourteen years after the discovery of dolastatin 10, the same molecule was isolated from a marine cyanobacterium, *Symploca* sp. VP642 collected from Palau [98]. The only difference between the two isolations was the yield (1 to 0.1 ppb from the sea hare vs. 10 ppm dry weight from the cyanobacterium). Overall, it was suggested that cyanobacteria were the ultimate producers of the dolastatin 10 and that the sea hare did not have the ability to concentrate the dietary molecules, resulting in the low yield. Dolastatin 10 exhibited significant cytotoxicity against KB and LoVo cells with IC_{50} values of 0.041 and 0.066 nM, respectively [98]. In addition, dolastatin 10 was a potent microtubule depolymerizer, in which the total loss of cellular microtubules was observed at a concentration of only 0.75 nM [98]. Exposure to dolastatin 10 caused the formation of abnormal multipolar mitotic spindles and the breakdown of the nucleus into micronuclei [98]. Unfortunately, the phase II clinical trial as a single agent was discontinued due to undesired peripheral toxicity.

Dolastatin 15 (**2**, Figure 4), a seven-subunit depsipeptide, was also isolated from the Indian Ocean sea hare *Dolabella auricularia* [137]. It was structurally related to dolastatin 10 (**1**). Despite the structural similarity, dolastatin 15 showed on average about seven times less cytotoxicity than dolastatin 10 [138]. Similar to dolastatin 10, it disrupted microtubule assembly through binding to the vinca domain of tubulin and induced apoptosis in cancer cells. Although dolastatin 15 has not been obtained from marine cyanobacteria, it is related to several dolastatin analogues isolated from cyanobacteria, suggesting dolastatin 15 also to be of cyanobacterial origin.

Both dolastatin 10 (**1**) and 15 (**2**) served as drug leads for the development of various synthetic analogues. TZT-1027 (**3**, Auristatin PE or soblidotin, Figure 4) was found to be superior to current anticancer drugs such as paclitaxel and vincristine in vitro. However, clinical phase I and II evaluation showed lack of efficacy and peripheral neuropathy [139, 140]. Two simplified synthetic analogues of dolastatin 15, LU-103793 (**4**, Cematodin, Figure 4) and ILX651 (**5**, Synthadotin or Tasidotin, Figure 4), were developed as drug candidates and entered clinical trials. LU103793 was a water-soluble analogue and has completed a phase II evaluation [141]. Unfortunately, clinical evaluation was discontinued due to

poor performance in clinical phase II [138]. ILX651, also a water-soluble analogue, was developed as a third generation of dolastatin 15 analogue. The metabolic stability and bioavailability of ILX651 was enhanced compared to LU-103793. It has completed a phase I evaluation in patients with advanced solid tumors, and the results showed that the compound was well tolerated and no cardiotoxicities were observed. It is now in phase II evaluation. Recently, another dolastatin 10 analogue, auristatin E, was developed as an antibody drug conjugate targeting CD30. This resulted in a highly effective and well tolerated drug brentuximab vedotin (**6**, Figure 4) [142]. It was recently approved by FDA for use in Hodgkin's lymphoma and anaplastic large cell lymphoma, and is now marketed as Adcetris by Seattle Genetics. Three other antibody conjugates of the auristatin E, glembatumumab vedotin (CDX-011), SGN-75, and ASG-5ME, are now in clinical phase I and II trials [143].

Symplostatin 1 (**7**, Figure 4), a structural analogue of dolastatin 10, was isolated from a Guamanian collection of *Symploca hydnoides* [93]. Dolastatin 10 was also obtained, again demonstrating the dietary origin of the dolastatins. Symplostatin 1 exhibited cytotoxicity against KB cells with an IC_{50} value of 0.4 nM [93]. It also induced 80% microtubule loss in A-10 cells at 1.3 nM. Overall, biological activities of symplostatin 1 were comparable to these of dolastatin 10, suggesting that its mechanism of action must be similar, if not identical, to that of dolastatin 10 [93, 144].

Symplostatin 3 (**8**, Figure 4), another analogue of dolastatin 10, was isolated from the organic extract of *Symploca* sp. VP452 collected in Hawaii [100]. The structure of symplostatin 3 only differed from that of dolastatin 10 in the C-terminal unit, where the dolaphenine unit had been substituted by a 3-phenyllactic acid moiety [97, 100]. Structurally, symplostatin 3 most closely resembled isodolastatin H (**9**, Figure 4), which was another dolastatin 10 analogue found in the Japanese sea hare *Dolabella auricularia* [145]. The 3-phenyllactic acid unit was connected via an ester linkage to the residual tetrapeptide [100]. Due to this structural difference, symplostatin 3 was found to be approximately a 100-fold less cytotoxic than dolastatin 10, and IC_{50} values of symplostatin 3 were 3.9 and 10.3 nM against KB and LoVo cells, respectively [100]. In addition, symplostatin 3 caused microtubule depolymerization as well as the breakdown of the nucleus into micronuclei. These microtubule effects of the molecule were indistinguishable from those of dolastatin 10 and symplostatin 1 [93, 98, 100].

Malevamide D (**10**, Figure 4), a peptide ester isolated from Hawaiian *Symploca hydnoides*, was an analogue of isodolastatin H [94]. As observed for symplostatin 3, the C-terminal residue of both

malevamide D and isodolastatin H was connected to a proline via an ester rather than an amide bond. The structure of malevamide D differs from dolastatin 10 at both the N- and C-terminal ends, where the former has L-Ile and 3-phenyl-1,2-propanediol moieties, respectively [16]. Malevamide D was found to be cytotoxic, displaying IC_{50} values ranging from 0.3 to 0.7 nM against P-388, A-549, HT-29, and MEL-28 cells.

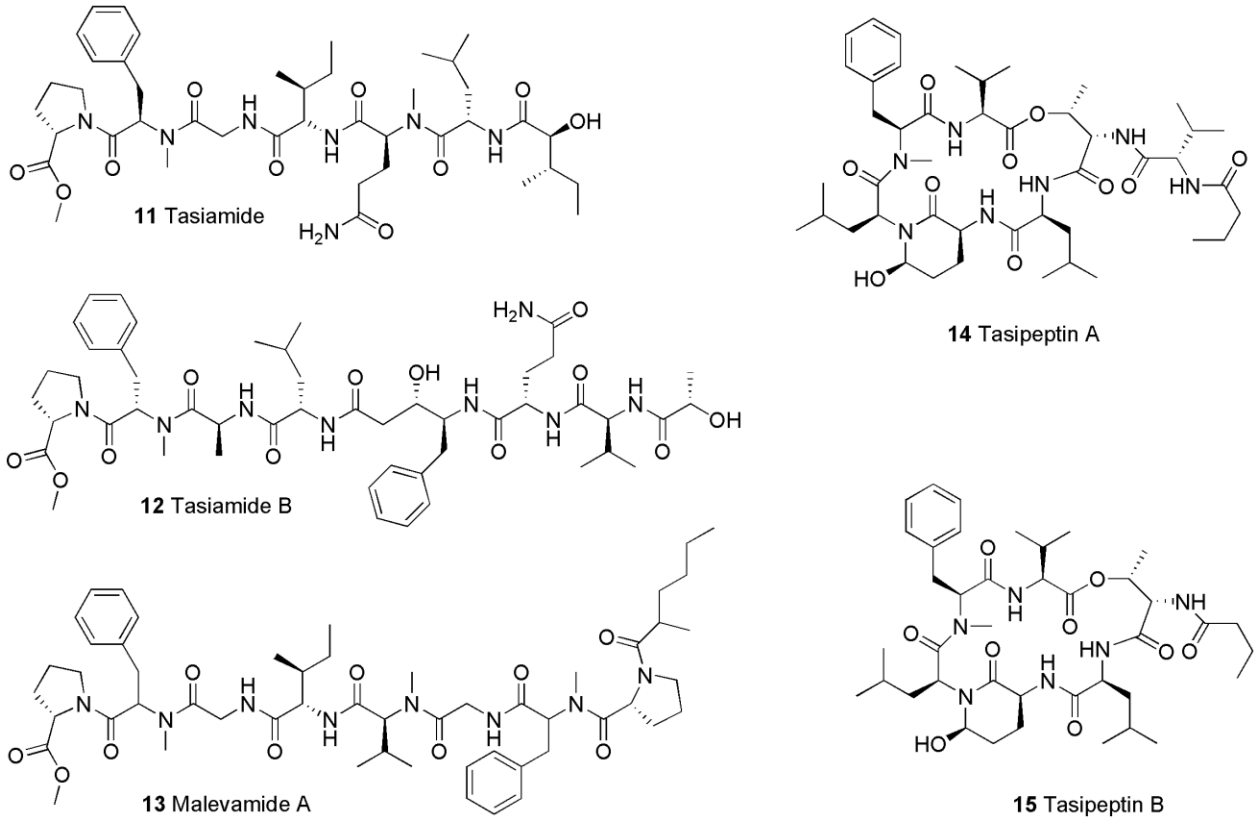

Figure 5. Structures of tasiamides, tasipeptins and malevamide A

Tasiamide (**11**) and tasiamide B (**12**) (Figure 5), linear peptides, were isolated from a *Symploca* sp. collected from Palau [101, 102]. The structure of tasiamide that comprised of seven amino acid-derived residues, while tasiamide B had an additional amino acid residue. The structure of tasiamide contained several features common to cyanobacterial peptides, including a hydroxy acid, two *N*-methylamides, and an ester. The closest structurally related compound of tasiamide was the linear lipopeptide malevamide A

(**13**, Figure 5), which shared the amino acid sequence from *O*-methylproline through isoleucine [146]. On the other hand, the structure of tasiamide B contained an unusual moiety 4-amino-3-hydroxy-5-phenylpentanoic acid (Ahppa), which was known as a component of protease inhibitors from *Candida* [147] and *Streptomyces* spp. [148]. This was the first report of the Ahppa from a marine cyanobacterium. Both tasiamide and tasiamide B were found to be cytotoxic against KB cells with IC_{50} values of 0.58 and 0.80 μM, respectively [101, 102]. Furthermore, tasiamide showed cytotoxicity against LoVo cells with an IC_{50} value of 4.2 μM [101]. Malevamide A however, was inactive against P-388, A-549, and HT-29 cells at 2 μM [146].

Two cyclic depsipeptides, tasipeptins A (**14**) and B (**15**) (Figure 5), were later isolated from the aqueous extract of the same *Symploca* sp. that produced tasiamide [149]. Both tasipeptins A and B were found to be cytotoxic against KB cells with IC_{50} values of 0.93 and 0.82 μM, respectively.

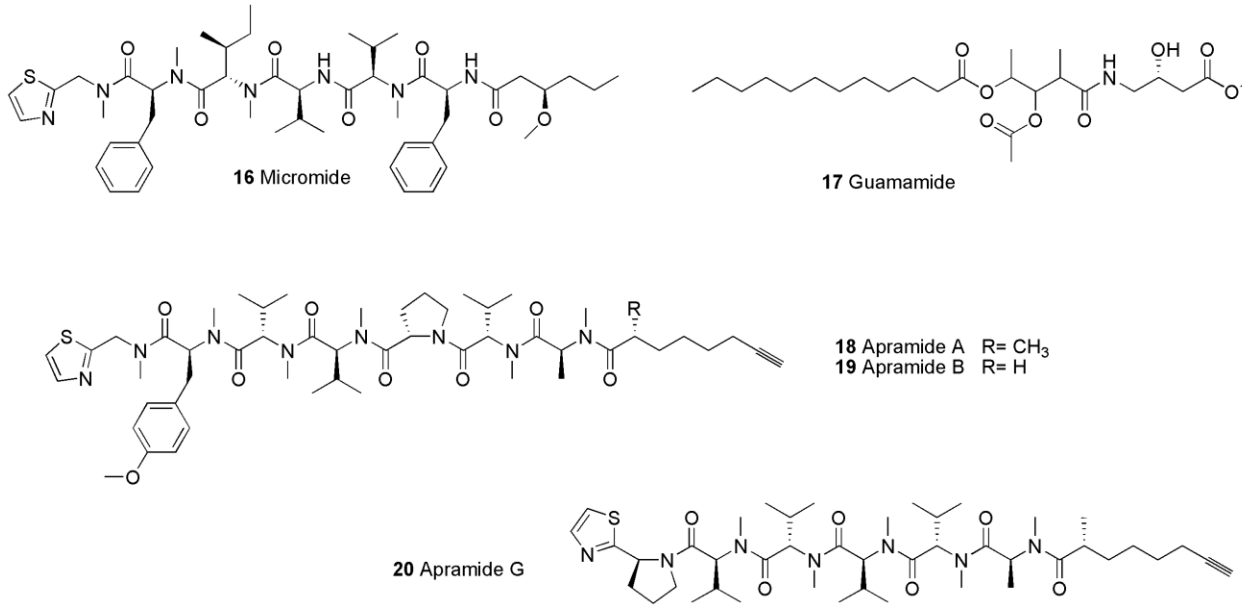

Figure 6. Structures of micromide, guamamide, and apramides

Micromide (**16**, Figure 6) was isolated from a Guamanian *Symploca* sp., along with guamamide (**17**, Figure 6) and apramides A, B, and G (**18-20**, Figure 6) [96]. The structure of micromide contained *N*-

methylated amino acids, a D-amino acid, and a modified cysteine moiety in the form of a thiazole ring. Furthermore, it had a unique β-methoxy acid moiety and a 3-methoxy-hexanoic acid. Micromide was found to be cytotoxic against KB cells with an IC_{50} value of 260 nM, and selective against solid tumor cells. On the other hand, the IC_{50} values of the apramides A, B, and G against KB cells were an order of magnitude lower than micromide. Guamamide showed cytotoxicity against KB cells with an IC_{50} value of 1.2 μM.

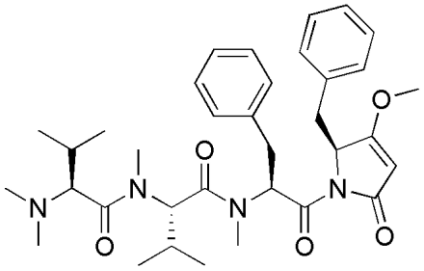

21 Belamide A

Figure 7. Structure of belamide A

Belamide A (**21**, Figure 7), a highly methylated tetrapeptide, was isolated as the major metabolite from a Panamanian *Symploca* sp. [99]. The structure of belamide A contained N-terminal *N*,*N*-dimethylvaline and C-terminal benzyl-methoxy-pyrrolinone moieties, both of which were characteristic residues of dolastatin 15 [99, 150]. In particular, the C-terminus of belamide A expanded the repertoire of linear peptides from marine cyanobacteria [16, 99]. This structural feature contributed to structure-activity relationship (SAR) studies and further, to the development of potential drug leads for this class of compounds. As opposed to the nanomolar activities against cancer cells for both dolastatins 10 and 15 [97, 137], belamide A showed only moderate cytotoxicity against MCF-7 and HCT-116 cells with IC_{50} values of 1.6 and 0.74 μM, respectively [16, 99]. Belamide A showed microtubule depolymerization in A-10 cells at 20 μM [99].

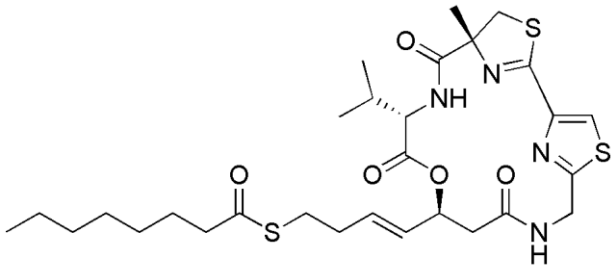

22 Largazole

Figure 8. Structure of largazole

Largazole (**22**, Figure 8), a cyclic depsipeptide, was isolated from a *Symploca* sp. collected from the Florida Keys [95]. The structure of largazole contained a substituted 4-methylthiazoline linearly fused to a thiazole. This unit had also been observed in didehydromirabazole isolated from a terrestrial cyanobacterium *Scytonema mirabile* [122]. It also contained a 3-hydroxy-7-mercaptohept-4-enoic acid unit and a thioester moiety. Both of these moieties have only been reported in the secondary metabolites produced by sponges, eukaryotic algae, and bacteria [151-154]. Largazole exhibited exceptional antiproliferative activity against transformed cells, i.e. MDA-MB-231 and U2OS cells with GI_{50} values of 7.7 and 55 nM, respectively. Interestingly, non-transformed cells were much less sensitive to the effects of largazole (GI_{50} values against NMuMG and NIH3Ts cells were 122 and 480 nM, respectively), suggesting that cancer cells were preferentially targeted [42, 95]. Largazole also showed significant growth inhibition of HT-29 and IMR-32 cells with GI_{50}/LC_{50} of 12 nM/22 nM and 16 nM/22 nM, respectively [95]. In addition, it was shown that largazole had in vitro and in vivo osteogenic acitivity with significant potential in bone formation, repair, and regeneration [155]. Moreover, it was revealed that largazole was a pro-drug, liberating largazole thiol [156].

2.2.2 *Lyngbya*

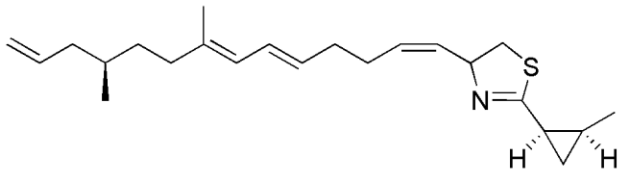

23 Curacin A

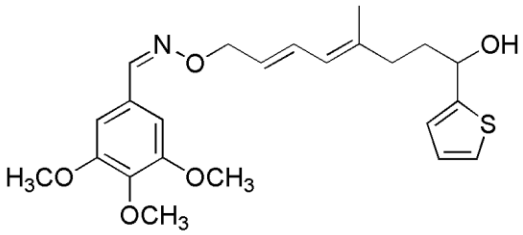

24 Synthetic analogue

Figure 9. Structures of curacin A and the synthetic analogue

Curacin A (**23**, Figure 9) was isolated from *Lyngbya majuscula* collected in Curçao [56]. The structure of curacin A consisted of a 2,4-disubstituted thiazoline ring and a lipophilic chain [157]. Brine shrimp assay-guided isolation led to isolation of the compound. Curacin A showed potent cytotoxicity in a variety of cancer cell lines at nanomolar concentrations. The mode of action was shown to be inhibition of tubulin polymerization [56]. Curacin A inhibited microtubule assembly through interaction at the colchicine binding site, and its binding behavior was similar to that of podophyllotoxin [158]. However, in vivo studies could not be imitated due to poor water solubility and instability of the compound. A series of semi-synthetic derivatives have been prepared using combinatorial synthesis in order to improve the solubility and stability [159]. One of these synthetic variants (**24**, Figure 9) is currently undergoing preclinical evaluation as potential anticancer drug [4].

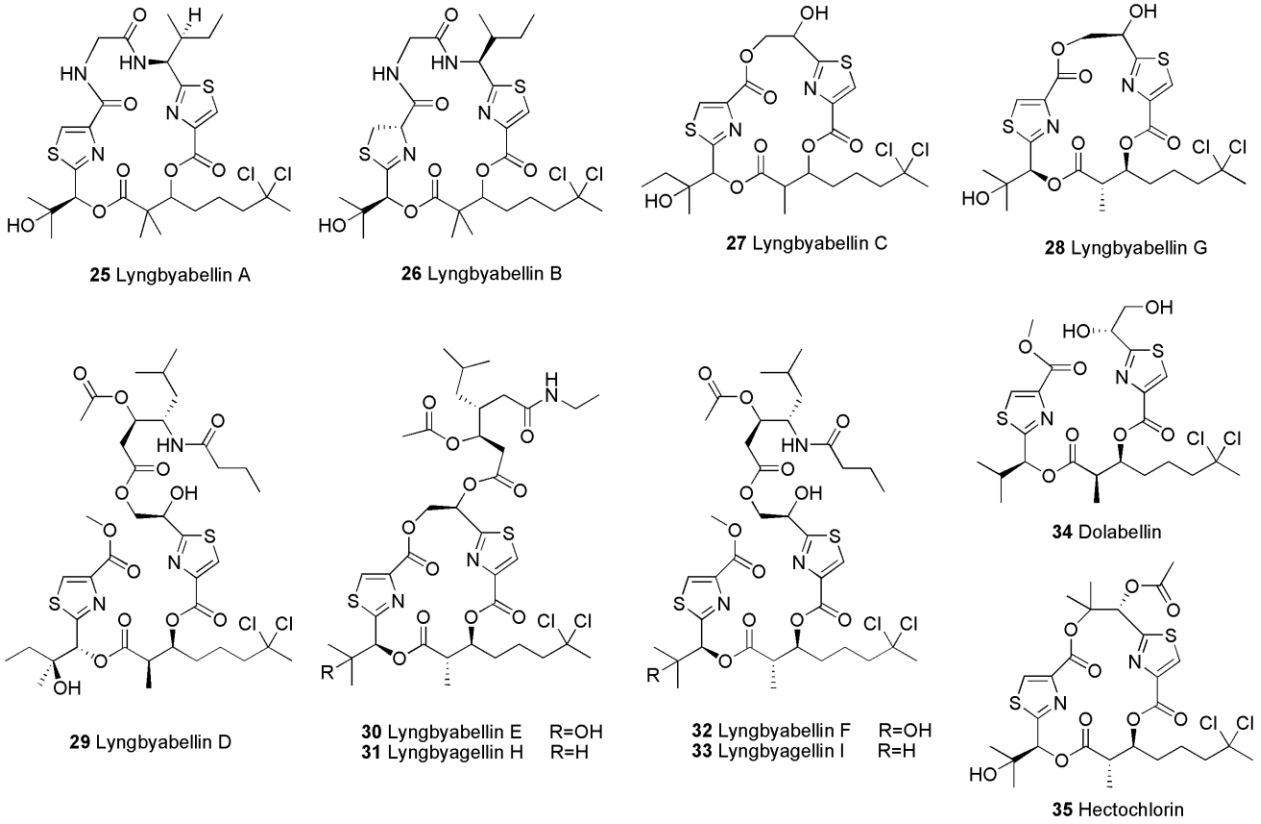

Figure 10. Structures of lyngbyabellins, dolabellin, and hectochlorin

Lyngbyabellins A-I (**25**-**33**, Figure 10) were isolated from *Lyngbya majuscula* and *Lyngbya* sp. collected from Guam, Palau, and Papua New Guinea [62, 63, 66, 73, 76, 83].

The structure of lyngbyabellin A (**25**) was similar to that of dolabellin (**34**, Figure 10), originally obtained from the sea hare *Dolabella auricularia*, in that both contained a dichlorinated β-hydroxy acid and two functionalized thiazole carboxylic acid moieties [63, 74]. Lyngbyabellin A exhibited cytotoxicity against KB and LoVo cells with IC_{50} values of 0.05 and 0.8 μM, respectively. In addition, it disrupted microfilament network in A-10 cells at concentrations ranging from 0.01 to 7.2 μM. Further investigation of the lyngbyabellin A-producing *L. majuscula* led to the isolation of lyngbyabellin B along with lyngbyapeptin A [73]. The structure of lyngbyabellin B differed from that of lyngbyabellin A in that the former contained a valine and a thiazole unit instead of an isoleucine and a thiazoline ring [63, 73]. Lyngbyabellin B was only slightly less cytotoxic than lyngbyabellin A against KB and LoVo cells with IC_{50} values of 0.1 and 1.2 μM, respectively.

Lyngbyabellin C (**27**) was isolated from a Palauan *Lyngbya* sp. along with lyngbyabellin A, lyngbyapeptins A-C, and palau'imide (**61**) (Figure 13) [80]. Lyngbyabellin C showed cytotoxicity against KB and LoVo cells with IC_{50} values of 2.1 and 5.3 μM, respectively. Re-collections of the Guamanian *Lyngbya* sp. [80] led to the isolation of lyngbyabellin D (**29**) and 15-norlyngbyapeptin A [83]. Lyngbyabellin D displayed an IC_{50} value of 0.1 μM against KB cells. Another collection of *L. majuscula* from Papua New Guinea led to the isolation of lyngbyabellins E-I (**28**, **30**-**33**) and dolabellin (**34**) [76]. The structures of lyngbyabellins were either cyclic or acyclic. However, it was found that one ester linkage in lyngbyabellin C was prone to methanolysis, yielding the linear form of the structure [80]. This conversion led to the speculation that the acyclic form of lyngbyabellins F and I could be derived by methanolysis of their cyclic forms, lyngbyabellins E and H, respectively [76]. Lyngbyabellins E-I displayed cytotoxicity against NCI-H460 and neuro-2a cells with IC_{50} values ranging from 0.2 to 4.8 μM. Dolabellin was originally isolated from *D. auricularia* however, it is now believed that the true producer of this compound was cyanobacteria in the diet.

Hectochlorin (**35**, Figure 10) was initially isolated from a cultured strain of *Lyngbya majuscula* collected from Jamaica, and subsequently from field collections made from Panama [66]. The structure of hectochlorin resembled those of dolabellin and lyngbyabellins A and B [63, 66, 73, 74]. Hectochlorin was found to be cytotoxic against CA46 cells with an LD_{50} value of 20 nM. Moreover, it was shown to induce hyperpolymerization of the eukaryotic actin filament, the same mode of action observed for lyngbyabellin B on the actin cytoskeleton [73]. In addition, hectochlorin was found to be a potent antifungal compound against *Candida albicans* [66].

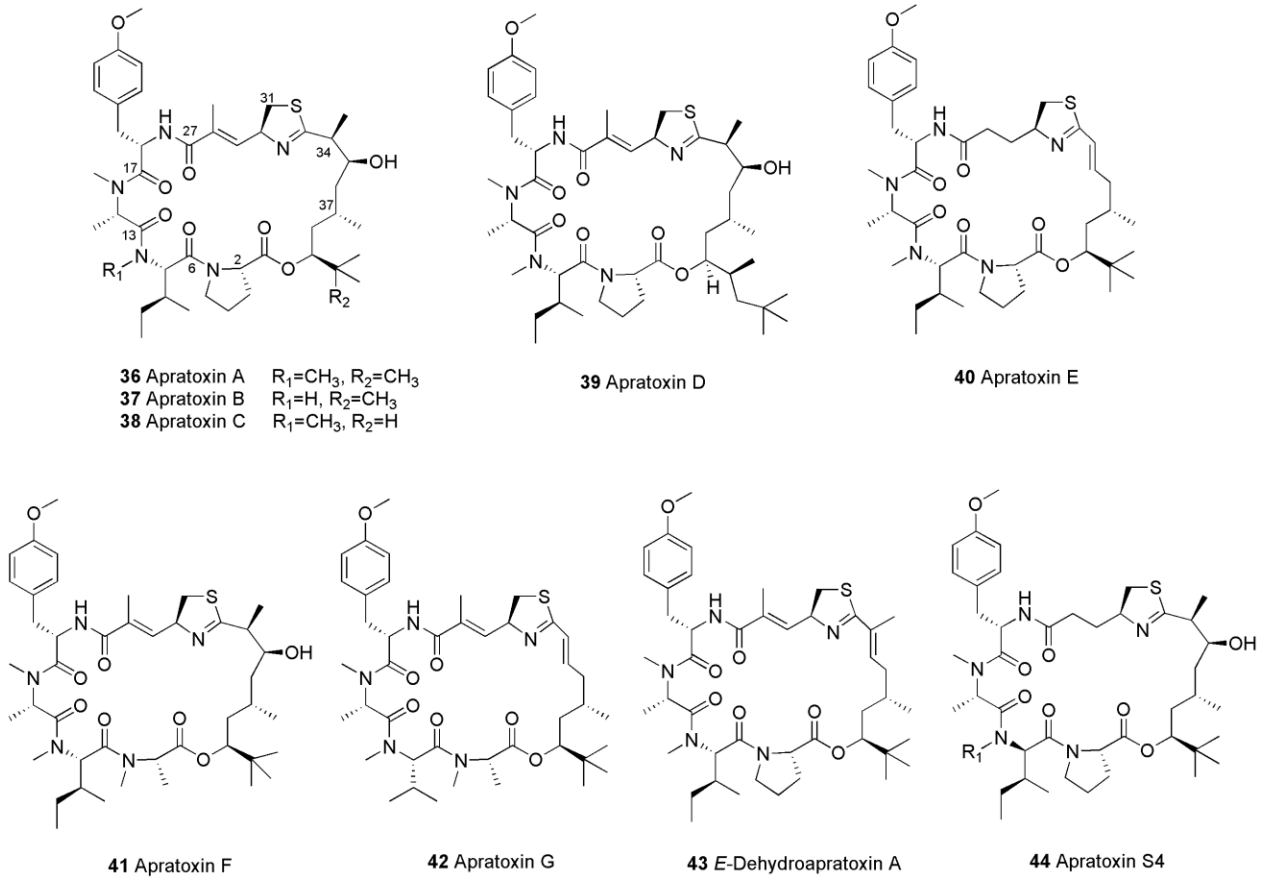

Figure 11. Structures of apratoxins and synthetic analogues

Apratoxins A-G (**36**-**42**, Figure 11), cyclic depsipeptides, were isolated from various *Lyngbya* spp, collected from Guam, Palau, Palmyra, and Papua New Guinea. Apratoxins were characterized by having five amino acid moieties and a polyketide chain as part of the cyclic carbon skeleton [16].

Apratoxin A (**36**), the first molecule of this series, was isolated from *Lyngbya majuscula*, collected in Guam [58]. Apratoxin A was found to be sensitive to acid, and it decomposed to the dehydro-derivative. Apratoxin A displayed significant cytotoxicity against a variety of human cancer cells with IC_{50} values ranging from 0.36 nM in LoVo cells to 0.52 nM in KB cells. Despite the subnanomolar cytotoxicity of the apratoxin A, it showed limited or no activity against colon and breast tumors at sublethal doses in vivo. Furthermore, animal toxicity and weight loss were observed at higher doses. Apratoxin B (**37**) and C (**38**), simple desmethyl analogues of apratoxin A, were isolated from *Lyngbya* sp., collected in Guam and Palau, respectively [59]. When compared to apratoxin A, apratoxin B and a semisynthetic analogue *E*-

dehydroapratoxin A (**43**) were significantly less cytotoxic, suggesting that the presence of *N*-methyl isoleucine moiety and hydroxyl group at C-35 were important features for biological activities. On the other hand, apratoxin C showed almost identical IC_{50} values as apratoxin A, indicating that the *tert*-butyl group was not essential for activity. Apratoxin D (**39**) was isolated from two other species, *Lyngbya majuscula* and *Lyngbya sordia*, both collected from Papua New Guinea [77]. The structure of apratoxin D had the same sequence of amino acid residues as apratoxins A and C while containing a new polyketide moiety, 3,7-dihydroxy-2,5,8,10,10-pentamethylundecanoic acid. Apratoxin D showed an IC_{50} value of 2.6 nM against NCI-H460 cells. This was nearly equipotent to that of apratoxin A, thus, indicating that the cytotoxicity was not impacted by the larger lipopeptide tail. Apratoxin E (**40**) was isolated from Guamanian *Lyngbya bouillonii* [51]. In comparison to apratoxin A, the structure of apratoxin E contained an olefinic methine and allylic methyl proton signals of the α,β-unsaturated modified cysteine spin system instead of a pair of methylene signals. Apratoxin E showed significant cytotoxicity against several cancer cells with IC_{50} values ranging from 21 to 72 nM, further suggesting that the α,β-unsaturation of the modified cysteine residue was not essential for the activity. The 5- to 15-fold reduced cytotoxicity compared with apratoxin A was attributed to the dehydration in the long-chain polyketide moiety, which could affect the conformation of the molecule. Most recently, apratoxins F (**41**) and G (**42**) were isolated from *Lyngbya bouillonii* collected from Palmyra Atoll [52]. The structure of both compounds contained an *N*-methyl alanine moiety at a position where all prior apratoxins have possessed a proline unit, adding fresh insights into the SAR of the apratoxin family. Both apratoxin F and G showed cytotoxicity against NCI-H460 cells with IC_{50} values of 2 and 14 nM, respectively.

The potent cytotoxicity, anticancer potential, and novel carbon skeleton led to the total synthesis of apratoxin A [160-162] and several total syntheses to develop SAR studies of this class of metabolites [163-165]. The results indicated that several disparate regions of the compound were important for maximal biological activity, while the lower regions from C-39 to the *tert*-butyl terminus and C-1 to C-5 were more tolerant of structural changes. In particular, SAR studies and medicinal chemistry efforts recently led to the identification of apratoxin S4 (**44**, Figure 11), which was an hybrid analogue of apratoxins A and E [166]. Apratoxin S4 was the first viable candidate of the apratoxin family in that it showed the tumor selectivity as well as increased antitumor activity and potency [166].

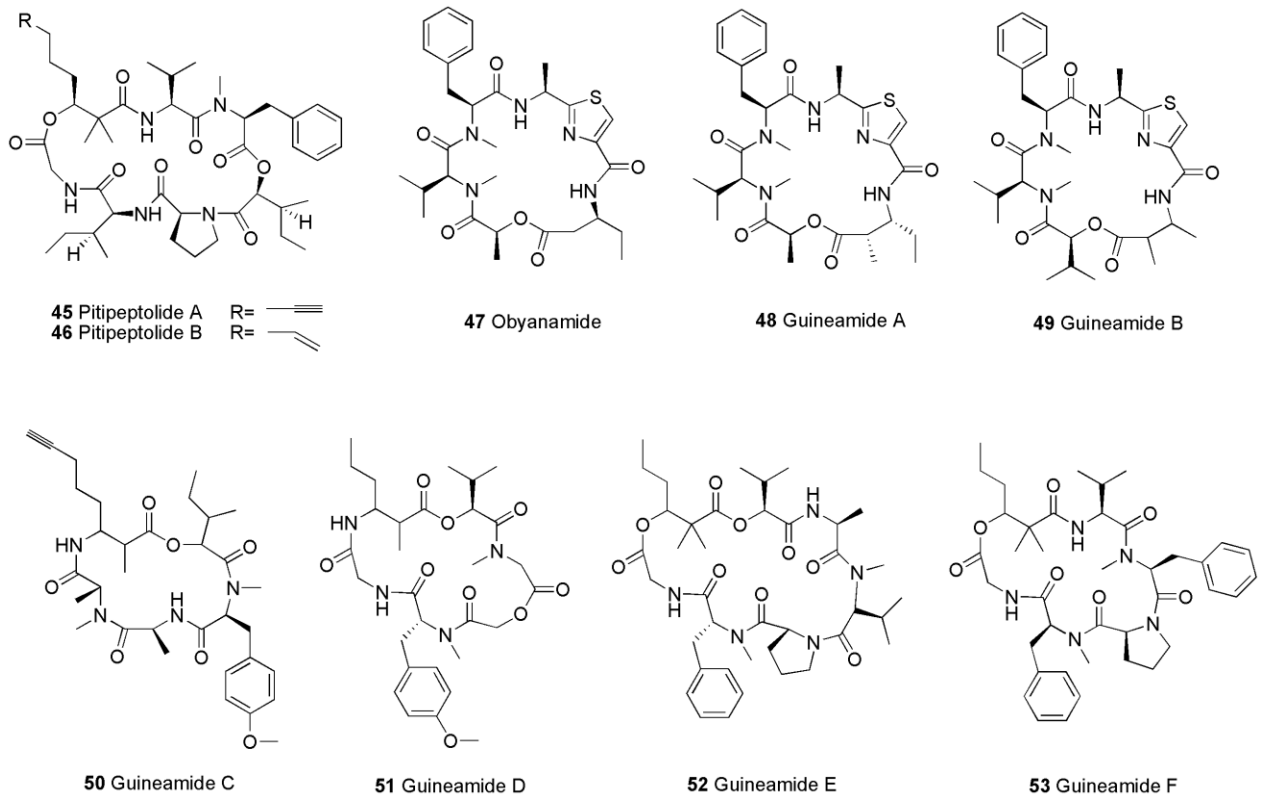

Figure 12. Structures of pitipeptolides, obyanamide, and guineamides

Pitipeptolides A (**45**) and B (**46**) (Figure 12), isolated from a Guamanian *Lyngbya majuscula*, were analogues of guineamide E (**52**) [64]. Both pitipeptolides A and B showed weak cytotoxicity against LoVo cells with IC_{50} values of 2.8 and 2.4 μM, respectively. In addition, pitipeptolide A was found to chemically defend *L. majuscula* from marine grazers including *Echinometra mathaei* (sea urchin), *Menaethius monoceros* (herbivorous crab), *Parhyale hawaiensis* (amphipod), and *Cymadusa imbroglio* (amphipod) [167].

Obyanamide (**47**, Figure 12), isolated from *Lyngbya confervoides* collected in Saipan, was an analogue of guineamide A (**48**) [54]. The structure of obyanamide differed from that of guineamide A by having 3-aminopentanoic acid (Apa) instead of Mapa moiety [54, 75]. Obyanamide showed moderate cytotoxicity against KB and LoVo cells with IC_{50} values of 0.9 and 5.2 μM, respectively.

Guineamides A-F (**48**-**53**, Figure 12) were isolated from a Papua New Guinea collection of *Lyngbya majuscula* [75]. The ring size of the six guineamides ranged from five to seven residues,

displaying different structural types. The structures of all six compounds possessed a number of *N*-methylated amino acids, and α-hydroxy, β-amino, and β-hydroxy acids. Of the β-amino acids, 2-methyl-3-aminopentanoic acid (Mapa), 2-methyl-3-aminobutanoic acid (Maba), and 2-methyl-3-amino-oct-7-ynoic acid (Maoya) were observed in guineamides A-C, respectively. The Mapa residue, in particular, has been reported as a component of several marine molluscan metabolites such as dolastatins D, 11, 12, and onchidin A [168-170]. The identification of guineamides in cyanobacteria further supported that these metabolites were diet-drived. The structures of both guineamides E and F contained a 2,2-dimethyl-3-hydroxyhexanoic acid (Dmhha) moiety. This represented the first report of such a residue in natural products [16, 75]. Moderate cytotoxicity against neuro-2a cells was observed for guineamides B and C with IC_{50} values of 15 and 16 μM, respectively, while guineamide A was inactive at 16 μM.

Ulongamides A-F (**54**-**59**, Figure 13), cyclic depsipeptides, were isolated from the apratoxin-producing cyanobacterium *Lyngbya* sp. collected from Palau. The structures of all ulongamides contained 3-amino-2-methylhexanoic acid (Amha), which had also been encountered in other cyanobacterial metabolites such as malevamide B (**60**) [146] and lyngbyastatin 3 (**101**) [171], as well as in kulokekahilide-1, a constituent of the cephalaspidean mollusk *Philinopsis speciosa* [172]. Ulongamide A differed from obyanamide (**47**, Figure 12) in the residue sequence, with the *N*-Me-Val and the *N*-Me-Phe residues being switched. In addition, obyanamide contained a different β-amino acid, 3-aminopentanoic acid (Apa) [54, 86]. All ulongamides, except ulongamide F lacking an aromatic amino acid moiety, displayed cytotoxicity against KB and LoVo cells with IC_{50} values ranging from 1 to 5 μM.

Palau'imide (**61**, Figure 13), a truncated analogue of dolastatin 15 (Figure 4), was isolated from *Lyngbya* sp. collected in Palau [80]. The structure of palau'imide contained a *N*-acylpyrrolinone unit, which had been found in cyanobacterial metabolites such as microcolins A and B [173]. It also contained an imide. There have been several reports of similar cytotoxic imides, e.g. majusculamide D and deoxymajusculamide D from a marine cyanobacterium [174] and mirabimides A-E (**139**-**143**, Figure 29) from a terrestrial cyanobacterium [122, 175]. Furthermore, the lipid chain in palau'imide had precedence in cyanobacterial metabolites such as malevamide A (**13**, Figure 5) [146]. Palau'imide exhibited moderate cytotoxicity against KB and LoVo cells with IC_{50} values of 1.4 and 0.36 μM, respectively [80].

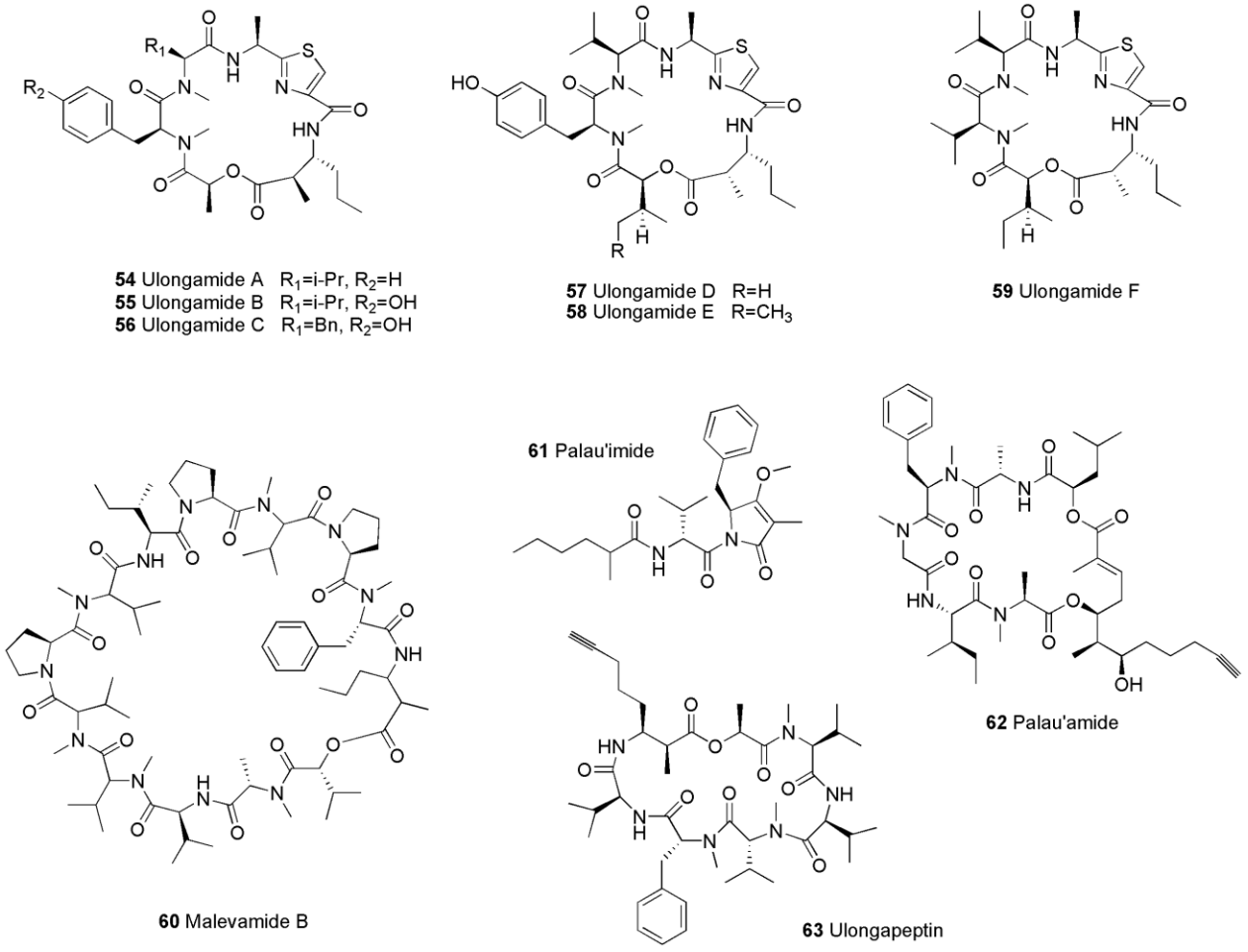

Figure 13. Structures of ulongamides, malevamide B, palau'imide, palau'amide, and ulongapeptin

Palau'amide (**62**, Figure 13), a cyclic depsipeptide, was isolated from a *Lyngbya* sp. collected in Palau [85]. The structure of palau'amide contained a terminal alkyne containing polyketide in addition to six amino acid-derived residues [16]. Palau'amide was cytotoxic against KB cells with an IC_{50} value of 13 nM. A structurally related minor compound was isolated along with palau'amide, which displayed an IC_{50} value against KB cells of 1 nM. However, the structure of the minor compound could not be assigned due to insufficient material for NMR experiments. These unsolved structural problems, combined with the remarkable cytotoxicity, led to the total synthesis and SAR studies. As a result, the stereoconfiguration of the palau'amide was corrected [84]. The synthetic palau'amide showed potent cytotoxicity against HeLa, A549, and BGC cells with IC_{50} values of 39, 19, and 26 nM, respectively.

Ulongapeptin (**63**, Figure 13), isolated from a Palauan *Lyngbya* sp., was another analogue of guineamide E (**52**) [87]. The structure of ulongapeptin contained a β-amino acid, 3-amino-2-methyl-7-octynoic acid (AMO), which had previously been identified in the mollusk metabolite onchidin [170, 176]. Ulongapeptin showed cytotoxicity against KB cells with an IC_{50} value of 0.63 μM.

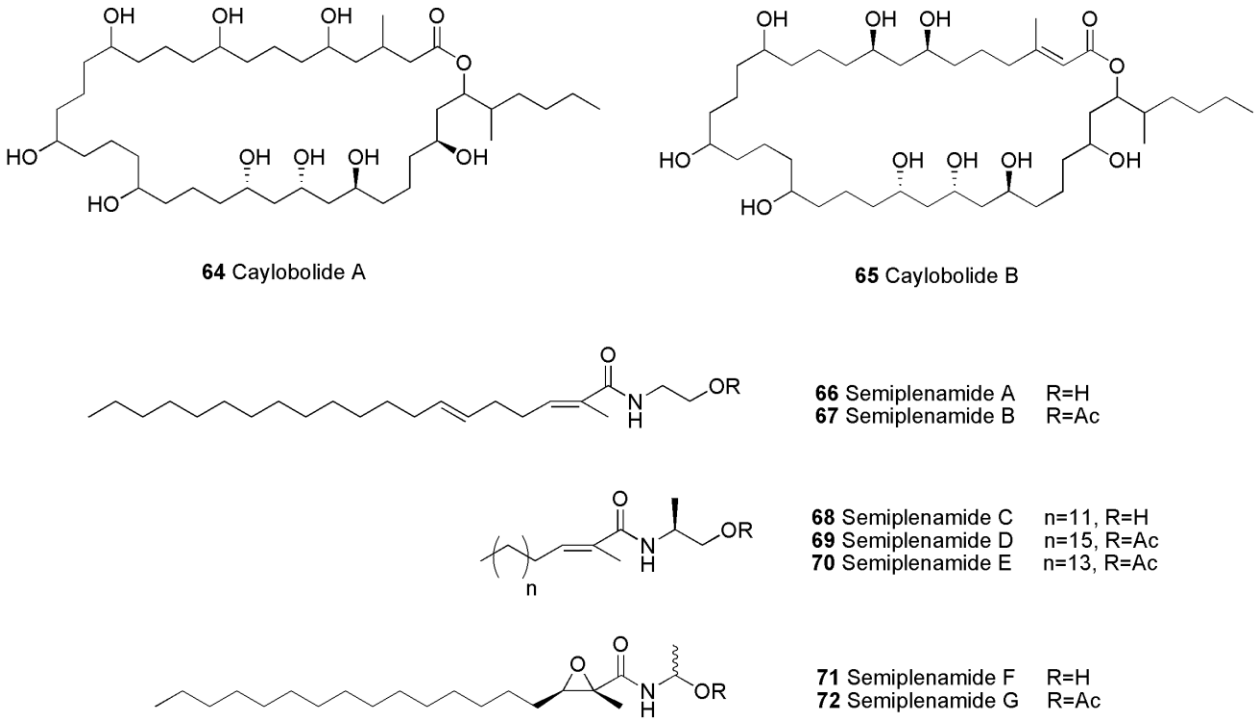

Figure 14. Structures of caylobolides and semiplenamides

Caylobolide A (**64**, Figure 14), a 36-membered lactone, was isolated from a *Lyngbya majuscula* collected in Bahamas [55]. The structure of caylobolide A contained a contiguous pentad of 1,5-diols and a 1,3,5-triol, which closely resembled amphidinol, a polyhydroxylated polyketide isolated from a marine dinoflagellate [177-179]. Caylobolide A showed moderate cytotoxicity against HCT-116 cells with an IC_{50} value of 9.9 μM. Caylobolide B (**65**, Figure 14) was later isolated from Floridian mixture of *Phormidium* spp., and exhibited cytotoxicity against HT-29 and HeLa cells with IC_{50} values of 4.5 and 12.2 μM, respectively [90]. The major activity of the extract was attributed to symplostatin 1. Due to the binary

mixture of two different *Phormidium* species, it was unclear whether caylobolide B and symplostatin 1 were produced by the same species.

Semiplenamides A-G (**66**-**72**, Figure 14), fatty acid amides, were isolated from *Lyngbya semiplena* collected from Papua New Guinea [78]. The structure of semiplenamides was similar to that of anandamide, an endogenous cannabinoid neurotransmitter. Semiplenamides A, B, and G showed weak affinity of the rat cannabinoid CB_1 receptor, while semiplenamide A displayed moderate inhibitory activity with an IC_{50} value of 18 μM against anadamide membrane transporter. In addition, all semiplenamides showed weak to moderate toxicity in the brine shrimp assay with LC_{50} values ranging from 1.4 to 19 μM.

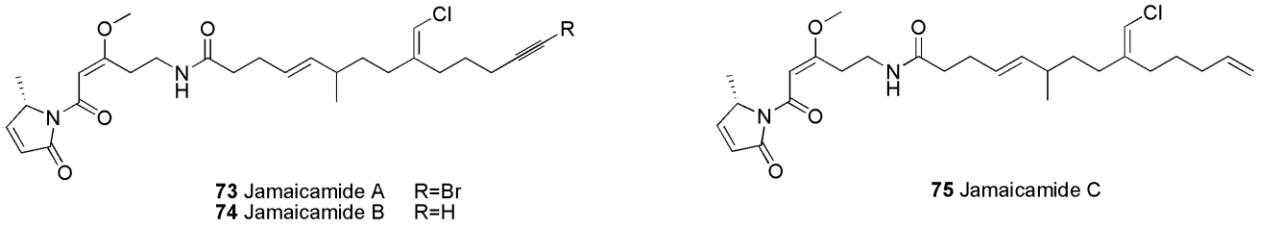

73 Jamaicamide A R=Br
74 Jamaicamide B R=H

75 Jamaicamide C

Figure 15. Structures of jamaicamides

Jamaicamides A-C (**73**-**75**, Figure 15), linear lipopeptides, were isolated from a *Lyngbya majuscula* collected in Jamaica [68]. The structures of jamaicamides were highly functionalized with a pyrrolinone ring system, a vinyl chloride, and a terminal alkynyl bromide or olefinic carbon [16, 68]. The alkynyl bromide moiety observed in jamaicamide A had rarely been found in nature. In fact, it has only been observed in veraguamides A, B, K, and L (Figure 28) from marine cyanobacteria [89, 91], and in fatty acid derivatives from Central Asian lichens [180, 181]. The pyrrolinone moiety has also been found in other *Lyngbya* metabolites, and is believed to be important for the biological activities of some of these natural products [182]. Jamaicamides A-C displayed cytotoxicity against NCI-H460 and neuro-2a cells with an LC_{50} value of approximately 15 μM. In addition, all three showed sodium channel-blocking activity at 5 μM, producing about half the response of saxitoxin applied at 0.15 μM [68].

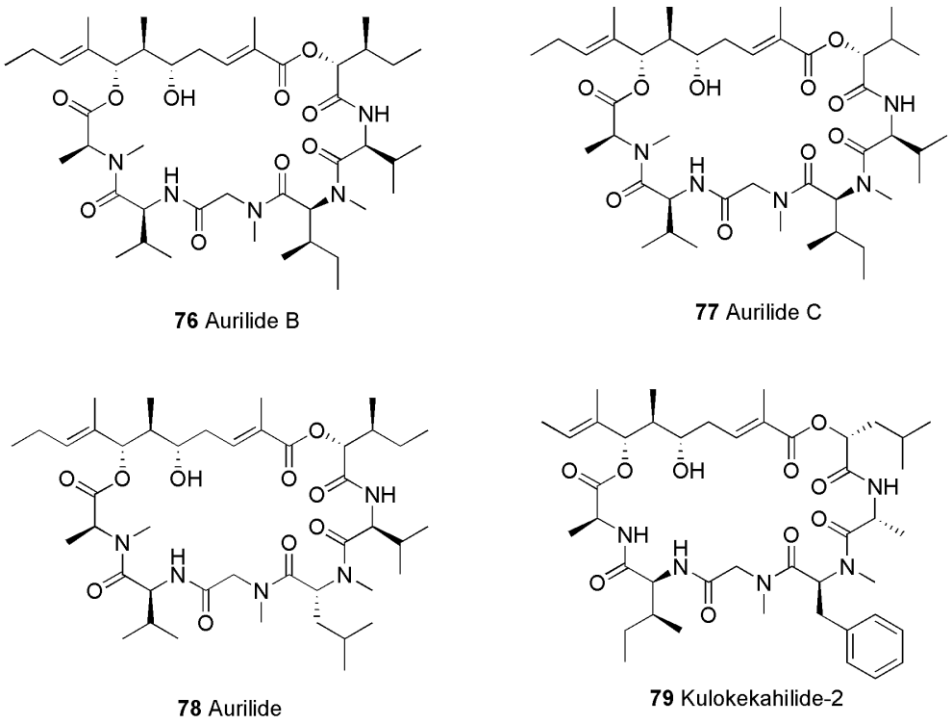

Figure 16. Structures of aurilides and kulokekahilide-2

Aurilides B (**76**) and C (**77**) (Figure 16) were isolated from a Papua New Guinea collection of *Lyngbya majuscula* [72]. Both compounds were closely related to aurilide (**78**, Figure 16), originally isolated from the sea hare *Dolabella auricularia* [183] The discovery of aurilides B and C further supported the cyanobacterial origin of aurilide [16]. Kulokekahilide-2 (**79**, Figure 16), derived from the sea hare *Philinopsis speciosa*, also shared structural similarities with the aurilides B and C, and its biosynthetic origin is likely from cyanobacteria [184]. Both aurilides B and C showed cytotoxicity against NCI-H460 and neuro-2a cells with LC_{50} values between 0.01 and 0.13 μM. Aurilide B was further evaluated in the NCI 60 cell line panel, and found to be highly cytotoxic with the mean GI_{50} value of less than 10 nM [72].

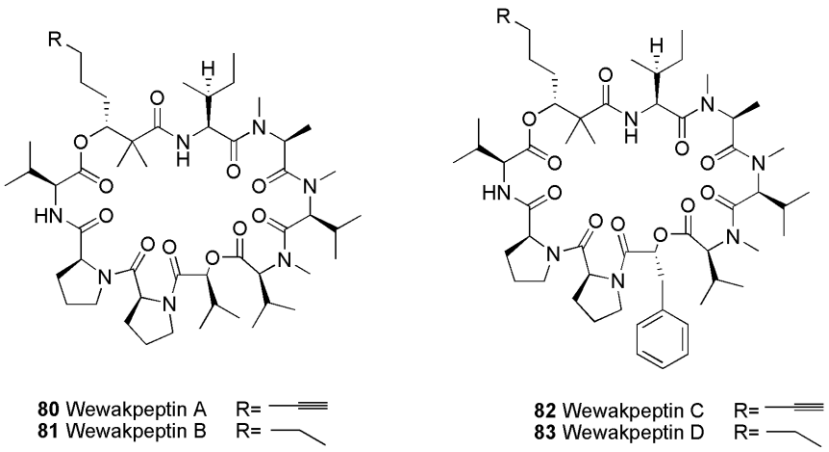

Figure 17. Structures of wewakpeptins

Wewakpeptins A-D (**80**-**83**, Figure 17), cyclic depsipeptides, were isolated from *Lyngbya semiplena* collected from Papua New Guinea [79]. The structures of wewakpeptins possessed a bis ester, 2,2-dimethyl-3-hydroxy-7-octynoic acid (Dhoya) or 2,2-dimethyl-3-hydroxyoctanoic acid (Dhoaa) residue, and a diprolyl group. Wewakpeptins A and B were found to be the most cytotoxic among these four depsipeptides with an LC_{50} value of approximately 0.4 μM against both the NCI-H460 and neuro-2a cells.

Grassypeptolide A (**84**, Figure 18), a bis-thiazoline containing cyclic depsipeptide, was isolated from *Lyngbya confervoides* collected in Florida Keys in 2008 [53]. The structure of grassypeptolide A contained a Maba moiety and 2-aminobutyric acid (Aba). The Maba moiety had also been observed in guineamide B (**49**) [75], while the Aba moiety had precedence only in sponge metabolites [185-187]. Furthermore, grassypeptolide A consisted of an unusually high number of D-amino acids and two thiazolines. The thiazoline rings flanking the D-Aba derived moiety were reminiscent of the lissoclinamides and the patellamides [188]. Grassypeptolide A displayed cytotoxicity against U2OS, HeLa, HT-29, and IMR-32 cells with IC_{50} values from 1.0 to 4.2 μM, while lissoclinamide 7 showed cytotoxicity with IC_{50} values ranging from 53.7 nM to 21.5 μM against T24, MRC5CV1, and normal lymphocytes [188, 189].

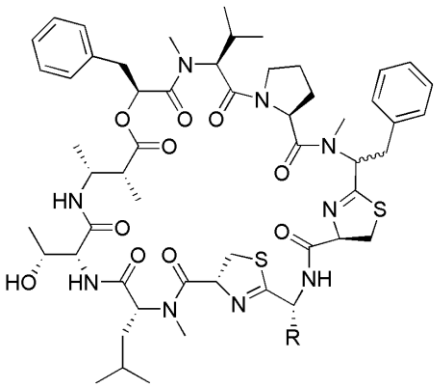

84 Grassypeptolide A R=CH_2CH_3, 28*R*
85 Grassypeptolide B R=CH_3, 28*R*
86 Grassypeptolide C R=CH_2CH_3, 28*S*
87 Grassypeptolide F R=CH_2CH_3, 28*R*
88 Grassypeptolide G R=CH_3, 28*R*

Figure 18. Structures of grassypeptolides

Grassypeptolides B (**85**) and C (**86**) were isolated along with grassypeptolide A (**84**) from a *Lyngbya confervoides* collected in Florida Keys in 2010 [190]. When compared to grassypeptolide A (**84**), replacement of the ethyl moiety by a methyl group in grassypeptolide B resulted in slightly reduced cytotoxicity (3−4-fold) while inversion of the Phe moiety to L-conformation in grassypeptolide C led to greater potency (16−23-fold). It was shown that grassypeptolides A and C arrested G1 phase cell cycle at lower concentrations, followed by G2/M phase arrest at higher concentrations. In addition, these two compounds demonstrated the ability to bind to metals such as Cu^{2+} and Zn^{2+}, and this was suggested as the potential mechanism of cytotoxicity.

Grassypeptolides F (**87**) and G (**88**) were isolated from *Lyngbya majuscula* collected from Palau [61]. The structural variations between grassypeptolides F and G and the grassypeptolides A-C were that Thr and *N*-Me-Leu in grassypeptolide A-C had been replaced by Val and *N*-Ne-Phe in grassypeptolides F and G. Both grassypeptolides F and G were found to moderately inhibit the activity of the transcription factor AP-1 with IC_{50} values of 5.2 and 6.0 μM.

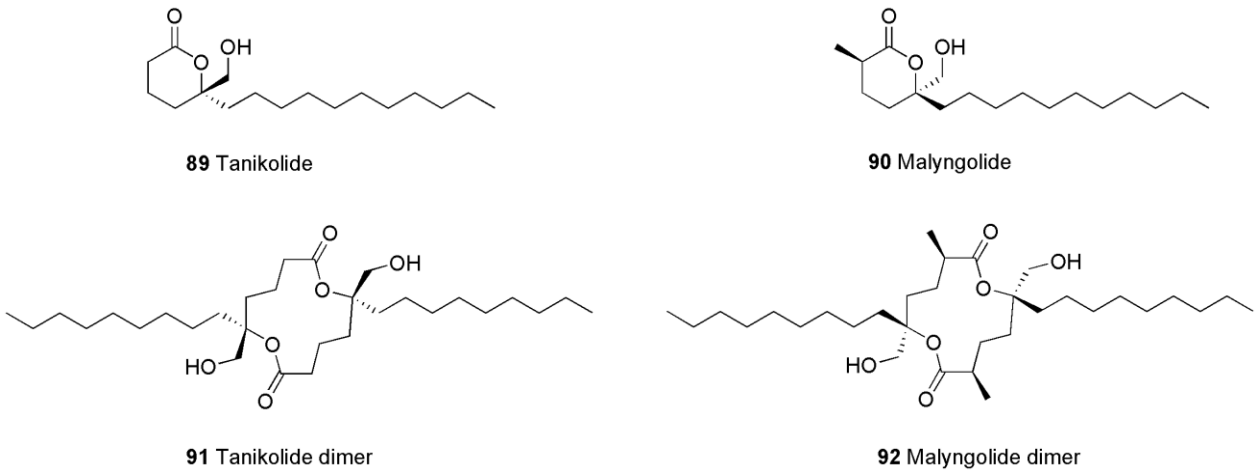

Figure 19. Structures of tanikolides and malyngolides

Tanikolide (**89**) and malyngolide (**90**) (Figure 19) were structurally related lactones obtained from *Lyngbya majuscula* [191, 192]. Both compounds possessed a β-hexalactone ring and an alkyl chain. In comparison with malyngolide, tanikolide lacked a methyl group at the lactone ring. Furthermore, the absolute configuration at C-5 was reversed. Tanikolide was toxic to brine shrimp toxicity (LC_{50} value of 10.1 μM). Dimer forms of the tanikolide and malyngolide (Figure 20) were later isolated from *L. majuscula* collected from Madagascar and Panama, respectively [69, 71]. Tanikolide dimer (**91**) was found to be a potent inhibitor of SIRT2 (NAD^+-dependent cytoplasmic sirtuin type 2), an HDAC-associated protein and a target for anticancer therapy, with IC_{50} values ranging from 176 nM to 2.4 μM [69]. Malyngolide dimer (**92**) exhibited cytotoxicity against NCI-H460 cells with an IC_{50} value of 9 μM as well as moderate antimalarial activity against chloroquine resistant *Plasmodium falciparum* (W2) [71]. Despite the significant structural similarity of two dimers, malyngolide dimer was inactive in SIRT2 assay.

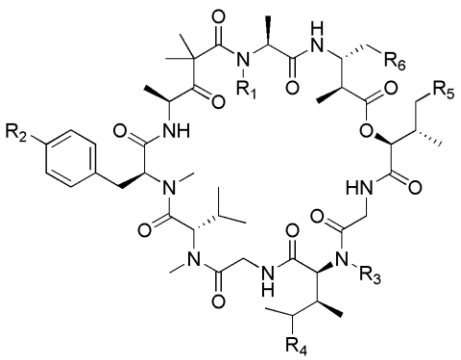

	R_1	R_2	R_3	R_4	R_5	R_6
93 Desmethoxymajusculamide C	H	H	CH_3	H	CH_3	H
94 Majusculamide C	H	OCH_3	CH_3	H	CH_3	H
95 57-Normajusculamide C	H	OCH_3	CH_3	H	H	H
96 Dolastatin 11	H	OCH_3	H	CH_3	CH_3	H
97 Dolastatin 12	CH_3	H	H	CH_3	CH_3	H
98 Lyngbyastatin 1	CH_3	OCH_3	H	CH_3	CH_3	H
99 Lyngbyastatin 3	CH_3	OCH_3	H	CH_3	CH_3	CH_3

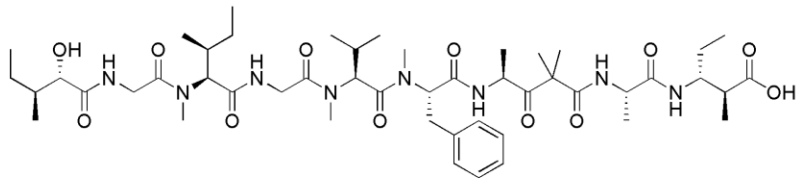

100 Linear hydrolysis form of desmethoxymajusculamide C

Figure 20. Structures of desmethoxymajusculamide C and related compounds

Desmethoxymajusculamide C (**93**, Figure 20), a cyclic depsipeptide, was isolated from a *Lyngbya majuscula* collected in Fiji [57]. The structure of desmethoxymajusculamide C was closely related to majusculamide C (**94**), 57-normajusculamide C (**95**), dolastatins 11 (**96**) and 12 (**97**), lyngbyastatins 1 (**98**) and 3 (**99**) [168, 171, 193-195]. There were five sites of variable *C*-, *N*-, and *O*-methylation, which gave rise to the metabolite diversity found in this structural class. Desmethoxymajusculamide C showed cytotoxicity against HCT-116 cells with an IC_{50} value of 20 nM. Interestingly, it was observed that the ring-opened, linear form of the desmethoxymajusculamide C (**100**) showed a similar level of cytotoxic activity against HCT-116 cells with an IC_{50} value of 16 nM. In addition, both cyclic and linear desmethoxymajusculamide C caused the complete loss of microfilament at 52 nM with dramatic changes in cell morphology in A-10 cells. At the same concentration, apoptosis and the breakdown of nuclei into apoptotic bodies were observed. It was presumed that the linear form of the molecule was as active as the cyclic form, since it adopted an active conformation similar to desmethoxymajusculamide C. Overall, this finding was discordant with the common point of view that the cyclic form is the bioactive form of the many peptides.

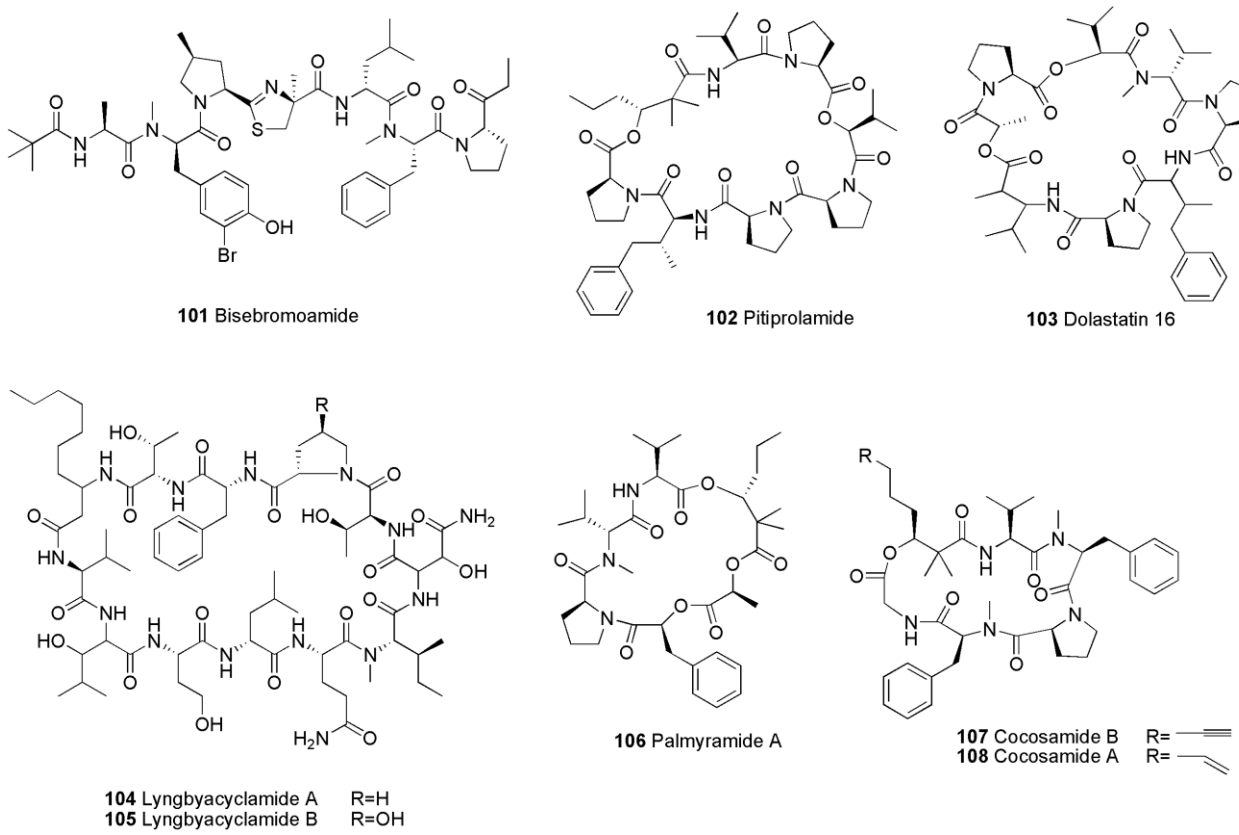

Figure 21. Structures of bisebromoamide, pitiprolamide, palmyramide A, lyngbyacyclamides, and cocosamides

Bisebromoamide (**101**, Figure 21), a linear peptide, was isolated from *Lyngbya* sp. collected in Okinawa [81]. The structure of bisebromoamide contained several unusual structural features, including a pivalic acid, a brominated tyrosine, a methylated proline, an α-methyl thiazoline ring, a D-leucine, and a 2-(2-oxo-propyl)pyrrolidine residue. Overall, the structure contained a high degree of D-amino acids and *N*-methylated amino acids along with modified amino acids of nonribosomal origin [81, 196]. Bisebromoamide exhibited cytotoxicity against a panel of 39 human cancer cells (JFCR39) at the Japanese Foundation for Cancer Research with the average GI_{50} value of 40 nM. Furthermore, it showed cytotoxicity against HeLa S3 cells with an IC_{50} value of 40 nM. In addition, it selectively inhibited the phosphorylation of ERK (extracellular signal regulated protein kinase) in NRK cells by PDFG (platelet-derived growth factor)-stimulation at 0.1-10 μM.

Investigation of a Guamanian *Lyngbya majuscula* led to the isolation of a cyclic peptide, pitiprolamide (**102**, Figure 21) [65]. The pitiprolamide had four proline moieties, corresponding to 50% of its amino acid residues, and the structure was related to dolastatin 16 (**103**) [197]. The structure of pitiprolamide also contained a Dmhha residue, which had previously been reported from guineamides E and F [75], and palmyramide A [70]. Pitiprolamide showed weak cytotoxicity against HCT116 and MCF-7 cells with an IC_{50} value of 33 μM.

Lyngbyacyclamides A (**104**) and B (**105**) (Figure 21) were isolated from a *Lyngbya* sp. collected in Okinawa [82]. The structures resembled those of laxaphycin B (**110**, Figure 22) [45] and lobocyclamide C [198]. Both lyngbyacyclamides A and B showed cytotoxicity against B16 mouse melanoma cells with IC_{50} values of 0.7 μM.

Palmyramide A (**106**, Figure 21) was isolated from a *Lyngbya majuscula* collected from Palmyra Atoll [70]. Palmyramide A contained three amino acids and three hydroxy acids as well as a Dmhha unit [75]. Palmyramide A showed weak cytotoxicity against NCI-H460 cells with an IC_{50} value of 39.7 μM. In addition, it was found to blocke the voltage gated sodium channel in neuro-2a cells.

Cocosamides A (**107**) and B (**108**) (Figure 21), cyclic depsipeptides, were isolated from Guamanian *Lyngbya majuscula*, along with malyngamide 3 [60]. The structures of cocosamides possessed 2,2-dimethyl-3-hydroxy-7-octenoic acid (Dhoea) and 2,2-dimethyl-3-hydroxy-7-octynoic acid (Dhoya) moieties, and were closely related to pitipeptolide A [60, 64]. Cocosamides A and B exhibited cytotoxicity against HT-29 cells with IC_{50} values of 24 and 11 μM, respectively. MCF-7 cells were slightly less susceptible to both compounds with IC_{50} values of 30 and 39 μM, respectively.

2.2.3 *Anabaena*

Laxaphycins A (**109**) and B (**110**) (Figure 22), cyclic lipopeptides, were obtained from both the terrestrial cyanobacterium *Anabaena laxa* [105, 106] and the tropic marine cyanobacterium *Anabaena torulosa* [199]. Both compounds have also been reported from an assemblage of 80% *Lyngbya majuscula* together with *Anabaena* sp. and *Oscillatoria* sp. [45]. Due to the high rate of *L. majuscula* in this assemblage and the high concentration of laxaphycins purified, it was suggested that *L. majuscula* was the source of the compounds [105, 106]. Laxaphycins A and B were co-produced by the same strain of the cyanobacterium, though structurally different. Laxaphycin A was a cyclic undecapeptide containing a 3-

aminooctanoic acid (Aoc) moiety, and laxaphycin B was a cyclic dodecapeptide containing a 3-aminodecanoid acid (Ade) residue. Laxaphycin A exhibited a weak antiproliferative effect on leukemia and solid cancer cells [199] however, it potentiated the anticancer effect of laxaphycin B on sensitive and resistant cancer cells. This synergistic effect was also observed in an antifungal assay [200].

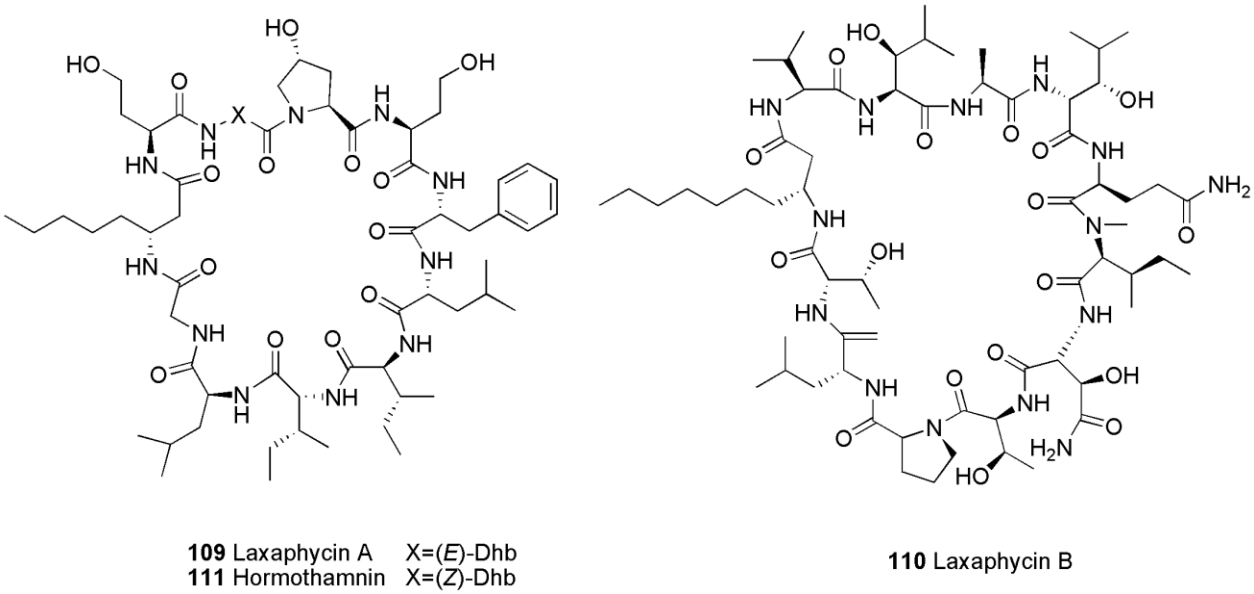

109 Laxaphycin A X=(*E*)-Dhb
111 Hormothamnin X=(*Z*)-Dhb

110 Laxaphycin B

Figure 22. Structures of laxaphycins and hormothamnin A

2.2.4 *Hormothamnion enteromorphoides*

Hormothamnin A (**111**, Figure 22), an cyclic undecapeptide, was isolated from the marine cyanobacterium *Hormothamnion enteromorphoides* [48]. The structure of hormothamnin A was similar to that of the laxaphycin A, except for configuration of Dhb residue. Hormothamnin A exhibited cytotoxicity against a variety of solid cancer cells, while laxaphycin A showed weak cytotoxicity. Thus, it was presumed that the configuration of the Dhb accounted for the cytotoxic activity observed for hormothamnin A.

2.2.5 *Synechocystis*

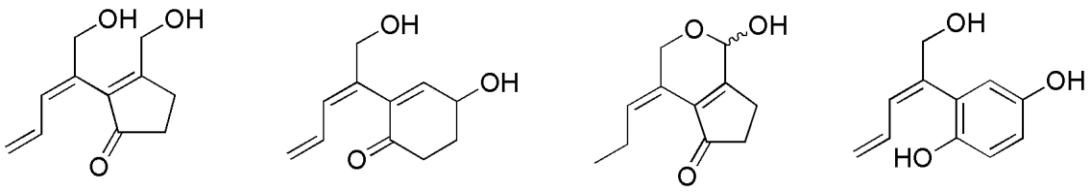

112 Nakienones A **113** Nakienones B **114** Nakienones C **115** Nakitriol

Figure 23. Structures of nakienones and nakitriol

Nakienone A (**112**, Figure 23) was isolated along with nakienones B (**113**) and C (**114**) and nakitriol (**115**) (Figure 23) from a dead coral, *Acropora* sp., which was completely covered with the cyanobacterium *Synechocystis* sp. [103]. Nakienone A was found to be cytotoxic against both KB and HCT-116 cells with IC_{50} values of 25 and 103 μM, respectively. Nakitriol was found to be non-selectively cytotoxic to EM9, XRS-6, UV20, and BR1 cells with an IC_{50} value of 103 μM.

2.2.6 *Geitlerineama*

Ankaraholides A (**116**) and B (**117**) (Figure 24) were isolated from a Madagascan *Geitlerinema* sp. along with swinholide A (**118**) [92]. The structures of ankaraholides A and B represented glycosylated forms of the swinholides. Ankaraholide A inhibited proliferation of NCI-H460, neuro-2a and MDA-MB-435 cells with IC_{50} values of 119, 262, and 8.9 nM, respectively. Furthermore, both ankaraholides A and B caused complete loss of the filamentous (F)-actin in A-10 cells at 30 and 60 nM, respectively, with dramatic changes in cell morphology. The biological activity of ankaraholide A was comparable to that of swinholide A, suggesting that the additional sugar moieties in ankaraholide A were not essential for its biological properties.

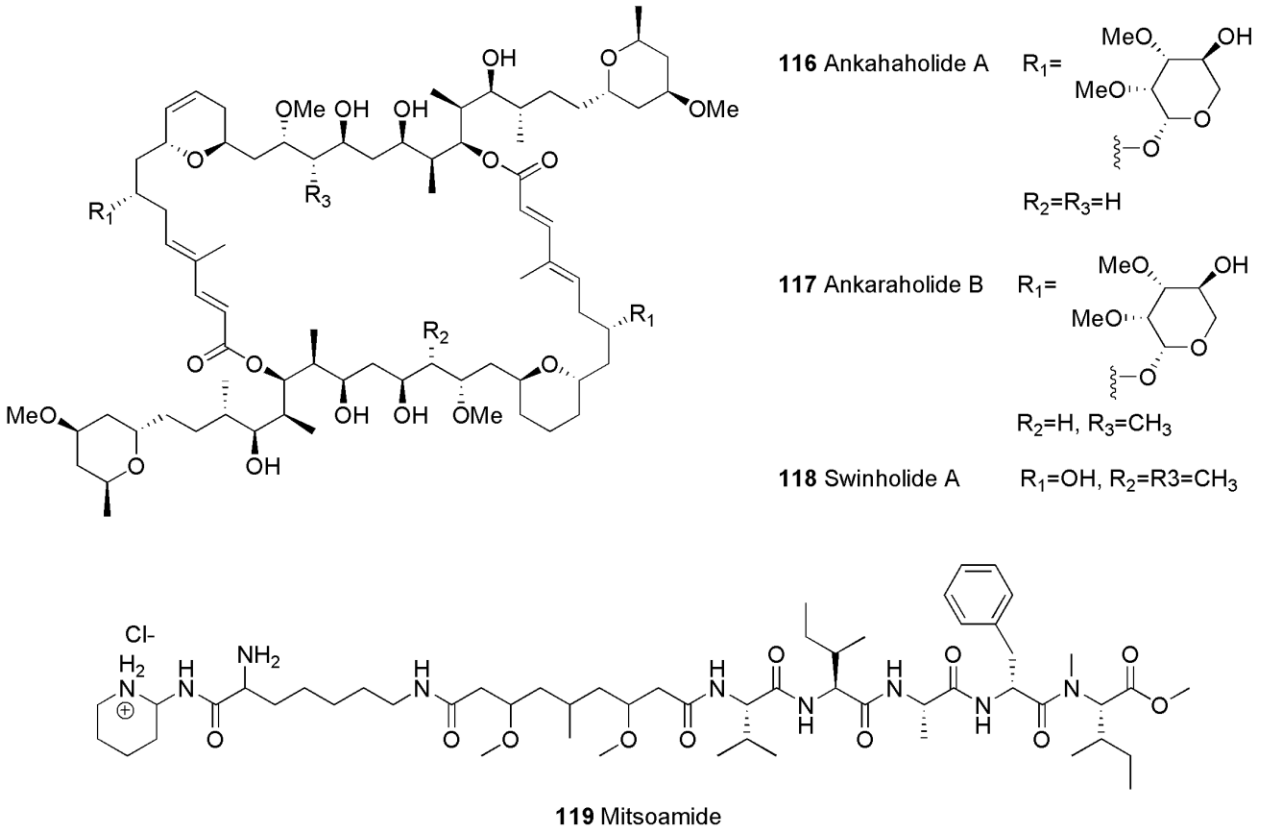

Figure 24. Structures of ankaraholides, swinholide A, and mitsoamide

Swinholide A (**118**, Figure 24), an asymmetric 44-membered dilactone ring macrolide, was originally isolated from the marine sponge *Theonella swinhoei* [47]. It had been suggested that symbiotic microorganisms were the true producers, since swinholides were produced by three taxonomically unrelated sponges [92]. Indeed, swinholide A was later isolated from *Symploca* cf. sp. collected from Fiji [92]. Swinholide A showed cytotoxicity against L1210 and KB cells with IC_{50} values of 0.04 and 0.05 μM, respectively [201]. The cytotoxic effects were exerted by disruption of the actin cytoskeleton [202].

Mitsoamide (**119**, Figure 24), a linear lipopeptide, was isolated from *Geitlerinema* sp. collected from Madagascar [46]. The structure of mitsoamide contained a 3,7-dimethoxy-5-methyl-nonanedioic acid (DMNA), a piperidine aminal moiety, and a homolysine. The central polyketide portion of the structure had amide linkages to amino acids at both termini, inconsistent with the established pathways for mixed NRPS/PKS pathways [46, 203]. Mitsoamide exhibited cytotoxicity against NCI-H460 cells with a LC_{50} value of 460 nM.

2.2.7 *Leptolyngbya*

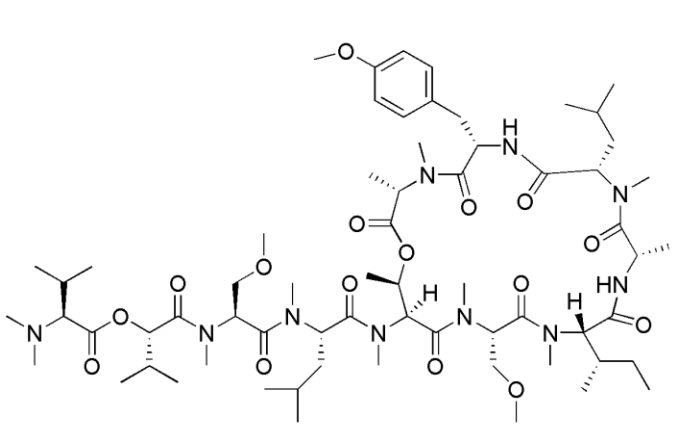

120 Coibamide A

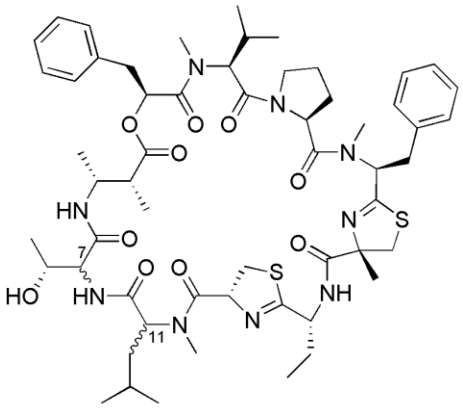

121 Grassypeptolide D 7*R*, 11*R*
122 Grassypeptolide E 7*S*, 11*S*

Figure 25. Structures of coibamide A and grassypeptolides D and E

Coibamide A (**120**, Figure 25), a cyclic depsipeptide, was isolated from *Leptolyngbya* sp. collected in Panama [49]. The structure of coibamide A contained a linear section ending with an *N*,*N*-dimethyl valine at the amino terminus, and showed a high level of *N*- and *O*-methylation. Coibamide A displayed potent cytotoxicity against NCI-H460 and neuro-2a cells with LC_{50} values of less than 23 nM. However, it did not interfere with tubulin or actin in cytoskeletal assays. It was shown that coibamide A had the highest potency against MDA-MB-231, LOXIMVI, HL-60 (TB), and SNB-75 cells with GI_{50} values of 2.8, 7.4, 7.4, and 7.6 nM, respectively. In addition, coibamide A was COMPARE negative [204], indicating that it likely inhibited cancer cell proliferation via a novel mechanism [49].

Grassypeptolides D (**121**) and E (**122**) (Figure 25) were isolated along with dolastatin 12 (**99**) from *Leptolyngbya* sp. collected in the Red Sea [50]. The structures of these compounds were closely related to that of grassypeptolide C (**86**, Figure 18). Both grassypeptolides D and E showed cytotoxicity against HeLa cell (IC_{50} values of 335 and 192 nM, respectively) and mouse neuro-2a blastoma cells (IC_{50} values of 599 and 407 nM, respectively).

2.2.8 *Oscillatoria*

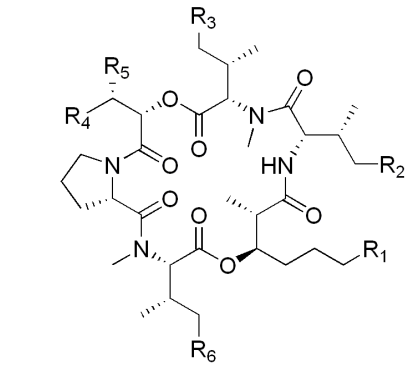

Veraguamides		R_1	R_2	R_3	R_4	R_5	R_6
123	A	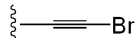	H	H	Et	Me	H
124	B	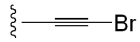	H	H	Me	Me	H
125	C		H	H	Et	Me	H
126	D		H	H	Et	Me	Me
127	E		Me	Me	Et	Me	H
128	F		H	H	Ph	H	H
128	G		H	H	Et	Me	H
130	H		H	H	Me	Me	H
131	I	Et	H	H	Et	Me	H
132	J	Et	H	H	Me	Me	H

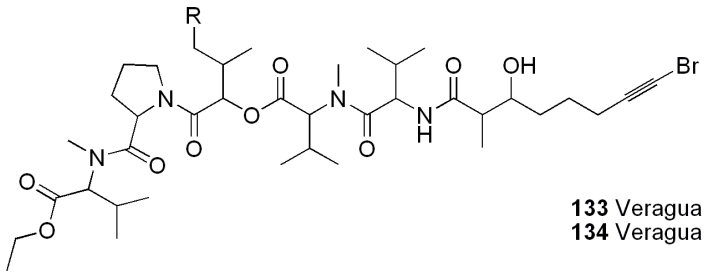

133 Veraguamide K R=Me
134 Veraguamide L R=H

Figure 26. Structures of veraguamides

Veraguamides A-C (**123**-**125**) and H-L (**130**-**134**) (Figure 26), cyclic depsipeptides, were isolated from *cf. Oscillatoria margaritifera* collected from the Coiba National park, Panama [89]. A parallel effort from a Guamanian *Symploca* cf. *hydnoides* led to the isolation of veraguamides A-C as well as several new derivatives D-G (**126**-**129**) [91]. The structures of veraguamides were characterized by the presence of an invariant proline residue, multiple *N*-methylated amino acids, an α-hydroxy acid, and a C_8-polyketide-derived β-hydroxy acid moiety with a characteristic terminus of either an alkynyl bromide, alkyne, or vinyl group. Veraguamide A, the major component, showed cytotoxic activity against NCI-H460 cells with a LD_{50} value of 141 nM, while veraguamides B, C, K, and L exhibited cytotoxicity in the low micromolar range.

Biological activities of veraguamides H-I could not be determined due to insufficient quantities [89]. Veraguamides A-G showed moderate to weak cytotoxicity against HT-29 and HeLa cells [91].

2.2.9 Mixed assemblage

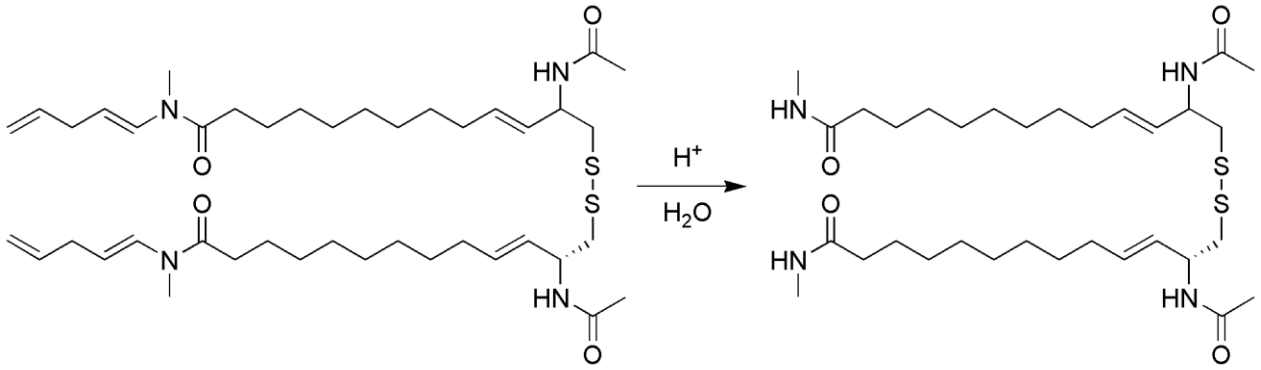

135 Somocystinamide A

Acid treated-derivative

Figure 27. Structures of somocystinamide A and the acid treated derivative

Somocystinamide A (**135**, Figure 27), an unusual disulfide dimer, was isolated from a mixed assemblage of *Lyngbya majuscula* and *Schizothrix* sp. collected in Fiji [88]. Somocystinamide A was highly sensitive to acidic conditions, and rapidly converted to a structurally simplified derivative (Figure 27). The original form of the compound exhibited cytotoxicity against neuro-2a cells with an IC_{50} value of 1.8 μM [88]. Somocystinamide A was identified as a pluripotent inhibitor of angiogenesis as well as tumor cell proliferation, and the latter was largely attributed to induction of programmed cell death pathways [205]. In detail, the molecule initiated apoptosis via both the intrinsic and extrinsic pathways although the more sensitive pathway involved activation of caspase 8. Somocystinamide A selectively activated the caspase 8 pathway at low nanomolar concentration, which altered the cell membrane and caused apoptosis [205]. The molecule also induced cell death via caspase-8-independent pathways in micromolar concentrations. The acid-derivative decomposition product of somocystinamide A, on the other hand, was not biologically active [88].

2.3 Cytotoxic secondary metabolites from freshwater/terrestrial cyanobacteria

2.3.1 Order Nostocales

2.3.1.1 *Anabaena affinis*

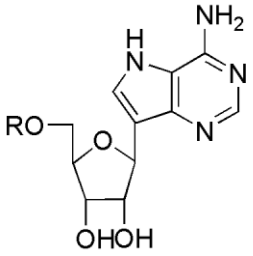

136 9-Deazaadenosine R=H
137 9-Deazaadenosine 5'-α-D-glucopyranoside R=Glucose

Figure 28. Structures of the cytotoxic compounds from *Anabaena affinis*

9-Deazaadenosine (**136**) and its glucopyranose analogue (**137**) (Figure 28) were isolated from a cultured *Anabaena affinis* VS-1, obtained from a water-bloom sample collected from Star Lake, Norwich, VT [104]. These compounds were the first reported naturally occurring pyrrolo[3,2-d]pyrimidine derivatives. Both 9-deazaadenosine and its 5'-α-D-glycopyranoside showed cytotoxicity against L1210 cells with IC_{50} values of 0.02 and 0.007 μM, respectively. In addition, long treatment of 9-deazaadenosine resulted in inhibitions of RNA, DNA, and protein synthesis. The mechanism of action for this compound was suggested as a translation inhibitor via its incorporation into RNA [206].

2.3.1.2 *Scytonema*

Scytonemin (**138**, Figure 29), a yellow-brown sunscreen pigment, which occurs predominantly in the extracellular sheaths of many cyanobacteria [207]. Nearly 300 cyanobacterial species have been described with yellow to brown sheaths in Geitler's monograph and more than 30 cyanobacteria species have been found to contain the scytonemin [207]. The characteristic absorption maximum of scytonemin was in the spectral region 325-425 nm (UV-A), 250 nm (UV-B), and 280-320 nm (UV-C) [208] and was

shown that scytonemin provides significant protection to cyanobacteria against UV damage. The structure of scytonemin was composed of indolic and phenolic subunits, and derived from condensation of a L-tryptophan and a 3-indole pyruvic acid, followed by coupling to *p*-hydroxyphenylpyruvic acid. Scytonemin inhibited human *polo*-like kinase, a serine/threonine kinase involved in regulating the G_2/M cell cycle [209].

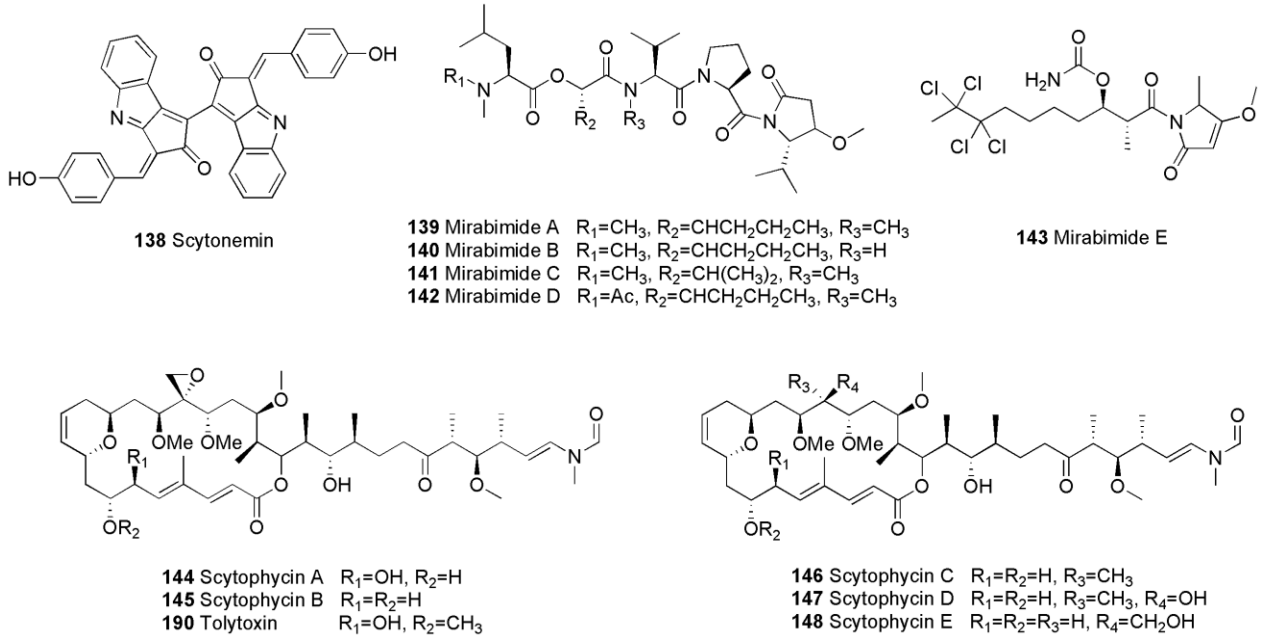

Figure 29. Structures of the cytotoxic compounds from the genus *Scytonema*

Mirabimides A-E (**139**-**143**, Figure 29), *N*-acylpyrrolinones, were isolated from a cultured cyanobacterium *Scytonema mirabile* (Dilwyn) Bornet (BY-8-1), collected from Mr. Tantalus, Oahu, HI [122, 175]. Mirabimide E was structurally and pharmacologically interesting in that it contained a tetrachlorinated ethylene moiety, and showed solid tumor selectivity against L1210, colon adenocarcinoma 38, colon CX-1, and LML cells with zones of inhibition of 300-430, 800, 330, and 400 zone units (200 zone units = 6 mm), respectively, at 5 µg/disk.

Scytophycins A-E (**144**-**148**, Figure 29), polyketide-derived macrolides, were isolated from cultured terrestrial cyanobacteria *Scytonema pseudohofmanni* Bharadwaja BC-1-2 and ATCC 53141 [210, 211]. These compounds were structurally related to tolytoxin (**190**) and biogenetically related to the marine natural products swinholide A (**118**, Figure 24), ulapualides A and B, and kabiramide C [211]. Scytophycins A and B showed cytotoxicity against KB cells with an IC_{50} value of 1.2 μM and both showed moderate activity against P-388 and B16 cells intraperitoneally implanted in mice. These compounds also displayed strong antifungal activity against some phytopathogenic fungi. Scytophycins C-E were found to be less cytotoxic and less fungicidal.

2.3.1.3 *Cylindrospermum*

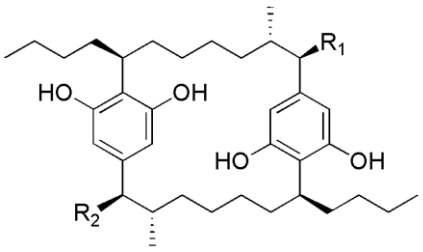

149 Cylindrocyclophane A $R_1=R_2=OH$
150 Cylindrocyclophane B $R_1=OH$, $R_2=OAc$
151 Cylindrocyclophane C $R_1=OH$, $R_2=H$
152 Cylindrocyclophane D $R_1=R_2=OAc$
153 Cylindrocyclophane E $R_1=OAc$, $R_2=H$
154 Cylindrocyclophane F $R_1=R_2=H$

Figure 30. Structures of the cytotoxic compounds from the genus *Cylindrospermum*

Cylindrocyclophane A (**149**, Figure 30), a [7.7]paracyclophane, was isolated from *Cylindrospermum licheniforme* Küzing [109]. Cylindrocyclophanes B-F (**150**-**154**) were later isolated from *C. licheniforme* ATCC 29204, ATCC 29412, and UTEX 2014 [212]. The ATCC 29204 strain produced cylindrocyclophanes B-D along with cylindrocyclophane A, while ATCC 29412 and UTEX 2014 produced cylindrocyclophanes D-F as the major components. All of these cylindrocyclophanes exhibited cytotoxicity with IC_{50} values ranging from 0.8 to 8.0 μM, but none showed selectivity toward murine or human solid tumor cells in the Corbett assay.

2.3.1.4 *Nostoc*

6-Cyano-5-methoxy-12-methylindolo[2,3,-a]carbazole (**155**, Figure 31) was isolated from a cultured *Nostoc sphaericum* EX-5-1, obtained from a mud sample collected at the University of Hawaii [121]. The structure of the heterocyclic indolo[2,3-a]carbazole system has also been found in metabolites isolated from other organisms such as in staurosporine from *Streptomyces staurosporeus* [213], in acriflavins from *Arcyria denudate* [214], and rebeccamycin from *Nocardia aerocoligenes* [215]. Compound **155** showed cytotoxicity against KB and LoVo cells with a MIC value of 15.4 μM and antiviral activity against herpes simplex type 2.

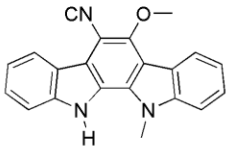

155 6-Cyano-5-mehoxy-12-methylindolo[2,3,-a]carbazole

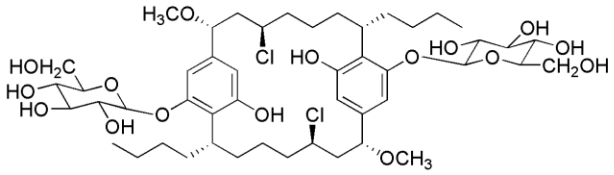

156 Nostocyclophane A

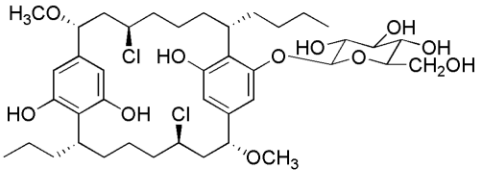

157 Nostocyclophane B

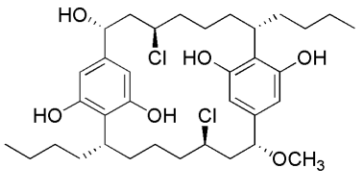

158 Nostocyclophane C

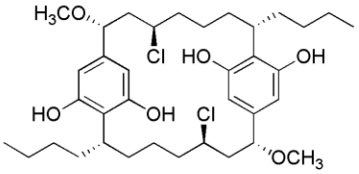

159 Nostocyclophane D

Figure 31. Structures of the cytotoxic compounds from the genus *Nostoc*

Nostocyclophanes A-D (**156**-**159**, Figure 31), chlorine-containing [7.7]paracyclophanes, were isolated from *Nostoc linckia* (Roth) Bornet ex Bornet & Flahault (UTEX B1932) [112]. Nostocyclophane D displayed cytotoxicity against KB and LoVo cells with an IC_{50} value of 0.77 μM. Nostocyclophanes A-C, minor compounds, displayed cytotoxicity against KB and LoVo cells with IC_{50} values ranging from 1.5 to 3.0 μM.

Cryptophycin 1 (**160**, Figure 32), a cyclic depsipeptide, was isolated from a cultured *Nostoc* sp. (ATCC 53789) [116]. It was initially identified as an antifungal compound [216], but later found to be

cytotoxic against KB, LoVo, and SKOV3 cells with IC_{50} values of 9.2, 10, and 20 pM, respectively [37]. Cryptophycin 1 and over 25 cryptophycin analogues have been obtained from the cultured *Nostoc* sp. (GSV 224) [119, 217-219]. These structures had different patterns of chlorination (none-, mono-, and di-) on the tyrosine residue and different absolute configurations of the α-carbon on the tyrosine ring as well as of the epoxide. The structural differences also included the presence or absence of a 2-methyl as well as double bond substitution [37]. Cryptophycin 52 (**161**, LY355703, Figure 25), a synthetic derivative of cryptophycin 1, was structurally closely related to that of cryptophycin 1 and only contained an additional methyl group. Both cryptophycin 1 and 52 inhibited the polymerization of microtubules, and cryptophycin 52 was the most potent suppressor of microtubule dynamics studied to date [220]. The high level of toxicity of cryptophycin 52 eventually led to the termination of clinical trials. However, cryptophycin is still a lead compound and synthetic efforts are continuing.

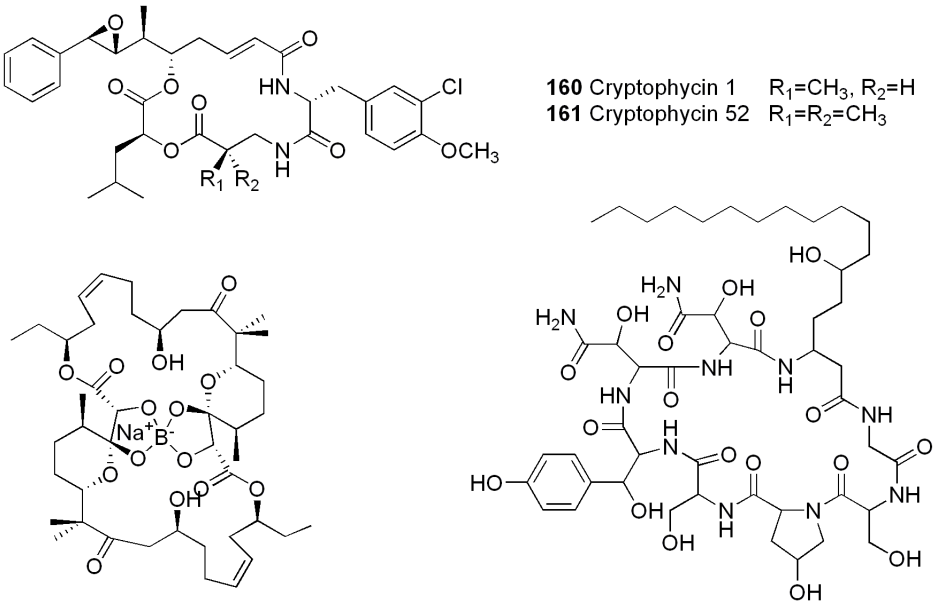

Figure 32. Structures of the cytotoxic compounds from the genus *Nostoc*

Borophycin (**162**, Figure 32), a boron-containing metabolite, was isolated from a cyanobacterium *Nostoc linckia* (Roth) Bornet ex Bornet & Flahault (UH isolate GA-5-23) [113]. The structure of borophycin

was composed of two identical halves, and the overall structure was similar to those of boromycin [221] and aplasmomycin [222]. However, the biosynthesis of borophycin differed from those of boromycin and aplasmomycin in that borophycin was derived from acetate and methionine as a starter unit, not from propionate [113]. Borophycin was found to be cytotoxic against LoVo and KB cells with MIC values of 0.077 and 3.9 μM, respectively.

Nostofungicidine (**163**, Figure 32), a cyclic lipopeptide, was isolated from a field-collected terrestrial *Nostoc commune*, obtained on the campus of Okayama University [111]. The structure of nostofungicidine contained a β-amino acid, 3-amino-6-hydroxy stearic acid (Ahs), and was the first report of Ahs in natural product. Furthermore, it contained β-hydroxy-α-amino acids, which had previously been found in antifungal cyclic peptides such as pneumocandins [223] and xylocandins [224]. Long chain α-hydroxy-β-amino acids found in the structure of nostofungicidine had also been found in other cyanobacterial metabolites such as calophycin (**187**, Figure 34) [107], puwainaphycins [225], and microginin [226]. Nostofungicidine showed cytotoxicity against NSF-60 cells with an IC_{50} value of 1.5 μM and antifungal activity against *Aspergillus candidus* with an MIC value of 1.5 μM.

Nostophycin (**164**, Figure 33), a 22-membered cyclic peptide, was isolated from a cultured *Nostoc* sp. strain 152, along with hepatotoxic microcystins [115]. The structure of nostophycin was composed of seven amino acid moieties including a β-amino acid 3-amino-2,5-dihydroxy-8-phenyloctanoic acid (Ahoa) and two D-amino acids, D-glutamine and D-*allo*-isoleucine. These amino acids were also observed in the microcystins, and it was assumed that biosynthetic pathways of these compounds were closely related [115]. Nostophycin exhibited 40% growth inhibition against L1210 cells at 11 μM, while it did not show any activity against a wide spectrum of bacteria and fungi.

Comnostins A-E (**164**-**169**, Figure 33), diterpenoids, were isolated from a cultured terrestrial cyanobacterium *Nostoc commune* (EAWAG 122b) [110]. The occurrence of diterpenoids in cyanobacteria is rare, and only few have been reported including tolypodiol from *Tolypothrix nodosa* [227] and noscomin (**325**, Figure 57) from *Nostoc commune* (EAWAG 122b) [228]. Comnostin B exhibited cytotoxicity against KB and Caco-2 cells with MIC values of 1.22 and 0.42 μM, respectively, while comnostins A-E displayed moderate antibacterial activity against *Escherichia coli*, *Staphylococcus epidermidis*, and *Bacillus cereus*.

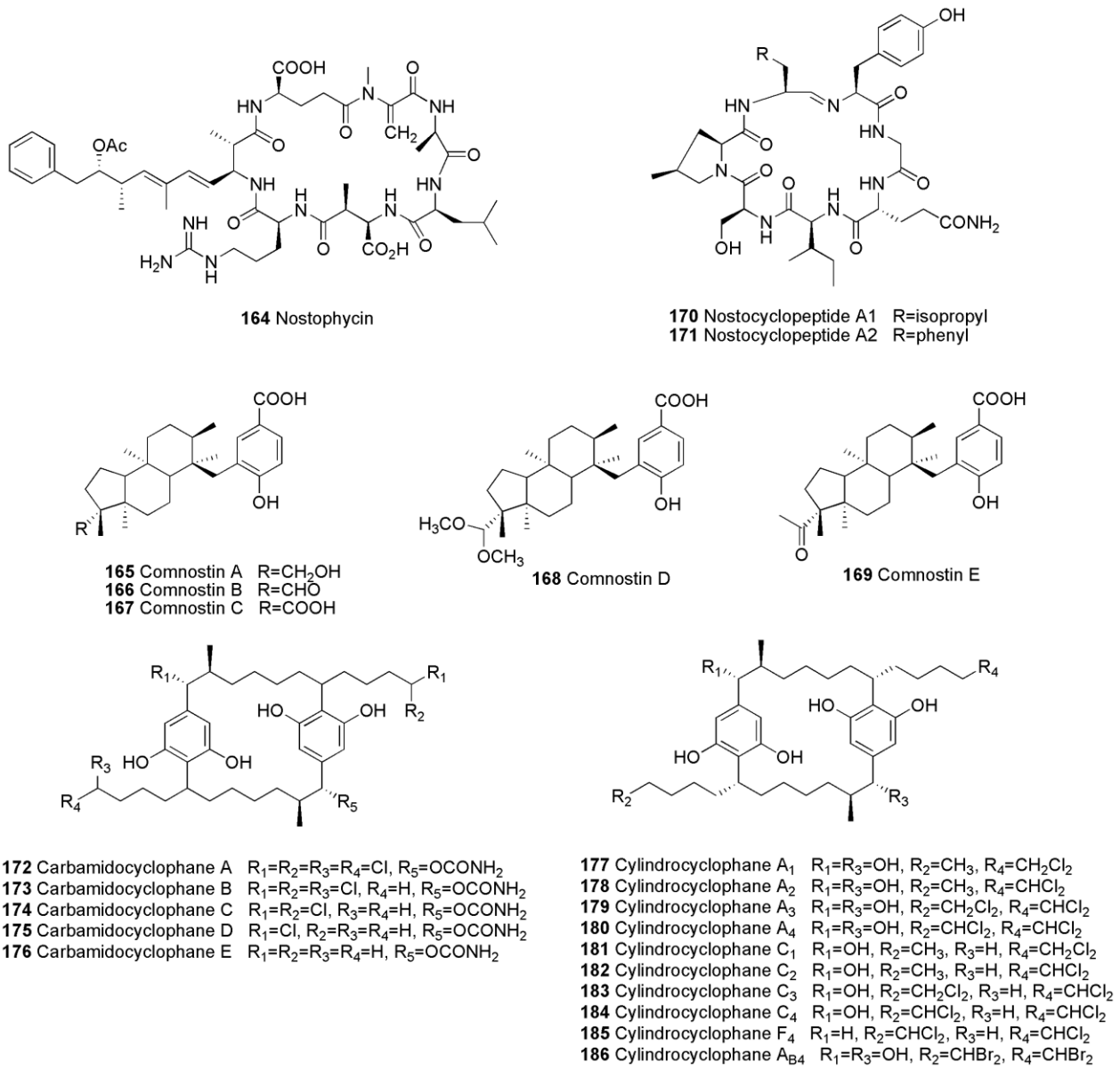

Figure 33. Structures of the cytotoxic compounds from the genus *Nostoc*

Nostocyclopeptides A1 (**170**) and A2 (**171**) (Figure 33), cyclic heptapeptides, were also isolated from the cryptophycin-producing *Nostoc* sp. (ATCC 53789) [117]. Both *Nostoc* sp. ATCC 53789 and *Nostoc* sp. GSV 224 displayed similar HPLC spectra, indicating the presence of cryptophycins. However, the 16S rRNA gene analysis indicated that there was a 2.8% homology difference between the two species [117]. Furthermore, both species were genetically different in that the genes that encoded for the biosynthesis of nostopeptolides (**305**-**307**, Figure 55) were present in GSV 224, but not in ATCC 53789.

Conversely, nostocyclopeptides were produced by ATCC 53789, but not by GSV 224. The structures of these nostocyclopeptides contained a unique imino linkage in the macrocyclic ring. The nostocyclopeptides A1 and A2 displayed cytotoxicity against KB and LoVo cells with an average IC_{50} value of 1 μM. No antifungal and antibacterial activities were observed. Neither of compound showed inhibition of proteases such as trypsin, thrombin, plasmin, chymotrypsin, elastase, and papain.

Carbamidocyclophanes A-E (**172**-**176**, Figure 33) were isolated from a cultured *Nostoc* sp. CAVN 10, obtained from a soil sample collected in Northern Vietnam [118]. The structures of carbamidocyclophanes were different from those of cylindrocyclophanes (**149**-**154**) previously obtained from *Cylindrospermum licheniforme* in that carbamidocyclophanes possessed carbamido substituents at the 1,14-positions. All of the carbamidocyclophanes contained at least one chlorine moiety except carbamidocyclophane E. Carbamidocyclophanes A-C showed cytotoxicity against FI and MCF-7 cells with IC_{50} values ranging from 0.86 and 5.1 μM. The MIC values of these compounds against *Staphylococcus aureus* ATCC 6538 were determined as 0.1, 0.04, and 0.06 mM, respectively.

Cylindrocyclophanes A_1-A_4 (**177**-**180**), C_1-C_4 (**181**-**184**), and F_4 (**185**) (Figure 33) along with cylindrocyclophanes A (**149**), C (**151**), and F (**154**) were isolated from a cultured cyanobacterium *Nostoc* sp. UIC 10022A obtained from a soil sample collected from Chicago, Illinois [120]. Several of the compounds showed cytotoxicity against HT-29 cells with IC_{50} values ranging from 0.9 to 2.8 μM as well as inhibition of 20S proteasome. Cylindrocyclophane A_{B4} (**186**) was a semi synthetic analogue obtained by the incorporation of bromine. Both cylindrocyclophanes A_4 and A_{B4} showed similar level of cytotoxicity against HT-29 cells.

2.3.1.5 *Calothrix*

Calophycin (**187**, Figure 34), a cyclic decapeptide, was isolated from a cultured *Calothrix fusca* (Kützing) Bornet & Flahault EU-10-1, obtained from a sample collected from a pond in an abandoned irrigation canal, Waimano Stream, Oahu [107]. The structure of calophycin contained nine α-amino acids, a *N*-methylated amino acid, prolyl, and valyl moieties. It also contained a β-amino acid 3-amino-2-hydroxy-4-methylpalmitoyl (Hamp), which was also present in puwainaphycin E isolated from *Anabaena* sp. BQ-16-1 [229, 230]. Calophycin showed cytotoxicity against KB cells with an IC_{50} value of 0.2 μM.

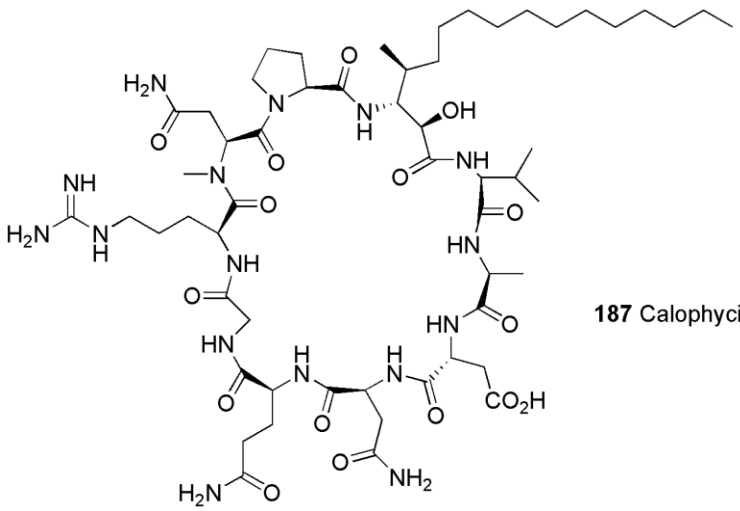

187 Calophycin

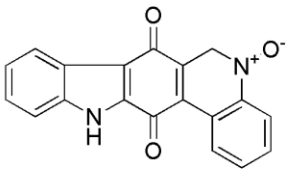

188 Calothrixin A
189 Calothrixin B N5-deoxy

Figure 34. Structures of the cytotoxic compounds from the genus *Calothrix*

Calothrixins A (**188**) and B (**189**) (Figure 34), indolo[3,2-j]phenanthridine alkaloids, were isolated from a cultured *Calothrix* sp. CAN 95/2, obtained from the sample collected in the Australian Capital Territory [108]. The structure of calothrixins A and B was a fused pentacyclic ring system containing both indole and quinoline portions. Calothrixin A was found to be relatively insoluble, while calothrixin B was more soluble. Both compounds showed growth inhibition of the chloroquine-resistant strain of *Plasmodium falciparum* at nanomolar concentrations. However, both compounds also showed cytotoxicity against HeLa cells with IC_{50} values of 20 and 350 nM, respectively.

2.3.1.6 *Tolypothrix*

Tolytoxin (**190**, Figure 31), a macrocyclic lactone, was first isolated from a culture of the terrestrial cyanobacterium *Tolypothrix conglutinate* var. *colorata* Ghose, collected from Fanning Island. It was later isolated along with 6-hydroxyscytophycin B, 19-*O*-demethylscytophycin C, and 6-hydroxy-7-*O*-methylscytophycin E from *Scytonema mirabile*, *Scytonema burmanicum* Skuja, and *Scytonema ocellatum* (DD-8-1, FF-65-1, and FF-66-3) [125]. The structure of tolytoxin was closely related to the scytophycin class of compounds and it was found to be 6-hydroxy-7-*O*-methylscytophycin B. Tolytoxin showed cytotoxicity against several human cells with IC_{50} values ranging from 0.52 to 8.4 nM [231].

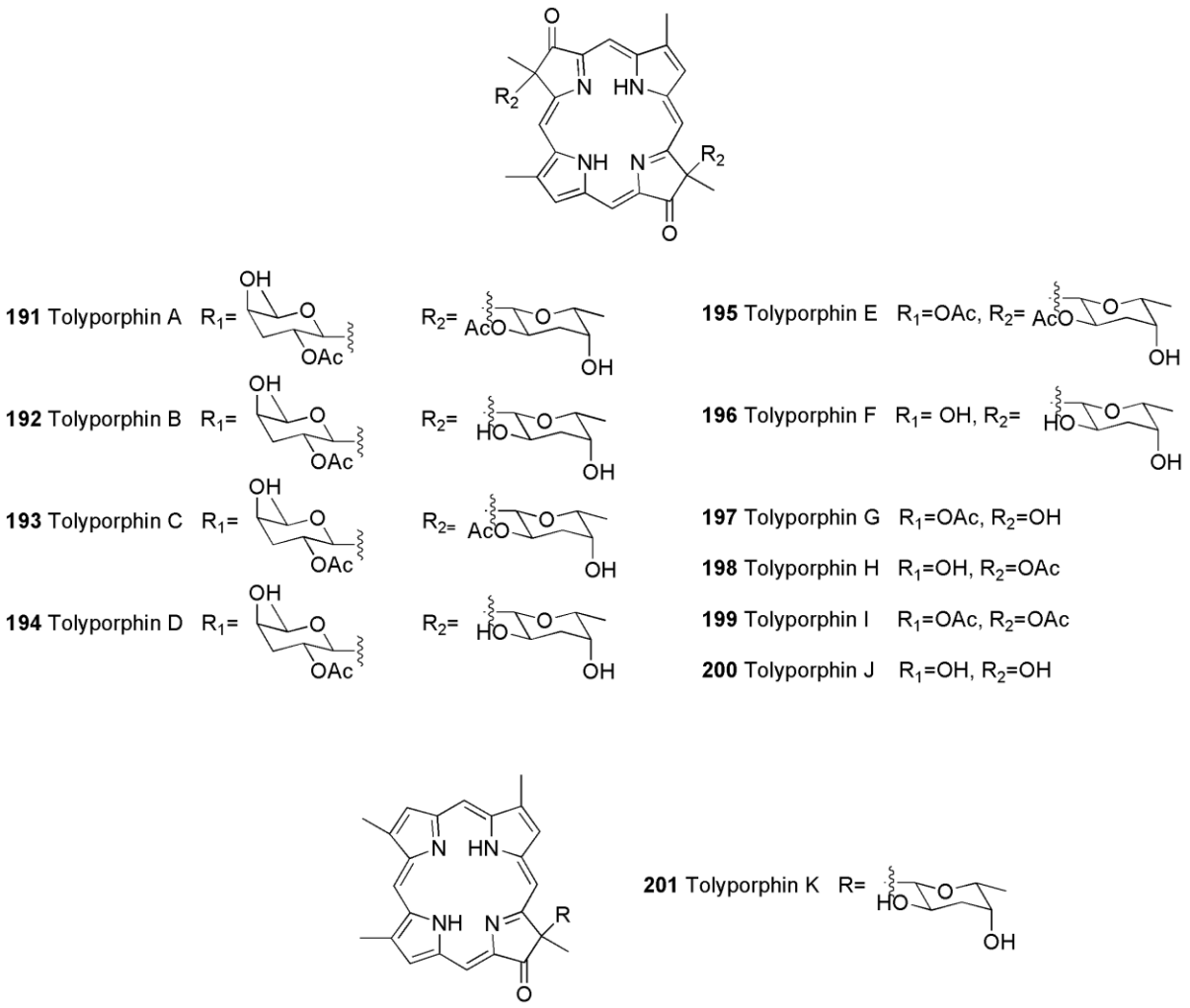

Figure 35. Structures of the cytotoxic compounds from the genus *Tolypothrix*

Tolyporphins A-K (**191**-**201**, Figure 35) were isolated from a cultured cyanobacterium *Tolypothrix nodosa* Bharadwaja (UH strain HT-58-2), obtained from a soil sample collected at Nan Madol, Pohnpei [126-128]. The structures of tolyporphins were unique naturally occurring porphinoids. All the compounds, except tolyporphins J and K, showed cytotoxicity against MCF-7/ADR cells with an IC_{50} value of less than 0.2 μM. It was found that tolyporphin A potentiated the cytotoxicity of adriamycin or vinblastine in SK-VLB cells at doses as low as 1.3 μM as well as increased the accumulation of [^{3}H]vinblastine in MCF-7/ADR cells.

2.3.2 Order Stigonematales

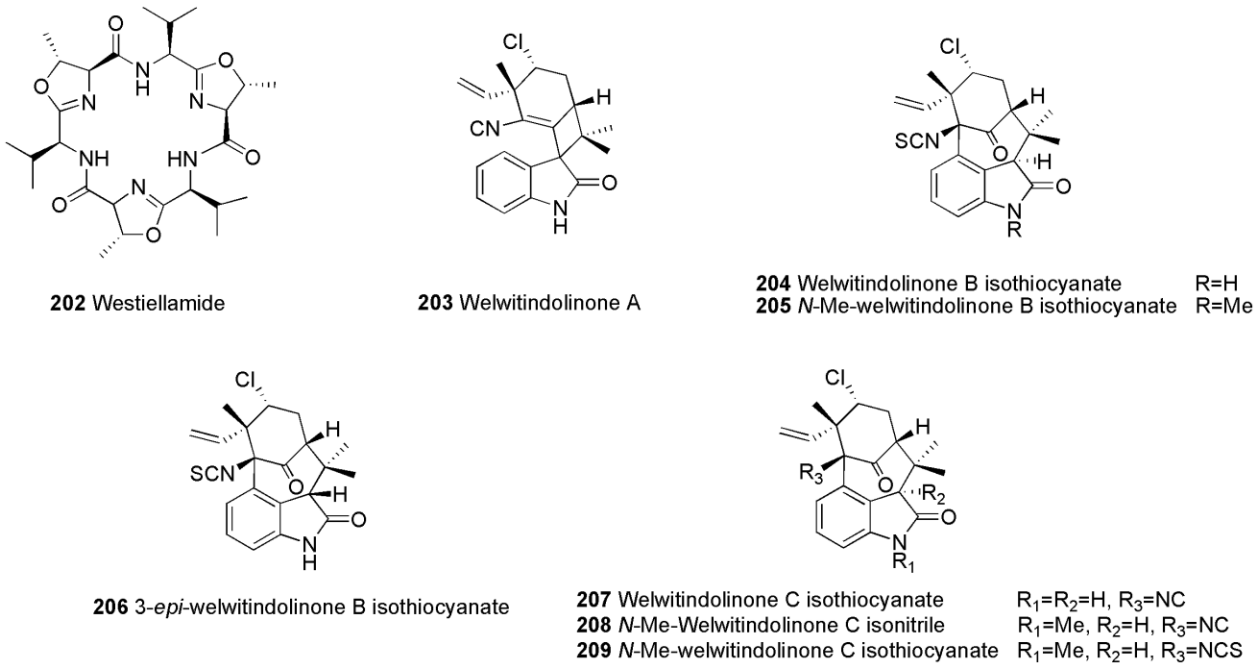

Figure 36. Structures of the cytotoxic compounds from the order Stigonematales

2.3.3.1 *Westiellopsis*

Westiellamide (**202**, Figure 36), a bistratamide-related cyclic peptide, was isolated from a cultured *Westiellopsis prolifica* Janet, obtained from a freshwater mud sample on the island of Oahu, Hawaii [133]. Westiellamide contained repeating valine and methyl-oxazoline residues. The isolation of westiellamide from a cyanobacterium provided evidence that cyanobacteria are the true source of the bistratamides isolated from the tunicate *Lissoclinum patella.* Westiellamide inhibited the growth of KB and LoVo cells with ED_{50} values of 3.7 μM.

2.3.3.2 *Hapalosiphon*

Welwitindolinones (**203**-**209**, Figure 36) were isolated from *Hapalosiphon welwitichii*, obtained from a freshwater sample collected at the Australian Institute of Marine Sciences in Queensland, Australia [132]. Both welwitindolinone C isothiocyanate (**207**) and *N*-methylwelwitindolinone C isonitrile (**208**)

showed cytotoxicity against MCF-7 cells with IC_{50} values of 0.12 µM, while the isothiocyanate derivative of *N*-methylwelwitindolinone C (**209**) was less cytotoxic with an IC_{50} value of 3.03 µM. *N*-methylwelwitindolinone C isothiocyanate (**209**) was found to potentiate cytotoxicity of actinomycine D and daunomycin against MCF-7/ADR cells, while it failed to sensitize these cells to cisplain, indicating **209** to be an antagonist of the P-glycoprotein MDR pump.

2.3.3 Order Oscillatoriales

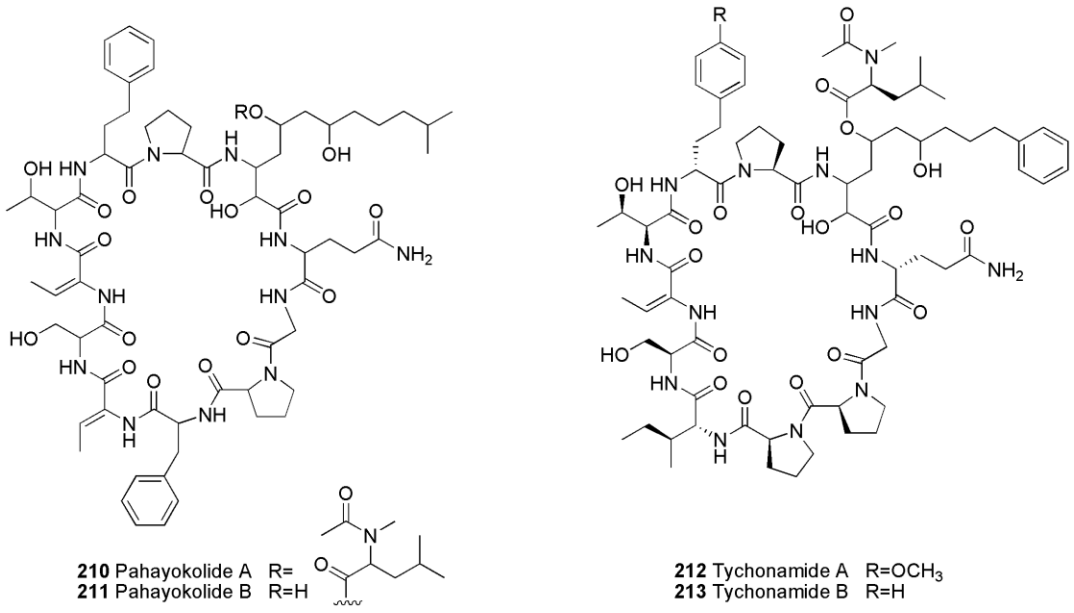

Figure 37. Structures of the cytotoxic compounds from the order Oscillatoriales

2.3.3.1 *Lyngbya*

Pahayokolides A (**210**) and B (**211**) (Figure 37), cyclic peptides, were isolated from a cultured *Lyngbya* sp. 15-2, obtained from a floating periphyton mat collected in the Florida Everglades [129, 130]. The structures of pahayokolides contained a polyhydroxy β-amino acid 3-amino-2,5,7,8-tetrahydroxy-10-methylundecanoic acid (AThmU) moiety. Pahayokolide A also contained a pendant *N*-acetyl-*N*-methyl leucine, while this was absent in pahayokolide B. Pahayokolide A showed cytotoxicity against a set of human cancer cells such as NCI-H460, A498, SKOV3, HT-29, U251, SKBR3, SKMEL28, and CEM with

IC_{50} values ranging from 2.13 and 44.57 μM. It also showed growth inhibition against Gram−negative bacteria, yeast, and green algae.

2.3.3.2 *Tychonema*

Tychonamides A (**212**) and B (**213**) (Figure 37) were isolated from a cultured *Tychonema* sp., obtained from a sample collected from a pond near a sugar factory in Wierthe, Germany [131]. The structures of both compounds contained a novel β-amino acid 3-amino-2,5,7-trihydroxy-8-phenyloctanoic acid (Atpoa). Both compounds showed cytotoxicity against a panel of 37 cancer cells with mean IC_{50} values of 0.6 and 2.2 μM, respectively. Furthermore, tychonamide B showed activity against tumor cell suspensions derived from solid tumor xenografts with a mean IC_{50} value of 1.6 μM. In addition, tychonamide A showed antiprotozoal activity against *Trypanosoma brucei rhodesiense* with an IC_{50} value of 0.07 μM.

2.3.4 Order Chroococcales

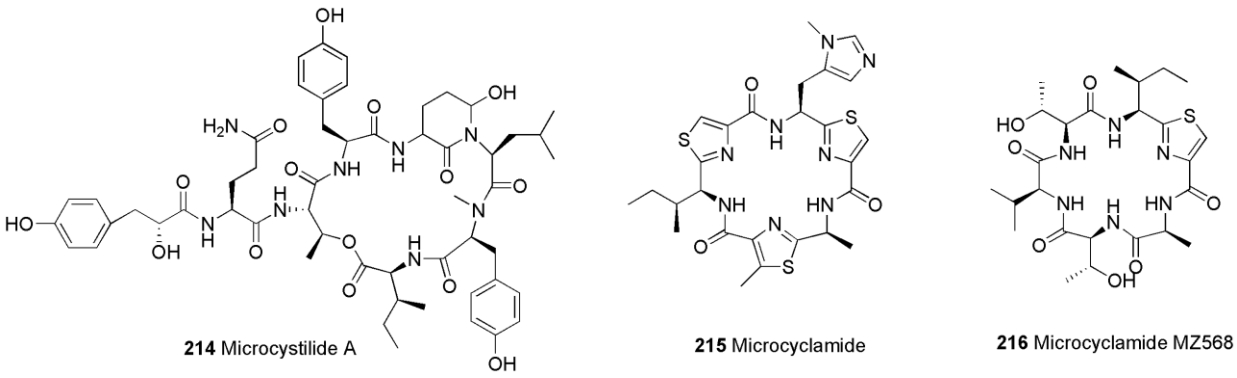

Figure 38. Structures of the cytotoxic compounds from the order Chroococcales

2.3.4.1 *Microcystis*

Microcystilide A (**214**) (Figure 38), a cyclic depsipeptide, was isolated from the microcystins-producing cyanobacterium *Microcystis aeruginosa* (NO-15-1840) [232]. The structure of microcystilide A

was similar to that of dolastatin 13, obtained from the sea hare *Dolabella auricularia*. Unlike microcystins, microcystilide A did not contain a 3-amino-9-methoxy-2,6,8-trimethyl-10-phenyl,4,6-decadienoic acid (Adda) moiety. Microcystilide A was found to be cytotoxic against HCT116 and HCTVP35 cell lines (IC_{50} values of 0.46 μM) and in a cell differentiation assay using HL-60 cells at 0.46 μM.

Microcyclamide (**215**, Figure 38), a cyclic hexapeptide, was isolated from a cultured *Microcystis aeruginosa* (NIES-298) [135]. The structure of microcyclamide contained a five-membered heterocycle, consisting of two thiazoles and one methyloxazole, and was the first cyclic hexapeptide found in *M. aeruginosa*. Microcyclamide showed cytotoxicity against P388 with an IC_{50} value of 2.0 μM.

Microcyclamide MZ568 (**216**, Figure 38), a thiazole-containing cyclic hexapeptide, was isolated from a *Microcystis* sp. bloom sample, collected in a fishpond at Kibbutz Ma'ayan-Tzvi, Israel [134]. The structure of microcyclamide MZ568 was derived from one cysteine and two threonine/serine moieties. Microcyclamide MZ568 exhibited cytotoxicity against Molt-4 cell line with 36% cell growth inhibition at 1.8 μM.

Chapter 3. BIOLOGICAL EVALUATION OF CULTURED CYANOBACTERIA

3 Biological Evaluation of Cultured Cyanobacteria

3.1 Introduction

Identification of molecular probes and potential anticancer drug candidates from natural sources can be achieved by screening extracts, fractions, or pure compounds using a variety of assay strategies, i.e. target-based screening and/or phenotypic screening [4].

Target-based screening has become more common as the molecular bases of cancer have been elucidated. It aims at specific molecular markers responsible for the development of malignant cancer phenotypes, and is thought to lead to improved efficacy and selectivity of cancer treatments [233-236]. In addition, target-based screening can be applied to both small-molecule screening using high-throughput formats as well as for biologic-based approaches to identify monoclonal antibodies [237]. However, the targeted molecular markers may not be relevant to cancer pathogenesis, nor do they provide a sufficient therapeutic index. Most targets exist in the cellular environment, and compounds identified by target-based assays may not be specific to the target [237]. The active compounds may have high affinity to other cellular molecules with no relationship to the pathogenesis of cancer. In addition, most molecular targets interact with other proteins within cellular pathways or networks, and inhibition of a specific molecular target may change the expression or the relative levels of interacting proteins [236]. In addition, this screening approach precludes targeting loss or alteration of target function that are often observed in cancer cells such as p53 mutations [233]. Furthermore, the target-based approach is limited by our knowledge of biology and targets that can be used for in vitro screening [233].

On the other hand, a specific molecular target is not the primary determinant in a phenotypic approach. As opposed to target-based screening, the phenotypic approach accounts for any mutation or other physiological changes that occur during tumorigenesis. Results obtained by phenotypic screening can be more effectively related to therapeutic impact, than by those obtained through target-based assays. In addition, phenotypic screening identifies compounds that are physically able to interact with their target protein within cells [233, 236]. This initial confirmation of cell permeability can eliminate potential problems associated with molecular target inhibitors that may later lack activity in a cellular environment [233, 236]. However, the use of phenotypic assays can be challenging for the optimization of the molecular properties of drug candidates due to the lack of knowledge of real molecular targets. In addition, the phenotypic approach is considered to be of lower throughput than the target-based assay approach [237].

Analysis of the new molecular entities (NMEs) and new biologics that were approved by the US Food and Drug Administration (FDA) between 1999 and 2008 indicated that the contribution of the phenotypic screening to the discovery of first-in-class small molecule drugs exceeded that of target-based approches [237]. In detail, the 259 agents were divided into three categories, i.e. 75 first-in-class drugs, 164 follower drugs, and 20 imaging agents. Out of the 75 first-in-class drugs, 28 (37%) were discovered via phenotypic screening, while 17 (23%) were discovered based on target-based screenings (Figure 39). For follower drugs, on the other hand, it was shown that 83 (51%) out of 164 drugs approved by FDA during the same period were discovered via target-based screenings, while only 30 (18%) were based on phenotypic screenings (Figure 39). It was presumed that this reversal of the trend between the first-in-class and follower drugs was the result of drug developers drawing on knowledge of previously identified molecular mechanisms to more effectively use target-based bioassays [237]. Overall, this analysis indicated that the phenotypic screening was the most successful approach to discover small-molecule first-in-class NMEs, despite the current focus in drug discovery on target-based approaches.

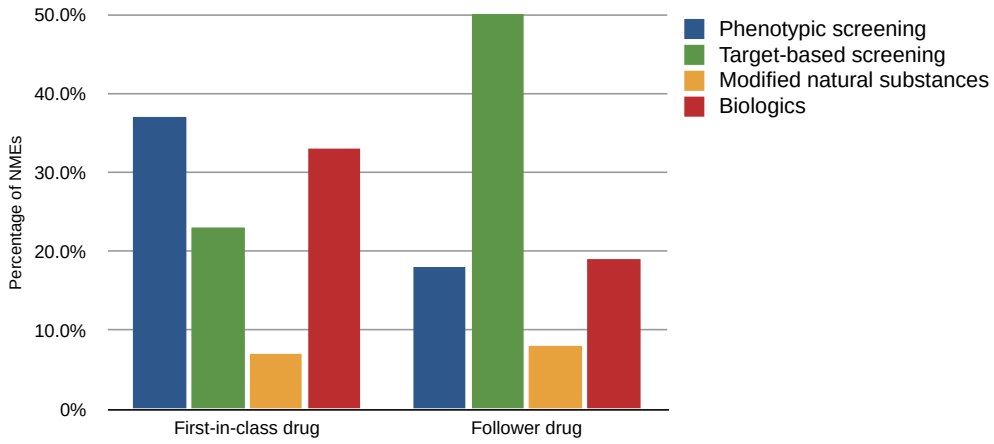

Figure 39. The distribution of new drugs discovered between 1999 and 2008, according to the discover strategy. The graph illustrates the number of new molecular entities (NMEs) in each category (This figure was adapted from the original article by Swinney, D. C. and Anthony, J. [237]).

The aim of this study was to identify cyanobacterial strains with significant biological activities using two bioassay systems; cytotoxicity as a phenotypic assay and 20S proteasome inhibition as a target-based screening. Unialgal strains of cyanobacteria were acquired from established culture collections as well as obtained from samples collected in the field. All strains were cultured under a controlled environment. Cultured strains were harvested and extracted. The extracts were screened for cytotoxicity against a set of human cancer cells and for 20S proteasome inhibition. The resulting active strains were cultured at larger scale for further chemical investigation.

3.2 Cyanobacteria culture collection

3.2.1 Acquisition of cyanobacteria strains

Cyanobacteria strains were obtained from external collections, i.e. the Culture Collection of Algae at the University of Texas at Austin (UTEX) [238], the Provasoli-Guillard National Culture Collection of Marine Phytoplankton (CCMP) [239], the Culture Collection at the University of Göttingen, Germany (SAG) [240], and the Culture Collection of Autotrophic Organisms at the Academy of Sciences of the Czech Republic (CCALA) [241]. Cyanobacteria strains were also isolated from samples obtained from the field. Multiple techniques such as isolation by streak plate, micropipette, and serial dilution were used to obtain unialgal strains from the material collected in the field [242, 243].

3.2.2 Culture conditions

Each new strain acquired from commercial culture collections or isolated from samples in the field was cultured in a controlled environment. The temperature of the culture room was maintained at 20°C. Light was provided via white fluorescent lights with an 18/6 hour light/dark cycle and a mean illuminescence of 1.93 klx. Each strain was first introduced into 150 mL of inorganic media in a 250 mL Erlenmeyer flask. After approximately two weeks (when there was sufficient growth in stock cultures), the cultivated biomass was used to inoculate one culture of 300 mL of medium in a 1 L Fernback flask and two 2 L of media in a 2.8 L Fernback flask under aeration. These cultures were allowed to grow for 4-8 weeks. The biomass from the 300 mL was used to create cryopreservation stocks. The biomass from the two 2 L was harvested and used to create an initial extract.

Freshwater strains were cultured in Allen, Z, Z45, or DY-V medium while marine strains were cultured in ES (enriched seawater medium) or f/2 medium (Table 3). For strains that were acquired from the culture collections, media with a high defree of similarity to those used by the source collection were chosen. Protocol for all media used in this study was adapted from the protocols described by Andersen *et al*. [244] and Falch *et al*. [38] with slight modifications to allow for the use of a common set of stock solutions.

TABLE 3. CONCENTRATED STOCK OF MEDIA NUTRIENTS (UNIT: MOLARITY, M)

	Freshwater				Marine	
Component	Allen	DY-V	Z	Z45	f/2	ES
C (CO_3)	1.89×10^{-4}	-	-	-	3.33×10^{-3}	3.33×10^{-3}
N (NO_3+NH_4)	1.76×10^{-2}	2.35×10^{-4}	5.74×10^{-3}	5.74×10^{-3}	8.83×10^{-4}	2.05×10^{-4}
P (PO_4)	2.15×10^{-4}	7.06×10^{-6}	3.99×10^{-4}	5.74×10^{-3}	3.62×10^{-5}	2.18×10^{-5}
S (SO_4)	1.52×10^{-4}	2.03×10^{-4}	1.04×10^{-4}	1.04×10^{-4}	2.77×10^{-2}	2.77×10^{-2}
Fe	3.59×10^{-7}	3.70×10^{-6}	1.00×10^{-6}	1.00×10^{-6}	1.34×10^{-5}	5.97×10^{-6}
Fe: Chelator*	0.01	0.17	1.00	1.00	1.15	1.11

*Chelator is citrate for Allen and EDTA for all others.

3.2.3 Extract library

For each strain, the biomass from 2 × 2 L of cultures was harvested by centrifugation, and freeze-dried. The lyophilized biomass was repeatedly macerated with methanol/dichloromethane (1:1 v/v) at room temperature, and the solvent was evaporated *in vacuo*. The dried crude extract was stored at -20°C until used. From each dried extract, approximately 10-15 mg was dissolved in DMSO to create a 10 mg/mL library solution. 96-well formatted polypropylene tubes were used to store 1 mL of the library solutions, and the material archive was stored at -80°C for further biological evaluations.

3.3 Biological evaluation

The evaluation of cytotoxicity against a set of human cancer cell lines designated HT-29, NCI-H460, MCF-7, and SF268 was performed. Furthermore, a human cancer cell panel consisting of 12 different cancer cells was used to evaluate cytotoxicity of selected cyanobacteria strains. In addition,

inhibition of 20S proteasome, an established target for cancer therapy, was evaluated. All of these assays were performed on both the extract and pure compounds.

3.3.1 Cytotoxicity assay

In order to evaluate cytotoxicity against HT-29, cells were propagated in RPMI 1640 media supplemented with fetal bovine serum (10% v/v), 100 units/mL penicillin, and 100 µg/mL streptomycin at 37°C in 5% CO_2 atmosphere. Monolayer cultures were released by treatment with trypsin, and suspended in media. Prepared cells were plated at 2.5×10^3 cells per well in a 96-well microtiter plate and incubated for 16 h at 37°C in 5% CO_2 atmosphere, then the samples and a positive control, vinblastine, were added. After 72 h incubation under the same condition of cell culture, an MTS assay was performed using a commercially available kit (CellTiter 96® Aqueous One Solution Cell Proliferation Assay, Promega Corp, Madison, Wisconsin) according to the manufacturer's instructions. The absorbance was measured at 490 nm using a Tecan Genios Promicroplate reader. Cytotoxicity of the samples were measured against NCI-H460, MCF-7, and SF268 as described previously [245] with slight modifications. The modified procedures were summarized as followed. NCI-H460 and SF268 cells were seeded at 1×10^3 and 3.4×10^3 cells per 50 µL, respectively. The fixed plates were tapped for drying instead of using air dry before adding 10 mM Tris base. SpectroMax was used to read the absorbance at 562 nm. Average replicate values from the plate reader were converted to percent survival using Excel. ED_{50} values and curve fitting data were calculated using CompuSyn.

The cytotoxicity assay for HT-29 was performed at The Ohio State University, Columbus, Ohio. The cytotoxicity assay for NCI-H460, MCF-7, and SF268 was performed at North Carolina Central University, Durham, North Carolina.

An average cytotoxicity value was also measured for selected cyanobacteria strains using 12 different human cancer cells designated BT549, DU4475, MDA-MB-468, and MDA-MB-231 for breast, PC3, LNCaP-FGC, and Du145 for prostate, NCI-H460 and SHP-77 for lung, and NCT116 for colon, A2780/DDP-S for ovarian, and CCRG-CEM for leukemia. The assay was performed at the Bristol-Myers Squibb corporate.

3.3.2 20S proteasome assay

The 20S proteasome assay was performed according to the protocol provided with the BIOMOL 20S proteasome Assay Kit (BIOMOL International LP, Plymouth Meeting, PA, USA). The samples, bortezomib as a positive control, and 20S proteasome fraction were diluted in the assay buffer (6.05 g Tris HCl, 1.86 g KCl, 0.58 g NaCl, and 95.2 mg $MgCl_2$ in 1L H_2O, pH 7.5). The enzyme reaction started adding Suc-LLVY-AMC substrate with a final concentration of 10 μM. The plates were incubated for 15 min, and the chymotrypsin-like proteasome activity was determined by measuring fluorescence of the substrate. Fluorescence was measured using a Tecan Genios Promicroplate reader with an excitation wavelength of 360 nm and an emission wavelength of 460 nm. The assay was performed at the University of Illinois at Chicago, Chicago, Illinois.

3.4 Results and discussion

A total of 306 cyanobacterial strains were added to the extract library from May 2008 to June 2011. Of these, 131 strains were acquired from commercial culture colections, and 176 strains were isolated from field samples collected from various regions of the United States. Out of these 176 strains, the taxonomy of 37 strains were not determined and thus, these strains were removed from following analyses. None of these 37 strains were active in either biological assay system used for this study.

The 269 cyanobacterial strains in the extract library belong to all five orders of cyanobacteria: Chroococcales (31), Pleurocapsales (5), Oscillatoriales (106), Nostocales (114), and Stigonematales (13). The largest single source of strains was from isolates obtained at the University of Illinois at Chicago (UIC) using samples collected in the field (52%) (Table 4). The largest external source of commercial strains was the Culture Collection of Algae at the University of Texas at Austin (UTEX) (30%).

269 extracts were prepared from the 269 cyanobacteria strains and evaluated for their cytotoxicity against a variety of human cancer cells as well as for 20S proteasome inhibition. In both assays, the cyanobacteria in the order Stigonematales provided the highest hit rates although most of the screened strains were filamentous cyanobacteria belonging to the orders Nostocales and Oscillatoriales (Table 5 and Figure 30).

TABLE 4. STRAINS BY CULTURE SOURCE AND TAXONOMIC ORDER

	Source*					
Order	UTEX	CCMP	SAG	CCALA	UIC	**Total**
Chroococcales	7	5	2	1	16	**31**
Pleurocapsales	3	-	1	-	1	**5**
Oscillatoriales	31	8	5	-	62	**106**
Nostocales	35	8	10	2	59	**114**
Stigonematales	5	-	5	2	1	**13**
Total	**81**	**21**	**23**	**5**	**139**	**269**

* UTEX= Culture Collection of Algae at the University of Texas at Austin, CCMP= Provasoli-Guillard National Center for Culture of Marine Phytoplankton, SAG= Culture Collection of Algae at the University of Göttingen, Germany, CCALA= Culture Collection of Autotrophic Organisms at the Academy of Sciences of the Czech Republic, UIC= Isolated from field collected samples at the University of Illinois at Chicago.

Three of the thirteen strains from the order Stigonematales were cytotoxic. On the other hand, 5 of 114 strains in the order Nostocales and 1 of 104 in the order Oscillatoriales exhibited cytotoxicity. Four strains (3691, 10035, 1693, and 1829) did not display cytotoxicity against HT-29 cells, while exhibiting activity against NCI-H460, MCF-7, and SF268 cells. On the other hand, one strain (4a) of the order Nostocales showed cytotoxicity only against HT-29 cells. No strains of the two non-filamentous orders, Chroococcales and Pleurocapsales, showed significant cytotoxicity against any cancer cells used in this study (tested at 20 µg/mL). None of extracts from the order Oscillatoriales displayed cytotoxicity against HT-29 cells tested at 20 µg/mL.

TABLE 5. ACTIVITY DATA FROM INITIAL SCREENING GROUPED BY TAXONOMIC ORDER

	Bioassay*				
Order	HT-29	NCI-H460	MCF-7	SF268	20S Proteasome
Chroococcales	-	-	-	-	-
Pleurocapsales	-	-	-	-	-
Oscillatoriales	-	0.9% (1)	0.9% (1)	0.9% (1)	0.9% (1)
Nostocales	4.4% (5)	4.4% (5)	4.4% (5)	4.4% (5)	2.6% (3)
Stigonematales	7.7% (1)	23.1% (3)	23.1% (3)	23.1% (3)	23.1% (3)
Total	**2.2%**	**3.3%**	**3.3%**	**3.3%**	**2.6%**

* Number denotes hit rate with total number of active strains in parenthesis. A dash (-) denotes none active.

Two strains of the order Stigonematales (1693 and 1829) and two strains of the order Nostocales (1832 and 10035) were further evaluated for their cytotoxicity against a cancer cell panel consisting of 12 different cancer cells, and all 4 strains showed significant cytotoxicity (Table 6). Other cytotoxic strains were not evaluated against this cancer cell panel.

As a result of the 20S proteasome inhibition, seven strains were found to be active (Table 6). Again, the cyanobacteria (1693, 1829, and 4679) of the order Stigonematales provided the highest hit rate (23.1%). One strain (3691) of the order Oscillatoriales and three strains (1832, 4a, and 10022a) of the order Nostocales showed significant 20S proteasome inhibitory activities. Whereas, none of strains of the two orders, Chroococcales and Pleurocapsales, were active.

The initial analysis of 20S proteasome inhibition resulted in a hit rate of 13.4%, and the cyanobacteria of all orders, except Pleurocapsales, had high hit rates. The hit rates of Chroococcales and Oscillatoriales were 22.8% and 15.1%, respectively. Nostocales and Stigonematales displayed 14.0% and 38.5% hit rates, respectively. It was later determined that the high hit rates were in part due to false positives, resulting from color interferences of cyanobacterial pigments presented in the crude extracts.

TABLE 6. LIST OF ACTIVE CYANOBACTERIA STRAINS

Strain ID	Scientific Name	Target*					
		HT-29 (ED_{50})	NCI-H46[b]	MCF-7 (% inhibition)	SF268	Cancer cell panel [a] (ED_{50})	20S Proteasome (% inhibition)
Order Oscillatoriales							
3691	*Lyngbya* sp.	-	98.0	81.0	100.0	ND	79.8
Order Nostocales							
1832	*Nostoc muscorum*	10.8	86.0	62.8	66.3	3.5	88.0
4a	*Nostoc* sp.	11.5	-	-	-	ND	96.1**
10022a	*Nostoc* sp.	2.0	100	87.8	100	ND	91.1
10047	*Nostoc* sp.	7.2	100	93.7	61.6	ND	-
10062	*Nostoc* sp.	13.1	100	72.9	77.2	ND	-
10035	*Nostoc* sp.	-	42.8	54.6	46.7	16.0	-
Order Stigonematales							
1693	*Westiellopsis prolifica*	-	100.0	94.9	100.0	2.5	96.1
1829	*Fischerella muscicola*	-	72.0	55.0	63.0	5.3	86.8
20931	*Westiellopsis* sp.	13.5	88.0	49.0	41.0	ND	-
4679	*Fischerella* sp.	-	-	-	-	ND	94.9

A dash (-) denotes inactive. *HT-29 Human colon cancer cell, NCI-H460 Human large lung cancer cell, MCF-7 Human breast cancer cell, SF268 Human glioblastoma cancer cell, and 20S proteasome, an established target for cancer therapy. [a] A panel of 12 human cancer cells designated BT549 (Breast), DU4475 (Breast), MDA-MB-468 (Breast), NCI-H466 (Lung), PC3 (Prostate), SHP-77(Lung), LNCaP-FGC (Prostate), NCT116 (Colon), MDA-MB-231 (Breast), A2780/DDP-S (Ovarian), DU145 (Prostate), CCRG-CEM (Leukemia). **Assay was performed at 50 µg/mL (others tested at 100 µg/mL). ND represents not determined.

Chapter 4. CHEMICAL INVESTIGATIONS ON BIOACTIVE STRAINS OF CULTURED CYANOBACTERIA

4 Chemical Investigations on Bioactive Strains of Cultured Cyanobacteria

Based on the initial bioassay results, five cyanobacterial strains were cultured in large scale. Extracts of each strain were prepared using the procedure described in the section 3.2.3. Each dried extract was mixed with HP20SS resin (Diaion®). This mixture was prepared as a slurry and the mixture was dried using a centrifugal evaporator. The dried material was poured into a HP20SS resin-containing plastic column fitted with a frit and subjected to an 8-step elution, in which 50-150 mL of each solvent (100% H_2O, 20% 2-propanol, 40% 2-propanol, 60% 2-propanol, 70%, 2-propanol, 80% 2-propanol, 90% 2-propanol, and 100% 2-propanol) was used to generate eight fractions (F1-F8, respectively). Approximately 10-15 mg of each fraction was dissolved in DMSO to create a 10 mg/mL fraction library solution. The fractions were stored in 96-well formatted polypropylene tubes and daughter plates were prepared for biological evaluation. The material archive containing all fractions was stored at -80°C for further usage. The remaining of each fraction was used for bioassay-guided fractionation.

A. *Fischerella* sp. (SAG 46.79)

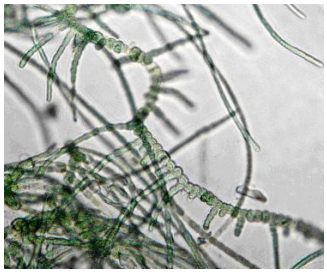

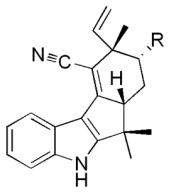

12-*epi*-fischerindole I nitrile (**217**) R=Cl
Deschloro 12-*epi*-fischerindole I nitrile (**218**) R=H

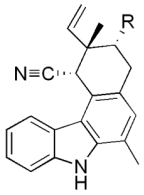

12-*epi*-fischerindole W nitrile (**219**) R=Cl
Deschloro 12-*epi*-fischerindole W nitrile (**220**) R=H

Figure 40. Photomicrograph of *Fischerella* sp. (SAG 46.79) and isolated compounds

Chemical investigation of the cultured cyanobacterium *Fischerella* sp. (SAG strain number 46.79) led to the isolation of four nitrile-containing indole alkaloids, namely 12-*epi*-fischerindole I nitrile (**217**), deschloro 12-*epi*-fischerindole I nitrile (**218**), 12-*epi*-fischerindole W nitrile (**219**), and deschloro 12-*epi*-fischerindole W nitrile (**220**) along with a known metabolite hapalosin (**221**). The structures were determined by detailed spectroscopic analyses of 1D and 2D NMR and HRESIMS data. All isolates were evaluated for cytotoxicity against human cancer cells and for 20S proteasome inhibition. Deschloro 12-*epi*-fischerindole I nitrile (**218**) was found to be weakly cytotoxic against HT-29 cells with an ED_{50} value of 23 μM. Hapalosin (**221**) showed weak cytotoxicity against HT-29 and MCF-7 cells with ED_{50} values of 22 and 27 μM, respectively, as well as moderate 20S proteasome inhibition with an IC_{50} value of 12 μM. Compounds **217**-**220** all contain a nitrile moiety as opposed to the isonitrile found in all fischerindoles reported to date. Compounds **219** and **220** also display a new carbon skeleton, in which a six-membered ring replaced the five-membered ring normally found in fischerindole-type alkaloids.

A.1 Taxonomic description of the genus *Fischerella*

According to Komárek *et al*., the genus *Fischerella* belongs to the family Fischerellaceae in the order Stigonematales in the phylum Cyanobacteria, domain Bacteria [246]. The order Stigonematales is characterized by the formation of true branching, where multiple planes of division occur during binary fission. Eight families with 48 genera are recognized by Anagnostidis and Komárek, and the genera exhibit

the highest degree of morphological complexity and differentiation within the cyanobacteria [247]. The most frequently represented genera in culture are *Fischerella* (Born. et Flah.) Gom. 1895, *Hapalosiphon* Näg. in Küz. ex Born. et Flah. 1886, and *Mastigocladus* Cohn ex Kirchner 1898 [248]. The current taxonomic description of *Fischerella* by Komárek *et al*. is as follows [246].

> The thallus is composed of morphologically diverse, uniseriate or multiseriate, usually creeping filaments and more or less erect uniseriate branches. Most species produce feltlike, rarely compact mats. Creeping trichomes with barrel-shaped cells sometimes occur within a gelatinous matrix. Trichomes are generally moniliform and enveloped by thick, sometimes from outside wavy or slightly lamellated, colored sheaths. Erect true branches (with T-type branching), usually unilateral, arise after longitudinal cell division in basal trichomes. Branches, primarily cylindrical, are generally composed of cylindrical elongated cells in colorless sheaths. Cell contents are slightly granular, with thylakoids distributed irregularly. Heterocytes are intercalary, subspherical in basal trichomes, and cylindrical in branches. Akinetes (known only in a few species) occur occasionally and irregularly in basal trichomes. Cell division occurs mainly via horizontal (crosswise), perpendicular fission. Reproduction occurs via uniseriate hormogonia separating from the ends of branches. Hormogonia liberated under wet or humid conditions, and are usually morphologically distinct from other cells in branches and contain aerotopes (gas vacuoles).

The complex variety of forms and developmental stages of *Fischerella* such as primary and secondary trichomes, hormogonia, unicells, and amorphous cell aggregates makes it difficult to differentiate any single stage of the genus *Fischerella* from other genera such as *Stigonema* and *Hapalosiphon*. The developing patterns of main axis and branches can be a key to distinguish between *Fischerella* and *Stigonema*. However, there is no clear boundary separating these three genera for all described species [247].

SAG 46.79 was isolated by Schwabe, G. H. in 1970 and deposited in The Culture Collection of Algae at the University of Göttingen. It was purchased and maintained under laboratory conditions, and further used for biological and chemical evaluations.

A.2 Compounds previously isolated from cyanobacteria of the order Stigonematales

Branched, filamentous cyanobacteria belonging to the order Stigonematales have produced a variety of biologically active secondary metabolites including indole alkaloids. Over 70 indole alkaloids have been described since the first report of hapalindoles A (**222**) and B (**223**) from *Hapalosiphon fontinalis* in 1984 [249]. Representative classes of the indole alkaloids include hapalindoles (**222**-**248**),

hapalindolinones (**249** and **250**), hapaloxindoles (**251**-**253**), fontonamides (**254** and **255**), hapalonamides (**256**-**258**), ambiguines (**259**-**277**), fischerindoles (**278**-**282**), and welwitindolinones (**203**-**209** and **283**-**285**) (Figure 41). All of these have tri- to hexacyclic carbon skeletons derived from L-tryptophan and geraniol pyrophosphate, and possess diverse biological activities including antibacterial, antifungal, and antialgal activities.

The genus *Fischerella* has been reported to produce many of these indole alkaloids (Table 7). Fischambiguines A (**276**) and B (**277**) were recently reported from *Fischerella ambigua*, and fischambiguine B showed strong inhibitory activity against *Mycobacterium tuberculosis* (Figure 41). Besides the indole alkaloids, fischerellins A (**292**) and B (**293**) have also been reported as anticyanobacterial and antifungal compounds from *Fischerella muscicola* (Figure 42). The structures of both compounds contained a pyrrolidinone ring and a polyunsaturated side chain. In particular, fischerellin A, a potent photosystem-II inhibitor, inhibited the growth of cyanobacteria and higher plants. Furthermore, ambigols A-C (**286**-**288**), tijipanazole D (**289**), and 2,4-dichlorobenzoid acid (**286**) were obtained from *Fischerella ambigua* (Figure 42). Ambigols A-C were highly chlorinated and contained aromatic rings. *Fischerella* sp. also produced γ-linolenic acid (GLA) (**291**) with a broad-spectrum antibacterial activity (*Staphylococcus aureus*, *Escherichia coli*, *Salmonella typhi*, *Pseudomonas aeruginosa*, and *Enterobacter aerogenes*). In addition, microcystin-LR (**294**), a hepatotoxic compound, has been detected in *Fischerella* sp. by HPLC-MS, and a nucleotide sequence putatively involved in microcystine synthesis has been identified in this genus (Figure 42).

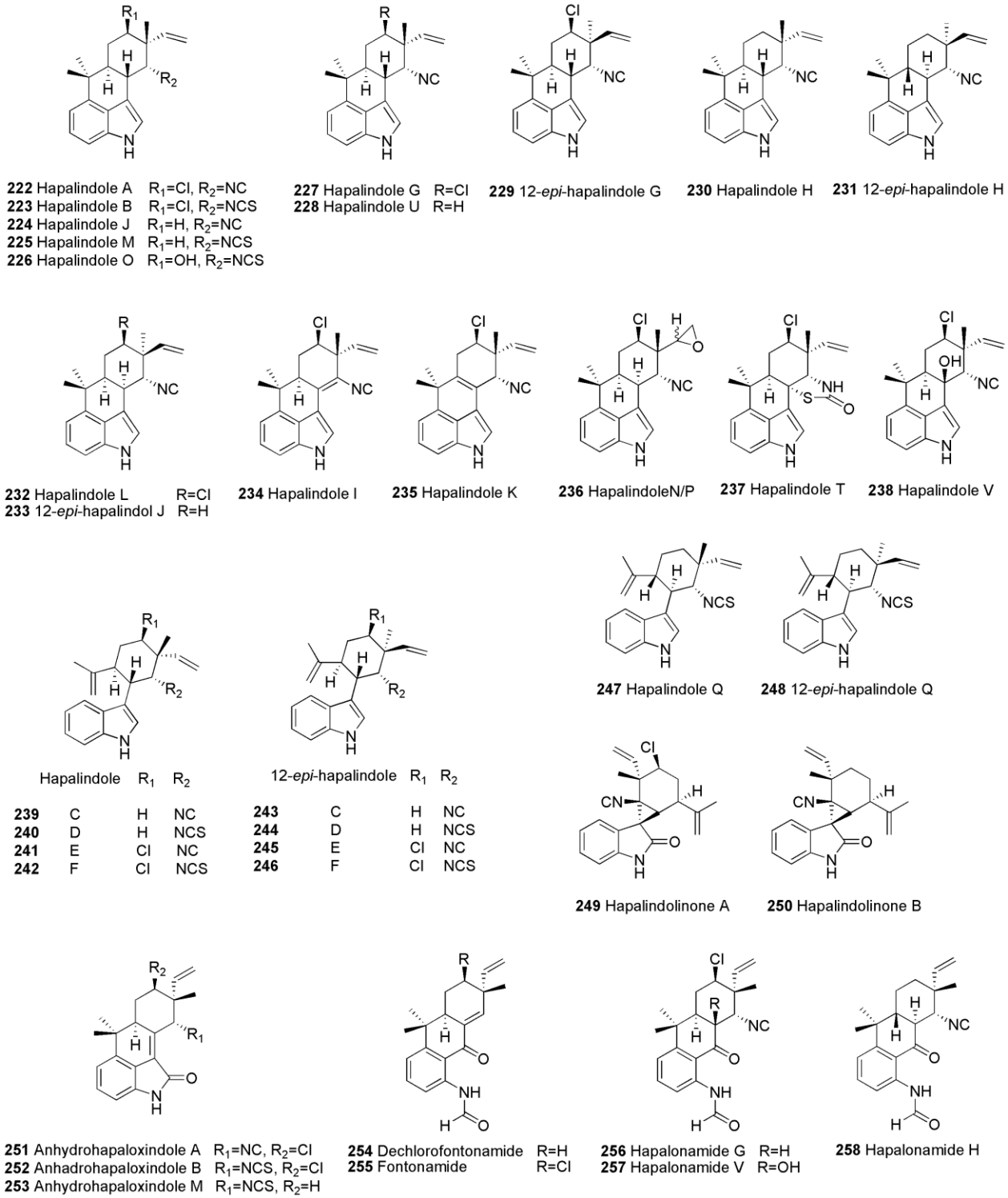

Figure 41. Structures of hapalindole-type alkaloids from the order Stigonematales

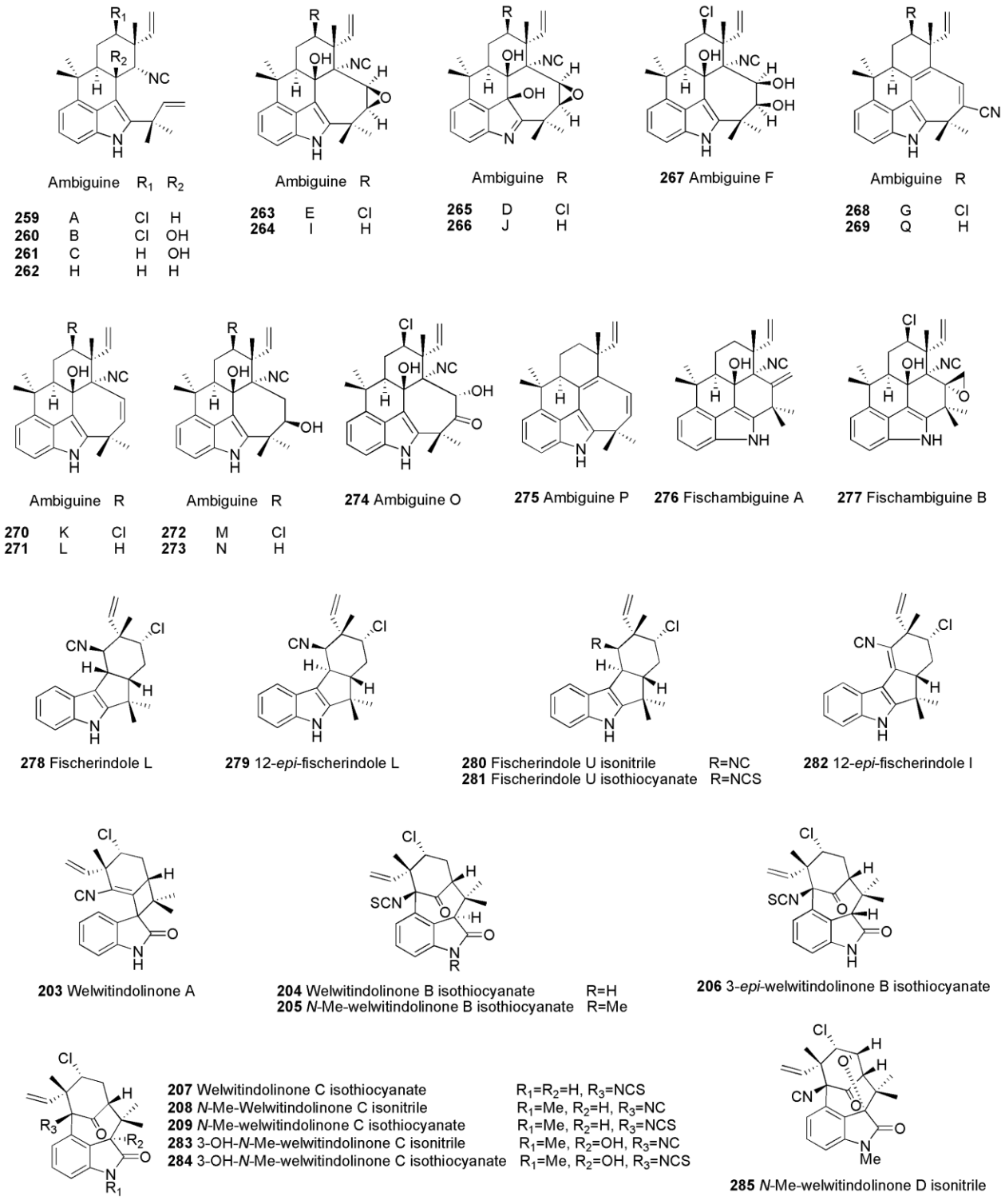

Figure 41 (continued). Structures of hapalindole-type alkaloids from the order Stigonematales

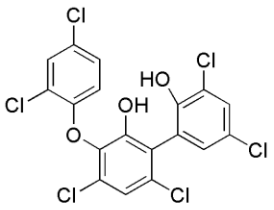

286 Ambigol A

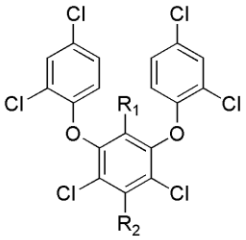

287 Ambigol B R_1=H, R_2=OH
288 Ambigol C R_1=OH, R_2=H

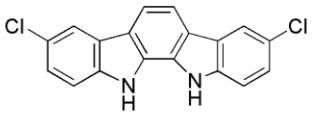

289 Tjipanazole D

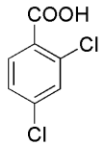

290 2,4-dichlorobenzoic acid

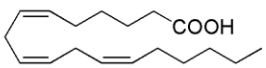

291 γ-linolenic acid (GLA)

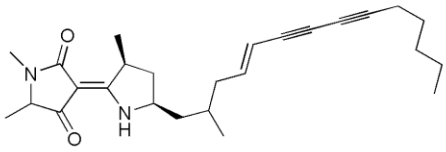

292 Fischerellin A

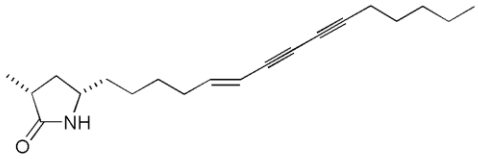

293 Fischerellin B

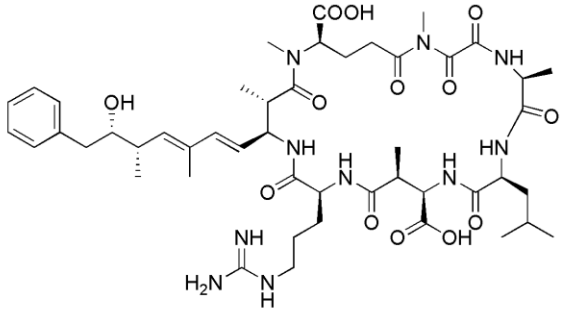

294 Microcystin-LR

Figure 42. Structures of miscellaneous compounds from the genus *Fischerella*

TABLE 7. COMPOUNDS FROM CYANOBACTERIA BELONGING TO THE GENUS *FISCHERELLA*

Source	Compound	Activity	Reference
Fischerella ambigua	ambigols A-C (**286**-**288**)	antibacterial, cytotoxic, and antialgal	[250, 251]
	2,4-dichlorobenzoic acid (**290**)		
	tjipanazole D (**289**)		
	ambiguines A-F (**259**-**261**, **265**, **263**, **267**)	antifungal	[252, 253]
	ambiguines A-C (**259**-**261**), E (**263**), F (**267**), I (**264**), and K-O (**270**-**274**)	antibacterial	[254, 255]
	fischambiguines A (**276**) and B (**277**)		
	hapalindoles G (**227**) and H (**230**)		
	ambiguines G (**268**) and Q (**269**) nitriles		
Fischerella ambigua ATCC 55210	ambiguines B-F (**260**, **261**, **265**, **263**, **267**)	antifungal	[256]
	hapalindole G (**227**) and H (**230**)		
Fischerella ATCC 43239	12-*epi*-hapalindole C isonitrile (**243**)	insecticidal, antibacterial, and antifungal	[257]
	12-*epi*-hapalindole E (**245**)		
	12-*epi*-hapalindole J isonitrile (**233**)		
	hapalindole L (**232**)		
Fischerella ATCC 53558	hapalindolinones A (**249**) and B (**250**)	vasopressin antagonists	[258, 259]
Fischerella muscicola	fischerellins A (**292**) and B (**293**)	antifungal and algicidal	[260, 261]
	fischerindole L (**278**)	antifungal	[262]
Fischerella sp.	ambiguines H-J (**262**, **264**, **266**)	antibacterial and antimycotic	[253]
	12-*epi*-hapalindole H (**231**)		
	fischerellin A (**292**)	antifungal and antialgal	[263]
	12-*epi*-hapalindole F (**246**)		
	hapalindole T (**237**)	antibacterial	[264]
	3-OH-*N*-Me-welwitindolinone C isonitrile (**283**)	antifungal	[265]
	3-OH-*N*-Me-welwitindolinone C isothiocyanate (**284**)		
	N-Me-welwitindolinone D isonitrile (**285**)		
	microcystin-LR (**294**)	hepatotoxic	[266]
	γ-linolenic acid (GLA) (**291**)	broad-spectrum antibacterial	[267]

A.3 Chemical investigations of the cultured cyanobacterium *Fischerella* sp. (SAG 20.93)

A.3.1 Experimental

A.3.1.1 General experimental procedures

Optical rotations were measured with a Perkin-Elmer 241 polarimeter. UV spectra were recorded on a Varian Cary 50 Bio spectrophotometer. 1D and 2D NMR spectra were obtained at room temperature on a Bruker Avance DRX 600 MHz spectrometer with a 5 mm CPTXI Z-gradient probe. ^{13}C NMR spectra were obtained on a Bruker AV 900 MHz NMR spectrometer with a 5 mm ATM CPTCI Z-gradient probe. ^{1}H and ^{13}C chemical shifts were referenced to a residual proton, 7.27 and 77.2 ppm in $CDCl_3$, 2.50 and 39.5 ppm in DMSO-d_6, respectively. HRESIMS were obtained using a Shimadzu IT-TOF spectrometer.

A.3.1.2 Biological material

Fischerella sp. was acquired from the Culture Collection of Algae at the University of Gottingen (SAG strain number 46.79). The cyanobacterium was grown in a 2.8 L Fernback flask containing 2 L of inorganic media (Z media) under aeration [244]. Cultures were illuminated with fluorescent lamps at 1.93 klx with an 18/6 hours light/dark cycle. The temperature of the culture room was maintained at 22°C. After eight weeks, the biomass of the cyanobacterium was harvested by centrifugation and then lyophilized. The same conditions were used for all three cultures.

A.3.1.3 Extraction and isolation

The lyophilized biomass (1.1 g) from 2 L of culture was extracted with CH_2Cl_2/MeOH (1:1 v/v) at room temperature and the solvent was evaporated *in vacuo*. The extract (147.8 mg) was redissolved in CH_2Cl_2/MeOH (1:1 v/v) and mixed with Diaion® HP20SS resin. The mixture was dried *in vacuo* and the dried mixture was fractionated on a Diaion® column using a step gradient with increasing amount of 2-propanol in water to afford eight fractions. Fraction 5, eluting with 70% 2-propanol, displayed 75% inhibition of 20S proteasome at 50 ppm. Fraction 5 was subjected to a reversed-phase HPLC column (Varian C_8 Dynamax, 10 x 250 mm, flow rate 3 mL/min) with 75-95% MeOH/H_2O gradient over 45 min to yield hapalosin (0.7 mg, t_R 36 min) as the 20S proteasome active component. A second extract (176.9 mg) was prepared from a second culture (2.5 g from 2 x 2 L of culture). By the procedure described above, eight fractions were obtained. Fractions 5 and 6, eluted with 70% and 80% 2-propanol, respectively, were

subjected to HPLC-ESI-TOF-MS analysis (Varian Microsorb C_8, 2.0 x 250 mm, flow rate 0.2 mL/min) with 30-100% MeOH gradient over 35 min containing 0.1% acetic acid. The analysis of MS spectra indicated the presence of potentially new indole alkaloids. Fraction 5 was subjected to reversed-phase HPLC column (Varian C_8 Dynamax, 10 x 250 mm, flow rate 3 mL/min) with 70-85% MeOH/H_2O over 80 min to yield **233** (0.3 mg, t_R 25 min), **218** (0.6 mg, t_R 29 min), and **220** (0.4 mg, t_R 22 min). Fraction 6 was further subjected to reversed-phase HPLC with a 70-80% MeOH/H_2O gradient over 80 min and yielded **221** (0.5 mg, t_R 29 min), **218** (0.2 mg, t_R 34 min), **219** (0.6 mg, t_R 34 min), and **220** (0.5 mg, t_R 24 min). Due to the degradations of **219** and **220** in DMSO-d_6, a third extract (299.5 mg extract from 2 x 2 L culture) was purified by the same procedure to produce **217** (0.3 mg) and **218** (0.1 mg), **219** (0.5 mg) and **220** (0.7 mg). Material obtained for **219** and **220** was used to complete the structure elucidations in $CDCl_3$.

A.3.1.3.1 12-*epi*-Fischerindole I nitrile (217)

Amorphous white powder; $[\alpha]_D^{25}$ -44.0º (*c* 0.07, $CHCl_3$); UV (MeOH) λ_{max} (log ε) 223 (6.10) 277 (5.76) 323 (5.84); IR ν_{max} 3283, 2962, 2924, 2852, 2204, 1715, 1616, 1474, 1453 cm^{-1}; ^1H and ^{13}C NMR data, see Table 8; HRESIMS *m/z* 335.1331 ($[M-H]^-$, calcd for $C_{21}H_{20}ClN_2$, 335.1393).

A.3.1.3.2 Deschloro 12-*epi*-fischerindole I nitrile (218)

Amorphous white powder; $[\alpha]_D^{25}$ -115.6º (*c* 0.07, $CHCl_3$); UV (MeOH) λ_{max} (log ε) 221 (6.75) 277 (5.30) 321 (5.46); IR ν_{max} 3743, 3290, 2953, 2926, 2856, 2200, 1686, 1617, 1455 cm^{-1}; ^1H and ^{13}C NMR data, see Table 8; HRESIMS *m/z* 301.1718 ($[M-H]^-$, calcd for $C_{21}H_{21}N_2$, 301.1783).

A.3.1.3.3 12-*epi*-Fischerindole W nitrile (219)

Amorphous white powder; $[\alpha]_D^{25}$ -22.0º (*c* 0.05, $CHCl_3$); UV (MeOH) λ_{max} (log ε) 237 (5.49) 262 (5.15) 298 (5.03) 328 (4.73); ^1H and ^{13}C NMR data, see Table 9; HRESIMS *m/z* 333.1175 ($[M-H]^-$, calcd for $C_{21}H_{18}ClN_2$, 333.1236).

A.3.1.3.4 Deschloro 12-*epi*-fischerindole W nitrile (220)

Amorphous white powder; $[\alpha]_D^{25}$ -18.3º (*c* 0.08, $CHCl_3$); UV (MeOH) λ_{max} (log ε) 237 (5.67) 262 (5.32) 298 (5.22) 328 (4.91); ^1H and ^{13}C NMR data, see Table 9; HRESIMS *m/z* 299.1556 ($[M-H]^-$, calcd for $C_{21}H_{19}N_2$, 299.1626).

A.3.2 Chemical structures of the isolates

A.3.2.1 Structures of new compounds from *Fischerella* sp. (SAG 46.79)

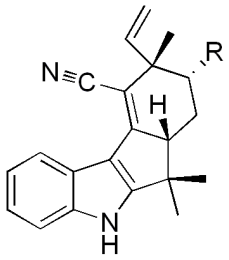

12-*epi*-fischerindole I nitrile (**217**) R=Cl
Deschloro 12-*epi*-fischerindole I nitrile (**218**) R=H

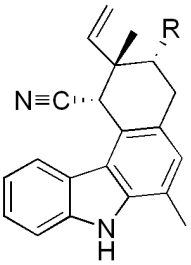

12-*epi*-fischerindole W nitrile (**219**) R=Cl
Deschloro 12-*epi*-fischerindole W nitrile (**220**) R=H

Figure 43. Structures of new compounds isolated from *Fischerella* sp. (SAG 46.79)

A.3.2.2 Structure of a previously reported compound, hapalosin (221), from *Fischerella* sp. (SAG 46.79)

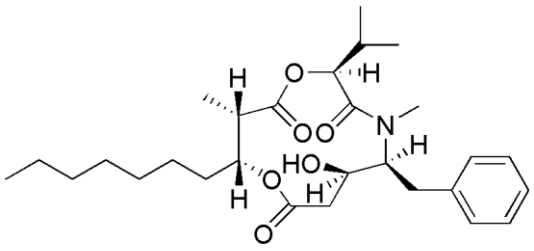

221 Hapalosin

Figure 44. Structure of hapalosin

A.3.3 Structure elucidation

A.3.3.1 12-*epi*-fischerindole I nitrile (217) and deschloro 12-*epi*-fischerindole I nitrile (218)

12-*epi*-Fischerindole I nitrile (**217**) was obtained as a white amorphous powder. The HRESIMS pseudo-molecular $[M-H]^-$ ion at *m/z* 335.1331 indicated a molecular formula of $C_{21}H_{21}ClN_2$. The presence of a chlorine atom was confirmed by the 3:1 molecular ion cluster at *m/z* 335/337.

Interpretation of the ^{1}H NMR and COSY spectra of **217** (Table 8, Figure 45) revealed a 1,2-disubstituted indole moiety [δ_H 12.01 (H-1), 8.20 (H-4), 7.41 (H-7), 7.16 (H-6), and 7.10 (H-5)], a vinyl group [δ_H 5.94 (H-20), 5.29 (H-21*E*), and 5.05 (H-21*Z*)], and three methyl singlets [δ_H 1.49 (H_3-19), 1.42 (H_3-18), and 1.12 (H_3-17)]. Furthermore, an isolated spin system consisting of two methines [δ_H 4.46 (H-13) and 3.26 (H-15)] connected by a methylene [δ_H 2.13 (H-14$_{eq}$) and 2.00 (H-14$_{ax}$)] was observed. Together, these findings indicated that **217** was a 2,3-disubstituted indole of the fischerindole class.

The ^{13}C NMR spectrum of **217** displayed all 21 carbon resonances, required by the molecular formula. Thirteen resonances appeared in the range between 90 and 150 ppm, and eight of these (δ_C 163.2, 141.6, 122.7, 122.0, 121.7, 121.1, 113.1, and 112.8) were assigned to an indole moiety. The carbon resonances at δ_C 141.4 and 117.1 and at δ_C 156.0 and 96.6 were assigned to a vinyl group and a tetra substituted double bond, respectively. The final carbon resonance at δ_C 120.6 was attributed to a nitrile moiety.

These fragments were connected based on correlations observed in the HMBC spectrum (Table 8 and Figure 45). The indole moiety was confirmed by correlations from H-4 to C-3, C-6, and C-8, and from H-5 to C-7 and C-9. This indole moiety was connected to the *gem*-dimethyl group at C-16 by correlations from both H_3-17 and H_3-18 to C-2. Correlations from both H_3-17 and H_3-18 to C-16 and C-15 further connected this group to the H_{13}-H_{15} fragment. The vinyl and H_3-19 methyl groups were placed on C-12, and in turn connected to C-13 by correlations from H-20 to C-11, C-12, and C-19, and from H_3-19 to C-11, C-12, C-13, and C-20. Moreover, correlations from H-15 to C-10, C-11, C-14, C-16, C-18, and C-22, established the fischerindole ring system, and placed the nitrile moiety at C-11.

^{1}H and ^{13}C data of the structurally related 12-*epi*-fischerindole I isonitrile [132] were available for comparison with those of **1**. However, only carbon chemical shifts were compared since spectra of the 12-*epi*-fischerindole I isonitrile were recorded in CD_2Cl_2. A comparison of the ^{13}C NMR chemical shifts of **217** with those reported for the structurally related 12-*epi*-fischerindole I isonitrile indicated that the major differences were observed at C-22 (δ_C 164.8 vs 120.6 in **217**) and surrounding carbons [C-3 (δ_C 141.0 vs

δ_C 112.8 in **217**), C-10 (δ_C 140.7 vs 156.0 in **217**), and C-11 (δ_C 113.0 vs 96.6 in **217**)]. This difference in carbon chemical shifts further confirmed that a nitrile moiety had replaced the isonitrile moiety found in 12-*epi*-fischerindole I isonitrile. Based on these findings, the structure of **217** was established as 12-*epi*-fischerindole I nitrile.

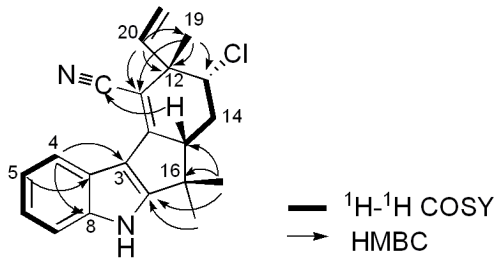

Figure 45. Key COSY and HMBC correlations of 12-*epi*-fischerindole I nitrile (**217**)

The HRESIMS of deschloro 12-*epi*-fischerindole I nitrile (**218**) displayed a pseudo-molecular $[M-H]^-$ ion at *m/z* 301.1718, corresponding to the molecular formula $C_{21}H_{22}N_2$, indicating the absence of a chlorine atom.

Examination of NMR spectra revealed **218** to be closely related to **217** (Table 8). The major difference being that the H-13 methine signal (δ_H 4.46) in the ^{1}H NMR spectrum of **217** had been replaced by methylene signals [δ_H 1.84 (H-13$_{eq}$) and 1.61 (H-13$_{ax}$)] in **218**.

Similarly in the ^{13}C NMR spectrum, the C-13 methine (δ_C 66.4) in **217** had been replaced by a methylene carbon (δ_C 35.4) in **234**. Analysis of COSY spectrum of **234** further indicated the presence of a CH-CH_2-CH_2 spin system from C-15 to C-13, and the planar structure of **234** was determined to be the deschloro derivative of **217**, deschloro 12-*epi*-fischerindole I nitrile.

TABLE 8. NMR DATA OF 12-*EPI*-FISCHERINDOLE I NITRILE (**217**) AND DESCHLORO 12-*EPI*-FISCHERINDOLE I NITRILE (**218**) IN DMSO-d_6.

Position	**217**			**218**		
	δ_C, mult.[a]	δ_H, mult. (*J* in Hz)[b]	HMBC[b]	δ_C, mult.[c]	δ_H, mult. (*J* in Hz)[b]	HMBC[b]
1		12.01, br s	2, 7, 8, 9		12.01, br s	
2	163.2, C			163.0, C		
3	112.8, C			113.3, C		
4	121.7, CH	8.20, d (7.9)	3, 6, 8	121.3, CH	8.21, d (8.1)	3, 6, 8
5	121.1, CH	7.10, dd (7.9, 7.9)	7, 9	120.4, CH	7.07, dd (8.1, 8.1)	7, 9
6	122.7, CH	7.16, dd (7.9, 7.9)	4, 8	122.0, CH	7.13, dd (8.1, 8.1)	4, 8
7	113.1, CH	7.41, d (7.9)	5	112.5, CH	7.38, d (8.1)	5
8	141.6, C			141.1, C		
9	122.0, C			121.49, C		
10	156.0, C			156.3, C		
11	96.6, C			96.8, C		
12	44.9, C			39.8, C		
13_{ax}	66.4. CH	4.46, dd (12.0, 3.0)	20	35.4, CH_2	1.61, ddd (12.6, 2.4)	15, 16, 19, 20
13_{eq}					1.84, ddd (12.6, 5.4, 2.4)	11, 14, 15, 16
14_{ax}	29.7, CH_2	2.00, ddd (12.0)		18.1, CH_2	1.48, dddd (12.6, 2.4)	15, 16
14_{eq}		2.13, ddd (12.0, 5.4, 3.0)			1.67, m	13, 16
15	58.1, CH	3.26, dd (12.0, 5.4)	10, 11, 14, 16, 18, 22	58.5, CH	2.92, dd (12.6, 5.4)	10, 11, 14, 16, 18, 22
16	40.5, C			40.1, C		
17	25.3, CH_3	1.12, s	2, 15, 16, 18	25.0, CH_3	1.07, s	2, 15, 16, 18
18	24.9, CH_3	1.42, s	2, 15, 16, 17	24.7, CH_3	1.40, s	2, 15, 16, 17
19	24.0, CH_3	1.49, s	11, 12, 13, 20	27.2, CH_3	1.32, s	11, 12, 13, 20
20	141.4, CH	5.94, dd (17.2, 10.5)	11, 12, 19	146.1, CH	5.80, ddd (17.2, 10.4)	11, 12, 13, 19
21*E*	117.1, CH_2	5.29, d (10.5)	12	113.6, CH_2	5.45, d (10.4)	12
21*Z*		5.05, d (17.2)	12, 20		4.91, d (17.2)	12, 20
22	120.6, C			121.40, C		

[a] Chemical shift determined from gHSQC and gHMBC experiments recorded at 600 MHz. [b] Recorded at 600 MHz. [c] DEPTQ experiment recorded at 226 MHz.

A.3.3.2 12-*epi*-fischerindole W nitrile (219) and deschloro 12-*epi*-fischerindole W nitrile (220)

12-*epi*-Fischerindole W nitrile (**219**) was obtained as a white amorphous powder. The HRESIMS pseudo-molecular $[M-H]^-$ ion at *m/z* 333.1175 indicated a molecular formula of $C_{21}H_{19}ClN_2$. The presence of a chlorine atom was confirmed by the 3:1 molecular ion cluster at *m/z* 333/335.

Unlike **217** and **218**, the NMR spectra of **219** were recorded in $CDCl_3$ since the structure was found to be unstable in DMSO-d_6. Despite the use of different solvents, some notable changes in chemical shifts between **219** and **217** were observed. A comparison of the ^{1}H NMR spectra of **219** and **217** (Table 1 and 2) revealed that the methine (H-15) and one of the *gem*-dimethyl singlets (H_3-17) in **217** had disappeared, while two new methine singlets [δ_H 7.30 (H-16) and δ_H 4.79 (H-11)] had appeared. Furthermore, the chemical shift of H_3-18 (δ_H 1.42) had shifted downfield (δ_H 2.41). Similarly in the ^{13}C NMR spectra, two quaternary carbons C-11 (δ_C 96.6) and C-16 (δ_C 40.5) found in **217** had been replaced by two methines [δ_C 41.0 (C-11) and 112.4 (C-16)]. Moreover, the methine at C-15 (δ_C 58.1) found in **217** had been replaced by a new carbon at δ_C 125.0. In addition, a new carbon at δ_C 124.7 (C-17) in **219** had replaced one of the *gem*-dimethyls in **217**. Together, these findings indicated that the five-membered ring found in **217** had been rearranged in **219**.

Three spin systems, H-4 to H-7, H-13 to H-14, and H-20 to H_2-21, were observed in the COSY spectrum of **219** (Table 9 and Figure 46) and it indicated that the H_{13}-H_{15} sequence observed in both **217** and **219** was shortened to a H_{13}-H_{14} sequence in **219**. This finding along with chemical shift changes in the ^{13}C NMR spectra between **217** and **219** indicated that a new six-membered ring had been introduced in **219** by incorporation of one of the *gem*-dimethyls from **217** into the ring.

The fragments from the COSY spectrum were connected by analysis of HMBC correlations to determine the planar structure of **219**. Similar as observed for both **217** and **218**, the connectivity of the indole moiety in **219** was established by correlations from H-4 to C-3, C-6, and C-8, from H-5 to C-7, and from H-7 to C-9. The vinyl and H_3-19 methyl groups were positioned on C-12 by correlations from H-20 to C-12 and C-19 as well as from H_3-19 to C-12 and C-20. Both of these groups were further connected to the H_{13}-H_{14} fragment and to C-11 by correlations from both H-20 and H_3-19 to C-11 as well as from H_3-19 to C-13. The position of the nitrile moiety at C-11 and the connectivity from C-11 to C-10 and from C-10 to C-3 were determined by correlations from H-11 to C-3, C-12, C-13, C-19, C-20, and C-22. The planar structure of **219** was completed by the correlations observed from H_3-18 to C-2, C-17, C-16, from both H-14_{ax} and H-16 to C-10, and from H_2-14 to C-15. Together, these findings indicated that 12-*epi*-fischerindole

W nitrile (**219**) possess a new carbon skeleton in which the five-membered ring, found in all previously known fischerindoles, has been replaced with a six-membered ring.

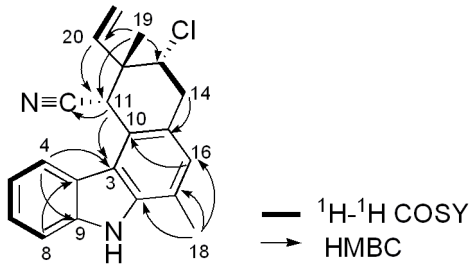

Figure 46. Key COSY and HMBC correlations of 12-*epi*-fischerindole W nitrile (**219**)

The HRESIMS of deschloro 12-*epi*-fischerindole W nitrile (**220**) displayed a pseudo-molecular $[M-H]^-$ ion at *m/z* 299.1556, corresponding to the molecular formula $C_{21}H_{20}N_2$, indicating the absence of a chlorine atom.

Again, $CDCl_3$ was used to record NMR spectra for **220** since the structure was found to be unstable in DMSO-d_6. The NMR spectra of **220** were similar to that of **219**. A comparison of the ^{1}H NMR spectra of **219** and **220** (Table 9) indicated that the H-13 methine signal (δ_H 4.72) found in **219** had been replaced by a new methylene [δ_H 2.23 (H-13$_{ax}$) and δ_H 1.98 (H-13$_{eq}$)]. Analogously, this was observed in the ^{13}C NMR spectra, where the C-13 methine signal (δ_C 62.7) found in **219** had been replaced by a new methylene carbon (δ_C 31.5).

In the COSY spectrum of **220**, a CH_2-CH_2 spin system designated for C-13 and C-14 was also present. Together, these findings indicated **220** to be the deschloro derivative of **219**, deschloro 12-*epi*-fischerindole W nitrile.

TABLE 9. NMR DATA OF 12-*EPI*-FISCHERINDOLE W NITRILE (**219**) AND DESCHLORO 12-*EPI*-FISCHERINDOLE W NITRILE (**220**) IN $CDCL_3$.

Position	**219**			**220**		
	δ_C, mult.[a]	δ_H, mult. (*J* in Hz)[b]	HMBC[b]	δ_C, mult.[c]	δ_H[b], mult. (*J* in Hz)[b]	HMBC[b]
1		8.15, br s			8.08, br s	
2	134.8, C			135.6, C		
3	124.8, C			124.4, C		
4	122.3, CH	8.15, d (7.8)	3, 6, 8	122.4, CH	8.21, d (7.8)	3, 8
5	120.2, CH	7.34, dd (7.8, 7.8)	7	119.8, CH	7.32, dd (7.8, 7.8)	7, 9
6	125.8, CH	7.48, dd (7.8, 7.8)	4, 8	125.3, CH	7.45, dd (7.8, 7.8)	8
7	111.0, CH	7.50, d (7.8)	9	110.7, CH	7.49, d (7.8)	9
8	139.7, C			139.7, C		
9	122.0, C			121.4, C		
10	118.0, C			118.8, C		
11	41.0, CH	4.79, s	3, 12, 13, 19, 20, 22	39.4, CH	4.57, s	12, 13, 15, 22
12	42.6, C			37.8, C		
13_{ax}	62.7, CH	4.72, dd (11.5, 5.8)	20	31.5, CH_2	2.23, m	
13_{eq}					1.98, dd (13.2, 6.4)	
14_{ax}	36.0, CH_2	2.97, dd (16.6, 11.5)	10, 13, 15	24.3, CH_2	2.90, dd (17.2, 6.4)	15
14_{eq}		3.46, dd (16.6, 5.8)	12, 13, 15, 20		2.71, m	
15	125.0, C [d]			126.0, C		
16	112.4, CH	7.30, s	10, 17, 18	111.7, CH	7.27, s	10, 15, 18
17	124.7, C			125.7, C		
18	20.6, CH_3	2.41, s	2, 16, 17	20.6, CH_3	2.39, s	2, 16, 17
19	24.8, CH_3	1.76, s	11, 12, 13, 20	27.4, CH_3	1.59, s	11, 12, 13, 20
20	135.6, CH	6.00, dd (17.5, 11.0)	11, 12, 19	141.3, CH	5.80, dd (17.5, 11.0)	
21*E*	117.3, CH_2	5.12, d (11.0)	12	114.0, CH_2	4.94, d (11.0)	12
21*Z*		5.02, d (17.5)	12, 20		4.09, d (17.5)	12
22	118.6, C			119.1, C		

[a] DEPTQ experiment recorded at 226 MHz. [b] Recorded at 600 MHz. [c] Chemical shift determined from gHSQC and gHMBC experiments recorded at 600 MHz. [d] Chemical shift determined from gHMBC experiment recorded at 600 MHz.

A.3.3.3 Configurational analysis of nitrile-containing fischerindoles

The relative stereoconfigurations of **217**-**220** were deduced based on ^{1}H-^{1}H coupling constant analysis and/or correlations observed in 1D selective or 2D NOESY spectra.

Large coupling constants between H-14$_{ax}$ and H-13 (J=12.0 Hz) and H-14$_{ax}$ and H-15 (J=12.0 Hz) were observed for 12-*epi*-fischerindole I nitrile (**217**), indicating both H-13 and H-15 to be in axial orientations. The NOE correlations between H-13 and H-14$_{eq}$, H-15, and H$_3$-19 in the 2D NOESY spectrum further supported all to be in the same plane (Figure 47). Based on these findings, the relative configuration of **230** was determined as 12*R**, 13*R**, and 15*R**. The NOE correlation between H-15 and H$_3$-18 was supported H$_3$-18 also to be in the same plane. Deschloro 12-*epi*-fischerindole I nitrile (**218**) also displayed a large coupling constant between H-14$_{ax}$ and H-15 (J=12.6 Hz), indicating the H-15 to be in the axial orientation. 1D selective NOESY experiments were further performed to firmly determine the relative stereoconfiguration of **218**. Irradiation at the resonance frequency of H-15 (δ_H 2.92) produced NOE correlations with H-14$_{eq}$ and H-13$_{ax}$. Irradiation of the H-13$_{ax}$ (δ_H 1.61) produced NOE correlations to H-15 and H$_3$-19, indicating these to be in the same plane, and the relative stereoconfiguration of **218** was determined as 12*R** and 15*R**.

12-*epi*-Fischerindole W nitrile (**219**) displayed a large coupling constant between H-14$_{ax}$ and H-13 (J=11.5 Hz), suggesting that H-13 was in the axial orientation. In addition, the 2D NOESY spectrum of **219** displayed NOE correlations between H-11 and H$_3$-19 and H-13$_{ax}$, indicating all to be in the same plane (Figure 47). Thus, the relative stereoconfiguration of **219** was established as 11*R**, 12*R**, and 13*R**. Due to decomposition of 12-*epi*-fischerindole W nitrile (**220**), no NOESY NMR experiments were obtained. However, we assume that the relative stereoconfiguration of **220** is 11*R** and 12*R** as depicted since **219** and **220** likely share a common biosynthesis.

Figure 47. Key NOESY correlations of 12-e*pi*-fischerindole I nitrile (**217**, left) and 12-*epi*-fischerindole W nitrile (**219**, right)

A.4 Biological activity of the compounds isolated from *Fischerella* sp. (SAG 46.79)

Cytotoxicity of the isolates was evaluated using a set of human cancer cell lines designated HT-29 colon, NCI-H460 large lung, MCF-7 breast, and SF268 glioblastoma.

Deschloro 12-*epi*-fischerindole I nitrile (**218**) was found to be weakly cytotoxic against HT-29 cells with an IC_{50} value of 23 µM, and hapalosin (**221**) also showed similar IC_{50} values of 22 and 27 µM against HT-29 and MCF-7 cells, respectively. However, both **218** and **221** were found to be inactive against all other cancer cells displaying IC_{50} values of higher than 40 µM.

All isolates were also evaluated for the inhibition of 20S proteasome activity, and only hapalosin showed mild activity with an IC_{50} value of 12 µM.

It should be noted that 12-*epi*-fischerindole W nitrile (**219**) and deschloro 12-*epi*-fischerindole W nitrile (**220**) were found to be structurally unstable in DMSO-d_6. Thus, it is inevitable that degradation products of **219** and **220** were evaluated in all biological assays.

A.5 Conclusion

The bioassay-guided chemical investigation of the cyanobacterium *Fischerella* sp. led to the isolation of four new fischerindoles. Most hapalindole-type alkaloids reported to date have either isonitrile or isothiocyanate substituents. The only report of a nitrile moiety is in ambiguine G and Q nitriles, and both are thought to be the products of rearrangements of ambiguine isonitrile precursors.[7, 13] All four isolates reported here are unusual fischerindole-type indole alkaloids in that they all contain a nitrile moiety.

Interestingly, the only difference between the previously reported 12-*epi*-fischerindole I isonitrile [132] and 12-*epi*-fischerindole I nitrile (**217**) is that the isonitrile has been replaced by a nitrile. This placement indicates a different biosynthetic origin of the nitrile moiety in **217**, rather than it being the product from a rearrangement of an isonitrile precursor as suggested for ambiguine G and Q nitriles.

12-*epi*-Fischerindole W nitrile (**219**) and deschloro 12-*epi*-fischerindole W nitrile (**220**) both contain a new ring system for fischerindole-type alkaloids, where the five-membered ring of the fischerindole skeleton has been expanded to a six-membered ring. Thus, the finding of compounds **219** and **220** suggests that a new biosynthetic pathway may be present in this cyanobacterium.

B. *Westiellopsis* sp. (SAG 20.93) and *Fischerella muscicola* (UTEX LB1829)

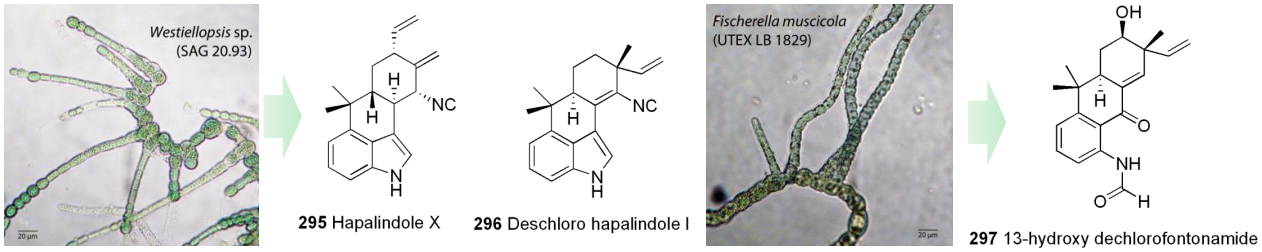

Figure 48. Photomicrographs of *Westiellopsis* sp. (SAG 20.93) and *Fischerella muscicola* (UTEX LB1829) and isolated compounds

Chemical investigation of two cultured cyanobacteria, *Westiellopsis* sp. (SAG strain number 20.93) and *Fischerella muscicola* (UTEX strain number LB1829), led to the isolation of three hapalindole-type alkaloids, namely hapalindole X (**295**), deschloro hapalindole I (**296**), and 13-hydroxy dechlorofontonamide (**297**), along with ten known indole alkaloids, hapalindoles A (**222**), C (**239**), G (**227**), H (**230**), I (**234**), J (**224**), and U (**228**), hapalonamide H (**258**), anhydrohapaloxindole A (**251**), and fischerindole L (**278**) and fischerellins A (**292**) and B (**293**). The structures were determined by a combination of spectroscopic analyses mainly based on 1D and 2D NMR and HRESIMS data. Selected compounds were evaluated for cytotoxicity and exhibited weak to moderate cytotoxicity against HT-29, MCF-7, NCI-H460, SF268, and IMR90 cells. All compounds, except **239**, were evaluated for 20S proteasome inhibition and displayed either weak or no inhibition at 25 µg/mL. Selected compounds were also evaluated for antimicrobial activity, and **295** and **222**, and **258** showed potent activity against both *M. tuberculosis* and *C. albicans* with MIC values ranging from 0.6 to 2.5 µM.

B.1 Taxonomic description of the genus *Westiellopsis*

According to Janet, M., the genus *Westiellopsis* belongs to the family Fischerellaceae in the order Stigonematales next to Chondrogloea in the phylum Cyanobacteria, domain Bacteria [268]. The taxonomic descritipns of *Westiellopsis* by Janet M. is as follows.

Westiellopsis gen. nov.

Thallus filamentous with true branching; filaments of two kinds, primary filaments slightly thicker and more or less creeping, secondary filaments, thinner and generally growing erect; filaments without a sheath and consisting of one row of cells; heterocysts intercalary; the dilated terminal portions of the secondary branches, by profuse transverse and longitudinal division, for, clusters of rounded cells (pseudohormocysts) the contents of which escape as gonidia and develop into new plants.

Westiellopsis prolifica sp. nov.

Characters same as for the genus; main filaments torulose and consisting of short barrel-shaped cells, 8-12 μ broad and as long as broad or slightly longer; branch-filaments thinner and elongate, not constricted at the crosswalls, with elongate cylindrical cells, 4-6 μ broad; heterocysts oblongcylindrical, 5.5-6 μ broad and 10.5-22 μ long. Gonidia formed singly from each cell of the pseudohormocyst, 8.5-9 μ in diameter.

SAG 20.93 was isolated by S. Vallisuta in 1986 and deposited in The Culture Collection of Algae at the University of Göttingen. UTEX LB1829 was isolated by Tiwari, G. L. and deposited in The Culture Collection of Algae at the University of Texas at Austin (http://web.biosci.utexas.edu) in 1971. Both strains were purchased, maintained under laboratory conditions, and used for biological and chemical evaluations.

B.2 Compounds previously isolated from cyanobacteria of the genus *Westiellopsis*

The cyanobacteria belonging to the genus *Westiellopsis* have produced cytotoxic indole alkaloids, westiellamide (**203**) and welwitindolinones (**204**-**209**), and chemical and biological properties of these compounds are summarized in the chapter 2.

B.3 Chemical investigation of the cultured cyanobacteria *Westiellopsis* sp. (SAG 20.93) and *Fischerella muscicola* (UTEX LB1829)

B.3.1 Experimental

B.3.1.1 General experimental procedures

Optical rotations were measured with a Perkin-Elmer 241 polarimeter. UV spectra were recorded on a Varian Cary 50 Bio spectrophotometer. IR spectra were obtained on a FTIR-410 Fourier transform infrared spectrometer. 1D and 2D NMR spectra were obtained at room temperature on a Bruker Avance DRX 600 MHz spectrometer with a 5 mm CPTXI Z-gradient probe. ^{13}C NMR spectrum was obtained on a

Bruker AV 900 MHz NMR spectrometer with a 5 mm ATM CPTCI Z-gradient probe. ^{1}H and ^{13}C chemical shifts were referenced to the corresponding solvent peaks. HRESIMS were obtained using a Shimadzu IT-TOF spectrometer.

B.3.1.2 Biological material

Westiellopsis sp. and *Fischerella muscicola* were acquired from the culture collections of Algae at the University of Göttingen (SAG strain number 20.93) and at the University of Texas at Austin (UTEX strain number LB1829), respectively. Each cyanobacterium was grown in a 2.8 L Fernback flask containing 2 L of inorganic media (Z media for SAG 20.93 and BG-12 media for UTEX LB1829) under aeration.[23] Cultures were illuminated with fluorescent lamps at 1.93 klx with an 18/6 hours light/dark cycle at 22 °C. After eight weeks, the biomass of each cyanobacterium was harvested by centrifugation, and lyophilized.

B.3.1.3 Extraction and isolation

The lyophilized biomass (1.00 g) of *Westiellopsis* sp., from total of 4 L culture, was extracted by maceration with CH_2Cl_2/MeOH (1:1 v/v) at room temperature and the solvent was evaporated *in vacuo*. The extract (330.7 mg) was redissolved in CH_2Cl_2/MeOH (1:1 v/v) and mixed with Diaion® HP20SS resin. The mixture was dried *in vacuo* and the dried mixture was fractionated on a Diaion® column using a step gradient with increasing amount of 2-propanol in water to afford eight fractions. Fractions 5-7, eluting with 70%, 80%, and 90% 2-propanol, respectively, displayed cytotoxicity against HT-29 cells. Fractions 5 and 6 were subjected to HPLC-ESIMS analysis (Varian Microsob C_8, 2.0 x 250 mm, flow rate 0.2 mL/min) with 30-100% MeOH gradient over 35 min containing 0.1% formic acid. The analysis of MS spectra indicated the presence of potentially new indole alkaloids. Fractions 5 and 6 were combined and further subjected to reversed-phase HPLC column (Alltima C_8 Dynamax, 10 x 250 mm, flow rate 3 mL/min) with 70-85% MeOH/H_2O gradient over 40 min and yielded **295** (1.05 mg, t_R 40.0 min) and **296** (0.62 mg, t_R 42.8 min) along with **258** (1.02 mg, t_R 16.0 min), **228** (0.66 mg, t_R 26.2 min), **239** (0.41 mg, t_R 28.5 min), **227** (0.29 mg, t_R 29.3 min), **224** (2.92 mg, t_R 30.5 min), **222** (5.15 mg, t_R 32.4 min), **230** (4.18 mg, t_R 37.8 min), and **234** (0.64 mg, t_R 43.5 min). The extract (327.0 mg) of *Fischerella muscicola* was obtained from the lyophilized biomass (6.26 g from 13 L culture) as described above. Eight fractions were obtained using the Diaion fractionation protocol described above. The combined fractions 5-7 (70%, 80%, and 90% 2-

propanol) were subjected to reversed-phase HPLC column (Alltima C_8, 10 x 250 mm, flow rate 3.0 mL/min) with 80% MeOH isocratic to yield **297** (0.94 mg, t_R 15.2 min) along with **278** (1.09 mg, t_R 13.3 min), **224** (1.14 mg, t_R 14.1 min), **222** (3.86 mg, t_R 15.9 min), and **234** (0.49 mg, t_R 17.6 min), **292** (1.06 mg, t_R 18.8 min) and **293** (1.27 mg, t_R 21.7 min). Fraction 6 was subjected to reversed-phase HPLC (Alltima C_8, 10 x 250 mm, flow rate 3.0 mL/min) with 70-85% MeOH/H_2O gradient over 50 min and yielded anhydrohapaloxindole A (1.13 mg, t_R 26.8 min).

B.3.1.3.1 Hapalindole X (295)

Yellow amorphous powder; $[\alpha]^{25}_D$ +138.0° ($CHCl_3$, *c* 0.14); UV (MeOH) λ_{max} (log *ε*) 223 (6.48) 275 (7.32); IR (neat) ν_{max} 3410, 2969, 2142, 1630, 1437, 1374, 1093, 920, 825, 776, 749 cm^{-1}; ^1H and ^{13}C NMR, see Table 10; HRESIMS *m/z* 303.1853 $[M+H]^+$ (calcd for $C_{21}H_{23}N_2$, 303.1861).

B.3.1.3.2 Deschloro hapalindole I (296)

White amorphous powder; $[\alpha]^{25}_D$ +11.0° ($CHCl_3$, *c* 0.05); UV (MeOH) λ_{max} (log *ε*) 223 (8.31) 247 (7.63) 280 (7.32) 324 (7.67); IR (neat) ν_{max} 3478, 2924, 2135, 1683, 1601, 1457, 1377, 1207, 1138, 1056, 843, 749, 724 cm^{-1}; ^1H and ^{13}C NMR, see Table 11; HRESIMS *m/z* 303.1863 $[M+H]^+$ (calcd for $C_{21}H_{23}N_2$, 303.1861).

B.3.1.3.3 13-hydroxy dechlorofontonamide (297)

Pale yellow amorphous powder; $[\alpha]^{25}_D$ -45.6° ($CHCl_3$, *c* 0.05); UV (MeOH) λ_{max} (log *ε*) 207 (4.99) 238 (5.40) 287 (5.27) 343 (4.83); IR (neat) ν_{max} 3750, 3200, 1698, 1654, 1599, 1507, 1252, 902, 813 cm^{-1}; ^1H and ^{13}C NMR, see Table 12; HRESIMS *m/z* 324.1630 $[M-H]^-$ (calcd for $C_{20}H_{22}NO_3$, 324.1600).

B.3.2 Chemical structures of the isolates

B.3.2.1 Structures of new compounds from *Westiellopsis* sp. (SAG 20.93) and *Fischerella muscicola* (UTEX LB1829)

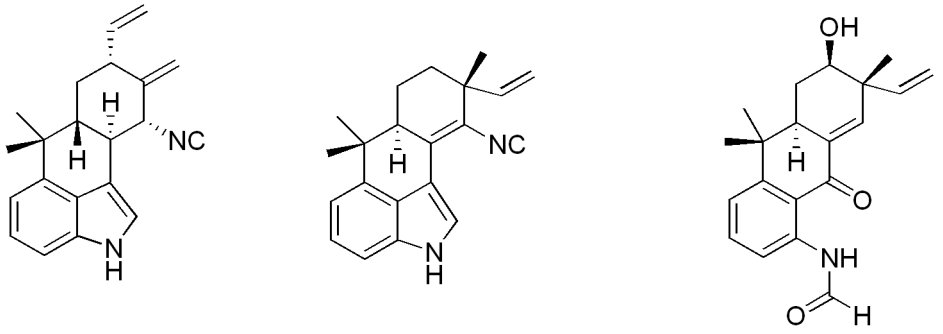

295 Hapalindole X **296** Deschloro hapalindole I **297** 13-hydroxy dechlorofontonamide

Figure 49. Structures of new compounds isolated from *Westiellopsis* sp. (SAG 20.93) and *Fischerella muscicola* (UTEX LB1829)

B.3.2.2 Structures of known compounds isolated from *Westiellopsis* sp. (SAG 20.93) and *Fischerella muscicola* (UTEX LB1829)

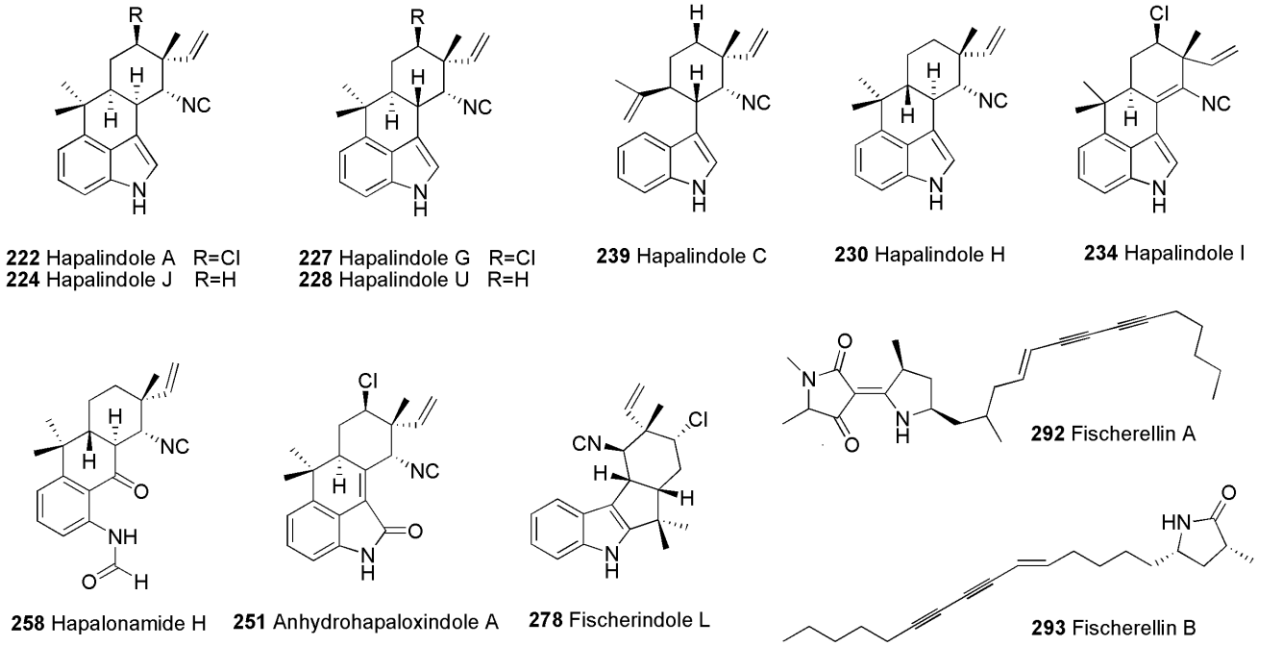

Figure 50. Structures of previously known compounds isolated from *Westiellopsis* sp. (SAG 20.93) and *Fischerella muscicola* (UTEX LB1829)

B.3.3 Structure elucidation

B.3.3.1 Hapalindole X (295)

Hapalindole X (**295**) was obtained as a yellow amorphous powder. The HRESIMS pseudo-molecular $[M+H]^+$ ion at *m/z* 303.1853 indicated a molecular formula of $C_{21}H_{22}N_2$.

The UV absorptions [λ_{max} (log ε) 223 (6.48) 275 (7.32) nm] and the ^{1}H NMR signals [δ_H 8.07 (H-1), 7.67 (H-2), 7.18 (H-6 and 7), and 7.02 (H-5)] indicated the presence of an indole moiety. The resonances at δ_H 5.94 (H-20), 5.19 (H-21*E*), and 5.14 (H-21*Z*) and at δ_H 1.48 (H_3-17) and 1.08 (H_3-18) showed the presence of a vinyl and two methyl groups, respectively. The two resonances at δ_H 5.45 (H-19a) and 5.06 (H-19b) were assigned to an exomethylene moiety. In addition, one methylene [δ_H 2.11 (H-14_{eq}) and 1.37 (H-14_{ax})] and four methines [δ_H 4.24 (H-11), 3.08 (H-10), 2.64 (H-13), and 1.77 (H-15)] were observed.

Correlations observed in the COSY spectrum connected these latter resonances and the vinyl group to form a spin system (Figure 51 and Table 10).

The ^{13}C NMR spectrum of **295** displayed all 21 carbon resonances, required by the molecular formula. Of the thirteen resonances observed between 100 and 160 ppm, eight resonances (δ_C 140.7, 133.7, 125.2, 123.3, 118.8, 113.4, 113.2, and 108.54) were assigned to the indole moiety and two resonances at δ_C 139.1 and 116.3 were attributed to the vinyl group. The carbon resonances at δ_C 144.7 and 108.53 were attributed to an exomethylene moiety, and the final carbon resonance at δ_C 159.5 was assigned to an isonitrile moiety.

These partial structures were connected by correlations observed in the HMBC spectrum (Figure 51 and Table 10). A correlation from H-5 to C-16 connected the indole moiety to the *gem*-dimethyl group. Correlations from both H_3-17 and H_3-18 to C-15 further connected this group to the large H-11 to H_2-21 fragment established in the COSY spectrum. The exomethylene moiety was placed at C-12 by a HMBC correlation from H-19a to C-12, and connected to C-11 and C-13 by correlations from both H-19a and H-19b to C-11 and C-13. The final connectivity from C-10 to C-3 was determined by a correlation from H-10 to C-3, and completed the planar structure of **295**. Although a direct correlation from H-11 to C-22 was not observed, the ^{13}C NMR chemical shift at δ_C 159.5 and a characteristic IR peak at 2142 cm^{-1} indicated the presence of an isonitrile. The position of the isonitrile at C-11 was determined based on the ^{13}C NMR chemical shift of C-11 (δ_C 63.0).

The relative stereoconfiguration of **295** was determined by correlations observed from 2D NOESY spectrum (Table 1). Correlations observed between H-13 and H-15, H-11, and H-14_{eq} indicated H-11, H-13, and H-15 all to be in the same plane. Correlations observed between H-14_{ax} and H-10 indicated these to be in the opposite plane. Thus, the relative configuration of **295** was established as 10*S**, 11*R**, 13*R**, and 15*R**.

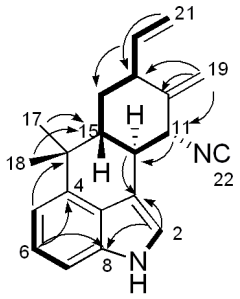

Figure 51. Key COSY (▬) and HMBC (⟶) correlations of hapalindole X (**295**)

TABLE 10. NMR DATA OF HAPALINDOLE X (**295**) IN $CDCL_3$

Position	δ_C, mult.[a]	δ_H	mult. (*J* in Hz)[b]	HMBC[b]	NOESY[b]
1		8.07	br s		2
2	118.8, CH	7.67	t (1.7)	3, 8, 9	1, 10, 11
3	113.4, C				
4	140.7, C				
5	113.2, CH	7.02	d (6.8)	7, 9, 16	17, 18
6	123.3, CH	7.18	t (6.8)	4, 8	
7	108.54, CH	7.18	d (6.8)	5, 9	
8	133.7, C				
9	125.2, C				
10	42.7, CH	3.08	t (11.1)	2, 3, 11, 15	11, 14_{ax}, 15, 18
11	63.0, CH	4.24	d (11.1)	10, 12	10, 13, 15
12	144.7, C				
13	45.9, CH	2.64	br t		11, 14_{eq}, 15, 20
14_{eq}	33.1, CH_2	2.11	dt (12.6, 3.0)	10, 12	13, 14_{ax}, 15
14_{ax}		1.37	d (12.6)	10, 12, 13, 15, 20	10, 14_{eq}, 18
15	48.7, CH	1.77	ddd (12.6, 11.1, 3.0)		11, 13, 14_{eq}
16	37.9, C				
17	25.08, CH_3	1.48	s	4, 15, 16, 18	5
18	25.05, CH_3	1.08	s	4, 15, 16, 17	5, 10
19a	108.53, CH_2	5.45	t (1.7)	11, 12, 13	11, 19b
19b		5.06	t (1.7)	11, 13	19a, 20
20	139.1, CH	5.94	ddd (17.6, 10.4, 7.8)	13, 14	14_{ax}, 21*E*, 21*Z*
21*E*	116.3, CH_2	5.19	dd (10.4, 1.7)	13	
21*Z*		5.14	dt (17.6, 1.7)	13, 20	13, 20
22	159.5, C				

[a] Recorded at 225 MHz.
[b] Recorded at 600 MHz.

B.3.3.2 Deschloro hapalindole I (296)

Deschloro hapalindole I (**296**) was obtained as a white amorphous powder. The HRESIMS pseudo-molecular $[M+H]^+$ ion at *m/z* 303.1863 indicated a molecular formula of $C_{21}H_{22}N_2$.

The ^{1}H NMR signals of an indole moiety [δ_H 8.32 (H-1), 7.89 (H-2), 7.20 (H-6 and H-7), and 7.04 (H-5)], a vinyl group [δ_H 5.94 (H-20), 5.21 (H-21*E*), and 5.18 (H-21*Z*)], and three methyl singlets [δ_H 1.52 (H_3-17), 1.36 (H_3-19), and 1.04 (H_3-18)] indicated **296** to be a hapalindole-type alkaloid. The UV absorptions [λ_{max} (log ε) 223 (8.31) 247 (7.63) 280 (7.32) 324 (7.67)] were markedly similar as those reported for hapalindole I [269]. A comparison of the ^{1}H NMR chemical shifts indicated that the major differences were observed at H-13 [δ_H 4.14 vs δ_H 1.76 (H-13$_{eq}$) and 1.72 (H-13$_{ax}$) in **296**] and H-14 [H-14$_{eq}$ (δ_H 2.41 vs δ_H 1.97 in **296**) and H-14$_{ax}$ (δ_H 2.23 vs δ_H 1.83 in **2**)]. In addition, minor differences in the ^{1}H NMR chemical shifts between **296** and hapalindole I were observed [H-21*E* (δ_H 5.46 vs δ_H 5.21 in **296**), H-21Z (δ_H 5.36 vs δ_H 5.18 in **296**), H-20 (δ_H 5.85 vs δ_H 5.94 in **296**), and H_3-19 (δ_H 1.47 vs δ_H 1.36 in **296**)]. This, combined with a molecular formula, indicated **296** to be the deschloro derivative of hapalindole I. The planar structure was confirmed by correlations observed in the COSY and HMBC spectra (Figure 52 and Table 11). The presence of an isonitrile moiety was confirmed by a characteristic IR peak at 2135 cm^{-1}.

The 2D NOESY spectrum was analyzed to determine the relative stereoconfiguration of **296**. Correlations observed between H-14$_{ax}$ and H_3-18 and H_3-19, and between H-15 and H-13$_{ax}$, H-14$_{eq}$, and H_3-17 indicated H-15 and H_3-19 to be in the opposite plane. Thus, the relative configuration of **296** was established as 12*R** and 15*S**, which is identical to that observed for hapalindole I.

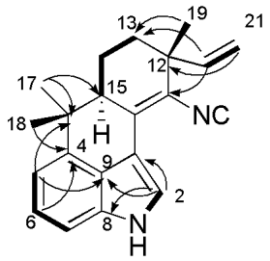

Figure 52. Key COSY (▬) and HMBC (⟶) correlations of deschloro hapalindole I (**296**)

TABLE 11. NMR DATA OF DESCHLORO HAPALINDOLE I (**296**) IN $CDCL_3$

Position	δ_C, mult.[a]	δ_H	mult. (*J* in Hz)[b]	HMBC[b]	NOESY[b]
1		8.32	br s		
2	123.3, CH	7.89	d (2.4)	3, 8, 9	
3	109.9, C				
4	140.7, C				
5	114.5, CH	7.04	m	4, 7, 9, 10, 16	17, 18
6	124.4, CH	7.20	m	4, 5, 8	
7	109.2, CH	7.20	m	5, 9	
8	133.1, C				
9	124.9, C				
10	132.4, C				
11	121.6, C				
12	40.6, C				
13_{eq}	35.8, CH_2	1.76	m	12, 19	19
13_{ax}		1.72	m		15
14_{eq}	20.1, CH_2	1.97	m	13	15
14_{ax}		1.83	m	13	18, 19
15	47.4, CH	2.66	dd (9.6, 6.6)	10, 11, 16, 17	13_{ax}, 14_{eq}, 14_{ax}, 17
16	38.9, C				
17	24.6, CH_3	1.52	s	4, 5, 16, 18	
18	26.1, CH_3	1.04	s	4, 5, 16, 17	14_{ax}
19	23.6, CH_3	1.36	s	11, 12, 13, 20	
20	145.2, CH	5.94	dd (17.4, 10.8)	11, 12, 13, 20	13_{ax}, 19
21*E*	114.7, CH_2	5.21	d (10.8)	12	19
21*Z*		5.18	d (17.4)	12, 20	19
22	[c]				

[a] Chemical shifts determined from gHSQC and gHMBC experiments recorded at 600 MHz.
[b] Recorded at 600 MHz.
[c] Signal not observed.

B.3.3.3 13-hydroxy dechlorofontonamide (297)

13-hydroxy dechlorofontonamide (**297**) was obtained as a pale yellow amorphous powder. The HRESIMS pseudo-molecular $[M-H]^-$ ion at *m/z* 324.1630 indicated a molecular formula of $C_{20}H_{23}NO_3$.

The ^1H NMR chemical shifts of **297** closely resembled those reported for dechlorofontonamide [270], with major differences being observed at H-13 [δ_H 1.73 (H-13_{eq}) and 1.64 (H-13_{ax}) vs δ_H 4.05 in **297**] and H-14 [H-14_{eq} (δ_H 1.96 vs δ_H 2.32 in **297**) and H-14_{ax} (δ_H 1.69 vs δ_H 2.09 in **297**)]. In addition, some minor differences in the ^1H NMR chemical shifts were observed at H-21*E* (δ_H 5.05 vs δ_H 5.20 in **297**), H-21Z (δ_H 5.01 vs δ_H 5.18 in **297**), H-20 (δ_H 5.85 vs δ_H 5.92 in **297**), and H_3-19 (δ_H 1.19 vs δ_H 1.35 in **297**). Together, these findings indicated **297** to be the hydroxy derivative of dechlorofontonamide, consistent with the molecular formula of $C_{20}H_{23}NO_3$.

The hydroxy group was placed at C-13 by analysis of the COSY spectrum, which indicated a CH-CH_2-CH spin system from C-15 to C-13, combined with the ^{13}C NMR chemical shift of C-13 (δ_C 64.8).

The relative stereoconfiguration of **297** was determined by analysis of 2D NOESY spectrum. Correlations observed between H-13 and H-15 and H-14_{eq} indicated H-13 and H-15 to be in the same plane. Correlations observed between H-14_{ax} and H_3-18 and H_3-19 indicated H-15 and H_3-17 to be in the opposite plane. Thus, the relative configuration of **297** was established as 12*R**, 13*S**, and 15*S**, which is identical to those reported for both fontonamide and dechlorofontonamide.

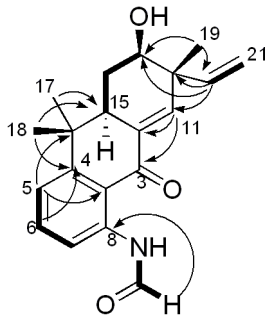

Figure 53. Key COSY (▬) and HMBC (⟶) correlations of 13-hydroxy dechlorofontonamide (**297**)

TABLE 12. NMR DATA OF 13-HYDROXY DECHLOROFONTONAMIDE (**297**) IN $CDCL_3$

Position	δ_C, mult.[a]	δ_H	mult. (*J* in Hz)[b]	HMBC[b]	NOESY[b]
1		11.67	s		2
2	159.9, CH	8.47	s	8	1
3	188.9, C				
4	153.7, C				
5	118.8, CH	7.19	d (8.2)	5, 9,16	17
6	135.3, CH	7.51	t (8.2)	4, 8	5
7	119.3, CH	8.59	d (8.2)	5	
8	140.8, C				
9	133.8, C				
10	133.6, C				
11	144.5, CH	7.10	d (2.4)	3, 10, 13, 15, 20	19
12	44.0, C				
13	64.8, CH	4.05	dd (12.8, 3.4)	14, 15, 19, 20	14_{eq}, 15, 20
13-OH		1.54	s		
14_{eq}	30.8, CH_2	2.32	ddd (12.8, 6.0, 3.4)	10, 12, 13	13, 15, 17
14_{ax}		2.09	q (12.8)	12, 13, 16	18, 19
15	44.2, CH	2.82	ddd (12.8, 6.0, 2.4)	11, 14, 16, 18	13, 17
16	37.8, C				
17	24.2, CH_3	1.44	s	4, 15, 16, 18	5
18	25.4, CH_3	1.04	s	4, 15, 16, 17	
19	19.9, CH_3	1.35	s	11, 12, 13, 20	11, 20, 21*Z*
20	142.9, CH	5.92	dd (17.4, 10.7)	11, 12, 13, 19	19
21*E*	115.1, CH_2	5.20	d (10.7)	12, 13	
21*Z*		5.18	d (17.4)	12, 20	19

[a] Chemical shifts determined from gHSQC and gHMBC experiments recorded at 600 MHz.
[b] Recorded at 600 MHz.

B.4 Biological activity of the compounds isolated from *Westiellopsis* sp. (SAG 20.93) and *Fischerella muscicola* (UTEX LB 1829)

Selected compounds were evaluated for cytotoxicity against HT-29, MCF-7, NCI-H460, and SF268 cancer cells, and IMR90 cells (Table 13). Hapalindole X (**295**) showed moderate cytotoxicity against all four cancer cells and relatively low cytotoxicity against IMR90 cells. The most cytotoxic compound was hapalindole H with IC_{50} values ranging from 8.5 to 31.9 μM, while 13-hydroxy dechlorofontonamide (**297**) was inactive in all cell lines tested.

Mo *et al* previously reported antimicrobial activities of hapalindole-related alkaloids [254, 255], and selected compounds were further evaluated for antimicrobial activity against a panel of microorganisms including *M. tuberculosis*, *M. smegmatis*, *C. albicans*, *E. coli*, and *A. baumanii* as well as for Vero cell toxicity (Table 14). Hapalindole X (**295**) displayed antimicrobial activities against both *M. tuberculosis* and *C. albicans* with MIC values of 2.5 μM with moderate cytotoxicity in the Vero cell assay with an IC_{50} value of 35.2 μM. Hapalindole I (**234**) showed inhibitory activity against *M. tuberculosis* with a MIC value of 2.0 μM with no detectable cytotoxicity against Vero cells. Hapalindole A (**222**) was the most active compound against *M. tuberculosis* with a MIC value of less than 0.6 μM. Both deschloro hapalindole I (**296**) and 13-hydroxy dechlorofontonamide (**297**) showed no antimicrobial activity. None of the evaluated compounds inhibited the growth of *A. baumanii*. Only hapalindole A (**222**) inhibited the growth of the gram-negative bacteria *E. coli* (MIC value of 8.0 μM).

TABLE 13. CYTOTOXIC ACTIVITY OF SELECTED COMPOUNDS ISOLATED FROM *WESTIELLOPSIS* SP. (SAG 20.93) AND *FISCHERELLA MUSCICOLA* (UTEX LB1829)

	IC_{50} (μM)				
	HT-29 [a]	MCF-7 [b]	NCI-H460 [c]	SF268 [d]	IMR90 [e]
Hapalindole X (**295**)	24.8	35.4 ± 2.8	23.0 ± 4.6	23.5 ± 9.5	113.2 ± 13.2
13-hydroxy dechlorofontonamide (**297**)	NA	>100	>100	>100	>100
Hapalindole I (**234**)	NA	>100	68.5 ± 11.0	93.1 ± 14.0	>100
Hapalindole J (**224**)	28.6	43.7 ± 10.0	12.0 ± 1.9	16.9 ± 3.4	39.1 ± 6.6
Hapalindole A (**222**)	31.3	30.7 ± 7.1	17.0 ± 4.8	16.3 ± 7.1	39.1 ± 10.2
Hapalindole U (**228**)	52.6	>100	>100	>100	>100
Hapalindole C (**239**)	52.6	>100	53.7 ± 15.5	88.6 ± 17.6	>100
Hapalindole H (**246**)	10.8	16.3 ± 3.3	8.5 ± 3.7	10.6 ± 4.5	31.9 ± 11.6
Anhydrohapaloxindole A (**251**)	NT	56.7 ± 10.5	18.7 ± 6.2	26.0 ± 9.0	80.1 ± 24.5
Fischerindole L (**278**)	48.2	28.3 ± 8.1	15.1 ± 2.6	17.4 ± 8.6	46.3 ± 13.7
Camptothecin	NT	0.08 ± 0.1	0.002 ± 0.0	0.07 ± 0.1	0.43 ± 0.5

[a] Human colon adenocarcinoma. [b] Human breast carcinoma. [c] Human large cell lung carcinoma. [d] Human glioblastoma cancer cell. [e] Human lung fibroblast normal cell. IC_{50} values were obtained by averaging the results from three independent experiments. NT represents not tested. NA represents not active.

TABLE 14. MIC AND IC_{50} VALUES FOR SELECTED COMPOUNDS ISOLATED FROM AND *WESTIELLOPSIS* SP. (SAG 20.93) AND *FISCHERELLA MUSCICOLA* (UTEX LB1829)

	MIC (μM)						IC_{50} (μM)
	M. Tuberculosis [a]	*M. smegmatis* [b]	*C. albicans* [c]	*S. aureus* [d]	*E. coli* [e]	*A. baumanii* [f]	Vero
Hapalindole X (**295**)	2.5	78.8	2.5	9.1	> 100	> 100	35.2
Deschloro hapalindole I (**296**)	> 100	> 100	> 100	> 100	> 100	> 100	> 100
13-hydroxy dechlorofontonamide (**297**)	> 100	> 100	> 100	> 100	> 100	> 100	> 100
Hapalindole I (**234**)	2.0	> 100	> 100	> 100	> 100	> 100	> 100
Hapalindole J (**224**)	4.3	39.0	0.7	8.4	> 100	> 100	31.9
Hapalindole A (**222**)	< 0.6	18.2	1.2	3.9	8.0	> 100	25.6
Anhydrohapaloxindole A (**251**)	16.2	>100	1.9	27.3	> 100	> 100	79.9
Hapalonamide H (**258**)	1.2	34.3	< 0.6	> 100	> 100	> 100	13.6
Fischerindole L (**278**)	22.0	63.0	1.2	6.4	> 100	> 100	< 9.2
Fischerellin A (**292**)	43.1	>100	> 100	> 100	> 100	> 100	94.8
Fischerellin B (**293**)	23.0	>100	> 100	> 100	> 100	> 100	> 100
Rifampin	0.20[g]						
Streptomycin		0.24[g]					
Amphotericin B			0.11[g]				
Ampicillin				0.54[g]			
Gentamycin					1.09[g]		
Deoxycycline						0.17[g]	

[a] *Mycobacterium tuberculosis*. [b] *Mycobacterium smegmatis*. [c] *Candida albicans*. [d] *Staphylococcus aureus*. [e] *Escherichia coli*. [f] *Acinetobacter baumannii*. [g] Results in μg/mL.

B.5 Conclusion

The bioassay-guided investigation of two cultured cyanobacteria, *Westiellopsis* sp. and *Fischerella muscicola*, both belonging to the order Stigonematales, led to the isolation of three new hapalindole-type alkaloids.

Hapalindole X (**295**) represents the first example of a tetracyclic hapalindole with an exocyclic methylene moiety. This moiety was found at C-12, a position substituted with a vinyl group and a methyl group in all previously reported tetracyclic hapalindoles. In hapalindole X (**295**), the vinyl group was moved at C-13 and suggesting the presence of a new biosynthetic pathway in this organism.

Most hapalindoles have been reported in both chlorinated and deschlorinated forms, and we herein report the isolation of deschlorinated hapalindole I (**296**).

Hapalonamides are considered oxidation products of the hapalindoles [271], and it can be assumed that 13-hydroxy dechlorofontonamide (**297**) is the oxidation product of hapalindole A (**222**).

C. *Nostoc* sp. (UIC 10047)

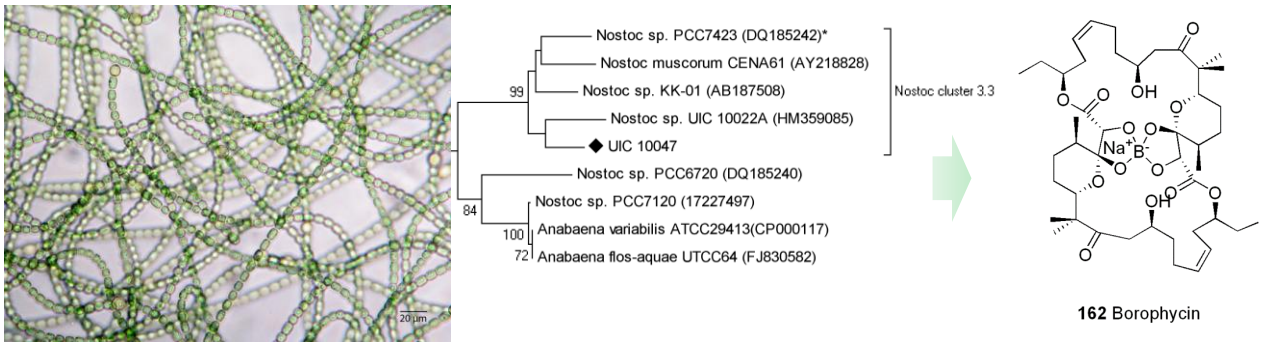

Figure 54. Photomicrograph of *Nostoc* sp. UIC 10047 and the isolate, borophycin (**162**)

Chemical investigation of the cultured cyanobacterium *Nostoc* sp. UIC 10047, isolated from a sample collected near east branch of DuPage River in Hidden Lake Forest Preserve in Illinois, led to the isolation of a known boron-containing compound, borophycin (**162**). The structure of borophycin (**162**) was confirmed by 1D and 2D NMR and MS data. Borophycin (**162**) showed cytotoxicity against HT-29, NCI-H460, MCF-7, SF268, and IMR90 cells with ED_{50} values ranging from 0.49 to 1.5 µM.

C.1 Taxonomic description of the genus *Nostoc*

According to Komárek *et al*., the genus *Nostoc* belongs to the family Nostocaceae in the order Nostocales in the phylum Cyanobacteria, domain Bacteria [246]. The genus *Nostoc* is characterized by the formation of heterocyte. The current taxonomic description of *Nostoc* by Komárek *et al*. is as follows.

> The thallus is microscopic or macroscopic, gelatinous, spherical or irregular gelatinous mats or flat colonies, smooth or warty at the surface, often with superficial mucilaginous exterior. Filamentous are typically coiled, forming irregular, loose, or dense clusters, concentrated near the colony surface. The sheath is mucilaginous, firm, wide, and sometimes yellow to brownish, but visible only in young colonies and confluent with common mucilage. The mucilage of the colony is sometimes colored, yellowish green or brownish. Trichomes are isopolar, sometimes very long, curled inside the colony, often moniliform. Cells are a barrel shaped and spherical, a uniform, shape and size along trichome, pale to bright blue-green or olive green. Heterocysts are barrel shaped or spherical, solitary, developing at ends of trichomes or intercalary. Akinetes are ellipsoidal, only slightly larger than vegetative cells, arising in rows between heterocysts. Cells

divide perpendicularly to the trichome axis; meristematic zones are unknown. Colony morphology changes during development, and reproduction is specific for each subgenus; motile hormogonia develop between heterocysts, by akinete germination or filament disintegration.

UIC 10047 was isolated from a sample collected near east branch of DuPage River in Hidden Lake Forest Preserve in DuPage, Illinois in June 14, 2007 (N41º45.55' W88º03.19'), and cultured under laboratory conditions.

C.2 Compounds previously isolated from cyanobacteria of the genus *Nostoc*

Several classes of natural products such as peptides, polyketides, alkaloids, terpenoids, have been isolated from cyanobacteria belonging to the genus *Nostoc* (Figures 55-58 and Table 15).

Nostocyclamide (**298**) and nostocyclamide M (**299**) (Figure 55), cyclic peptides from *Nostoc* sp., contain thiazole and oxazole moieties [272, 273]. Nostocyclamide showed inhibitory activity against the diatom *Navicula minima* and toxicity against *Brachionus calyciflorus*. Nostocyclamide M displayed allelopathic eddets against related cyanobacterial strains as well as grazer toxicity. Nostocyclin (**300**) (Figure 55), a 3-amino-6-hydroxy-2-piperidone-containing cyclic peptide from a *Nostoc* sp., inhibited protein phosphatase-1 activity [274]. It was not toxic in an intraperitoneal mouse assay or in the brine shrimp assay. Nostopeptins A (**301**) and B (**302**) (Figure 55), cyclic depsipeptides from *Nostoc minutum*, contained 3-amino-6-hydroxy-2-piperidone and showed inhibition of elastase with IC_{50} values of 1.3 and 11.0 μM as well as chymotrypsin with IC_{50} values of 1.4 and 1.6 μM, respectively [275]. Microviridins G (**303**) and H (**304**) (Figure 55), large polycyclic peptides, were isolated from *Nostoc munutum* and inhibited elastase [276]. Nostopeptolides A1-A3 (**305**-**307**) (Figure 55), cyclic depsipeptides, were obtained from a cryptophycin-producing *Nostoc* sp. [277]. None of the nostopeptolides showed antifungal, antibacterial, or inhibition of peptidase activities. Nostopeptin BN920 (**308**), nostoginins BN741 (**309**) and BN578 (**310**), and banyascyclamides A-C (**311**-**313**) (Figure 55) were isolated from the same *Nostoc* sp. [278]. Nostopeptin BN920, nostoginins BN578 and BN741 showed inhibition of several proteases such as serine endopeptidase, chymotrypsin, aminopeptidases, and bovine aminopeptidases. Insulapeptolides A-H (**314**-**321**) (Figure 55), amino-hydroxy-piperidone containing peptides from *Nostoc insulare*, showed inhibition of elastase and chymotrypsin [279].

TABLE 15. COMPOUNDS ISOLATED FROM CYANOBACTERIA BELONGING TO THE GENUS *NOSTOC*

Source	Compound	Activity	Reference
Nostoc commune	noscomin (**325**)	Antibacterial	[228]
	comnostins A-E (**171**-**175**)	Antibacterial	[110]
	nostofungicidine (**165**)	Antifungal, Cytotoxic	
Nostoc commune EAWAG 122b	8-[(5-carboxy-2,9-epoxy)benzyl]-2,5-dihydroxy-1,1,4a,7,8-pentamethyl-1,2,3,4,4a,6,7,8,9,10,10a-dodecahydrophenanthrene (**327**)	Antibacterial	[280]
	1,8-dihydroxy-4-methylanthraquinone (**323**)	Antibacterial	
	4-hydroxy-7-methylindan-1-one (**330**)	Antibacterial	
Nostoc insulare	insulapeptolides A –H (**314**-**321**)	Elastase inhibitor	[279]
	4,4′-dihydroxybiphenyl (**331**)	Cytotoxic	
	norharmane (**323**)	Cytotoxic	[281]
Nostoc linkia UTEX B1932	nostocyclophanes A-D (**158**-**161**)	Cytotoxic	[112]
Nostoc minutum NIES-26	microviridins G (**303**) and H (**304**)	Elastase inhibitor	[276]
	nostopeptins A (**301**) and B (**302**)	Elastase inhibitor	[275]
Nostoc muscorum	muscoride A (**324**)	Antibacterial	[282]
Nostoc sp.	nostocyclin (**300**)	Phosphatase inhibitor	
Nostoc sp. 152	nostophycin (**170**)	Cytotoxic	[115]
	microcystin-LR (**298**)	Hepatotoxic	[283]
Nostoc sp. 31	nostocyclamide (**298**)	Antialgal	[272]
	nostocyclamide M (**299**)	Antialgal	[272, 273]
Nostoc sp. 78-12A	nostocarboline (**324**)	Trypsin and acetylcholinesterase	[284]
Nostoc sp. ATCC 53789	cryptophycin (**145**)	Cytotoxic	[216]
	nostocyclopeptides A1 (**147**) and A2 (**148**)	Cytotoxic	[117]
Nostoc sp. CAVN 10	carbamidocyclophanes A-E (**166**-**170**)	Cytotoxic	[118]
Nostoc sp. GSV224	cryptophycins	Cytotoxic	[217, 219, 285]
	nostopeptolides A1-A3 (**305**-**307**)	-	[277]
Nostoc sp. TAU IL-220	nostocyclyne A (**326**)	Antibacterial	[286]
Nostoc sp. TAU IL-235	nostopeptin BN920 (**308**)	Chymotrypsin inhibitor	[278]
	nostoginin BN741 (**309**)	Bovine aminopeptidase N inhibitor	
	nostoginin BN578 (**310**)	Bovine aminopeptidase N inhibitor	
	banyascyclamides A-C (**311**-**313**)	-	
Nostoc sp. UIC 10022A	cylindrocyclophanes A_1-A_4 (**183**-**186**), C_1-C_4 (**187**-**190**), F_4 (**191**), A (**151**), C (**153**), and F (**156**)	20S proteasome inhibitor and cytotoxic	
Nostoc sphaericum	indolocarbazole (**157**)	Cytotoxic, antiviral	
Nostoc spongiaeforme	nostocine A (**328**)	Antialgal, Toxic	[287]
	borophycin (**162**)	Cytotoxic	[113]

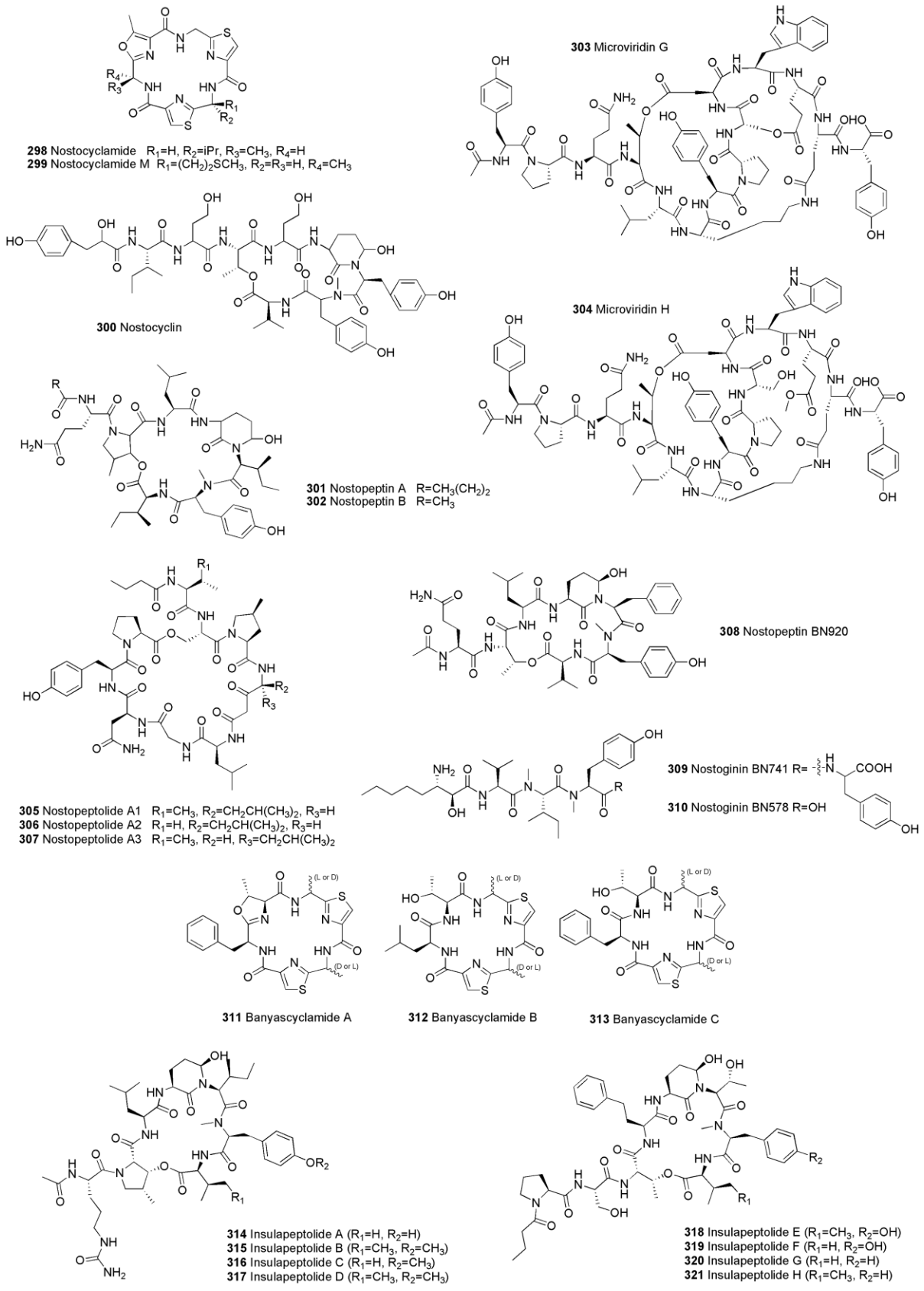

Figure 55. Structures of peptides from the genus *Nostoc*

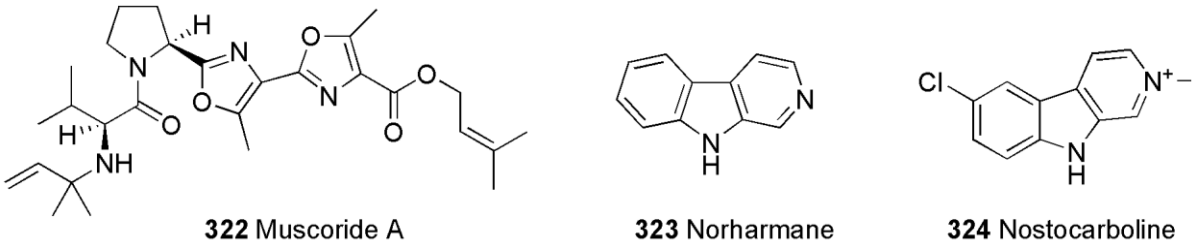

Figure 56. Structures of alkaloids from the genus *Nostoc*

Muscoride A (**322**) (Figure 56), an oxazole containing peptic alkaloid from *Nostoc muscorum*, contained two contiguous methyloxazoles and a N-(2-methyl-3-buten-2-yl)valine. It howed weak antibacterial activity against *Bacillus subtilis* and *Escherichia coli* [288]. Norharmane (**323**) (Figure 56) from *Nostoc insulare* had a similar structure to nostocarboline and showed algicidal, antibacterial, and antifungal activities with MIC values of 8-160 µg/mL [281, 289]. Nostocarboline (**324**) (Figure 56), a carbolinium alkaloid from *Nostoc* sp., was described as a cholinesterase inhibitor and showed growth inhibition of various cyanobacteria strains with MIC values of 1 µM [284].

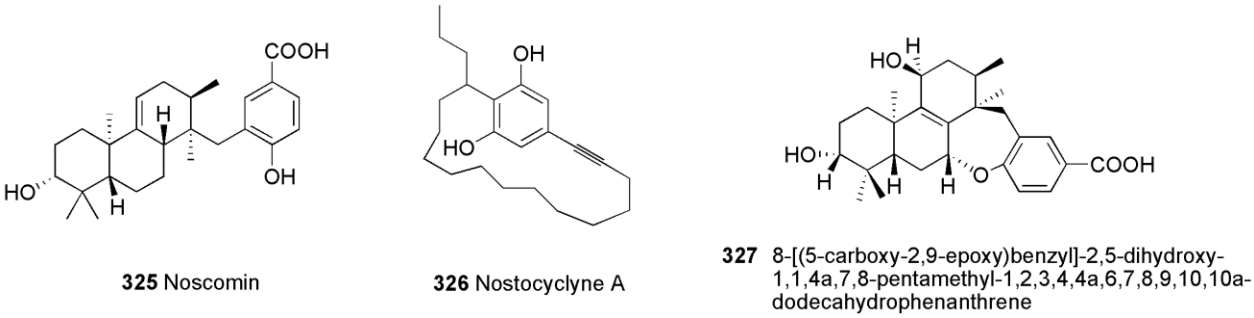

Figure 57. Structures of terpenoids from the genus *Nostoc*

Noscomin (**325**) (Figure 57) and comnostins A-E (**171**-**175**) are diterpenoids isolated from *Nostoc commune* [110, 228]. Noscomin showed antibacterial activity against *Bacillus cereus* and *Staphylococcus*

epidermidis with MIC values of 75 and 25 µM, respectively. Nostocyclyne A (**326**) (Figure 57), an acetylene-containing (1,4)-cyclophane, was obtained from a *Nostoc* sp., and showed weak inhibition of photosynthesis in green algae [286, 290]. 8-[(5-carboxy-2,9-epoxy)benzyl]-2,5-dihydroxy-1,1,4a,7,8-pentamethyl-1,2,3,4,4a,6,7,8,9,10,10a-dodecahydrophenanthrene (**327**) (Figure 57), a meroterpenoid from *Nostoc commune*, displayed a selective antibacterial activity against *Staphylococcus epidermidis* [280].

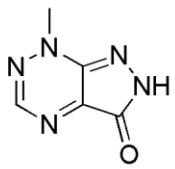

328 Nostocine A

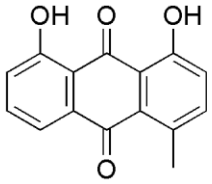

329 1,8-dihydroxy-4-methylanthraquinone

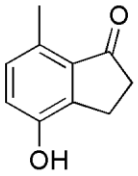

330 4-hydroxy-7-methylindan-1-one

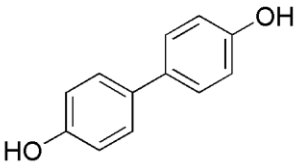

331 4,4'-dihydroxybiphenyl

Figure 58. Structures of miscellaneous compounds from the genus *Nostoc*

Nostocine A (**328**) (Figure 58), a violet pigment from *Nostoc spongiaeforme*, showed a broad spectrum of growth inhibition of several microorganisms, algae, and cultured plants. This suggested nostocine A to be a potential allelochemical [287]. An anthraquinone 1,8-dihydroxy-4-methylanthraquinone (**329**) and an indane derivative 4-hydroxy-7-methylindan-1-one (**330**) (Figure 58) were isolated from *Nostoc commune*, and 1,8-dihydroxy-4-methylanthraquinone was the first report of anthraquinone from cyanobacteria. Both compounds showed moderate antibacterial activity against *Staphylococcus epidermidis* and *Bacillus cereus* [280]. A simple phenolic compound 4,4′-dihydroxybiphenyl (**331**) (Figure 58) from *Nostoc insulare* showed moderate inhibitory activity against *Candida albicans* and *Bacillus cereus* with MIC values of 172 µM [289].

C.3 Chemical investigation of the cultured cyanobacterium *Nostoc* sp. (UIC 10047)

C.3.1 Experimental

C.3.1.1 General experimental procedures

^{1}H NMR spectrum was obtained at room temperature on a Bruker Avance DRX 600 MHz spectrometer with a 5 mm CPTXI Z-gradient probe. ^{13}C NMR spectrum was obtained on a Bruker AV 900 MHz NMR spectrometer with a 5 mm ATM CPTCI Z-gradient probe. ^{1}H and ^{13}C chemical shifts were referenced to the corresponding solvent peaks. HRESIMS were obtained using a Shimadzu IT-TOF spectrometer.

C.3.1.2 Biological material

Nostoc sp. (UIC 10047) was isolated from a field-collected sample near east branch DuPage River by bridge from Hidden Lake Forest Preserve in DuPage, Illinois (N41° 45.55' W88° 03.19'). The unialgal strain (UIC 10047) was obtained by micropipette [291], and grown in 2.8 L Fernback flask containing 2 L of inorganic media (Z media) under aeration [244]. Cultures were illuminated with fluorescent lamps at 1.93 klx with an 18/6 hours light/dark cycle at 22°C. After eight weeks, the biomass of the cyanobacterium was harvestsed by centrifugation and lyophilized.

C.3.1.3 Taxonomic identification

C.3.1.3.1 Morphological characterization

Morphological studies were performed using the cultivated UIC 10047 strain. The microscopic observation for morphological characterization was conducted using a Zeiss Axiostar Plus light microscope equipped with a Canon PowerShot A620 camera. The following parameters were selected to characterize its morphology: thallus morphology, shape of trichome, morphology of terminal cells, shape and arrangement of vegetative cells, presence and arrangement of heterocysts, and akinetes. Identification of the phenotype was performed according to the systems by Komárek *et al*. [246]. These morphological analyses were consistent with the diagnosis of the genus *Nostoc*.

C.3.1.3.2 DNA extraction, PCR, and sequencing

Approximately 1.4 g of biomass obtained from cultured material was pretreated with 5.5 mL of lysozyme (10 mg/mL) at 37°C for 30 min, followed by incubation with 55 µL of proteinase K (10 mg/mL) at 50°C for 1 h. DNA was extracted using the Wizard Genomic DNA purification kit (Promega). Concentration and purity of the isolated DNA was measured on a Thermo nanodrop 1000 spectrophotometer. The 16S rRNA genes were PCR-amplified using the cyanobacteria-specific primers 16s106F and 16s1509R [292]. Reaciton volumes were 26 µL containing 1 µL of DNA, 12.5 µL of 2× *Taq* PCR Master Mix, 1 µL of each primer (10 µM) and 10.5 µL of H_2O. The reaction was performed in a Bio-Rad C1000 thermal cycler as following reaction program: initial denaturation of 2 min at 95°C, 26 amplification cycles of 50 s at 95°C, 50 s at 47°C, and 2 min at 72°C, and final extention for 5 min at 72°C. PCR purification kit (Qiagen) and sequence with the primers 16s106F and 16s1509R as well as internal middle primers CYA359F and CYA781R [293].

C.3.1.3.3 Phylogenetic analysis

Phylogenetic and molecular evolutionary analyses were conducted using MEGA 5.05. The resulting sequence chromatograms were visually inspected, and the total sequence of 1,286 nucleotides were aligned with 41 cyanobacterial species obtained from GenBank as well as *Gloeobacter violaceus* PCC7421 as an outgroup. Cyanobacterial reference strains were selected from ***Bergey's Manual*** and only sequences of at least 1 kb were recovered from GenBank. Based on the initial morphological analysis, reference strains for the genus *Nostoc* were also selected (*Nostoc punctiforme* PCC73062, and *Nostoc* spp. PCC6720, PCC7120, and PCC7423). The strains previously collected from Illinois and Michigan area and identified as *Nostoc* by our group were also added (*Nostoc* sp. 10022A and 10062). Furthermore, strains for the genus *Trichormus* were included since in could not be ultimately distinguished from the *Nostoc* entirely based on the morphological characteristics [294]. In addition, a BLAST search was conducted using the 16S rRNA gene sequence of the UIC10047 and resulting strains with high sequence similarities were included (*Nostoc* sp. PCC7120, *Anabaena variabilis* ATCC29413, *Nodularia spumigena* CCY9414, and *Nostoc azollae* 0708). Multiple sequence alignment was performed using the ClustalW in MEGA 5.05 with default gap opening and extension penalties. The evolutionary history was inferred using three different methods (neighbor-joining, minimum evolution, and maximum likelihood). All three methods showed nearly identical topology particularly in the clade that includes UIC10047 with very similar

bootstrap values (the tree generated by neighbor-joining method shown in Figure 56). The resulting phylogenetic tree revealed that UIC10047 formed a monophyletic clade with *Nostoc muscorum* CENA61. *Nostoc* spp. PCC7423, KK-01, and UIC10022a, *Nostoc* sp. PCC7423 is a reference strain for *Nostoc* cluster 3.3, and thus the UIC10047 was designated within this cluster.

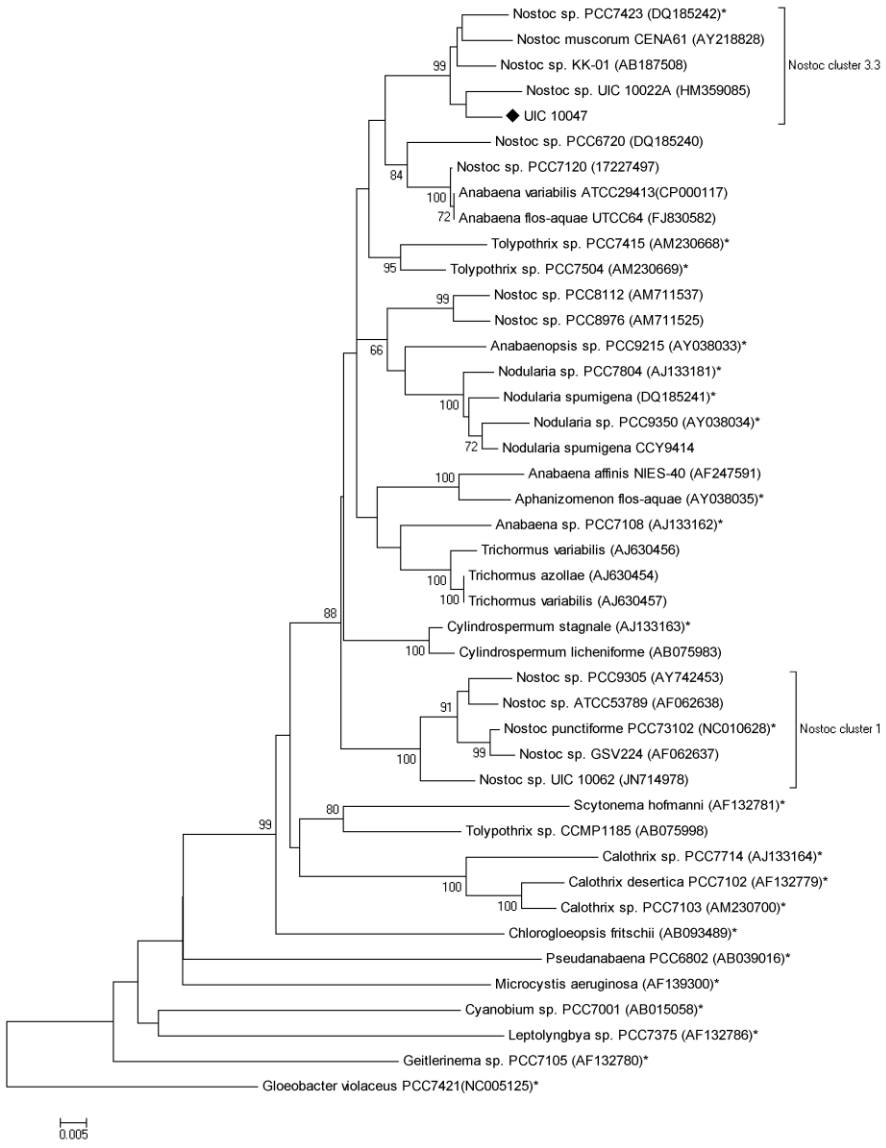

Figure 59. Phylogenetic relationships of 16S rRNA genes from cyanobacteria. Evolutionary distances were determined using the neighbor-joining analysis with 1,000 replicate bootstrap resampling to construct the phylogenetic tree. Strains were obtained from NCBI with the accession number given in parentheses. Strains marked with a (*) were obtained as Bergey's reference strains. Only bootstrap values above 65% were shown in the resulting tree.

C.3.1.4 Extraction and isolation

The lyophilized biomass (4.06 g) from 4 L of culture was extracted with CH_2Cl_2/MeOH (1:1 v/v) at room temperature and the solvent was evaporated *in vacuo*. The extract (279.9 mg) was redissolved in CH_2Cl_2/MeOH (1:1 v/v) and mixed with Diaion® HP20SS resin. The mixture was dried *in vacuo* and dried mixture was fractionated on a Diaion® column using a step gradient with increasing amount of 2-propanol in water to afford eight fractions. Fractions 5-8, eluting with 70%, 80%, 90%, and 100% 2-propanol, showed cytotoxicity against HT-29 cells. Fraction 6 was further subjected to a reversed-phase HPLC column (Onyx™ C_8 Monolithic, 4.6 × 100 mm, flow rate 4 mL/min) with 70-100% MeOH/H_2O gradient over 16 min to yield 24 subfractions. These 24 subfractions were evaluated for brine shrimp toxicity and subfractions 19-22 were found to be toxic. ^{1}H NMR spectra of these subfractions indicated subfractions 20 and 21 to be the same pure compound. The subfraction 20 was further subjected to ESI-TOF-MS (Flow injection with a flow rate 0.2 mL/min) with 50% MeOH isocratic over 2 min containing 0.1% formic acid. The analysis of the resulting MS indicated the sequtial loss of H_2O. The ^{1}H NMR spectrum and MS analysis indicated the bioactive compound to be a known boron-containing borophycin (**162**). The sub-fractionation procedure described above was repeatedly conducted to isolate more of **162**, material obtained from which was used to obtain DEPTQ spectrum and further confirmed the structure of **162**.

C.3.2 Struture elucidation

The structure of borophycin (**162**) was identified by a combined spectroscopic analyses based on 1D and 2D NMR and MS, and the data were found to be identical those previously reported for borophycin [113]. The NMR spectra of the compound **162** isolated from *Nostoc* sp. (UIC 10047) are presented in the APPENDIX (Figure 105-110).

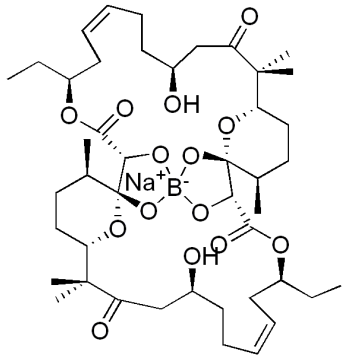

162 Borophycin

Figure 60. Structure of borophycin (**162**) isolated from *Nostoc* sp. UIC 10047

TABLE 16. NMR DATA OF BOROPHYCIN (**162**) IN DMSO-d_6 AND MEOD-d_4

	DMSO-d_6			MeOD-d_4	
Position	δ_C, mult.[a]	δ_H	mult. (J in Hz)[b]	δ_H	mult. (J in Hz)[b]
1	173.0, C				
2	78.6, CH	4.09		4.17	s
3	103.2, C				
4	35.8, CH	1.52		1.68	m
5	27.7, CH_2	1.52		1.60, 1.70	m
6	24.5, CH_2	1.20, 1.49		1.35, 1.58	m
7	72.3, CH	4.06		4.17	dd (11.5, 2.0)
8	49.8, C				
9	216.2, C				
10	42.0, CH_2	3.33, 2.44		2.53	dd (19.0, 0.5)
				3.39	dd (19.0 10.0)
11	66.2, CH	3.80		3.90	br t (10.0, 2.0)
12	36.5, CH_2	1.07, 1.26		1.20, 1.30	m
13	23.4, CH_2	2.50, 1.45		1.53	m
14	133.6, CH	5.52		5.56	dd (11.0, 4.0)
15	121.4, CH	5.35		5.40	td (11.0, 4.0)
16	28.5, CH_2	3.31		1.86	ddd (14.5, 4.0, 1.0)
				3.47	ddd (14.5, 12.5, 5)
17	75.8, CH	4.35		4.50	br dt (9.0, 5.0)
18	24.8, CH_2	1.70, 1.55		1.60, 1.77	m
19	10.5, CH_3	0.92		0.99	t (7.3)
20	16.5, CH_3	0.85		0.97	d (6.0)
21	22.5, CH_3	0.83		0.91	s
22	16.2, CH_3	0.86		0.96	s

C.4 Biological activity of the compound 162 isolated from *Nostoc* sp. (UIC 10047)

Borophycin (**162**) was evaluated for cytotoxic activity against a set of human cancer cells designated HT-29, NCI-H460, MCF-7, and SF268 using the methods described in section 3.3.1. and showed ED_{50} values of 1.0, 0.57, less than 0.49, and 1.50 µM, respectively. The compound also showed cytotoxicity against human lung fibroblasts IMR90 cells with an ED_{50} value of 0.5 µM, indicating it to be non-tumor selective.

C.5 Conclusion

Borophycin (**162**), the major component of *Nostoc* sp., possess significant cytotoxicity against HT-29, NCI-H460, MCF-7, SF268 cancer cells as well as IMR90 cells. The structurally related boron-containing compounds, boromycin [221, 295] and aplasmomycin [222, 296], have been reported from a terrestrial strain of *Streptomyces antibioticus* and a marine strain of *Streptomyces griseus*.

In our study, the method for isolation of the borophycin was standardized using brine shrimp assay-guided fractionation. UIC 10047 strain was mass cultured for more isolation of the compound, which will be subjected to further *in vivo* hollow fiber assay.

D. *Oscillatoria* sp. (UIC 10109)

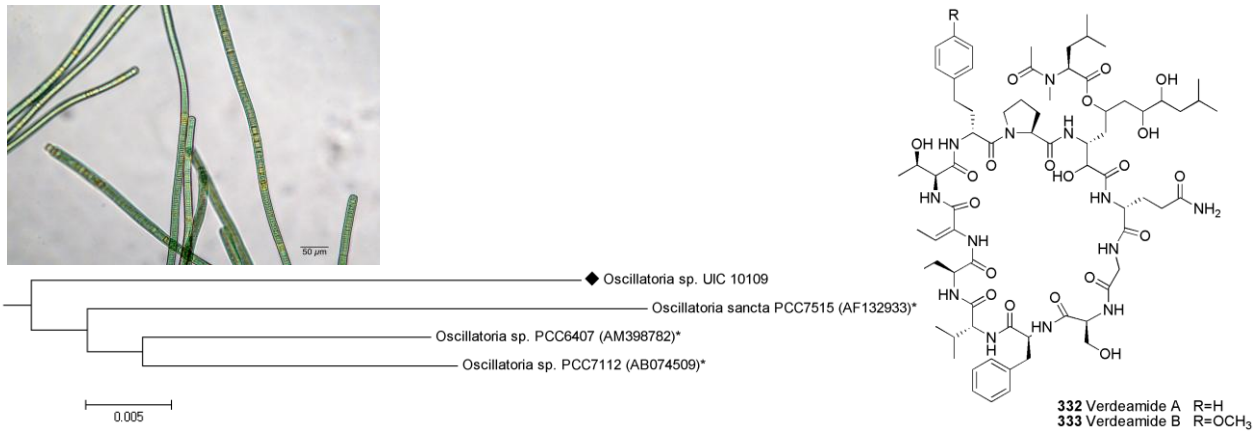

Figure 61. Photomicrograph of *Oscillatoria* sp. UIC 10109 and isolated compounds

Chemical investigation of the cultured cyanobacterium *Oscillatoria* sp. (UIC 10109), obtained from a sample collected from Puerto Rico, led to the isolation of two cyclic peptides, verdeamides A (**332**) and B (**333**), both containing the β-amino acid 3-amino-2,5,7,8-tetrahydroxy-10-methylundecanoic acid (Aound). The structures of these peptides were determined by detailed spectroscopic analyses of 1D and 2D NMR as well as MS/MS fragmentation. The absolute configurations of the amino acids were determined by Marfey's and advanced Marfey's methods after acid hydrolysis. Both verdeamides A (**332**) and B (**333**) were evaluated for cytotoxicity against a set of human cancer cells as well as for inhibition of the 20S proteasome, an established target for cancer treatment. Both compounds exhibited significant cytotoxicity and 20S proteasome inhibition against SW-620, NCI-H23, and MDA-MB-435 cells with ED_{50} values ranging from 0.7 to 4.4 µM.

D.1 Taxonomic description of the genus *Oscillatoria*

According to Komárek *et al*., the genus *Oscillatoria* belongs to the family Oscillatoriaceae in the order Oscillatoriales in the phylum Cyanobacteria, domain Bacteria [246]. The current taxonomic description of *Oscillatoria* by Komárek *et al*. is as follows.

> The thallus is usually flat, macroscopic, smooth, layered, rarely leathery, arranged in mats, less frequently in solitary trichomes. Trichomes are straight or slightly irregularly undulating, cylincrical , sometimes screwlike coiled at the ends, motile, gliding or oscillating in left-handed or right-handed rotation, usually wider than 6.8 µm (up to 70 µm), not constricted or constricted at the cross walls. Sheaths are usually absent, although they may occur under suboptimal conditions. Cells are short and discoid, always with lengths less than one half to one eleventh that of their widths; cell contents without aerotopes are homogeneous or sometimes contain large prominent granules. Cell division occurs in a rapid sequence transversely to the trichome axis. Reproduction occurs via trichome disintegration (sometimes completely) into short motile hormogonia, with the aid of necridia.

UIC 10109 strain was isolated from a sample collected from Puerto Rico (N18°20.490′ W65°365′), cultured under laboratory conditions, and used for biological and chemical evaluations.

D.2 Compounds previously isolated from cyanobacteria of the genus *Oscillatoria*

Filamentous cyanobacteria of the genus *Oscillatoria* have produced a variety of peptides and miscellaneous compounds such as fatty acids (Figure 62 and Table 17).

Oscillapeptins A-F (**334**-**339**) (Figure 62), Ahp-containing cyclic depsipeptides, were isolated from cultured *Oscillatoria agardhii* (NIES-204, -205, and -596) [297, 298]. Oscillapeptin A was found to be an elastase and chymotrypsin inhibitor. Oscillapeptins B, C, and E inhibited chymotrypsin and/or elastase activity, while oscillapeptin F showed inhibition of trypsin and plasmin. Oscillapeptin G (**340**) (Figure 62) was first isolated from a cultured terrestrial *O. agardhii* (NIES-610) as a tyrosinase inhibitor and later isolated from *O. agardhii* (CYA-128) collected from Lake Verijärvi in Finland [299]. The structure of oscillapeptin G contained glyceric acid and homotyrosine residues, in addition to the Ahp moiety observed in other oscillapeptins [300]. Oscillapeptin G inhibited both elastase and chymotrypsin with IC_{50} values of 1.1 and 11.4 µM, respectively.

Agardhipeptins A (**341**) and B (**342**) [301], and microviridins D-F (**343**-**345**) and I (**346**) were isolated from *Oscillatoria agardhii* (NIES-204) [299, 302]. The agardhipeptins A and B were identified as cyclic hepta- and octapeptide, respectively. Agardhipeptin A showed weak inhibition of plasmin with an IC_{50} value of 77 µM. Microviridins D-F showed inhibition of elastase with IC_{50} values of 0.3, 0.3, and 3.6 µM, respectively. Microviridins D and E also showed inhibition of chymotrypsin with IC_{50} values for both compounds of 0.6 µM, while microviridin F showed no inhibition of chymotrypsin at 60 µM. Microviridin I showed inhibition of elastase with an IC_{50} value of 0.2 µM [299].

Aeruginosins 205A (**347**) and 205B (**348**) were isolated from *Oscillatoria agardhii* (NIES-205), and both of these compounds showed inhibition of trypsin with IC_{50} values for both compounds of 0.08 μM [303]. Oscillaginins A (**349**) and B (**350**) were isolated from a cultured freshwater *Oscillatoria agardhii* [304]. Oscillaginin A was found to be a chlorine-containing linear tetrapeptide, and oscillaginin B was the deschlorinated derivative of oscillaginin A.

The cultured *Oscillatoria agardhii* strain 97 obtained from Lake Maarianallas in Finland produced oscillapeptilides 97-A (**351**) and 97-B (**352**), oscillacyclin (**353**), and anabaenopeptins B (**354**) and F (**356**) [299]. Oscillapeptilides 97-A and -B were cyclic depsipeptides and oscillapeptilide 97-B was a desmethyl derivative of the oscillapeptilide 97-A. Both compounds showed inhibitions of elastase with IC_{50} values of 0.7 and 12.5 μM, and inhibitions of chymotrypsin with IC_{50} values of 0.4 and 10.5 μM, respectively. The structures of anabaenopeptins B and F contained a ureido linkage. Anabaenopeptin F was also isolated from *O. agardhii* (NIES-204 and -610) along with anabaenopeptin E (**355**) and oscillamide Y (**357**) [305, 306]. Anabaenopeptins G (**358**) and H (**359**) were isolated from a cultured *O. agardhii* (NIES-595) and found to be a potent carboxypeptidase A inhibitors [307].

Portoamides A-D (**360**-**363**), cyclic dodecapeptides, were recently reported from a cultured freshwater *Oscillatoria* sp. [308]. The structures of portoamides contained a β-amino acid 3-amino-2,5,7,8-tetrahydroxy-10-methylundecanoic acid (Aound) moiety. Mixture of portoamides A and B showed complete inhibition of *C. vulgaris* with an IC_{50} value of 8.5 μM. In addition, this mixture showed growth inhibitions of the green microalgae *Ankistrodesmus falcatus* and *Chlamydomonas reinhardtii* as well as the cyanobacterium *Cylindrospermumopsis raciborskii*. The mixture of both compounds also showed cytotoxicity against NCI-H460 cells with an IC_{50} value of 0.4 μM, which was 10-fold more active than the individual portoamides A and B.

Coriolic acid (**368**) and α-dimorphecolic acid (**369**), unsaturated hydroxyl fatty acids, were isolated from *Oscillatoria redekei* [309]. Both compounds were found to inhibit the growth of Gram-positive bacteria such as *Bacillus subtilis* SBUG 14, *Micrococcus flavus* SBUG 16, and *Staphylococcus aureus* SBUG 11 and ATCC25923.

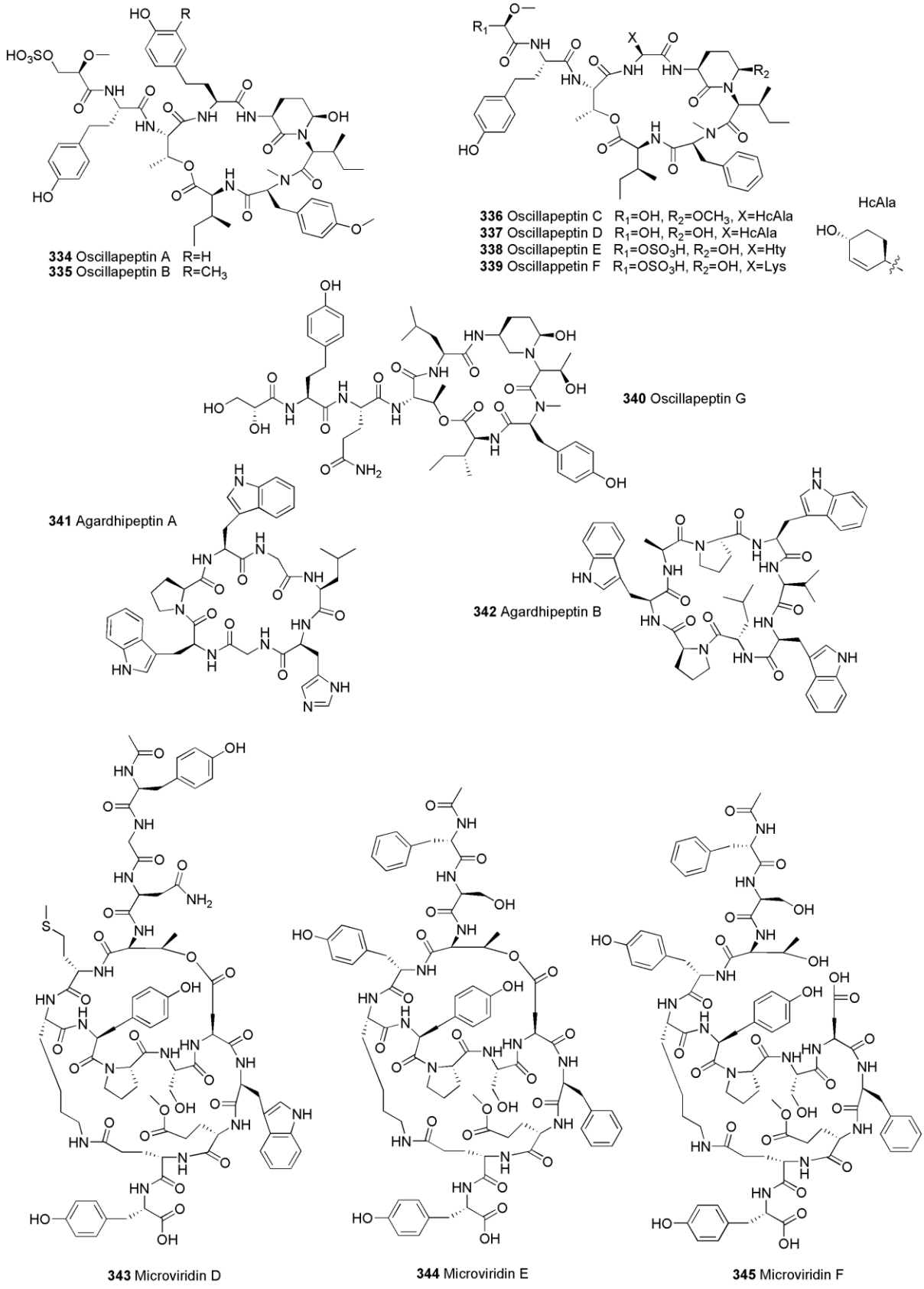

Figure 62. Structures of compounds from the genus *Oscillatoria*

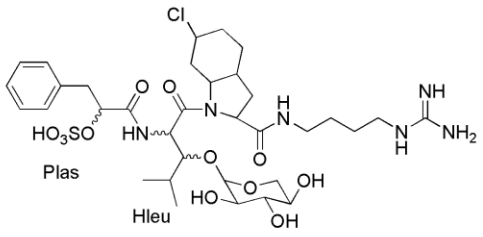

347 Aeruginosin 205A L-Plas, (2R,3*S*)-Hleu
348 Aeruginosin 205B D-Plas, (2S,3*R*)-Hleu

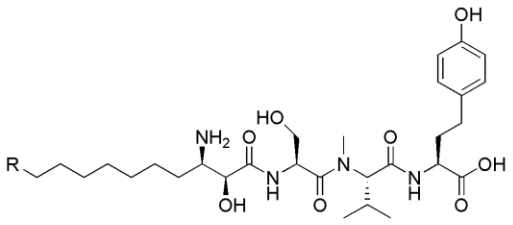

349 Oscillaginin A R=Cl
350 Oscillaginin B R=H

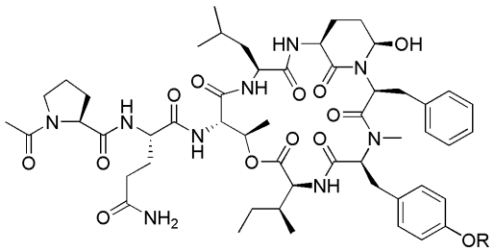

351 Oscillapeptilide 97-A R=CH3
352 Oscillapeptilide 97-B R=H

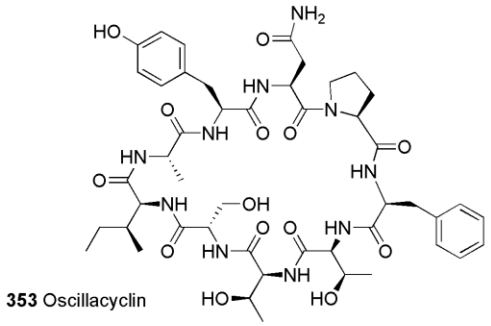

353 Oscillacyclin

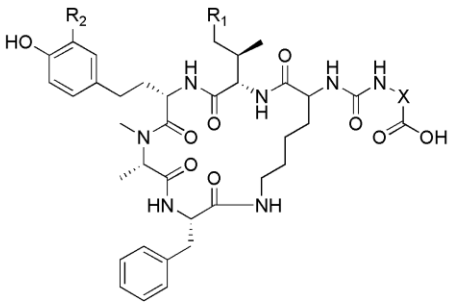

354 Anabaenopeptin B R_1=R_2=H, X=Arg
355 Anabaenopeptin E R_1=R_2=CH_3, X=Arg
356 Anabaenopeptin F R_1=CH_3, R_2=H, X=Arg
357 Oscillamide Y R_1=CH_3, R_2=H, X=Tyr

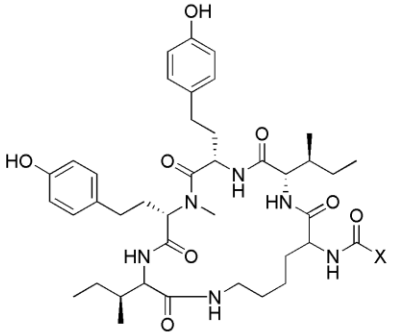

358 Anabaenopeptin G X=Tyr
359 Anabaenopeptin H X=Arg

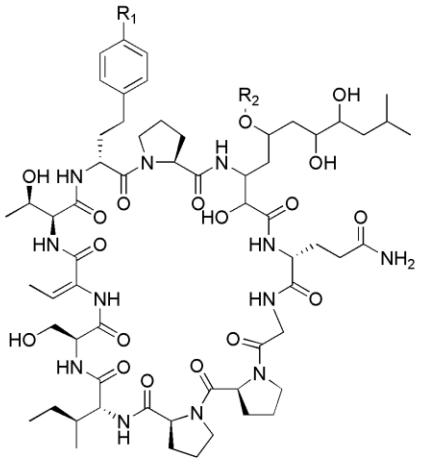

360 Portoamide A R_1=OCH_3, R_2=*
361 Portoamide B R_1=H, R_2=*
362 Portoamide C R_1=OCH_3, R_2-H
363 Portoamide D R_1=R_2=H

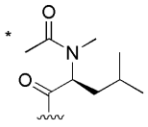

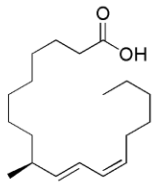

364 α-dimorphecolic acid

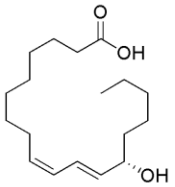

365 Coriolic acid

Figure 62 (Continued). Structures of compounds from the genus *Oscillatoria*

TABLE 17. COMPOUNDS FROM CYANOBACTERIA BELONGING TO THE GENUS *OSCILLATORIA*

Source	Compound	Class	Reference
Oscillatoria agardhii	oscillaginins A (**349**) and B (**350**)	peptide	[304]
	oscillamide Y	peptide	[305]
Oscillatoria agardhii (NIES-596)	oscillapeptin F (**339**)	peptide	[297]
Oscillatoria agardhii (CYA128)	oscillapeptin G (**340**)	peptide	[299]
Oscillatoria agardhii (NIES-204)	agardhipeptins A (**341**) and B (**342**)	peptide	[302]
	anabaenopeptin E (**355**)	peptide	[306]
	oscillapeptins A (**334**) and B (**335**)	peptide	[297, 298]
	microviridins D-F (**343**-**345**) and I (**346**)	peptide	[299, 301]
	anabaenopeptins B (**354**) and F (**356**)	peptide	[299]
Oscillatoria agardhii (NIES-205)	aeruginosins 205A (**347**) and 205B (**348**)	peptide	[303]
Oscillatoria agardhii (NIES-595)	anabaenopeptins G (**358**) and H (**359**)	peptide	[307]
	oscillapeptins C-E (**336**-**338**)	peptide	[297]
Oscillatoria agardhii (strain 97)	oscillapeptilides 97-A (**351**) and 97-B (**352**)	peptide	[299]
	oscillacyclin (**353**)	peptide	[299]
Oscillatoria redekei	coriolic acid (**368**)	fatty acid	[309]
	α-dimorphecolic acid (**369**)	fatty acid	[309]
Oscillatoria sp.	portoamides A-D (**360**-**363**)	peptide	[308]

D.3 Chemical investigation of the cultured cyanobacterium *Oscillatoria* sp. (UIC 10109)

D.3.1 Experimental

D.3.1.1 General experimental procedures

Optical rotations were measured with a Perkin-Elmer 241 polarimeter. UV spectra were recorded on a Varian Cary 50 Bio spectrophotometer. IR spectra were obtained on a FTIR-410 Fourier transform infrared spectrometer. 1D and 2D NMR spectra were obtained at room temperature on a Bruker Avance DRX 600 MHz spectrometer with a 5 mm CPTXI Z-gradient probe. ^{13}C NMR spectrum was obtained on a Bruker AV 900 MHz NMR spectrometer with a 5 mm ATM CPTCI Z-gradient probe. ^{1}H and ^{13}C chemical shifts were referenced to the corresponding solvent peaks. HRESIMS were obtained using a Shimadzu IT-TOF spectrometer.

D.3.1.2 Biological material

Oscillatoria sp. (UIC 10109) was isolated from sample collected from a rock with dripping water near the roadside embankment, in Puerto Rico (N18°20.490′ W65°365′, altitude 190 ft). The unialgal strain (UIC 10109) was obtained by micropipette [291], and grown in 2.8 L Fernback flask containing 2 L of inorganic media (Z media) under aeration. Cultures were illuminated with fluorescent lamps at 1.93 klx with an 18/6 hours light/dark cycle at 22°C. After seven weeks, the cells of the cyanobacterium were harvested and lyophilized.

D.3.1.3 Taxonomic identification

C.3.1.3.1 Morphological characterization

Morphological studies were performed using a cultivated UIC 10109 strain. The microscopic observation for morphological characterization was conducted using a Zeiss Axiostar Plus light microscope equipped with a Canon PowerShot A620 camera. The following parameters were selected to characterize its morphology: thallus morphology, shape of trichome, morphology of terminal cells, and size, shape and arrangement of vegetative cells. Identification of the phenotype was performed according to the systems by Komárek *et al*. [246]. These morphological analyses were consistent with the diagnosis of the genus *Oscillatoria*.

D.3.1.3.2 DNA extraction, PCR, and sequencing

Approximately 257.8 mg of biomass obtained from cultured material was pretreated with 2.5 mL of lysozyme (10 mg/mL) at 37°C for 30 min, followed by incubation with 25 µL of proteinase K (10 mg/mL) at 50°C for 1 h. DNA was extracted using the Wizard Genomic DNA purification kit (Promega). Concentration and purity of the isolated DNA was measured on a Thermo nanodrop 1000 spectrophotometer. The 16S rRNA genes were PCR-amplified using the cyanobacteria-specific primers 16s106F and 16s1509R [292]. Reaciton volumes were 26 µL containing 1 µL of DNA, 12.5 µL of 2x *Taq* PCR Master Mix, 1 µL of each primer (10 µM) and 10.5 µL of H_2O. The reaction was performed in a Bio-Rad C1000 thermal cycler as following reaction program: initial denaturation of 2 min at 95°C, 26 amplification cycles of 50 s at 95°C, 50 s at 47°C, and 2 min at 72°C, and final extention for 5 min at 72°C. PCR purification kit (Qiagen) and sequence with the primers 16s106F and 16s1509R as well as internal middle primers CYA359F and CYA781R [293].

D.3.1.3.3 Phylogenetic analysis

Phylogenetic and molecular evolutionary analyses were conducted using MEGA 5.05. The resulting sequence chromatograms were visually inspected, and the total sequence of 1320 nucleotides were aligned with 35 cyanobacteria species obtained from GenBank as well as *Gloeobacter violaceus* PCC7421 as an outgroup. Cyanobacterial reference strains were selected from *Bergey's Manual* and only sequences of at least 1 kb were recovered from GenBank. Based on the initial morphological analysis, reference strains from the genus *Oscillatoria* were also selected (*Oscillatoria* spp. PCC 6407 and PCC 7112, and *Oscillatoria sancta* PCC 7515). Multiple sequence alignment was performed using the ClustalW in MEGA 5.05 with default gap opening and extension penalties. The evolutionary history was inferred using three different methods (neighbor-joining, minimum evolution, and maximum likelihood). All three methods showed nearly identical topology particularly in the clade that includes UIC 10109 with very similar bootstrap values (the tree generated by neighbor-joining method shown in Figure 51). The resulting phylogenetic tree revealed that UIC 10109 formed a monophyletic clade with reference strains for *Oscillatoria*, and thus the UIC 10109 was determined as *Oscillatoria* sp.

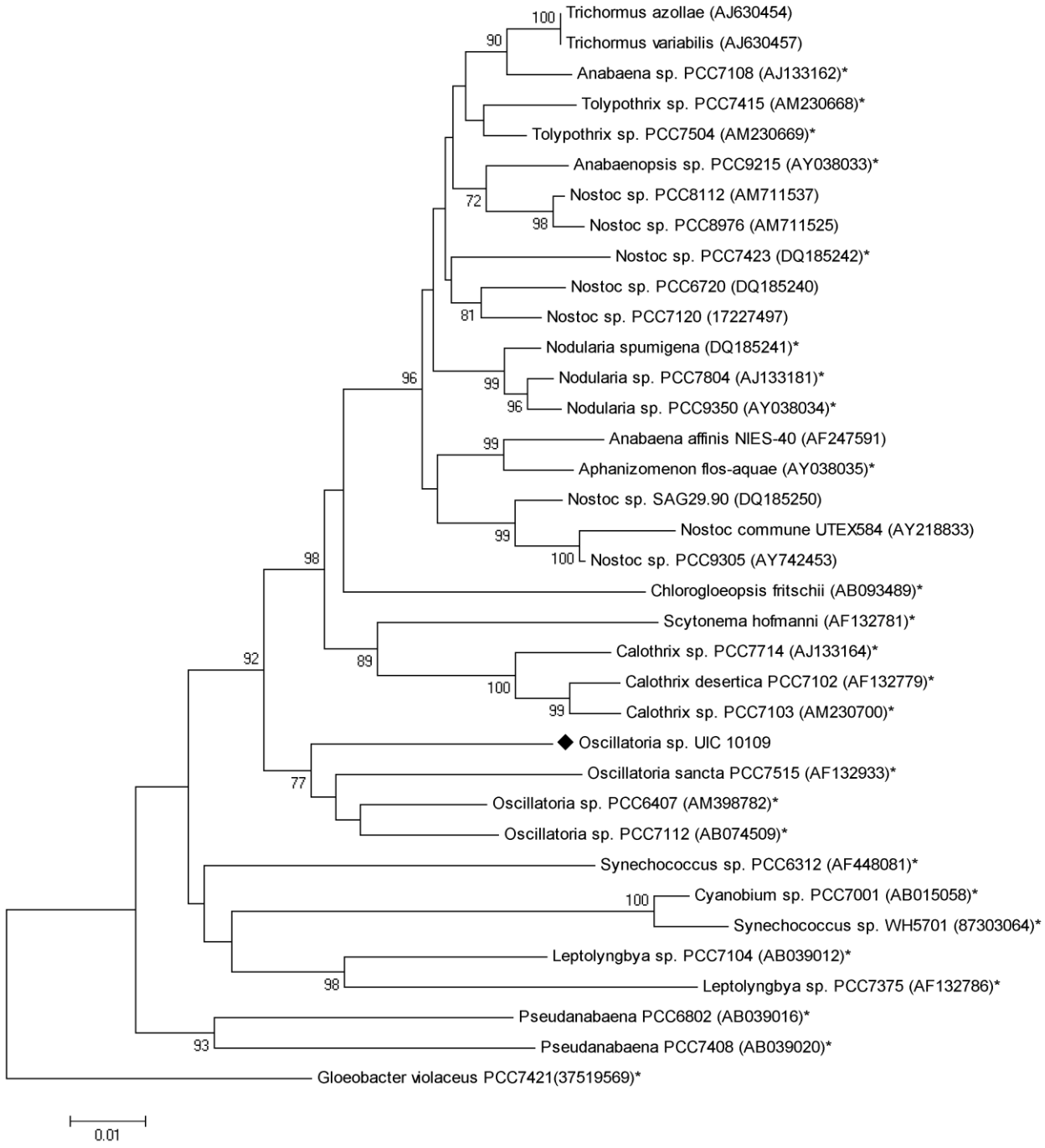

Figure 63. Phylogenetic relationships of 16S rRNA genes from cyanobacteria. Evolutionary distances were determined using the neighbor-joining analysis with 1,000 replicate bootstrap resampling to construct the phylogenetic tree. Strains were obtained from NCBI with the accession number given in parentheses. Strains marked with a (*) were obtained as Bergey's reference strains. Only bootstrap values above 75%.

D.3.1.4 Extraction and isolation

The lyophilized biomass (4.06 g) from 4 L of culture was extracted with CH_2Cl_2/MeOH (1:1 v/v) at room temperature and the solvent was evaporated *in vacuo*. The extract (279.9 mg) was redissolved in CH_2Cl_2/MeOH (1:1 v/v) and mixed with Diaion® HP20SS resin. The mixture was dried *in vacuo* and the dried mixture was fractionated on a Diaion® column using a step gradient with increasing amount of 2-propanol in water to afford eight fractions. Fractions 3 and 4, eluting with 40% and 60% 2-propanol, respectively, displayed cytotoxicity and 20S proteasome inhibition against MDA-MB-23 cells. Fractions 3 and 4 were subjected to HPLC-ESIMS analysis (Varian Microsob C_8, 2.0 × 250 mm, flow rate 0.2 mL/min) with 30-100% MeOH gradient over 35 min containing 0.1% formic acid. The analysis of MS spectra indicated the presence of potentially new large molecular weight peptides. Both fractions were further subjected to reversed-phase HPLC column (Varian C_8 Microsorb, 10 × 250 mm, flow rate 4 mL/min) with 65-75% MeOH/H_2O gradient over 40 min and yielded verdeamide A (3.0 mg, t_R 28.5 min) and verdeamide B (1.4 mg, t_R 25.2 min).

D.3.1.4.1 Verdeamide A (332)

Pale yellow oil; ^1H and ^{13}C NMR, see Table 18; HRESIMS *m/z* 1478.7601 [M+H]+ (calcd for $C_{71}H_{108}N_{13}O_{21}$, 1478.7782)

D.3.1.4.2 Verdeamide B (333)

Pale yellow amorphous powder; ^1H and ^{13}C NMR (Appendix 118-123) ; HRESIMS *m/z* 1508.7677 [M+H]+ (calcd for $C_{72}H_{110}N_{13}O_{22}$, 1508.7888)

D.3.1.5 Determination of absolute configuration

Approximately 0.5 mg of verdeamides A (**332**) and B (**333**) were hydrolyzed with 1 mL of 6 N HCl for 20 h at 110°C. The resulting acid hydrolysates were divided into two equal portions and evaporated to dryness. Each dried material was redissolved in 50 µL of H_2O and mixed with 20 µL of 1N $NaHCO_3$, 40 µL of 1-fluoro-2,4-dinitro-5-L-leucinamide (L-FDLA, 10 mg/mL in acetone), and 90 µL of acetone. The mixture was stirred for 1 h at 40°C. The reaction mixture was cooled to room temperature and then acidified with 20 µL of 2 N HCl. The resulting solution was dried and then redissolved in 300 µL of CH_3CN. Aliquots were subjected to reversed-phase HPLC-ESIMS analysis (Varian Microsorb C_{18}, 2.0 × 250 mm, flow rate 0.4

mL/min) with 20-65% CH_3CN gradient containing 0.1% formic acid over 50 min. The selective ion chromatograms of L-FDLA for hydrolysates of verdeamides A (**332**) and B (**333**) and for authentic standards were retrieved and retention times (t_R, min) were compared. The retention times of the L-FDLA derivatized amino acids in the hydrolysates of verdeamide A and B matched those of L-Pro (33.5), *N*-Me-L-Leu (45.8), D-Gln (31.7), L-Ser (27.8), L-Phe (41.6), D-Val (47.8), L-Thr (27.4), and D-Hphe (53.3). Retention times (t_R, min) of authentic amino acids were as follows: L-Pro (33.5), D-Pro (37.8), *N*-Me-L-Leu (45.7), *N*-Me-D-Leu (49.6), L-Gln (27.7), D-Gln (31.3), L-Ser（27.5), D-Ser (29.0), L-Phe (41.3), D-Phe (49.0), L-Val (37.6), D-Val (47.5), L-Thr (27.3), D-Thr (34.4), L-Hphe (44.4), and D-Hphe (52.9). For the absolute configurations of the *O*-Me-Htyr and Aound moieties, the advanced marfey's method was carried out as previously described [310-312]. Briefly, both L- and DL-FDLA derivatives of verdeamide B (**333**) were prepared and analyzed as described above, indicating the presence of D-O-Me-Htry and D-Aound.

D.3.2 Structure elucidation

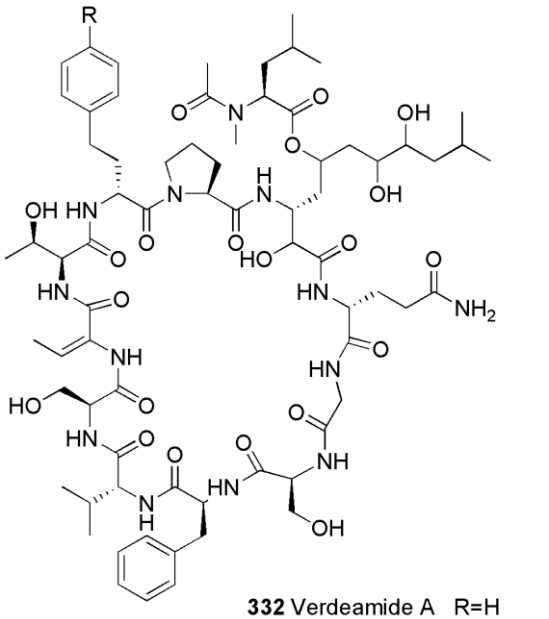

332 Verdeamide A R=H
333 Verdeamide B R=OCH_3

Figure 64. Structures of new compounds isolated from *Oscillatoria* sp. UIC 10109

Verdeamide A (**332**) was obtained as a pale yellow oil. The HRESIMS pseudo-molecular $[M+2H]^{2+}$ ion at *m/z* 739.8877, accompanied by a $[M+Na]^{+}$ ion peak at *m/z* 1500.7407, indicated a molecular formula of $C_{71}H_{107}N_{13}O_{21}$.

The ^{1}H NMR spectrum of verdeamide A (**332**) in DMSO-d_6 indicated the characteristic features of a peptide, including exchangeable amide NH signals, amino acid α-proton signals, and aliphatic methylene and methyl signals. However, exact analysis of NMR spectra of **332** was hindered due to the presence of multiple conformations in DMSO-d_6. Use of other solvents such as methanol-d_3 and -d_4, tetrahydrofuran-d_8, pyridine-d_5, acetone-d_6, and benzene-d_6 or combinations with H_2O was attempted to improve resolution of the NMR spectra. A combination of acetone-d_6 and water seemed to improve the resolution. However, water-suppression was needed, which led to the loss of α-proton signals. One major conformation with improved resolution was obtained using a mixture of acetone-d_6 and D_2O, in which water suppression was not needed, and 1D and 2D NMR spectra were obtained using this solvent system.

Extensive analysis of the COSY, TOCSY, HSQC, and HMBC spectra revealed the presence of nine standard amino acids: Pro, Gln, Gly, Ser (x2), Phe, Val, Thr, and Leu (Figure 65 and Table 18). HMBC correlations observed from *N*-Me (δ_H 2.08) to Leu C-2 (δ_C 54.8) and from *N*-Me (δ_H 2.08) and *N*-Ac (δ_H 2.90) to *N*-Ac (δ_C 172.4) revealed that Leu was methylated and acetylated at the *N*-terminus. The presence of homophenylalanine (Hphe) was determined by analyses of TOCSY and HMBC spectra. The TOCSY spectrum displayed one spin system from H-2 (δ_H 4.60) to H_2-4 (δ_H 2.72 and 2.58), and HMBC correlations from H_2-3 (δ_H 2.10 and 1.93) to C-5 (δ_C 141.0) connected this spin system to a benzene ring. The presence of dehydrobutyrine (Dhb) was evident by the presence of a highly diagnostic quartet of H-3 (δ_H 5.89) and a doublet of H-4 (δ_H 1.87). HMBC correlations from H-3 to C-1 (δ_C 165.1), C-2 (δ_C 129.3), and C-4 (δ_C 12.7) confirmed the Dhb moiety. A long spin system (H-2 to H-12) was observed in the TOCSY spectrum, indicating the presence of the β-amino acid 3-amino-2,5,7,8-tetrahydroxy-10-methylundecanoic acid (Aound).

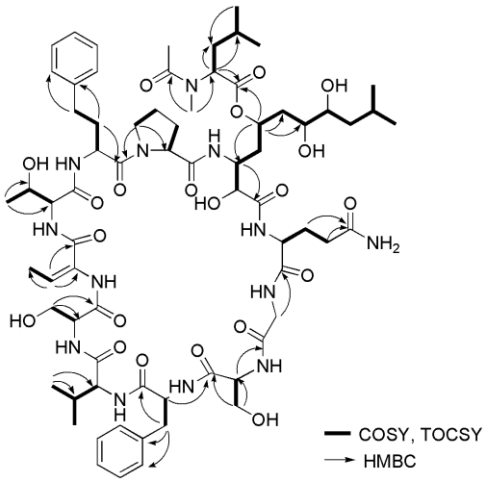

Figure 65. Key COSY and HMBC correlations of veradeamide A (**332**)

Due to the loss of NH amide protons in the NMR spectra obtained using a combination of acetone-d_6 and D_2O, the connectivity of amino acids was achieved by analyzing MS/MS fragmentations (Figure 66). The MS/MS spectrum of verdeamide A (**332**) showed a prominent neutral loss of 187 Da, corresponding to the ion fragment for *N*-Ac-*N*-Me-Leucine unit [131], followed by the ring cleavage between Pro and Hphe. The resulting linear fragment was subsequently fragmented, indicating the loss of each amino acid moiety and the sequence was found to be Hphe-Thr-Dhb-Ser1-Val-Phe-Ser2-Gly-Gln-Aound-Pro.

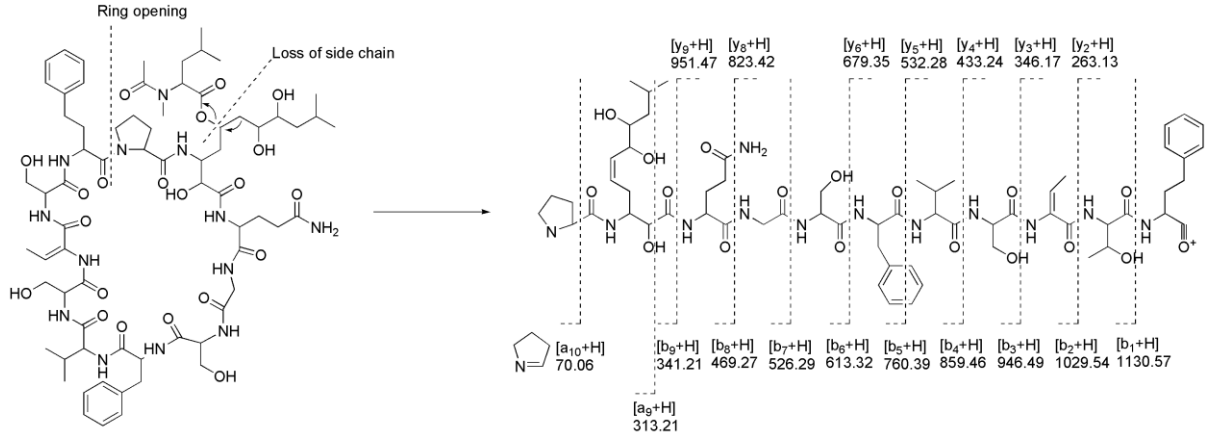

Figure 66. MS/MS fragmentation pattern of verdeamide A (**332**)

TABLE 18. ^{1}H AND ^{13}C NMR DATA OF VERDEAMIDES A (**332**) IN A COMBINATION OF ACETONE-d_6 AND D_2O

		δ_C [a]	δ_H	mult. (J in Hz) [b]			δ_C [a]	δ_H	mult. (J in Hz) [b]
Pro	1	[c]			Phe	6/8	130.2	7.14	m
	2	56.0	4.43	m		7	126.3	7.23	m
	3a	29.7	2.10	m	Ser2	1	[c]		
	3b					2	56.7	4.54	m
	4a	24.0	2.02	m		3a	61.8	3.92	m
	4b		1.85	m		3b		3.88	m
	5a	47.02	3.35	m	Gly	1	[c]		
	5b					2a	43.0	4.92	d (16.62)
Hphe	1	172.5				2b		3.98	d (16.62)
	2	50.9	4.60	m	Gln	1	[c]		
	3a	32.8	1.93	m		2	54.5	4.47	m
	3b		2.10	m		3a	27.8	2.14	m
	4a	31.3	2.72	m		3b		1.94	m
	4b		2.58	m		4a	31.4	2.40	m
	5	141.0				4b		2.13	m
	6/10	128.5	7.24	m		5	176.6		
	7/9	127.4	7.24	m	Aound	1	176.6		
	8	127.3	7.14	m		2	49.0	4.37	m
Thr	1	[c]				3	72.2	4.22	m
	2	58.6	4.55	m		4a	32.9	2.09	m
	3	65.9	3.92	m		4b		1.94	m
	4	19.3	1.15	d (6.48)		5	69.7	5.06	m
Dhb	1	165.1				6a	37.6	1.83	m
	2	129.3				6b		1.58	m
	3	125.3	5.89	q (7.38)		7	71.2	3.37	m
	4	12.7	1.87	d (7.38)		8	72.1	3.48	m
Ser1	1	170.4				9a	42.0	1.26	m
	2	56.7	4.22	m		9b			
	3a	60.8	3.64	m		10	24.1	1.77	m
	3b		3.64	m		11	23.2	0.86	m
Val	1	[c]				12	21.1	0.83	m
	2	60.6	4.07	d (7.44)	*N*-Ac-*N*-Me-Leu	1	[c]		
	3	29.2	2.17	m		2	54.8	5.15	d (11.34, 4.38)
	4	18.5	0.73	d (6.84)		3a	36.4	1.83	m
	5	18.0	0.80	d (6.84)		3b		1.71	m
Phe	1	173.0				4	24.6	1.43	m
	2	54.7	4.65	dd (7.86, 7.86)		5	20.8	0.88	d (6.6)
	3a	36.5	3.20	dd (13.74, 7.86)		6	22.7	0.83	d (6.6)
	3b		2.98	dd (13.74, 7.86)		*N*-Me	31.7	2.08	s
	4	137.3				*N*-Ac	172.4		
	5/9	129.3	7.25	m				2.90	s

[a] Chemical shift determined from gHSQC and gHMBC experiments recorded at 600 MHz. [b] Recorded at 600 MHz. [c] Not Assigned.

Verdeamide B **(333**) showed a ^{1}H NMR spectrum similar to that of verdeamide A (**332**), except with one additional singlet at δ_H 3.73, indicating the presence of a methoxy moiety. HMBC correlations from the methoxy moiety to C-8 (δ_C 158.0) of Htyr as well as from both H-6/10 and H-7/9 to C-8 (δ_C 158.0) of Htyr indicated the Htyr to be *O*-methylated. The molecular formula of $C_{72}H_{109}N_{13}O_{22}$ determined by the HRESIMS pseudomolecular $[M+2H]^{2+}$ ion at *m/z* 754.8909, accompanied by a $[M+Na]^{+}$ ion peak at *m/z* 1530.7507, further indicated the presence of an additional -OCH_2- fragment in verdeamide B. Together, verdeamide B (**333**) was found to be an analogue containing *O*-methylated homotyrosine instead of homophenylalanine observed in verdeamide A.

The absolute configurations of verdeamides A (**332**) and B (**333**) were assigned using FDLA-based marfey's and advanced marfey's analyses accompanied by both PDA and MS detection. Comparison of the retention times between L- and D- or DL-FLDA derivatized samples assigned an L configuration except Hphe, *O*-MeHtyr, Val, and Gln.

D.4 Biological activity of the compounds isolated from *Oscillatoria* sp. (UIC 10109)

Cytotoxicity of the isolates was evaluated using a set of human cancer cell lines designated SW-620 colon, NCI-H23 non-small cell lung, and MDA-MB-435 melanoma. Both verdeamides A (**332**) and B (**333**) were found to be cytotoxic against all three cell lines with ED_{50} values ranging from 4.4 to 0.8 μM, and showed the highest cytotoxicity against NCI-H23 cells with ED_{50} values of 0.8 and 0.9 μM, respectively.

Both verdeamides A (**332**) and B (**333**) were evaluated for inhibition of 20S proteasome and showed significant inhibitions against all three cell lines with ED_{50} values ranging from 3.1 to 0.7 μM. Again, both compounds showed the highest inhibitions of 20S proteasome against NCI-H23 cells with ED_{50} values of 0.7 μM.

D.5 Conclusion

The sample collected from Puerto Rico led to the isolation of a *Oscillatoria* sp. (UIC 10109), and the chemical investigation of the cyanobacterium led to the isolation of two new dodecapeptides, verdeamides A (**332**) and B (**333**). Both of these compounds contained an unusual β-amino acid moiety (3-amino-2,5,7,8-tetrahydroxy-10-methylundecanoic acid, Aound), and this moiety had previously been reported only for schizotrin A from *Schizotrix* sp. [313], pahayokolides from *Lyngbya* sp. [130], and

portoamides from *Oscillatoria* sp. [308]. The absolute configuration at Cβ of Anound moiety observed in both verdeamides A (**332**) and B (**333**) was assigned as D by advanced Marfey's analysis assuming that L-FDLA-L-Aound elutes before L-FDLA-D-Aound.

In this study, both verdeamides A (**332**) and B (**333**) showed significant inhibitions of 20S proteasome, which is an important controller of such as cell growth and programmed cell death, with ED_{50} values of 0.7 μM against NCI-H23 cells. This result strongly suggests that inhibition of 20S proteasome could be the molecular mechanism of these compounds, yet further experiments are needed to confirm this.

Chapter 5. CONCLUSION AND PERSPECTIVE

5 Conclusion and Perspective

5.1 Conclusion

In this study, over 300 cyanobacteria strains were cultured, harvested, and extracted between May 2008 and June 2011 to establish an extract library. Total of 306 cyanobacteria strain extracts were evaluated for both cytotoxicity and inhibition of 20S proteasome. Nine of the 306 screened strains displayed cytotoxicity against a set of cancer cells designated HT-29, NCI-H460, MCF-7, and SF268, or cancer cell panel consisting of 12 human cancer cells. Seven of the 306 screened strains also exhibited significant inhibition of 20S proteasome. Five of the seven were later found to be false positive due to color interference with the excitation or emission of the fluorescent enzyme in the assay. Most of the active strains for both cytotoxicity and 20S proteasome inhibition assays belonged to the filamentous orders Nostocales, Stigonematales, and Oscillatoriales. In addition, fractions of one cyanobacteria strain belonging to the order Oscillatoriales were found to be cytotoxic, while the extract did not show any significant activity. This was likely due to bioactive compounds present in the extracts below detection threshold. In total, five active strains, *Fischerella* sp. (SAG 46.79), *Westiellopsis* sp. (SAG 20.93), and *Fischerella muscicola* (UTEX LB1829) of the order Stigonematales, *Nostoc* sp. (UIC 10047) of the order Nostocales, and *Oscillatoria* sp. (UIC 10109) of the order Oscillatoriales were cultured for chemical investigation.

The organic extract of *Fischerella* sp. (SAG 46.79) exhibited significant inhibition of the 20S proteasome, and bioassay-guided fractionation led to the isolation of a previously known compound, hapalosin, as the active principle. A second culture of the same strain was prepared in an attempt to obtain any hapalosin analogues. The extract of the second culture did not inhibit 20S proteasome. However, HPLC-ESIMS analysis of the second extract indicated an intriguing chemical profile, and four nitrile-substituted fischerindole-type alkaloids, 12-*epi*-fischerindole I nitrile, deschloro 12-*epi*-fischerindole I nitrile, 12-*epi*-fischerindole W nitrile, and deschloro 12-*epi*-fischerindole W nitrile, were obtained from this extract. Of the more than 70 indole alkaloids isolated from cyanobacteria, only five have been classified as fischerindoles (fischerindole L, 12-*epi*-fischerindoles G and I, fischerindole U isonitrile, and fischerindole U isothiocyanate) [132, 262, 314]. The majority of these indole alkaloids contained an isonitrile or isothiocyanate moiety and only two were reported with a nitrile substituent (ambiguines G and Q) [255, 315]. Therefore, all four fischerindoles isolated in this study are unusual in that they all contain a nitrile moiety. It had been suggested that rearrangements of ambiguine isonitrile precursors led to the nitrile

products in ambiguine G and Q. However, the isolation of 12-*epi*-fischerindole I nitrile, only differing from 12-*epi*-fischerindole I isonitrile by the replacement of the isonitrile by a nitrile, indicated a different biosynthetic origin of the nitrile moiety in 12-*epi*-fischerindole I nitrile. The structures of 12-*epi*-fischerindole W nitrile and deschloro 12-*epi*-fischerindole W nitrile possessed a new fischerindole skeleton, expanding the five-membered ring to a six-membered ring. This also suggests a new biosynthetic pathway in this cyanobacterium.

Bioassay-guided fractionation of both *Westiellopsis* sp. (SAG 20.93) and *Fischerella muscicola* (UTEX LB1829) led to the isolation of three new hapalindole-type alkaloids along with ten previously reported indole alkaloids and two fischerellins. Hapalindole X was the first example of a tetracyclic hapalindole containing an exocyclic methylene moiety, suggesting the presence of a new biosynthetic pathway in this organism. Hapalindole X showed antimicrobial activities against *M. tuberculosis* and *C. albicans* with MIC values of 2.5 μM, with moderate cytotoxicity in the Vero cell assay. Hapalindole X also showed cytotoxicity against cancer cells with comparatively low cytotoxicity against IMR90 normal cells. Deschloro hapalindole I did not show antibacterial activity while hapalindole I exhibited inhibitory activity against *M. tuberculosis* with a MIC value of 2.0 μM, with no detectable cytotoxicity in the Vero cell assay. 13-hydroxy dechlorofontonamide was not active in cytotoxicity as well as against any microorganisms evaluated in this study.

Borophycin was isolated as the major active component from *Nostoc* sp. (UIC 10047) obtained from a sample collected from Hidden Lake Forest Preserve in Chicago, Illinois. This compound had been reported as a major constituent from a marine strain of *Nostoc linckia*, and shown to be cytotoxic without solid tumor or tumor selectivity [113]. Additional boron-containing compounds, boromycin and aplasmomycin, have been obtained from a terrestrial strain of *Streptomyces antibioticus* and a marine strain of *Streptomyces griseus*. However, studies have indicated that biosynthesis of borophycin was different from that of boromycin and aplasmomycin [113]. In this study, borophycin was found to be cytotoxic against HT-29, NCI-H460, and MCF-7 cancer cells with ED_{50} values of 1.0, 0.57, and 0.49 μM as well as IMR90 normal cells with an ED_{50} value of 0.5 μM.

Verdeamides A and B, cyclic dodecapeptides contained a unusual β-amino acid, 3-amino-2,5,7,8-tetrahydroxy-10-methylundecanoic acid (Aound). They were identified as the major biologically active compounds from *Oscillatoria* sp. (UIC 10109) obtained from a sample collected in Puerto Rico. Both peptides were found to be cytotoxic against SW-620, NCI-H23, and MDA-MB-435 cells with ED_{50} values

ranging from 0.8 to 3.0 μM for verdeamide A, and from 1.8 to 4.4 μM for verdeamide B. Both verdeamides A and B also showed the inhibition of 20S proteasome with ED_{50} values ranging from 0.7 to 3.1 μM.

In conclusion, this study showed cyanobacteria to be a promising source for the discovery of novel anticancer lead compounds. The diverse structures obtained in this study provided further evidence of the remarkable biosynthetic capacity of cyanobacteria. The high discovery rate of novel compounds from cyanobacteria can in part be explained by the relatively low number of investigation of cyanobacteria as a source for drugs as compared to other source organisms. In this study, total of 22 compounds were isolated from 5 strains of cyanobaceteria and 9 of 22 were found to be novel compounds. Most of the compounds exhibited moderate to strong cytotoxic activities or inhibition of 20S proteasome. Thus, we proposed that continued chemical and biological evaluations of this relatively untapped source organism can provide a great opportunity for the discovery of new anticancer lead compounds.

5.2 Perspective

5.2.1 Evaluation of biological activity of cyanobacteria

Both the present study and previous literature reports suggest that the filamentous cyanobacteria of the orders Nostocales, Stigonematales, and Oscillatoriales produce the majority of bioactive metabolites in cyanobacteria. Thus, it is recommended that our collection for future studies should be focused on the filamentous cyanobacteria from these orders.

5.3.2 Chemical and biological evaluation of isolated compounds

Four nitrile-containing fischerindoles were isolated from *Fischerella* sp. (SAG 46.79) along with a known cyclic depsipeptide, hapalosin. The structural classes of these compounds are quite different, yet all was obtained from the same strain. Given that the strain produced the nitrile-containing fischerindoles only during the second culture, it can be assumed that culture conditions might have been unintentionally disturbed. Therefore, it is suggested that future studies on this cyanobacterium should be carried out using different culture conditions such as different media, light intensity and duration, or use of elicitators to increase the production of bioactive fischerindole-type alkaloids or other hapalosin analogues.

Both *Westiellopsis* sp. (SAG 20.93) and *Fischerella muscicola* (UTEX LB1829) showed significant cytotoxicity against HT-29 cancer cells (*Westiellopsis* sp., ED_{50}=13.5 μg/mL) and against a cancer cell panel (*Fischerella muscicola*, ED_{50}=5.3 μg/mL). However, each isolated metabolite was found to be less

cytotoxic than the extract. This could be explained by either a synergistic effect among the isolates or possible degradation of the active ingredient(s) during purification. Therefore, it is recommended to evaluate mixtures of all isolated compounds along with the original extract. If synergistic effects are found, it would be of interest to explore which combination and ratio of the compounds show the highest activity.

Oscillatoria sp. (UIC 10109) was not selected for further chemical investigation, due to lack of significant biological activities observed in the initial biological screening of the extract. However, fractions of the *Oscillatoria* sp. were found to be active. Verdeamides A and B were isolated as the major bioactive metabolites and showed significant inhibition of the 20S proteasome as well as cytotoxicity. Biological evaluations of these compounds indicated the level of activity to be comparable for both cytotoxicity and 20S proteasome inhibition. This suggests that inhibition of the 20S proteasome may be the primary molecular mechanism of action for these compounds. The 20S proteasome plays an important role in controlling protein degradation through the ubiquitin-proteasome pathway. Ubiquitin is a polypeptide chain composed of 76 amino acids. Multi-enzyme cascade, E1 (ubiquitin-activating enzymes), E2 (ubiquitin-conjugating enzymes), and E3 (ubiquitin-protein ligases), activates ubiquitin in an ATP-dependent manner. Proteins covalently bound to the activated ubiquitin chains are recognized by 19S proteasome and destructed by 20S proteasome. Therefore, study of this pathway is suggested for follow-up experiments for detailed molecular mechanism of both compounds.

CITED LITERATURE

[1] Cancer Facts & Figures 2012 in American Cancer Society, **2012** (American Cancer Society, Atlanta)

[2] Cancer Facts & Figures 2011 in American Cancer Society, **2011** (American Cancer Society, Atlanta)

[3] Kinghorn, A. D., de Blanco, E. J. C., Chai, H. B., Orjala, J., Farnsworth, N. R., Soejarto, D. D., Oberlies, N. H., Wani, M. C., Kroll, D. J., Pearce, C. J., Swanson, S. M., Kramer, R. A., Rose, W. C., Fairchild, C. R., Vite, G. D., Emanuel, S., Jarjoura, D., Cope, F. O. Discovery of anticancer agents of diverse natural origin. *Pure. Appl. Chem.* **2009**, 81, 1051-1063.

[4] Singh, R. K., Tiwari, S. P., Rai, A. K., Mohapatra, T. M. Cyanobacteria: an emerging source for drug discovery. *J. Antibiot. (Tokyo)* **2011**, 64, 401-412.

[5] McAlpine, J., Romano, A., Ecker, D. Natural products, both small and large, and a focus on cancer treatment. *Curr. Opin. Drug Discov. Devel.* **2009**, 12, 186-188.

[6] Kinghorn, A. D. *Drug discovery from natural products*. In *Foy's principles of medicinal chmistry*; Eds. Lippincott Willams & Wilkins; Philadelphia; New York; London; Buenos Aires; Hong Kong; Sydney; Tokyo, **2007**, 6, pp 1.

[7] Kingston, D. G. A natural love of natural products. *J. Org. Chem.* **2008**, 73, 3975-3984.

[8] Harvey, A. L. Natural products in drug discovery. *Drug Discov. Today* **2008**, 13, 894-901.

[9] Galm, U., Shen, B. Natural product drug discovery: The times have never been better. *Chem. Biol.* **2007**, 14, 1098-1104.

[10] Kingston, D. G., Newman, D. J. Natural products as drug leads: An old process or the new hope for drug discovery? *IDrugs* **2005**, 8, 990-992.

[11] Paterson, I., Anderson, E. A. The renaissance of natural products as drug candidates. *Science* **2005**, 310, 451-453.

[12] Ortholand, J. Y., Ganesan, A. Natural products and combinatorial chemistry: back to the future. *Curr. Opin. Chem. Biol.* **2004**, 8, 271-280.

[13] Nisbet, L. J., Moore, M. Will natural products remain an important source of drug research for the future? *Curr. Opin. Biotechnol.* **1997**, 8, 708-712.

[14] Strohl, W. R. The role of natural products in a modern drug discovery program. *Drug Discov. Today* **2000**, 5, 39-41.

[15] Mayer, A. M. S., Gustafson, K. R. Marine pharmacology in 2001-2: Antitumour and cytotoxic compounds. *Eur. J. Canc.* **2004**, 40, 2676-2704.

[16] Tan, L. T. Bioactive natural products from marine cyanobacteria for drug discovery. *Phytochemistry* **2007**, 68, 954-979.

[17] Cragg, G. M., Grothaus, P. G., Newman, D. J. Impact of natural products on developing new anti-cancer agents. *Chem. Rev.* **2009**, 109, 3012-3043.

[18] Sausville, E. A., Johnson, J. I., Cragg, G. M., Decker, S. *Anticancer Agents*. In *Cancer drug discovery and development: New paradigms for a new millennium*; Eds. series, A. s.; American Chemical Society; **2001**, 796, pp 1-15.

[19] Newman, D. J., Cragg, G. M. Natural products as sources of new drugs over the last 25 years. *J. Nat. Prod.* **2007**, 70, 461-477.

[20] Chin, Y. W., Balunas, M. J., Chai, H. B., Kinghorn, A. D. Drug discovery from natural sources. *The AAPS Journal* **2006**, 8, E239-E253.

[21] Feling, R. H., Buchanan, G. O., Mincer, T. J., Kauffman, C. A., Jensen, P. R., Fenical, W. Salinosporamide A: A highly cytotoxic proteasome inhibitor from a novel microbial source, a marine bacterium of the new genus *Salinospora*. *Angew. Chem. Int. Ed.* **2003**, 42, 355-357.

[22] Feher, M., Schmidt, J. M. Property distributions: differences between drugs, natural products, and molecules from combinatorial chemistry. *J. Chem. Inf. Comput. Sci.* **2003**, 43, 218-227.

[23] Lam, K. S. New aspects of natural products in drug discovery. *Trens Microbiol.* **2007**, 15, 279-289.

[24] Henkel, T., Brunne, R. M., Muller, H. F. R. Statistical investigation into the structural complementarity of natural products and synthetic compounds. *Angew. Chem. Int. Ed.* **1999**, 38, 643-647.

[25] Williams, D. H., Stone, M. J., Hauck, P. R., Rahman, S. K. Why are secondary metabolites (natural products) biosynthesized? *J. Nat. Prod.* **1989**, 52, 1189-1208.

[26] Drahl, C., Cravatt, B. F., Sorensen, E. J. Protein-reactive natural products. *Angew. Chem. Int. Ed.* **2005**, 44, 5788-5809.

[27] Harvey, A. L. Medicines from nature: Are natural products still relevant to drug discovery? *Trends Pharmacol. Sci.* **1999**, 20, 196-198.

[28] Wase, N. V., Wright, P. C. Systems biology of cyanobacterial secondary metabolite production and its role in drug discovery. *Expert. Opin. Drug Discov.* **2008**, 3, 903-929.

[29] Singh, S., Kate, B. N., Banerjee, U. C. Bioactive compounds from cyanobacteria and microalgae: an overview. *Crit. Rev. Biotechnol.* **2005**, 25, 73-95.

[30] Fogg, G. E., Steward, W. D. P., Fay, P., Walsby, A. E. *The Blue-Green Algae*. In Eds. Academic Press; London, **1973**, pp

[31] Liu, X. J., Chen, F. Cell differentiation and colony alteration of *Nostoc flagelliforme*, an edible terrestrial cyanobacterium in different liquid suspension culture. *Folia Microbiol.* **2003**, 48, 619-625.

[32] Francis, G. Poisonous Australian Lake. *Nature (London)* **1878**, 18, 11-12.

[33] Moore, R. E., Corbett, T. H., Patterson, G. M. L., Valeriote, F. A. The search for new antitumor drugs from blue-green algae. *Curr. Pharm. Des.* **1996**, 2, 137-330.

[34] Donia, M. S., Hathaway, B. J., Sudek, S., Haygood, M. G., Rosovitz, M. J., Ravel, J., Schmidt, E. W. Natural combinatorial peptide libraries in cyanobacterial symbionts of marine ascidians. *Nat. Chem. Biol.* **2006**, 2, 729-735.

[35] Sielaff, H., Christiansen, G., Schwecke, T. Natural products from cyanobacteria: Exploiting a new source for drug discovery. *IDrugs* **2006**, 9, 119-127.

[36] Burja, A. M., Banaigs, B., Abou-Mansour, E., Burgess, J. G. Marine cyanobacgeria - a prolific source of natural products. *Tetrahedron* **2001**, 57, 9347-9377.

[37] Chlipala, G., Mo, S., Orjala, J. Chemodiversity in freshwater and terrestrial cyanobacteria. *Curr. Drug Targets* **2011**, 12, 1654-1673.

[38] Falch, B. S., Konig, G. M., Wright, A. D., Sticher, O. Biological activities of cyanobacteria: evaluation of extracts and pure compounds. *Planta Med.* **1995**, 61, 321-238.

[39] Gademann, K., Portmann, C. Secondary metabolites from cyanobacteria: Complex structures and powerful bioactivities. *Curr. Org. Chem.* **2008**, 12, 326-341.

[40] Harada, K. Production of secondary metabolites by freshwater cyanobacteria. *Chem. Pharm. Bull. (Tokyo)* **2004**, 52, 889-799.

[41] Jaspars, M., Lawton, L. Cyanobacteria - a novel source of pharmaceuticals. *Curr. Opin. Drug. Discov. Devel.* **1998**, 1, 77-84.

[42] Tidgewell, K., Clark, B. R., Gerwick, W. H. The natural products chemistry of cyanobacteria. *Chem. Biol.* **2010**, 2, 141-188.

[43] Engene, N., Rottacker, E. C., Kastovsky, J., Byrum, T., Choi, H., Ellisman, M. H., Komarek, J., Gerwick, W. H. *Moorea producens* gen. nov., sp. nov. and *Moorea bouillonii* comb. nov., tropical marine cyanobacteria rich in bioactive secondary metabolites. *Int. J. Syst. Evol. Microbiol.* **2012**, 62, 1171-1178.

[44] Engene, N., Choi, H., Esquenazi, E., Rottacker, E. C., Ellisman, M. H., Dorrestein, P. C., Gerwick, W. H. Underestimated biodiversity as a major explanation for the perceived rich secondary metabolite capacity of the cyanobacterial genus *Lyngbya*. *Environ. Microbiol.* **2011**, 13, 1601-1610.

[45] Bonnard, I., Rolland, M., Francisco, C., Banaigs, B. Total structure and biological properties of laxaphycins A and B, cyclic lipopeptides from the marine cyanobacterium *Lyngbya majuscula*. *Lett. Pept. Sci.* **1997**, 4, 289-292.

[46] Andrianasolo, E. H., Goeger, D., Gerwick, W. H. Mitsoamide: A cytotoxic linear lipopeptide from the Madagascar marine cyanobacterium *Geitlerinema* sp. *Pure Appl. Chem.* **2007**, 79, 593-602.

[47] Carmely, S., Kashman, Y. Structure of swinholide A, a new macrolide from the marine sponge, *Theonella swinhoei*. *Tetrahedron Lett.* **1985**, 26, 511-514.

[48] Gerwick, W. H., Jiang, Z. D., Agarwal, S. K., Farmer, B. T. Total structure of hormothamnin A, a toxic cyclic undecapeptide from the tropical marine cyanobacterium *hormothamnion enteromorphoides*. *Tetrahedron Lett.* **1992**, 48, 2313-2324.

[49] Medina, R. A., Goeger, D. E., Hills, P., Mooberry, S. L., Huang, N., Romero, L. I., Ortega-Barria, E., Gerwick, W. H., McPhail, K. L. Coibamide A, a potent antiproliferative cyclic depsipeptide from the Panamanian marine cyanobacterium *Leptolyngbya* sp. *J. Am. Chem. Soc.* **2008**, 130, 6324-6325.

[50] Thornburg, C. C., Thimmaiah, M., Shaala, L. A., Hau, A. M., Malmo, J. M., Ishmael, J. E., Youssef, D. T., McPhail, K. L. Cyclic Depsipeptides, Grassypeptolides D and E and Ibu-epidemethoxylyngbyastatin 3, from a Red Sea *Leptolyngbya* Cyanobacterium. *J. Nat. Prod.* **2011**, 74, 1677-1685.

[51] Matthew, S., Schupp, P. J., Luesch, H. Apratoxin E, a cytotoxic peptolide from a guamanian collection of the marine cyanobacterium *Lyngbya bouillonii*. *J. Nat. Prod.* **2008**, 71, 1113-1116.

[52] Tidgewell, K., Engene, N., Byrum, T., Media, J., Doi, T., Valeriote, F. A., Gerwick, W. H. Evolved diversification of a modular natural product pathway: Apratoxins F and G, two cytotoxic cyclic depsipeptides from a Palmyra collection of *Lyngbya bouillonii*. *ChemBioChem* **2010**, 11, 1458-1466.

[53] Kwan, J. C., Rocca, J. R., Abboud, K. A., Paul, V. J., Luesch, H. Total structure determination of grassypeptolide, a new marine cyanobacterial cytotoxin. *Org. Lett.* **2008**, 10, 789-792.

[54] Williams, P. G., Yoshida, W. Y., Moore, R. E., Paul, V. J. Isolation and structure determination of obyanamide, a novel cytotoxic cyclic depsipeptide from the marine cyanobacterium *Lyngbya confervoides*. *J. Nat. Prod.* **2002**, 65, 29-31.

[55] Macmillan, J. B., Molinski, T. F. Caylobolide A, a unique 36-membered macrolactone from a Bahamian *Lyngbya majuscula*. *Org. Lett.* **2002**, 9, 1535-1538.

[56] Gerwick, W. H., Proteau, P. J., Nagle, D. G., Hamel, E., Blokhin, A., Slate, D. L. Structure of curacin A, a novel antimitotic, antiproliferative, and brine shrimp toxic natural product from the marine cyanobacterium *Lyngbya majuscula*. *J. Org. Chem.* **1994**, 59, 1243-1245.

[57] Simmons, T. L., Nogle, L. M., Media, J., Valeriote, F. A., Mooberry, S. L., Gerwick, W. H. Desmethoxymajusculamide C, a cyanobacterial depsipeptide with potent cytotoxicity in both cyclic and ring-opened forms. *J. Nat. Prod.* **2009**, 72, 1011-1016.

[58] Luesch, H., Yoshida, W. Y., Moore, R. E., Paul, V. J., Corbett, T. H. Total structure determination of apratoxin A, a potent novel cytotoxin from the marine cyanobacterium *Lyngbya majuscula*. *J. Am. Chem. Soc.* **2001**, 123, 5418-5423.

[59] Luesch, H., Yoshida, W. Y., Moore, R. E., Paul, V. J. New apratoxins of marine cyanobacterial origin from Guam and Palau. *Bioorg. Med. Chem.* **2002**, 10, 1973-1978.

[60] Gunasekera, S. P., Owle, C. S., Montaser, R., Luesch, H., Paul, V. J. Malyngamide 3 and cocosamides A and B from the marine cyanobacterium *Lyngbya majuscula* from Cocos Lagoon, Guam. *J. Nat. Prod.* **2011**, 74, 871-876.

[61] Popplewell, W. L., Ratnayake, R., Wilson, J. A., Beutler, J. A., Colburn, N. H., Henrich, C. J., McMahon, J. B., McKee, T. C. Grassypeptolides F and G, Cyanobacterial Peptides from *Lyngbya majuscula*. *J. Nat. Prod.* **2011**, 74, 1686-1691.

[62] Milligan, K. E., Marquez, B. L., Williamson, R. T., Gerwick, W. H. Lyngbyabellin B, a toxic and antifungal secondary metabolite from the marine cyanobacterium *Lyngbya majuscula*. *J. Nat. Prod.* **2000**, 63, 1440-1443.

[63] Luesch, H., Yoshida, W. Y., Moore, R. E., Paul, V. J., Mooberry, S. L. Isolation, structure determination, and biological activity of Lyngbyabellin A from the marine cyanobacterium *Lyngbya majuscula*. *J. Nat. Prod.* **2000**, 63, 611-615.

[64] Luesch, H., Pangilinan, R., Yoshida, W. Y., Moore, R. E., Paul, V. J. Pitipeptolides A and B, new cyclodepsipeptides from the marine cyanobacterium *Lyngbya majuscula*. *J. Nat. Prod.* **2001**, 64, 304-307.

[65] Montaser, R., Abboud, K. A., Paul, V. J., Luesch, H. Pitiprolamide, a proline-rich dolastatin 16 analogue from the marine cyanobacterium *Lyngbya majuscula* from Guam. *J. Nat. Prod.* **2011**, 74, 109-112.

[66] Marquez, B. L., Watts, K. S., Yokochi, A., Roberts, M. A., Verdier-Pinard, P., Jimenez, J. I., Hamel, E., Scheuer, P. J., Gerwick, W. H. Structure and absolute stereochemistry of hectochlorin, a potent stimulator of actin assembly. *J. Nat. Prod.* **2002**, 65, 866-871.

[67] Suntornchashwej, S., Chaichit, N., Isobe, M., Suwanborirux, K. Hectochlorin and morpholine derivatives from the Thai sea hare, *Bursatella leachii*. *J. Nat. Prod.* **2005**, 68, 951-955.

[68] Edwards, D. J., Marquez, B. L., Nogle, L. M., McPhail, K., Goeger, D. E., Roberts, M. A., Gerwick, W. H. Structure and biosynthesis of the jamaicamides, new mixed polyketide-peptide neurotoxins from the marine cyanobacterium *Lyngbya majuscula*. *Chem. Biol.* **2004**, 11, 817-833.

[69] Gutierrez, M., Andrianasolo, E. H., Shin, W. K., Goeger, D. E., Yokochi, A., Schemies, J., Jung, M., France, D., Cornell-Kennon, S., Gerwick, W. H. Structural and synthetic investigations of tanikoide

dimer, a SIRT2 selective inhibitor, and tanikolide *Seco* acid from the Madagascar marine cyanobacterium *Lyngbya majuscula*. *J. Org. Chem.* **2009**, 74, 5267-5275.

[70] Taniguchi, M., Nunnery, J. K., Engene, N., Esquenazi, E., Byrum, T., Dorrestein, P. C., Gerwick, W. H. Palmyramide A, a cyclic depsipeptide from a Palmyra Atoll collection of the marine cyanobacterium *Lyngbya majuscula*. *J. Nat. Prod.* **2010**, 73, 393-398.

[71] Gutierrez, M., Tidgewell, K., Capson, T. L., Engene, N., Alejandro, A., Schemies, J., Jung, M., Gerwick, W. H. Malyngolide dimer, a bioactive symmetric cyclodepside from the Panamanian marine cyanobacterium *Lyngbya majuscula*. *J. Nat. Prod.* **2010**, 73, 709-711.

[72] Han, B., Gross, H., Goeger, D. E., Mooberry, S. L., Gerwick, W. H. Aurilides B and C, cancer cell toxins from a Papua New Guinea collection of the marine cyanobacterium *Lyngbya majuscula*. *J. Nat. Prod.* **2006**, 69, 572-575.

[73] Luesch, H., Yoshida, W. Y., Moore, R. E., Paul, V. J. Isolation and structure of the cytotoxin lyngbyabellin B and absolute configuration of lyngbyapeptin A from the marine cyanobacterium *Lyngbya majuscula*. *J. Nat. Prod.* **2000**, 63, 1437-1439.

[74] Sone, H., Kondo, T., Kiryu, M., Ishiwata, H., Ojika, M., Yamada, K. Dolabellin, a cytotoxic bisthiazole metabolite from the sea hare *Dolabella auricularia*: Structural determination and synthesis. *J. Org. Chem.* **1995**, 60, 4774-4781.

[75] Tan, L. T., Sitachitta, N., Gerwick, W. H. The guineamides, novel cyclic depsipeptides from a Papua New Guinea collection of the marine cyanobacterium *Lyngbya majuscula*. *J. Nat. Prod.* **2003**, 66, 764-771.

[76] Han, B., McPhail, K. L., Gross, H., Goeger, D. E., Mooberry, S. L., Gerwick, W. H. Isolation and structure of five lyngbyabellin derivatives from a Papua New Guinea collection of the marine cyanobacterium *Lyngbya majuscula*. *Tetrahedron* **2005**, 61, 11723-11729.

[77] Gutierrez, M., Suyama, T. L., Engene, N., Wingerd, J. S., Matainaho, T., Gerwick, W. H. Apratoxin D, a potent cytotoxic cyclodepsipeptide from papua new guinea collections of the marine cyanobacteria *Lyngbya majuscula* and *Lyngbya sordida*. *J. Nat. Prod.* **2008**, 71, 1099-1103.

[78] Han, B., McPhail, K. L., Ligresti, A., Di Marzo, V., Gerwick, W. H. Semiplenamides A-G, fatty acid amides from a Papua New Guinea collection of the marine cyanobacterium *Lyngbya semiplena*. *J. Nat. Prod.* **2003**, 66, 1364-1368.

[79] Han, B., Goeger, D., Maier, C. S., Gerwick, W. H. The wewakpeptins, cyclic depsipeptides from a Papua NEw Guinea collection of the marine cyanobacterium *Lyngbya semiplena*. *J. Org. Chem.* **2005**, 70, 3133-3139.

[80] Luesch, H., Yoshida, W. Y., Moore, R. E., Paul, V. J. Structurally diverse new alkaloids from Palauan collections of the apratoxin-producing marine cyanobacterium *Lyngbya* sp. *Tetrahedron* **2002**, 58, 7959-7966.

[81] Teruya, T., Sasaki, H., Fukazawa, H., Suenaga, K. Bisebromoamide, a potent cytotoxic peptide from the marine cyanobacterium *Lyngbya* sp.: Isolation, stereostructure, and biological activity. *Org. Lett.* **2009**, 11, 5062-5065.

[82] Maru, N., Ohno, O., Uemura, D. Lyngbyacyclamides A and B, novel cytotoxic peptides from marinc cyanobacteria *Lyngbya* sp. *Tetrahedron Lett.* **2010**, 51, 6384-6387.

[83] Williams, P. G., Luesch, H., Yoshida, W. Y., Moore, R. E., Paul, V. J. Continuing studies on the cyanobacterium *Lyngbya* sp.: Isolation and structure determination of 15-norlyngbyapeptin A and lyngbyabellin D. *J. Nat. Prod.* **2003**, 66, 595-598.

[84] Zou, B., Long, K., Ma, D. Total synthesis and cytotoxicity studies of a cyclic depsipeptide with proposed structure of palau'amide. *Org. Lett.* **2005**, 7, 4237-4240.

[85] Williams, P. G., Yoshida, W. Y., Quon, M. K., Moore, R. E., Paul, V. J. The structure of palau'amide, a potent cytotoxin from a species of the marine cyanobacterium *Lyngbya*. *J. Nat. Prod.* **2003**, 66, 1545-1549.

[86] Luesch, H., Williams, P. G., Yoshida, W. Y., Moore, R. E., Paul, V. J. Ulongamides A-F, new beta-amino acid-containing cyclodepsipeptides from Palauan collections of the marine cyanobacterium *Lyngbya* sp. *J. Nat. Prod.* **2002**, 65, 996-1000.

[87] Williams, P. G., Yoshida, W. Y., Quon, M. K., Moore, R. E., Paul, V. J. Ulongapeptin, a cytotoxic cyclic depsipeptide from a Palauan marine cyanobacterium *Lyngbya* sp. *J. Nat .Prod.* **2003**, 66, 651-654.

[88] Nogle, L. M., Gerwick, W. H. Somocystinamide A, a novel cytotoxic disulfide dimer from a Fijian marine cyanobacterial mixed assemblage. *Org. Lett.* **2002**, 4, 1095-1098.

[89] Mevers, E., Liu, W. T., Engene, N., Mohimani, H., Byrum, T., Pevzner, P. A., Dorrestein, P. C., Spadafora, C., Gerwick, W. H. Cytotoxic veraguamides, alkynyl bromide-containing cyclic depsipeptides from the marine cyanobacterium cf. *Oscillatoria margaritifera*. *J. Nat. Prod.* **2011**, 74, 928-936.

[90] Salvador, L. A., Paul, V. J., Luesch, H. Caylobolide B, a macrolactone from symplostatin 1-producing marine cyanobacteria *Phormidium* spp. from Florida. *J. Nat. Prod.* **2010**, 73, 1606-1609.

[91] Salvador, L. A., Biggs, J. S., Paul, V. J., Luesch, H. Veraguamides A-G, cyclic hexadepsipeptides from a dolastatin 16-producing cyanobacterium *Symploca* cf. hydnoides from Guam. *J. Nat. Prod.* **2011**, 74, 917-927.

[92] Andrianasolo, E. H., Gross, H., Goeger, D., Musafija-Girt, M., McPhail, K., Leal, R. M., Mooberry, S. L., Gerwick, W. H. Isolation of swinholide A and related glycosylated derivatives from two field collections of marine cyanobacteria. *Org. Lett.* **2005**, 7, 1375-1378.

[93] Harrigan, G. G., Luesch, H., Yoshida, W. Y., Moore, R. E., Nagle, D. G., Paul, V. J., Mooberry, S. L., Corbett, T. H., Valeriote, F. A. Symplostatin 1: A dolastatin 10 analogue from the marine cyanobacterium *Symploca hydnoides*. *J. Nat. Prod.* **1998**, 61, 1075-1077.

[94] Horgen, F. D., Kazmierski, E. B., Westenburg, H. E., Yoshida, W. Y., Scheuer, P. J. Malevamide D: Isolation and structure determination of an isodolastatin H analogue from the marine cyanobacterium *Symploca hydnoides*. *J. Nat. Prod.* **2002**, 65, 487-491.

[95] Taori, K., Paul, V. J., Luesch, H. Structure and activity of largazole, a potent antiproliferative agent from the floridian marine cyanobacterium, *Symploc*a sp. *J. Am. Chem. Soc.* **2008**, 130, 1806-1807.

[96] Williams, P. G., Yoshida, W. Y., Moore, R. E., Paul, V. J. Micromide and guamamide: cytotoxic alkaloids from a species of the marine cyanobacterium *Symploca*. *J. Nat. Prod.* **2004**, 67, 49-53.

[97] Pettit, G. R., Kamano, Y., Herald, C. L., Tuinman, A. A., Boettner, F. E., Kizu, H., Schmidt, J. M., Baczynskyj, L., Tomer, K. B., Bontems, R. J. The isolation and structure of a remarkable marine animal antineoplastic constituent: Dolastatin 10. *J. Am. Chem. Soc.* **1987**, 109, 6883-6885.

[98] Luesch, H., Moore, R. E., Paul, V. J., Mooberry, S. L., Corbett, T. H. Isolation of dolastatin 10 from the marine cyanobacterium *Symploca* species VP642 and total stereochemistry and biological evaluation of its analogue symplostatin 1. *J. Nat. Prod.* **2001**, 64, 907-910.

[99] Simmons, T. L., McPhail, K. L., Ortega-Barria, E., Mooberry, S. L., Gerwick, W. H. Belamide A, a new antimitotic tetrapeptide from a Panamanian marine cyanobacterium. *Tetrahedron Lett.* **2006**, 47, 3387-3390.

[100] Luesch, H., Yoshida, W. Y., Moore, R. E., Paul, V. J., Mooberry, S. L., Corbett, T. H. Symplostatin 3, a new dolastatin 10 analogue from the marine cyanobacterium *Symploca* sp. VP452. *J. Nat. Prod.* **2002**, 65, 16-20.

[101] Williams, P. G., Yoshida, W. Y., Moore, R. E., Paul, V. J. Tasiamide, a cytotoxic peptide from the marine cyanobacterium *Symploca* sp. *J. Nat. Prod.* **2002**, 65, 1336-1339.

[102] Williams, P. G., Yoshida, W. Y., Moore, R. E., Paul, V. J. The isolation and structure elucidation of tasiamide B, a 4-amino-3-hydroxy-5-phenylpentanoic acid containing peptide from the marine Cyanobacterium *Symploca* sp. *J. Nat. Prod.* **2003**, 66, 1006-1009.

[103] Nagle, D. G., Gerwick, W. H. Nakienones A-C and nakitriol, new cytotoxic cyclic C_{11} metabolites from an Okinawan cyanobacterial (*Synechocystis* sp.) overgrowth of coral. *Tetrahedron Lett.* **1995**, 36, 849-852.

[104] Namikoshi, M., Carmichael, W. W., Sakai, R., Jareserijman, E. A., Kaup, A. M., Rinehart, K. L. 9-Deazaadenosine and its 5'-α-D-glucopyranoside isolated from the cyanobacterium *Anabaena affinis* strain VS-1. *J. Am. Chem. Soc.* **1993**, 115, 2504-2505.

[105] Frankmolle, W. P., Larsen, L. K., Caplan, F. R., Patterson, G. M. L., Knubel, G., Levine, I. A., Moore, R. E. Antifungal cyclic peptides from the terrestrial blue-green alga *Anabaena laxa*. *J. Antibiot. (Tokyo)* **1992**, 45, 1451-1457.

[106] Frankmolle, W. P., Knubel, G., Moore, R. E., Patterson, G. M. L. Antifungal cyclic peptides from the terrestrial blue-green alga *Anabaena laxa*. II. Structures of laxaphycins A, B, D, and E. *J. Antibiot. (Tokyo)* **1992**, 45, 1458-1466.

[107] Moon, S. S., Chen, J. L., Moore, R. E., Patterson, G. M. L. Calophycin, a fungicidal cyclic decapeptide from the terrestrial blue-green alga *Calothrix fusca*. *J. Org. Chem.* **1992**, 57, 1097-1103.

[108] Rickards, R. W., Rothschild, J. M., Willis, A. C., Chazal, N. M. D., Kirk, J., Kirk, K., Saliba, K. J., Smith, G. D. Calothrixins A and B, novel pentacyclic metabolites from Calothrix cyanobacteria with potent activity against malaria parasites and human cancer cells. *Tetrahedron* **1999**, 55, 13513-13520.

[109] Moore, B. S., Chen, J. L., Patterson, G. M. L., Moore, R. E., Brinen, L. S., Kato, Y., Clardy, J. [7.7]Paracyclophanes from blue-green algae. *J. Am. Chem. Soc.* **1990**, 106, 6456-6457.

[110] Jaki, B., Orjala, J., Heilmann, J., Linden, A., Vogler, B., Sticher, O. Novel extracellular diterpenoids with biological activity from the cyanobacterium *Nostoc commune*. *J. Nat. Prod.* **2000**, 63, 339-343.

[111] Kajiyama, S.-i., Kanzaki, H., Kawazu, K., Kobayashi, A. Nostofungicidine, an antifungal lipopeptide from the field-grown terrestrial blue-green alga *Nostoc commune*. *Tetrahedron Lett.* **1998**, 39, 3737-3740.

[112] Chen, J. L., Moore, R. E., Patterson, G. M. L. Structures of nostocyclophanes A-D. *J. Org. Chem.* **1991**, 56, 4360-4364.

[113] Hemscheidt, T., Puglisi, M. P., Larsen, L. K., Patterson, G. M. L., Moore, R. E., Rios, J. L., Clardy, J. Structure and biosynthesis of borophycin, a new boeseken complex of boric acid from a marine strain of the blue-green alga *Nostoc linckia*. *J. Org. Chem.* **1994**, 59, 3467-3471.

[114] Banker, R., Carmeli, S. Tenuecyclamides A-D, cyclic hexapeptides from the cyanobacterium *Nostoc spongiaeforme* var. *tenue*. *J. Nat. Prod.* **1998**, 61, 1248-1251.

[115] Fujii, K., Sivonen, K., Kashiwagi, T., Hirayama, K., Harada, K. Nostophycin, a novel cyclic peptide from the toxic cyanobacterium *Nostoc* sp. 152. *J. Org. Chem.* **1999**, 64, 5777-5782.

[116] Smith, C. D., Zhang, X., Mooberry, S. L., Patterson, G. M., Moore, R. E. Cryptophycin: a new antimicrotubule agent active against drug-resistant cells. *Cancer Res.* **1994**, 54, 3779-3784.

[117] Golakoti, T., Yoshida, W. Y., Chaganty, S., Moore, R. E. Isolation and structure determination of nostocyclopeptides A1 and A2 from the terrestrial cyanobacterium *Nostoc* sp. ATCC53789. *J. Nat. Prod.* **2001**, 64, 54-59.

[118] Bui, H. T. N., Jansen, R., Pham, H. T. L., Mundt, S. Carbamidocyclophanes A-E, chlorinated paracyclophanes with cytotoxic and antibiotic activity from the Vietnamese cyanobacterium *Nostoc* sp. *J. Nat. Prod.* **2007**, 70, 678-681.

[119] Shih, C., Teicher, B. A. Cryptophycins: a novel class of potent antimitotic antitumor depsipeptides. *Curr. Pharm. Des.* **2001**, 7, 1259-1276.

[120] Chlipala, G. E., Sturdy, M., Krunic, A., Lantvit, D. D., Shen, Q., Porter, K., Swanson, S. M., Orjala, J. Cylindrocyclophanes with proteasome inhibitory activity from the cyanobacterium *Nostoc* sp. *J. Nat. Prod.* **2010**, 73, 1529-1537.

[121] Knubel, G., Larsen, L. K., Moore, R. E., Levine, I. A., Patterson, G. M. L. Cytotoxic antiviral indolocarbazoles from a blue-green alga belonging to the Nostocaceae. *J. Antibiot. (Tokyo)* **1990**, 43, 1236-1239.

[122] Carmeli, S., Moore, R. E., Patterson, G. M. L. Mirabimides A-D, new N-acylpyrrolinones from the blue-green alga *Scytonema mirabile*. *Tetrahedron* **1991**, 47, 2087-2096.

[123] Dillon, J. G., Castenholz, R. W. Scytonemin, a cyanobacterial sheath pigment, protects against uvc radiation: Implications for early photosynthetic life. *J. Phycol.* **1999**, 35, 673-681.

[124] Jung, J. H., Moore, R. E., Patterson, G. M. L. Scytophycins from a blue-green alga belonging to the nostocaceae. *Phytochemistry* **1991**, 30, 3615-3616.

[125] Carmeli, S., Moore, R. E., Patterson, G. M. L. Tolytoxin and new scytophycins from three species of *Scytonema*. *J. Nat. Prod.* **1990**, 53, 1533-1542.

[126] Prinsep, M. R., Caplan, F. R., Moore, R. E., Patterson, G. M. L., Smith, C. D. Tolyporphin, a novel multidrug resistance reversing agent from the blue-green alga *Tolypothrix nodosa*. *J. Am. Chem. Soc.* **1992**, 114,

[127] Prinsep, M. R., Patterson, G. M. L., Larsen, L. K., Smith, C. D. Further tolyporphins from the blue-green alga *Tolypothrix nodosa*. *Tetrahedron* **1995**, 51, 10523-10530.

[128] Prinsep, M. R., Patterson, G. M. L., Larsen, L. K., Smith, C. D. Tolyporphins J and K, two further porphinoid metabolites from the cyanobacterium *Tolypothrix nodosa*. *J. Nat. Prod.* **1998**, 61, 1133-1136.

[129] Berry, J. P., Gantar, M., Gawley, R. E., Wang, M., Rein, K. S. Pharmacology and toxicology of pahayokolide A, a bioactive metabolite from a freshwater species of *Lyngbya* isolated from the Florida Everglades. *Comp. Biochem. Physiol. C Toxicol. Pharmacol.* **2004**, 139, 231-238.

[130] An, T., Kumar, T. K., Wang, M., Liu, L., Lay, J. O., Jr., Liyanage, R., Berry, J., Gantar, M., Marks, V., Gawley, R. E., Rein, K. S. Structures of pahayokolides A and B, cyclic peptides from a *Lyngbya* sp. *J. Nat. Prod.* **2007**, 70, 730-735.

[131] Mehner, C., Muller, D., Krick, A., Kehraus, S., Loser, R., Gutschow, M., Maier, A., Fiebig, H.-H., Brun, R., Konig, G. M. A novel β-amino acid in cytotoxic peptides from the cyanobacterium *Tychonema* sp. *Eur. J. Org. Chem.* **2008**, 2008, 1732-1739.

[132] Stratmann, K., Moore, R. E., Bonjouklian, R., Deeter, J. B., Patterson, G. M. L., Shaffer, S., Smith, C. D., Smitka, T. A. Welwitindolinones, Unusual Alkaloids from the Blue-Green Algae

Hapalosiphon welwitschii and *Westiella intricata*. Relationship to Fischerindoles and Hapalindoles. *J. Am. Chem. Soc.* **1994**, 116, 9935-9942.

[133] Prinsep, M. R., Moore, R. E., Levine, I. A., Patterson, G. M. L. Westiellamide, a bistratamide-related cyclic peptide from the blue-green alga *Westiellopsis prolifica*. *J. Nat. Prod.* **1992**, 55, 140-142.

[134] Zafrir-Ilan, E., Carmeli, S. Two new microcyclamides from a water bloom of the cyanobacterium *Microcystis* sp. *Tetrahedron Lett.* **2010**, 51, 6602-6604.

[135] Ishida, K., Nakagawa, H., Murakami, M. Microcyclamide, a cytotoxic cyclic hexapeptide from the cyanobacterium *Microcystis aeruginosa*. *J. Nat. Prod.* **2000**, 63, 1315-1317.

[136] Tsukamoto, S., Painuly, P., Young, K. A., Yang, X., Shimizu, Y., Cornell, L. Microcystilide A: a novel cell-differentiation-promoting depsipeptide from *Microcystis aeruginosa* NO-15-1840. *J. Am. Chem. Soc.* **1993**, 115, 11046-11047.

[137] Pettit, G. R., Kamano, Y., Dufresne, C., Cerny, R. L., Herald, C. L., Schmidt, J. M. Isolation and structure of the cytostatic linear depsipeptide dolastatin 15. *J. Org. Chem.* **1989**, 54, 6005-6006.

[138] Tan, L. T. Filamentous tropical marine cyanobacteria: a rich source of natural products for anticancer drug discovery. *J. Appl. Phycol.* **2010**, 22, 659-676.

[139] Watanabe, J., Minami, M., Kobayashi, M. Antitumor activity of TZT-1027 (soblidotin). *Anticancer Res.* **2006**, 27, 1973-1981.

[140] Patel, S., Keohan, M. L., Saif, M. W., Rushing, D., Baez, L., Feit, K., DeJager, R., Anderson, S. Phase II study of intravenous TZT-1027 in patients with advanced or metastatic soft-tissue sarcomas with prior exposure to anthracycline-based chemotherapy. *Cancer* **2006**, 107, 2881-2887.

[141] Luesch, H., Harrigan, G. G., Goetz, G., Horgen, F. D. The cyanobacterial origin of potent anticancer agentsoriginallyisolated from sea hares. *Curr. Med. Chem.* **2002**, 9, 1791-1806.

[142] Katz, J., Janik, J. E., Younes, A. Brentuximab Vedotin (SGN-35). *Clin. Cancer Res.* **2011**, 17, 6428-6436.

[143] Gerwick, L., Moore, B. S. Lessons from the past and charting the future of marine natural products drug discovery and chemical biology. *Chem. Biol.* **2012**, 19, 85-98.

[144] Mooberry, S. L., Leal, R. M., Tinley, T. L., Luesch, H., Moore, R. E., Corbett, T. H. The molecular pharmacology of symplostatin 1: A new antimitotic dolastatin 10 analog. *Int. J. Cancer.* **2003**, 104, 512-521.

[145] Sone, H., Shibata, T., Fujita, T., Ojika, M., Yamada, K. Dolastatin H and isodolastatin H, potent cytotoxic peptides from the sea hare *Dolabella auricularia*: Isolation, stereostructures, and synthesis. *J. Am. Chem. Soc.* **1996**, 118, 1874-1880.

[146] Horgen, F. D., Yoshida, W. Y., Scheuer, P. J. Malevamides A-C, new depsipeptides from the marine cyanobacterium *Symploca laete-viridis*. *J. Nat. Prod.* **2000**, 63, 461-467.

[147] Sato, T., Shibazaki, M., Yamaguchi, H., Abe, K., Matsumoto, H., Shimizu, M. Novel *Candida albicans* aspartyl protease inhibitor. II. A new pepstatin-ahpatinin group inhibitor, YF-044P-D. *J. Antibiot.* **1994**, 47, 588-590.

[148] Omura, S., Imamura, N., Kawakita, K., Mori, Y., Yamazaki, Y., Masuma, R., Takahashi, Y., Tanaka, H., Huang, L. Y., Woodruff, H. B. Ahpatinins, new acid protease inhibitors containing 4-amino-3-hydroxy-5-pentanoic acid. *J. Antibiot.* **1986**, 39,

[149] Williams, P. G., Yoshida, W. Y., Moore, R. E., Paul, V. J. Tasipeptins A and B: New cytotoxic depsipeptides from the marine cyanobacterium *Symploca* sp. *J. Nat. Prod.* **2003**, 66, 620-624.

[150] Bai, R., Friedman, S. J., Pettit, G. R., Hamel, E. Dolastatin 15, a potent antimitotic depsipeptide derived from *Dolabella auricularia*. Interaction with tubulin and effect of cellular microtubules. *Biochem. Pharmacol.* **1992**, 43, 2637-2645.

[151] Horton, P., Inman, W. D., Crews, P. Enantiomeric Relationships and Anthelmintic Activity of Dysinin Derivatives from Dysidea Marine Sponges. *J. Nat. Prod.* **1990**, 53, 143-151.

[152] Roller, P., Au, K., Moore, R. E. *Chem. Commun.* **1971**,

[153] Perez Baz, J., Canedo, L. M., Fernandez, P. J. L., Silva, E. M. V. *J. Antibiot.* **1997**, 50, 738-741.

[154] Boger, D. G., Ichikawa, S. Total syntheses of thiocoraline and BE-22179: Establishment of relative and absolute stereochemistry. *J. Am. Chem. Soc.* **2000**, 122, 2956-2957.

[155] Lee, S. U., Kwak, H. B., Pi, S. H., K., Y. H., Byeon, S. R., Ying, Y., Luesch, H., Hong, J., Kim, S. H. In vitro and in vivo osteogenic activity of largazole. *ACS Med. Chem. Lett.* **2011**, 2, 248-251.

[156] Ying, Y., Taori, K., Kim, H., Hong, J., Luesch, H. Total synthesis and moelcular target of largazole, a histone deacetylase inhibitor. *J. Am. Chem. Soc.* **2008**, 130, 8455-8459.

[157] Okino, T. *Heterocycles from cyanobacteria*. In *Topics in heterocyclic chemistry*; Eds. Gupta, R. R.; Springer-Verlag; Berlin Heidelberg, **2006**, 5, pp 1-19.

[158] Blokhin, A. V., Yoo, H. D., Geralds, R. S., Nagle, D. G., Gerwick, W. H. Characterization ofthe interaction of the marine cyanobacterial natural product curacin A with the colchicine site of tubulin and initial structure-activity studies with analogues. *Mol. Pharmacol.* **1995**, 48, 523-531.

[159] Wipf, P., Reeves, J. T., Balachandran, R., Giuliano, K. A., Hamel, E., Day, B. W. Synthesis and biological evaluation of a focused mixture library of analogues of the antimitotic marine natural product curacin A. *J. Am. Chem. Soc.* **2000**, 122, 9391-9395.

[160] Chen, J., Forsyth, C. J. Total Synthesis of Apratoxin A. *J. Am. Chem. Soc.* **2003**, 125, 8734-8735.

[161] Chen, J., Forsyth, C. J. Total synthesis of the marine cyanobacterial cyclodepsipeptide apratoxin A. *Proc. Natl. Acad. Sci. USA* **2004**, 101, 12067-12072.

[162] Doi, T., Numajiri, Y., Munakata, A., Takahashi, T. Total synthesis of apratoxin A. *Org. Lett.* **2006**, 8, 531-534.

[163] Chen, J., Forsyth, C. J. Synthesis of the apratoxin 2,4-disubstituted thiazoline via an intramolecular aza-Witting reaction. *Org. Lett.* **2003**, 5, 1281-1283.

[164] Zou, B., Wei, J., Cai, G., Ma, D. Synthesis of an oxazoline analogue of apratoxin A. *Org. Lett.* **2003**, 5, 3503-3506.

[165] Gilles, A., Martinez, J., Cavelier, F. Supported synthesis of oxoapratoxin A. *J. Org. Chem.* **2009**, 74, 4298-4304.

[166] Chen, Q. Y., Liu, Y., Luesch, H. Systematic chemical mutagenesis identifies a potent novel apratoxin A/E hybrid with improved in vivo antitumor activity. *ACS Med. Chem. Lett.* **2011**,

[167] Cruz-Rivera, E., Paul, V. J. Chemical deterrence of a cyanobacterial metabolite against generalized and specilized grazers. *J. Chem. Ecol.* **2007**, 33, 213-217.

[168] Pettit, G. R., Kamano, Y., Kizu, H., Dufresne, C., Herald, C. L., Bontems, R. J., Schmidt, J. M., Boettner, F. E., Nieman, R. A. Isolation and structure of the cell growth inhibitory depsipeptides dolastatins 11 and 12. *Heterocycles* **1989**, 28, 553-558.

[169] Sone, H., Nemoto, T., Ishiwata, H., Ojika, M., Yamada, K. Isolation, structure, and synthesis of dolastatin D, a cytotoxic cyclic depsipeptide from the sea hard *Dolabella auricularia*. *Tetrahedron Lett.* **1993**, 34, 8449-8452.

[170] Rodriguez, J., Fernandez, R., Quinoa, E., Riguera, R., Debitus, C., Bouchet, P. Onchidine: A cytotoxic depsipeptide with C2 symmetry from a marine mollusc. *Tetrahedron Lett.* **1994**, 35, 9239-9242.

[171] Williams, P. G., Moore, R. E., Paul, V. J. Isolation and structure determination of lyngbyastatin 3, a lyngbyastatin 1 homologue from the marine cyanobacterium *Lyngbya majuscula*. Determination of the configuration of the 4-amino-2,2-dimethyl-3-oxopentanoic acid unit in majusculamide C, dolastatin 12, lyngbyastatin 1, and lyngbyastatin 3 from cyanobacteria. *J. Nat. Prod.* **2003**, 66, 1356-1363.

[172] Kimura, J., Takada, Y., Inayoshi, T., Nakao, Y., Goetz, G., Yoshida, W. Y., Scheuer, P. J. Kulokekahilide-1, a cytotoxic depsipeptide from the cephalaspidean mollusk *Philinopsis speciosa*. *J. Org. Chem.* **2002**, 67, 1760-1767.

[173] Koehn, F. E., Longley, R. E., Reed, J. K. Microcolins A and B, new immunosuppressive peptides from the blue-green alga *Lyngbya majuscula*. *J. Nat. Prod.* **1992**, 55, 613-619.

[174] Moore, R. E., Entzeroth, M. Majusculamide D and deoxymajusculamide D, two cytotoxins from *Lyngbya majuscula*. *Phytochemistry* **1988**, 27, 3101-3103.

[175] Paik, S., Carmeli, S., Cullingham, J., Moore, R. E., Patterson, G. M. L., Tius, M. A. Mirabimide E, an unusual *N*-Acylpyrrolinone from the blue-green alga *Scytonema mirabile*: Structure determination and synthesis. *J. Am. Chem. Soc.* **1994**, 116, 8116-8125.

[176] Fernandez-Suarez, M., Munoz, L., Fernandez, R., Riguera, R. Asymmetric synthesis of the β-amino acid methyl ester derivative of onchidin: (2S,3S)-methyl-3-amino-2-methyl-7-octynoate and its enantiomer. *Tetrahedron: Asymmestry* **1997**, 8, 1847-1854.

[177] Satake, K., Murata, M., Yasumoto, T. Amphidinol, a polyhydroxypolyene antifungal agent with an unprecedented structure, from a marine dinoflagellate, *Amphidinium klebsii*. *J. Am. Chem. Soc.* **1991**, 113, 9859-9861.

[178] Murata, M., Matsuoka, S., Matsumori, N., Paul, G. K., Tachibana, K. Absolute configuration of amphidinol 3, the first complete structure determination from amphidinol homologues: Application of a new configuration analysis based on carbon-hydrogen spin-coupling constants. *J. Am. Chem. Soc.* **1999**, 121, 870-871.

[179] Echigoya, R., Rhodes, L., Oshima, Y., Satake, M. The structures of five new antifungal and hemolytic amphidinol analogs from *Amphidinium carterae* collected in New Zealand. *Harmful Algae* **2005**, 4, 383-389.

[180] Rezanka, T., Dembitsky, V. Novel brominated lipidic compounds from lichens of Central Asia. *Phytochemistry* **1999**, 51, 963-968.

[181] Rezanka, T., Dembitsky, V. Brominated fatty acids from lichen *Acorospora gobiensis*. *Phytochemistry* **1998**, 50, 97-99.

[182] Zhang, L. H., Longley, R. E., Koehn, F. E. Antiproliferative and immunosuppressive properties of microcolin A, a marine-derived lipopeptide. *Life Sci.* **1997**, 60, 751-762.

[183] Suenaga, K., Mutou, T., Shibata, T., Itoh, T., Fujita, T., Takada, N., Hayamizu, K., Takagi, M., Irifune, T., Kigoshi, H., Yamada, K. Aurilide, a cytotoxic depsipeptide from the sea hare Dolabella auricularia: isolation, structure determination, synthesis, and biological activity. *Tetrahedron* **2004**, 60, 8509-8527.

[184] Nakao, Y., Yoshida, W. Y., Takada, Y., Kimura, J., Yang, L., Mooberry, S. L., Scheuer, P. J. Kulokekahilide-2, a cytotoxic depsipeptide from a cephalaspidean mollusk *Philinopsis speciosa*. *J. Nat. Prod.* **2004**, 67, 1332-1340.

[185] Fusetani, N., Sugawara, T., Matsunaga, S., Hirota, H. Orbiculamide A: A novel cytotoxic cyclic peptide from a marine sponge *Theonella* sp. *J. Am. Chem. Soc.* **1991**, 113, 7811-7812.

[186] Kobayashi, J., Itagaki, F., Shigemori, H., Ishibashi, M., Takahashi, K., Ogura, M., Nagasawa, S., Nakamura, T., Hirota, H., Ohta, T., Nozoe, S. Keramamides B-D: Novel peptides from the Okinawan marine sponge *Theonella* sp. *J. Am. Chem. Soc.* **1991**, 113, 7812-7813.

[187] Nakao, Y., Fujita, M., Warabi, K., Matsunaga, S., Fusetani, N. Miraziridine A, a novel cysteine protease inhibitor from the marine sponge *Theonella* aff. *mirabilis*. *J. Am. Chem. Soc.* **2000**, 122, 10462-10463.

[188] Hawkins, C. J., Lavin, M. F., Marshall, K. A., van den Brenk, A. L., Watters, D. J. Structure-activity relationships of the lissoclinamides: cytotoxic cyclic peptides from the ascidian *Lissoclinum patella*. *J. Med. Chem.* **1990**, 33, 1634-1638.

[189] Wipf, P., Fritch, P. C., Geib, S. J., Sefler, A. M. Conformational studies and structure-activity analysis of lissoclinamide 7 and related cyclopeptide alkaloids. *J. Am. Chem. Soc.* **1998**, 120, 4105-4112.

[190] Kwan, J. C., Ratnayake, R., Abboud, K. A., Paul, V. J., Luesch, H. Grassypeptolides A-C, cytotoxic bis-thiazoline containing marine cyclodepsipeptides. *J. Org. Chem.* **2010**, 75, 8012-8023.

[191] Singh, I. P., Milligan, K. E., Gerwick, W. H. Tanikolide, a toxic and antifungal lactone from the marine cyanobacterium *Lyngbya majuscula*. *J. Nat. Prod.* **1999**, 62, 1333-1335.

[192] Cardellina, J. H., Moore, R. E., Arnold, E. V., Clardy, J. Structure and absolute configuration of malyngolide, an antibiotic from the marine blue-green alga *Lyngbya majuscula* Gomont. *J. Org. Chem.* **1979**, 44, 4039-4042.

[193] Harrigan, G. G., Yoshida, W. Y., Moore, R. E., Nagle, D. G., Park, P. U., Biggs, J., Paul, V. J., Mooberry, S. L., Corbett, T. H., Valeriote, F. A. Isolation, structure determination, and biological activity of dolastatin 12 and lyngbyastatin 1 from *Lyngbya majuscula*/*Schizothrix calcicola* cyanobacterial assemblages. *J. Nat. Prod.* **1998**, 61, 1221-1225.

[194] Carter, D. C., Moore, R. E., Mynderse, J. S., Niemczura, W. P., Todd, J. S. Structure of majusculamide C, a cyclic depsipeptide from *Lyngbya majuscula*. *J. Org. Chem.* **1984**, 49, 236-241.

[195] Mynderse, J. S., Hunt, A. H., Moore, R. E. 57-Normajusculamide C, a minor cyclic depsipeptide isolated from *Lyngbya majuscula*. *J. Nat. Prod.* **1988**, 51, 1299-1301.

[196] Nunnery, J. K., Mevers, E., Gerwick, W. H. Biologically active secondary metabolites from marine cyanobacteria. *Curr. Opin. Biotechnol.* **2010**, 21, 787-793.

[197] Pettit, G. R., Xu, J.-p., Hogan, F., Williams, M. D., Doubek, D. L., Schmidt, J. M., Cerny, R. L., Boyd, M. R. Isolation and structure of the human cancer cell growth inhibitory cyclodepsipeptide dolastatin 16. *J. Nat. Prod.* **1997**, 60, 752-754.

[198] MacMillan, J. B., Ernst-Russel, M. A., de Ropp, J. S., Molinski, T. F. Lobocyclamides A-C, lipopeptides from a cryptic cyanobacteria mat containing *Lyngbya confervoides*. *J. Org. Chem.* **2002**, 67, 8210-8215.

[199] Bonnard, I., Rolland, M., Salmon, J. M., Debiton, E., Barthomeuf, C., Banaigs, B. Total structure and inhibition of tumor cell proliferation of laxaphycins. *J. Med. Chem.* **2007**, 50, 1266-1279.

[200] Frankmolle, W. P., Larsen, L. K., Caplan, F. R., Patterson, G. M. L., Knubel, G., Levine, I. A., Moore, R. E. Antifungal cyclic peptides from the terrestrial blue-green alga *Anabaena laxa*. I. Isolation and biological properties. *J. Antibiot. (Tokyo)* **1992**, 45, 1451-1457.

[201] Doi, M., Ishida, T. Molecular conformation of swinholide A, a potent cytotoxic dimeric macrolide from the Okinawan marine sponge *Theonella swinhoei*: X-ray cryastal structure of its diketone derivative. *J. Org. Chem.* **1991**, 56, 3629-3632.

[202] Bubb, M. R., Spector, I., Bershaksky, A. D., Korn, E. D. Swinholide A is a microfilament disrupting marine toxin that stabilizes actin dmers and severs actin filaments. *J. Biol. Chem.* **1995**, 270, 3463-3466.

[203] Weinig, S., Hecht, H. J., Mahmud, R., Muller, R. Melithiazole biosynthesis: Further insights into myxobacterial PKS/NRPS systems and evidence for anew subclass of methyl transferases. *Chem. Biol.* **2003**, 10, 939-952.

[204] Paull, K. D., Shoemaker, R. H., Hodes, L., Monks, A., Scudiero, D. A., Rubinsterin, L., Plowman, J., Boyd, M. R. Display and analysis of patterns of differential activity of drugs against human tumor cell lines: Development of mean graph and COMPARE algorithm. *J. Natl. Cancer Inst.* **1989**, 81, 1088-1092.

[205] Wrasidlo, W., Mielgo, A., Torres, V. A., Barbero, S., Stoletov, K., Suyama, T. L., Klemke, R. L., Gerwick, W. H., Carson, D. A., Stupack, D. G. The marine lipopeptide somocystinamide A triggers apoptosis via caspase 8. *Proc. Natl. Acad. Sci. U S A* **2008**, 105, 2313-2318.

[206] Glazer, R. I., Hartman, K. D., Knode, M. C. 9-Deazaadenosine. Cytocidal activity and effects on nucleic acids and protein synthesis in human colon carcinoma cells in culture. *Mol. Pharmacol.* **1983**, 24, 309-315.

[207] Garcia-Pichel, F., Castenholz, R. W. Characterization and biological implications of scytonemin, a cyanobacterial sheath pigment. *J. Phycol.* **1991**, 27, 395-409.

[208] Proteau, P. J., Gerwick, W. H., Pichel-Garcia, F., Castenholz, R. The structure of scytonemin, an ultraviolet sunscreen pigment from the sheaths of cyanobacteria. *Experientia.* **1993**, 49, 825-829.

[209] Stevenson, C. S., Capper, E. A., Roshak, A. K., Marquez, B., Eichman, C., Jackson, J. R., Mattern, M., Gerwick, W. H., Jacobs, R. S., Marshall, L. A. The identification and characterization of the marine natural produt scytonemin as a novel antiproliferative pharmacophore. *J. Pharmacol. Exp. Ther.* **2002**, 303, 858-866.

[210] Moore, R. E., Patterson, G. M. L., Mynderse, J. S., Barchi Jr., J., Norton, T. R., Furusawa, E., Furusawa, S. Toxins from cyanophytes belonging to the Scytonemataceae. *Pure Appl. Chem.* **1986**, 58, 263-271.

[211] Ishibashi, M., Moore, R. E., Patterson, G. M. L. Scytophycins, cytotoxic and antimycotic agents from the cyanophyte *Scytonema pseudohofmanni*. *J. Org. Chem.* **1986**, 51, 5300-5306.

[212] Moore, B. S., Chen, J. L., Patterson, G. M. L., Moore, R. E. Structures of cylindrocyclophanes A-F. *Tetrahedron* **1992**, 48, 3001-3006.

[213] Furasaki, A., Hashiba, N., Matsumoto, T., Hirano, A., Iwai, Y., Omura, S. X-ray crystal structure of staurosporine: A new alkaloid from a *Streptomyces* strain. *J. C. S. Chem. Comm.* **1978**, 1978, 800-801.

[214] Steglich, W., Steffan, B., Kopanski, L., Eckhardt, G. Indole pigments from the fruiting bodies of the slime mold *Arcyria denudata*. *Angew. Chem. Int. Ed. Engl.* **1980**, 19, 459-460.

[215] Nettleton, D. E., Doyle, T. W., Krishnan, B., Matsumoto, G. K., Clardy, J. Isolation and structure of rebeccamycin - A new antitumor antibiotic from *Nocardia aerucoligenes*. *Tetrahedron Lett.* **1985**, 26, 4011-4014.

[216] Schwartz, R. E., Hirsch, C. F., Sesin, D. F., Flor, J. E., Chartrain, M., Fromtling, R. E., Harris, G. H., Salvatore, M. J., Liesch, J. M., Yudin, K. Pharmaceuticals from cultured algae. *J. Ind. Microbiol.* **1990**, 5, 113-123.

[217] Trimurtulu, G., Ohtani, I., Patterson, G. M. L., Moore, R. E., Corbett, T. H., Valeriote, F. A., Demchik, L. Total structures of cryptophycins, potent antitumor depsipeptides from the blue-green alga *Nostoc* sp. strain GSV 224. *J. Am. Chem. Soc.* **1994**, 116, 4729-4737.

[218] Subbaraju, G. V., Golakoti, T., Patterson, G. M., Moore, R. E. Three new cryptophycins from *Nostoc* sp. GSV 224. *J. Nat. Prod.* **1997**, 60, 302-305.

[219] Chaganty, S., Golakoti, T., Heltzel, C., Moore, R. E., Yoshida, W. Y. Isolation and structure determination of cryptophycins 38, 326, and 327 from the terrestrial cyanobacterium *Nostoc* sp. GSV 224. *J. Nat. Prod.* **2004**, 67, 1403-1406.

[220] Al-awar, R. S., Corbett, T. H., Ray, J. E., Polin, L., Kennedy, J. H., Wagner, M. M., Williams, D. C. Biological evaluation of cryptophycin 52 fragment A analogues: Effect of the multidrug resistance ATP binding cassette transporters on antitumor activity. *Mol. Cancer Ther.* **2004**, 3, 1061-1067.

[221] Dunitz, J. D., Hawley, D. M., Miklos, D., Whiter, D. N. J., Berlin, Y., Marusic, R., Prelog, V. Structure of boromycin. *Helv. Chim. Acta.* **1971**, 54, 1709-1713.

[222] Nakamura, H., Iitaka, Y., Kitahar, T., Okazaki, T., Okami, Y. Structure of aplasmomycin. *J. Antibiot. (Tokyo)* **1977**, 30, 714-719.

[223] Morris, S. A., Schwartz, R. E., Sesin, D. F., Masurekar, P., Hallada, T. C., Schmatz, D. M., Bartizal, K., Henesens, O. D., Zink, D. L. Pneumocandin D_0, a new antifungal agent and potent inhibitor of Pneumocystis carinii. *J. Antibiot.* **1994**, 47, 755-764.

[224] Bisacchi, G. S., Hockstein, D. R., Koster, W. H., Parker, W. L., Rathnum, M., Unger, S. E. Xylocandin: A new complex of antifungal peptides. II. Structural studies and chemical modifications. *J. Antibiot.* **1987**, 40, 1520-1529.

[225] Moore, R. E., Bornemann, V., Niemczura, W. P., Gregson, J. M., L., C. J., Norton, T. R., Patterson, G. M. L., Helms, G. L. Puwainaphycin C, a cardioactive cyclic peptide from the blue-green alga *Anabaena* BQ-16-1. Use of two-dimensional ^{13}C-^{13}C and ^{13}C-^{15}N correlation spectroscopy in sequencing in amino acid units. *J. Am. Chem. Soc.* **1989**, 1111,

[226] Okino, T., Matsuda, H., Murakami, M., Yamaguchi, K. Microginin, an angiotensin-converting enzyme inhibitor from the blue-green alga *Microcystis aeruginosa*. *Tetrahedron Lett.* **1993**, 34, 501-504.

[227] Prinsep, M. R., Thomson, R. A., West, M. L., Wylie, B. L. Tolypodiol, an antiinflammatory diterpenoid from the cyanobacterium *Tolypothrix nodosa*. *J. Nat. Prod.* **1996**, 59, 786-788.

[228] Jaki, B., Orjala, J., Sticher, O. A novel extracellular diterpenoid with antibacterial activity from the cyanobacterium *Nostoc commune*. *J. Nat. Prod.* **1999**, 62, 502-503.

[229] Gregson, J. M., Chen, J. L., Patterson, G. M. L., Moore, R. E. Structures of puwainaphycins A-E. *Tetrahedron* **2001**, 48, 3727-3734.

[230] Moore, R. E. Cyclic peptides and depsipeptides from cyanobacteria: a review. *J. Ind. Microbiol.* **1996**, 16, 134-143.

[231] Patterson, G. M. L., Larsen, L. K., Moore, R. E. Bioactive natural products from blue-green algae. *J. Appl. Phycol.* **1994**, 6,

[232] Tsukamoto, S., Painuly, P., Young, K. A., Yang, X., Shimizu, Y. Microcystilide A: a novel cell-differentiation-promoting depsipeptide from *Microcystis aeruginosa* NO-15-1840. *J. Am. Chem. Soc.* **1993**, 115, 11046-11047.

[233] Balis, F. M. Evolution of anticancer drug discovery and the role of cell-based screening. *J. Natl. Cancer Inst.* **2002**, 94, 78-79.

[234] Gibbs, J. B. Mechanism-based target identification and drug discovery in cancer research. *Science* **2000**, 287, 1969-1973.

[235] Gibbs, J. B. Anticancer drug targets: growth factors and growth factor signaling. *J. Clin. Invest.* **2000**, 105, 9-13.

[236] Sausville, E. A., Johnson, J. I. Molecules for the millennium: How will they look? New drug discovery year 2000. *Br. J. Cancer* **2000**, 83, 1401-1404.

[237] Swinney, D. C., Anthony, J. How were new medicines discovered? *Nat. Rev. Drug Discov.* **2011**, 10, 507-519.

[238] Starr, R. C., Zeikus, J. A. UTEX - the culture collection of algae at the University-Of-Texas at Austin 1993 List of cultures. *J. Phycol.* **1993**, 29, 1-106.

[239] Andersen, R. A., Morton, S. L., Sexton, J. P. Provasoli-Guillard National Center for Culture of Marine Phytoplankton 1997 list of strains. *J. Phycol.* **1997**, 33, 1-75.

[240] Schlösser, U. G. SAG - Sammlung von Algenjulturen at the University of Göttingen. Catalogue of strains 1994. *Bot. Acta.* **1994**, 107, 113-186.

[241] Lukavský, J., Cepák, V., Komárek, J., Kašpárková, M., Takáčová, M. Catalogue of algal and cyanobacterial strains of culture collection of autotrophic organisms at Trebon. *Algological studies* **1992**, 63, 59-112.

[242] Andersen, R. A., Kawachi, M. *Traditional Microalgae Isolation Techniques*. In *Algal Culturing Techniques*; Eds. Andersen, R. A.; Elsevier Academic Press; Burlington, MA, **2005**, pp 83-100.

[243] Hoshaw, R. W., Rosowski, J. R. *Methods for microscopic algae*. In *Handbook of Phycological methods: Culture methods & Growth measurements*; Eds. Stein, J. R.; Cambridge University Press; Cambridge, **1973**, pp 53-68.

[244] Andersen, R. A., Berges, J. A., Harrison, R. J., Watanabe, M. M. *Recipes for Freshwater and Seawater Media*. In *Algal Culturing Techniques*; Eds. Andersen, R. A.; Elsevier Academic Press; Burlington, MA, **2005**, pp 429-538.

[245] Alali, F. Q., El-Elimat, T., Li, C., Qandil, A., Alkofahi, A., Tawaha, K., Burgess, J. P., Nakanishi, Y., Kroll, D. J., Navarro, H. A., Falkinhan, J. O., Wani, M. C., Oberlies, N. H. New colchicinoids from a native jordanian meadow saffron, *Colchicum brachyphyllum*: Isolation of the first naturally occurring dextrorotatory colchicinoid. *J. Nat .Prod.* **2005**, 68, 173-178.

[246] Komárek, J., Komáková, J., Kling, H. *Filamentous cyanobacteria*. In *Freshwater algae of North America*; Eds. Wehr, J. D., Sheath, R. G.; Elsevier; San Diego, **2003**, pp 184.

[247] Boone, D. R., Castenholz, R. W. *Subsection V. (Formerly Stigonematales Geitler 1925)*. In *Bergey's manual of systematic bacteriology*; Eds. Hoffmann, L., Castenholz, R. W.; Springer; New York, **2001**, 1, pp 589-599.

[248] Gugger, M. F., Hoffmann, L. Polyphyly of true branching cyanobacteria (Stigonematales). *Int. J. Syst. Evol. Microbiol.* **2004**, 54, 349-357.

[249] Moore, R. E., Cheuk, C., Patterson, G. M. L. Hapalindoles: New Alkaloids from the Blue-Green Alga *Hapalosiphon fontinalis*. *J. Am. Chem. Soc.* **1984**, 106, 6456-6457.

[250] Falch, B. S., Koenig, G. M., Wright, A. D., Sticher, O., Ruegger, H., Bernardinelli, G. Ambigol A and B: New biologically active polychlorinated aromatic compounds from the terrestrial blue-green alga *Fischerella ambigua*. *J. Org. Chem.* **1993**, 58, 6570-6575.

[251] Wright, A. D., Papendorf, O., Konig, G. M. Ambigol C and 2,4-dichlorobenzoic acid, natural products produced by the terrestrial cyanobacterium *Fischerella ambigua*. *J. Nat. Prod.* **2005**, 68, 459-461.

[252] Smitka, T. A., Bonjouklian, R., Doolin, L., Jones, N. D., Deeter, J. B. Ambiguine isonitriles, fungicidal hapalindole-type alkaloids from three genera of blue-green algae beloning to the Stigonemataceae. *J. Org. Chem.* **1992**, 57, 857-861.

[253] Raveh, A., Carmeli, S. Antimicrobial ambiguines from the cyanobacterium *Fischerella* sp. collected in Israel. *J. Nat. Prod.* **2007**, 70, 196-201.

[254] Mo, S., Krunic, A., Chlipala, G., Orjala, J. Antimicrobial ambiguine isonitriles from the cyanobacterium *Fischerella ambigua*. *J. Nat. Prod.* **2009**, 72, 894-899.

[255] Mo, S., Krunic, A., Santarsiero, B. D., Franzblau, S. G., Orjala, J. Hapalindole-related alkaloids from the cultured cyanobacterium *Fischerella ambigua*. *Phytochemistry* **2010**, 71, 2116-2123.

[256] Bonjouklian, R., Moore, R. E., Patterson, G. M. L., Smitka, T. A. U.S.**1994**.

[257] Becher, P. G., Keller, S., Jung, G., Sussmuth, R. D., Juttner, F. Insecticideal activity of 12-*epi*-hapalindole J isonitrile. *Phytochemistry* **2007**, 68, 2493-2497.

[258] Schwartz, R. E., Hirsch, C. F., Springer, J. P., Pettibone, D. J., Zink, D. L. Unusual cyclopropane-containing hapalindolinones from a cultured cyanobacterium. *J. Org. Chem.* **1987**, 52, 3704-3706.

[259] Schwartz, R. E., Hirsch, C. F., Sigmund, J. M., Pettibone, D. J. U.S.**1989**.

[260] Hagmann, L., Juttner, F. Fischerellin A, a Novel Photosystem-II-inhibiting Allelochemical of the Cyanobacterium *Fischerella muscicola* with Antifungal and Herbicidal Activity. *Tetrahedron Lett.* **1996**, 37, 6539-6542.

[261] Papke, U., Gross, E. M., Francke, W. Isolation, Identification and Determination of the Absolute Configuration of Fischerellin B. A New Algicide from the Freshwater Cyanobacterium. *Tetrahedron Lett.* **1997**, 38, 379-382.

[262] Park, A., Moore, R. E., Patterson, G. M. L. Fischerindole L, a New Isonitrile from the Terrestrial Blue-Green Alga *Fischerella muscicola*. *Tetrahedron Lett.* **1992**, 33, 3257-3260.

[263] Etchegaray, A., Rabello, E., Dieckmann, R., Moon, D. J., Fiore, M. F., von Doehren, H., Tsai, S. M., Neilan, B. A. Algicide production by the filamentous cyanobacterium *Fischerella* sp. CENA 19. *J. Appl. Phycol.* **2004**, 16, 237-243.

[264] Ravi, K. A., Arunima, S., Akhilesh, P. S., Deepali, Sureshwar, P. S., Gopal, N., Ranjana, S., Brahm, S. S. Identification of an antimicrobial entity from the cyanobacterium *Fischerella* sp. isolated from bark of *Azadirachta indica* (Neem) tree. *J. Appl. Phycol.* **2006**, 18, 33-39.

[265] Jimenez, J. I., Huber, U., Moore, R. E., Patterson, G. M. L. Oxidized Welwitindolinones from Terrestrial *Fischerella* spp. *J. Nat. Prod.* **1999**, 62, 569-572.

[266] Fiore, M. F., Genuaio, D. B., da Silva, C. S. P., Shishido, T. K., Moraes, L. A. B., Neto, R. C., Silva-Stenico, M. E. Microcystin production by a freshwater spring cyanobacterium of the genus *Fischerella*. *Toxicon* **2009**, 53, 754-761.

[267] Asthana, R. K., Srivastava, A., Singh, A. P., Deepali, Singh, S. P., Nath, G., Srivastava, R., Srivastava, B. S. Identification of an antimicrobial entity from the cyanobacterium *Fischerella* sp. isolated from bark of *Azadirachta indica* (Neem) tree. *J. Appl. Phycol.* **2006**, 18, 33-39.

[268] Janet, M. Westiellopsis prolifica, gen. et sp. nov., a new member of the Stigonemataceae. *Annals of Botany* **1941**, 5, 167-170.

[269] Moore, R. E., Cheuk, C., Yang, X. G., Patterson, G. M. L. Hapalindoles, Antibacterial and Antimycotic Alkaloids from the Cyanophyte *Hapalosiphon fontinalis*. *J. Org. Chem.* **1987**, 52, 1036-1043.

[270] Moore, R. E., Yang, X. G., Patterson, G. M. L., Bonjouklian, R., Smitka, T. A. Hapalonamides and Other Oxidized Hapalindoles from *Hapalosiphon fontinalis*. *Phytochemistry* **1989**, 28, 1565-1567.

[271] Moore, R. E., Yang, X. G., Patterson, G. M. L. Fontonamide and Anhydrohapaloxindole A, Two New Alkaloids from the Blue-Green Alga *Hapalosiphon fontinalis*. *J. Org. Chem.* **1987**, 52, 3773.

[272] Todorova, A. K., Juettner, F., Linden, A., Pluess, T., von Philipsborn, W. Nostocyclamide: A new macrocyclic, thiazole-containing allelochemical from *Nostoc* sp. 31 (Cyanobacteria). *J. Org. Chem.* **1995**, 60, 7891-7895.

[273] Juettner, F., Todorova, A. K., Walch, N., nov Philipsborn, W. Nostocyclamide M: A cyanobacterial cyclic peptide with allelopathic activity from *Nostoc* 31. *Phytochemistry* **2001**, 57, 613-619.

[274] Kaya, K., Sano, T., Beattie, K. A., Codd, G. A. Nostocyclin, a novel 3-amino-6-hydroxy-2-piperidone-containing cycic depsipeptide from the cyanobacterium *Nostoc* sp. *Tetrahedron Lett.* **1996**, 37, 6725-6728.

[275] Okino, T., Qi, S., Matsuda, H., Murakami, M., Yamaguchi, K. Nostopeptins A and B, elastase inhibitors from the cyanobacterium *Nostoc minutum*. *J. Nat. Prod.* **1997**, 60, 158-161.

[276] Murakami, M., Sun, Q., Ishida, K., Matsuda, H., Okino, T., Yamaguchi, K. Microviridins, elastase inhibitors from the cyanobacterium *Nostoc minutum* (NIES-26). *Phytochemistry* **1997**, 45, 1197-1202.

[277] Golakoti, T., Yoshida, W. Y., Chaganty, S., Moore, R. E. Isolation and structures of nostopeptolides A1, A2, and A3 from the cyanobacterium *Nostoc* sp. GSV224. *Tetrahedron* **2000**, 56, 9093-9102.

[278] Ploutno, A., Carmeli, S. Modified peptides from a water bloom of the cyanobacterium *Nostoc* sp. *Tetrahedron* **2002**, 58, 9949-9957.

[279] Mehner, C., Muller, D., Kehraus, S., Hautmann, S., Gutschow, M., Konig, G. M. New peptolides from the cyanobacterium *Nostoc insulare* as selective and potent inhibitors of human leukocyte elastase. *Chembiochem* **2008**, 9, 2692-2703.

[280] Jaki, B., Heilmann, J., Sticher, O. New antibacterial metabolites from the cyanobacterium *Nostoc commune* (EAWAG 122b). *J. Nat. Prod.* **2000**, 63, 1283-1285.

[281] Volk, R. B., Mundt, S. Cytotoxic and non-cytotoxic exometabolites of the cyanobacterium *Nostoc insulare*. *J. Appl. Phycol.* **2007**, 19, 55-62.

[282] Nagatsu, A., Kajitani, H., Sakakibara, J. Muscoride A: A new oxazole peptide alkaloids from freshwater cyanobacterium *Nostoc muscorum*. *Tetrahedron Lett.* **1995**, 36, 1299-1301.

[283] Sivonen, K., Namikoshi, M., Evans, W. R., Fardig, M., Carmichael, W. W., Rinehart, K. L. Three new microcystins, cyclic heptapeptide hepatotoxins, from *Nostoc* sp. strain 152. *Chem. Res. Toxicol.* **1992**, 5, 464-469.

[284] Becher, P. G., Baumann, H. I., Gademann, K., Juettner, F. The cyanobacterial alkaloid nostocarboline: An inhibitor of acetylcholinesterase and trypsin. *J. Appl. Phycol.* **2009**, 21, 103-110.

[285] Golakoti, T., Ogino, J., Heltzel, C. E., Lehusebo, T., Jensen, C. M., Larsen, L. K., Patterson, G. M. L., Moore, R. E., Mooberry, S. L., Corbett, T. H., Valeriote, F. A. Structure determination, conformational-analysis, chemical-stability studies, and antitumor evaluation of the cryptophycins-Isolation of 18 new analogs from *Nostoc* sp. strain GSV-224. *J. Am. Chem. Soc.* **1995**, 117,

[286] Ploutno, A., Carmeli, S. Nostocyclyne A, a novel antimicrobial cyclophane from the cyanobacterium *Nostoc* sp. *J. Nat. Prod.* **2000**, 63, 1524-1526.

[287] Hirata, K., Yoshitomi, S., Dwi, S., Iwabe, O., Mahakhant, A., Polchai, J., Miyamoto, K. Bioactivities of nostocine A produced by a freshwater cyanobacterium *Nostoc spongiaeforme* TISTR 8169. *J. Biosci. Bioeng.* **2003**, 95, 512-517.

[288] Hammerschmidt, F. J., Clark, A. M., El-Kashoury, E. A., El-Kawy, M. M. A., El-Fishawy, A. M. Chemical composition and antimicrobial activity of essential oils of *Jasonia candicans* and *J. montana*. *Planta Med.* **1993**, 59, 68-70.

[289] Volk, R. B., Furkert, F. H. Antialgal, antibacterial and antifungal activity of two metabolites produced and excreted by cyanobacteria during growth. *Microbiol. Res.* **2006**, 161, 180-186.

[290] Ben-Haim, Y., Banim, E., Kushmaro, A., Loya, Y., Rosenberg, E. Inhibition of photosynthesis and bleaching of zooxanthellae by the coral pathogen *Vibrio shiloi*. *Environ. Microbiol.* **1999**, 1, 223-229.

[291] Guillard, R. R. L. *In Algal Culturing Techniques*. In *Purification Methods for Microalgae*; Eds. Andersen, R. A.; Elsevier Academic Press; Burlington, MA, **2005**, pp 117-132.

[292] Martínez-Murcia, A. J., Acinas, S. G., Rodriguez-Valera, F. Evaluation of prokaryotic diversity by restrictase digestion of 16S rDNA directly amplified from hypersaline environments. *FEMS Microbiol. Ecol.* **1995**, 17, 247-256.

[293] Nübel, U., GarciaPichel, F., Muyzer, G. PCR primers to amplify 16S rRNA genes from cyanobacteria. *Appl. Environ. Microbiol.* **1997**, 63, 3327-3332.

[294] Rajaniemi, P., Hrouzek, P., Kastovska, K., Willame, R., Rantala, A., Hoffmann, L., Komárek, J., Sivonen, K. Phylogenetic and morphological evaluation of the genera *Anabaena*, *Aphanizomenon*, *Trichormus*, and *Nostoc* (Nostocales, Cyanoacteria). *Int. J. Syst. Evol. Microbiol.* **2005**, 55, 11-26.

[295] Hutter, R., Keller-Schierlein, W., Knusel, F., Prelog, V., Rodgers, G. C. J., Suter, P., Vogel, G., Voser, W., Zahner, J. The metabolic products of microorganisms. Boromycin. *Helv. Chim. Acta.* **1967**, 50, 1533-1539.

[296] Okami, Y., Okazaki, T., Kitahara, T., Umezawa, H. Studies on marine microorganisms. V. A new antibiotic, aplasmomycin, produced by a streptomycete isolated from shallow sea mud. *J. Antibiot. (Tokyo)* **1976**, 29, 1019-1025.

[297] Itou, Y., Ishida, K., Shin, H. J., murakami, M. Oscillapeptins A to F, serine protease inhibitors from the three strains of *Oscillatoria agardhii*. *Tetrahedron* **1999**, 55, 6871-6882.

[298] Shin, H. J., Murakami, M., Matsuda, H., Ishida, K., Yamaguchi, K. Oscillapeptin, an elastase and chymotrypsin inhibitor from the cyanobacterium *Oscillatoria agardhii* (NIES-204). *Tetrahedron Lett.* **1995**, 36, 5235-5238.

[299] Fujii, K., Sivonen, K., Naganawa, E., Harada, K. Non-toxic peptides from toxic cyanobacteria, *Oscillatoria agardhii*. *Tetrahedron* **2000**, 56, 725-733.

[300] Sano, T., Kaya, K. Oscillapeptin G, a tyrosinase inhibitor from toxic *Oscillatoria agardhii*. *J. Nat. Prod.* **1996**, 59, 90-92.

[301] Shin, H. J., Murakami, M., Matsuda, H., Yamaguchi, K. Microviridins D-F, serine protease inhibitors from the cyanobacterium *Oscillatoria agardhii* (NIES-204). *Tetrahedron* **1996**, 52, 8159-8168.

[302] Shin, H. J., Matsuda, H., Murakami, M., Yamaguchi, K. Agardhipeptins A and B, two new cyclic hepta-and octapeptide, from the cyanobacterium *Oscillatoria agardhii* (NIES-204). *Tetrahedron* **1996**, 52, 13129-13136.

[303] Shin, H. J., Matsuda, H., Murakami, M., Yamaguchi, H. Aeruginosins 205A and -B, serine protease inhibitory glycopeptides from the cyanobacterium *Oscillatoria agardhii* (NIES-205). *J. Org. Chem.* **1997**, 62, 1810-1813.

[304] Sano, T., Kaya, K. A 3-amino-10-chloro-2-hydroxydecanoic acid-containing tetrapeptide from *Oscillatoria agardhii*. *Phytochemistry* **1997**, 44, 1503-1505.

[305] Sano, T., Kaya, K. Oscillamide Y, a chymotrypsin inhibitor from toxic *Oscillatoria agardhii*. *Tetrahedron Lett.* **1995**, 36, 5933-5936.

[306] Shin, H. J., Matsuda, H., Murakami, M., Yamaguchi, K. Anabaenopeptins E and F, two new cyclic peptides from the cyanobacterium Oscillatoria agardhii (NIES-204). *J. Nat. Prod.* **1997**, 60, 139-141.

[307] Itou, Y., Suzuki, S., Ishida, K., Murakami, M. Anabaenopeptins G and H, potent carboxypeptidase A inhibitors from the cyanobacterium *Oscillatoria agardhii* (NIES-595). *Bioorg. Med. Chem. Lett.* **1999**, 9, 1243-1246.

[308] Leao, P. N., Pereira, A. R., Liu, W. T., Ng, J., Pevzner, P. A., Dorrestein, P. C., Konig, G. M., Vasconcelos, V. M., Gerwick, W. H. Synergistic allelochemicals from a freshwater cyanobacterium. *Proc. Natl. Acad. Sci. U S A* **2010**, 107, 11183-11188.

[309] Mundt, S., Kreitlow, S., Jansen, R. Fatty acids with antibacterial activity from the cyanobacterium *Oscillatoria redekei* HUB 051. *J. Appl. Phycol.* **2003**, 15, 263-267.

[310] B'Hymer, C., Montes-Bayon, M., Caruso, J. A. Marfey's reagent: Past, present, and future uses of 1-fluoro-2,4-dinitrophenyl-5-L-alanine amide. *J. Sep. Sci.* **2003**, 26, 7-19.

[311] Bhushan, R., Bruckner, H. Marfey's reagent for chiral amino acid analysis: A review. *Amino Acids* **2004**, 27, 231-247.

[312] Bonnard, I., Manzanares, I., Rinehart, K. L. Stereochemistry of kahalalide F. *J. Nat. Prod.* **2003**, 66, 1466-1470.

[313] Pergament, I., Carmell, S. Schizotrin A: A novel antimicrobial cyclic peptide from a cyanobacterium. *Tetrahedron Lett.* **1994**, 35, 8473-8476.

[314] Richter, J. M., Ishihara, Y., Masuda, T., Whitefield, B. W., Llamas, T., Pohjakallio, A., Baran, P. S. Enantiospecific total synthesis of the hapalindoles, fischerindoles, and welwitindolinones via a redox economic approach. *J. Am. Chem. Soc.* **2008**, 130, 17938-17954.

[315] Huber, U., Moore, R. E., Patterson, G. M. L. Isolation of a Nitrile-Containing Indole Alkaloid from the Terrestrial Blue-Green Alga *Hapalosiphon delicatulus*. *J. Nat. Prod.* **1998**, 61, 1304-1306.

APPENDIX

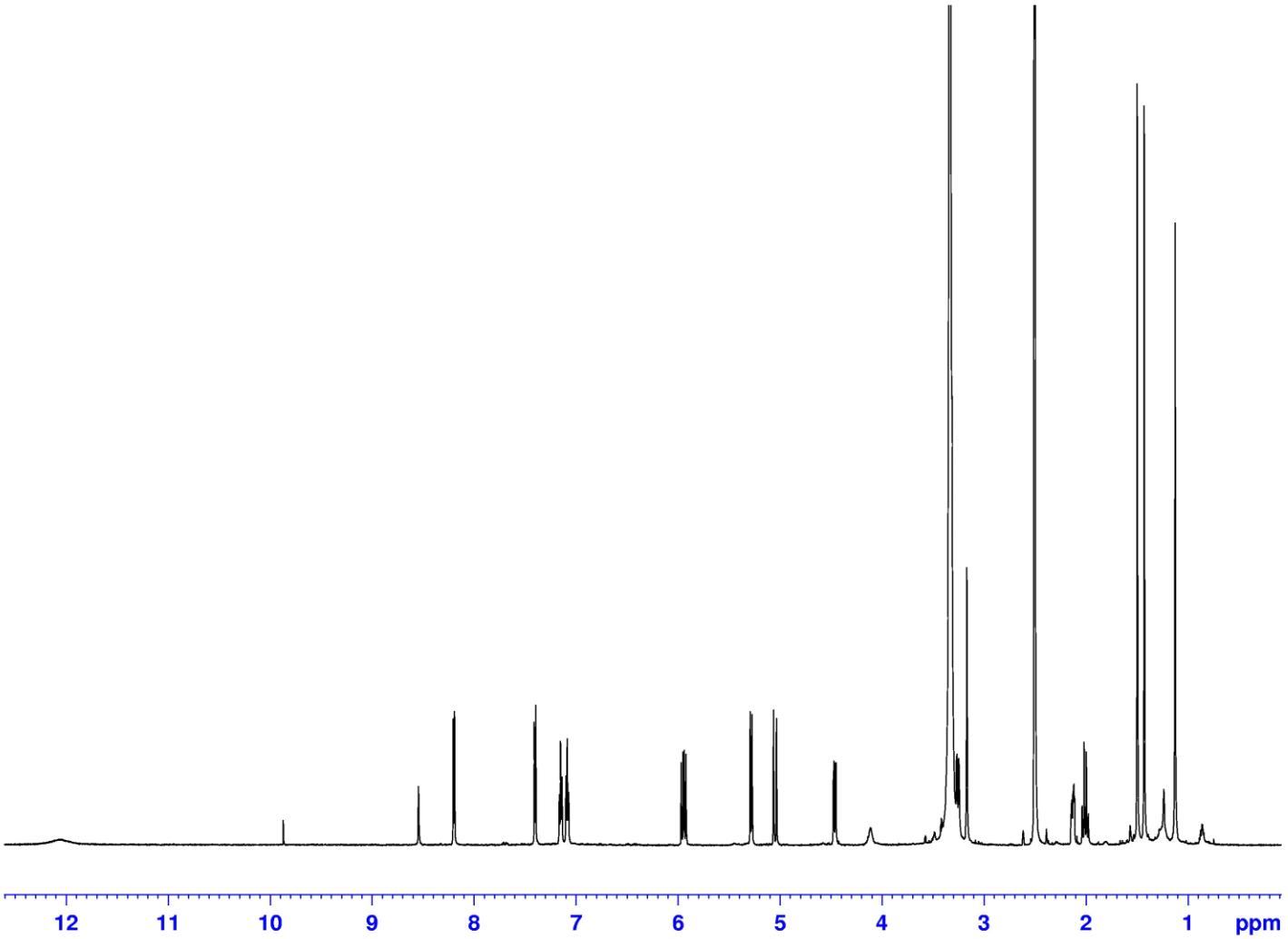

Figure 67. ^{1}H NMR spectrum (600 MHz, DMSO-d_6) of 12-*epi*-fischerindole I nitrile (**217**)

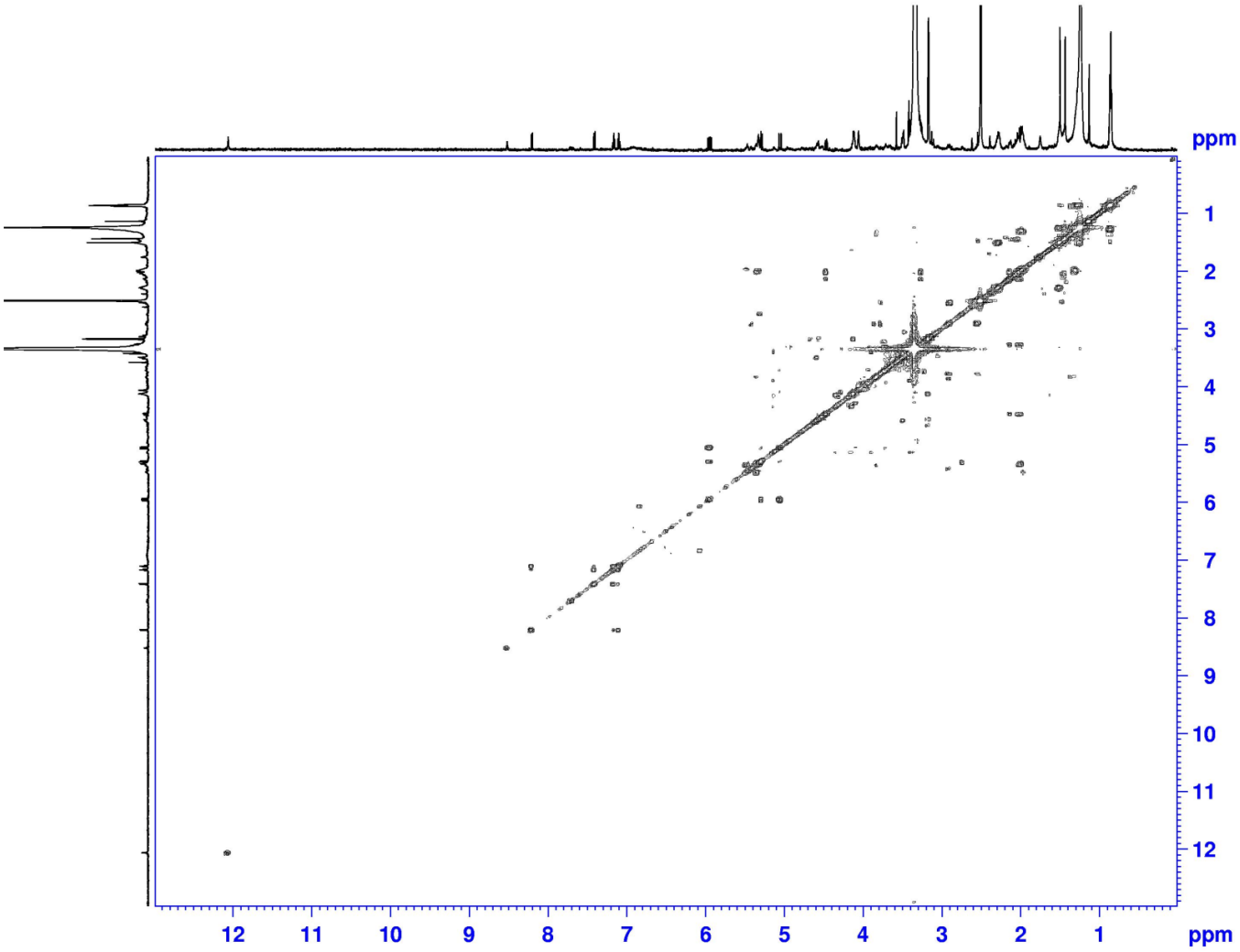

Figure 68. COSY spectrum (600 MHz, DMSO-d_6) of 12-*epi*-fischerindole I nitrile (**217**)

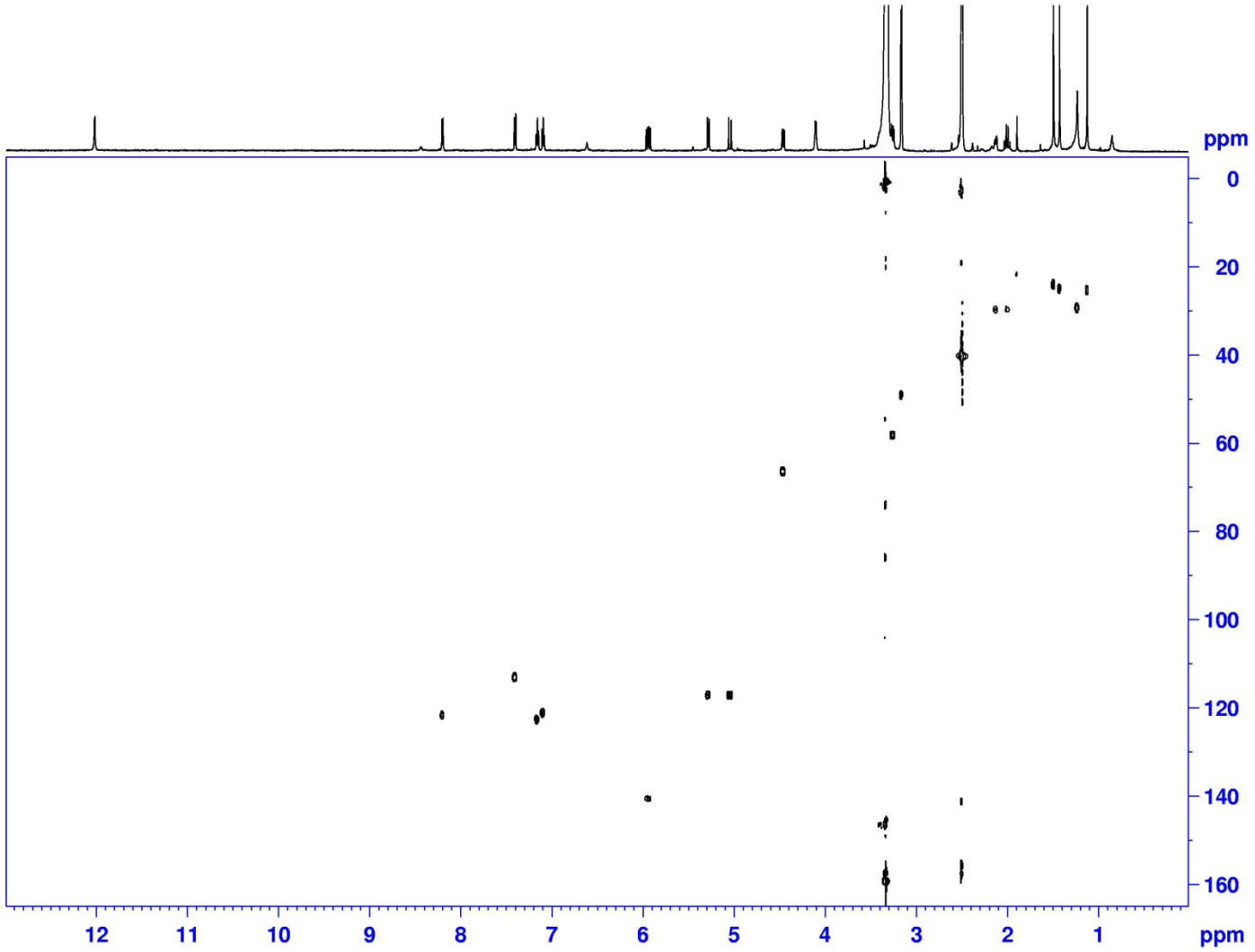

Figure 69. HSQC spectrum (600 MHz, DMSO-d_6) of 12-*epi*-fischerindole I nitrile (**217**)

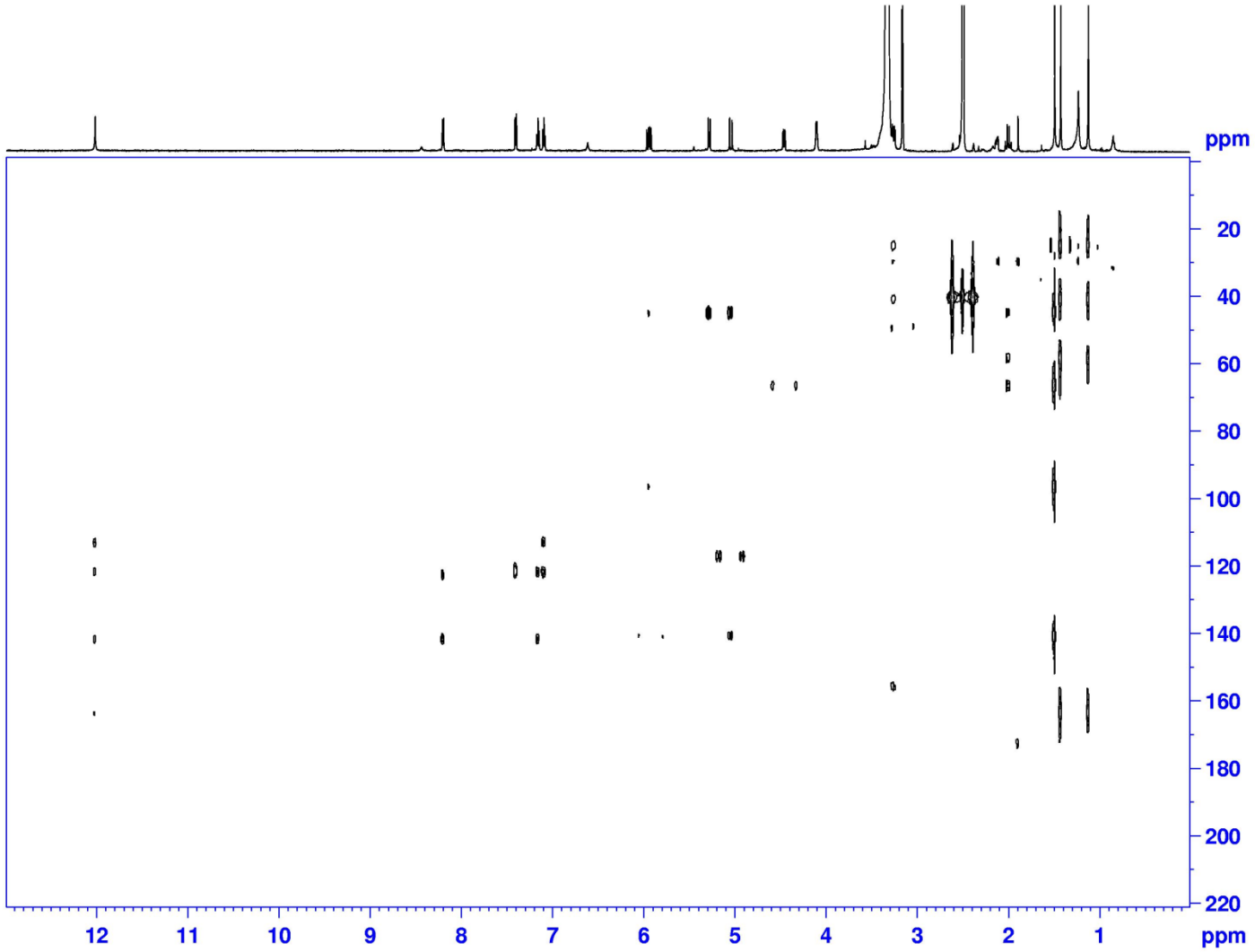

Figure 70. HMBC spectrum (600 MHz, DMSO-d_6) of 12-*epi*-fischerindole I nitrile (**217**)

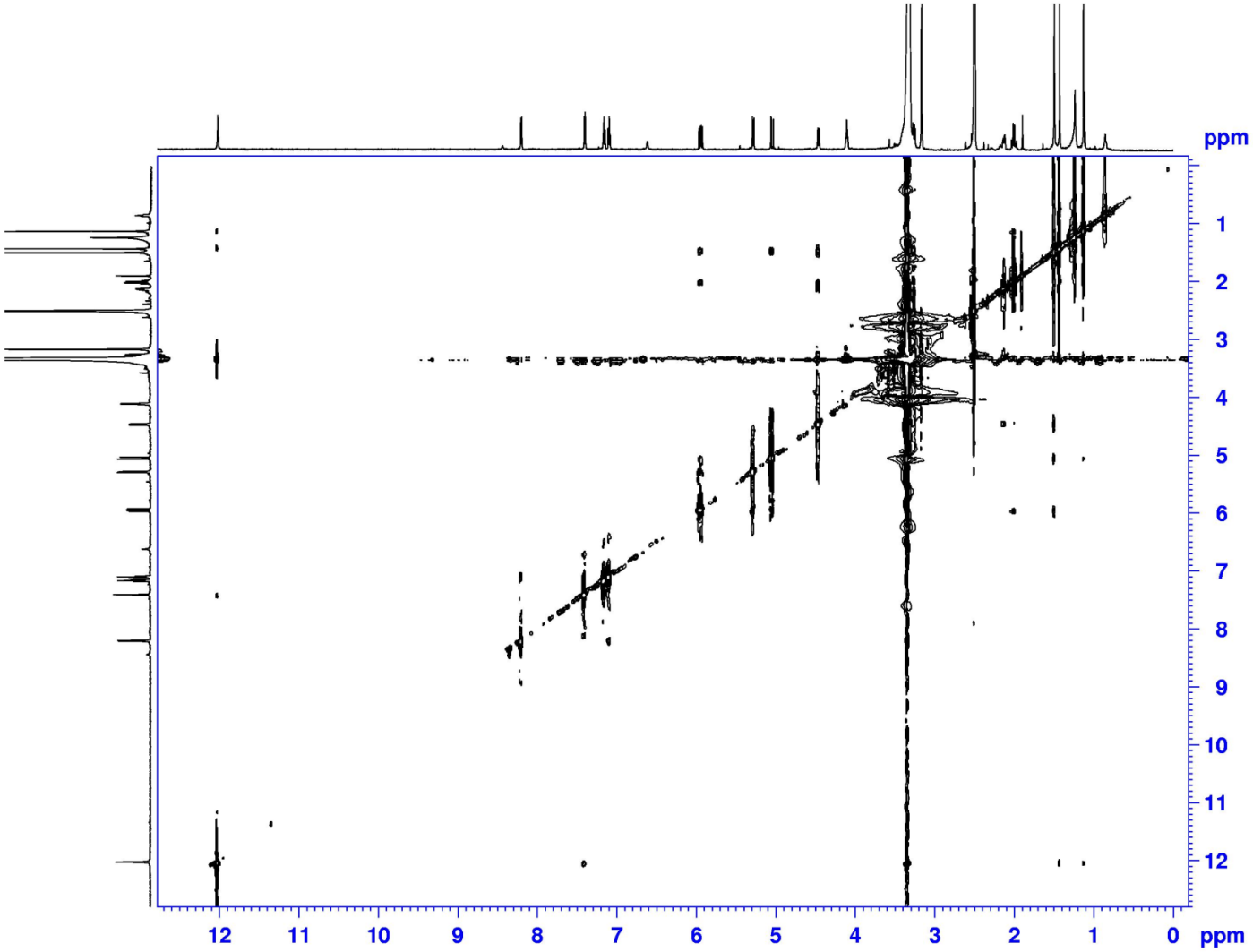

Figure 71. NOESY spectrum (600 MHz, DMSO-d_6) of 12-*epi*-fischerindole I nitrile (**217**)

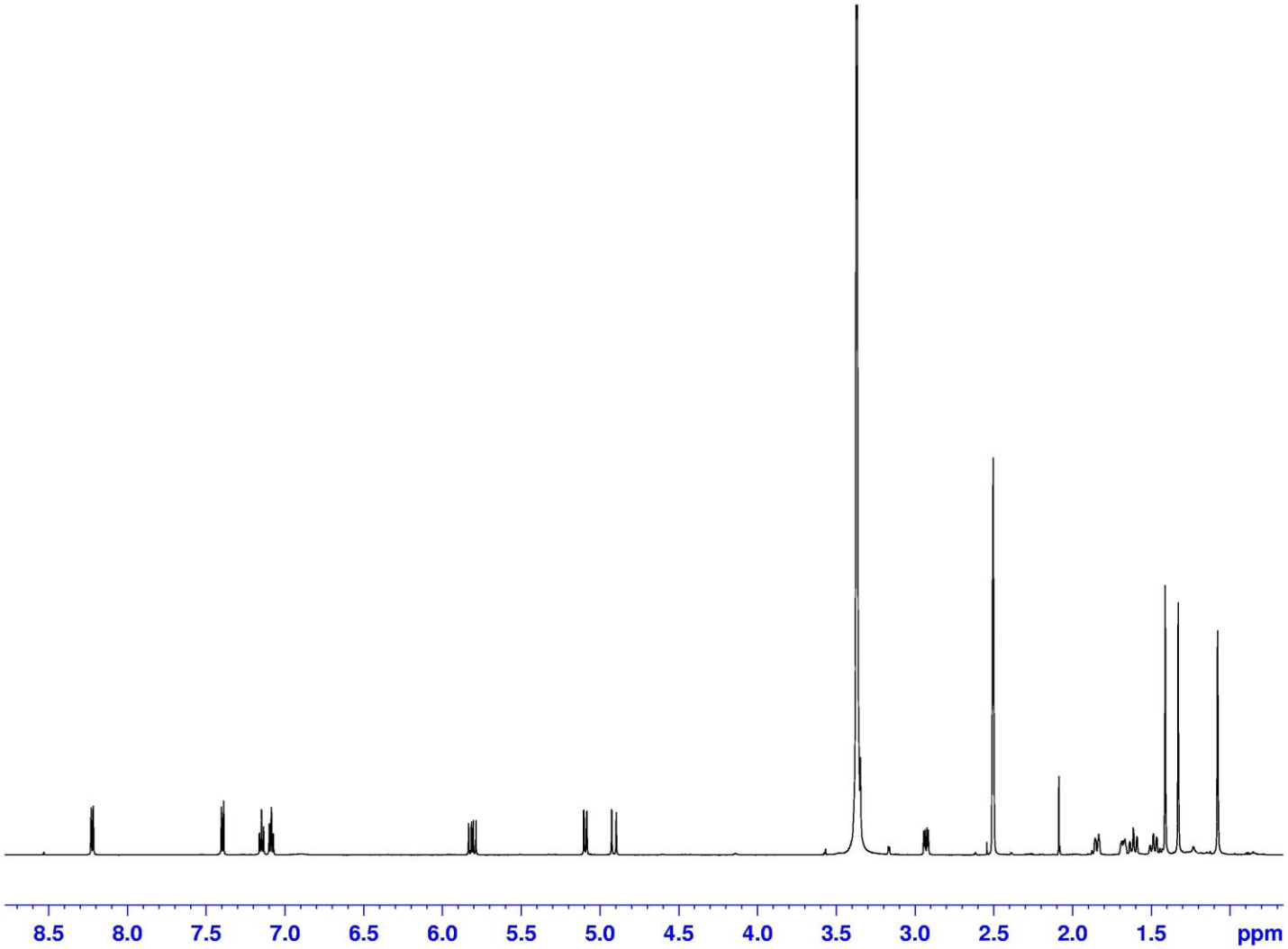

Figure 72. ^{1}H NMR spectrum (600 MHz, DMSO-d_6) of deschloro 12-*epi*-fischerindole I nitrile (**218**)

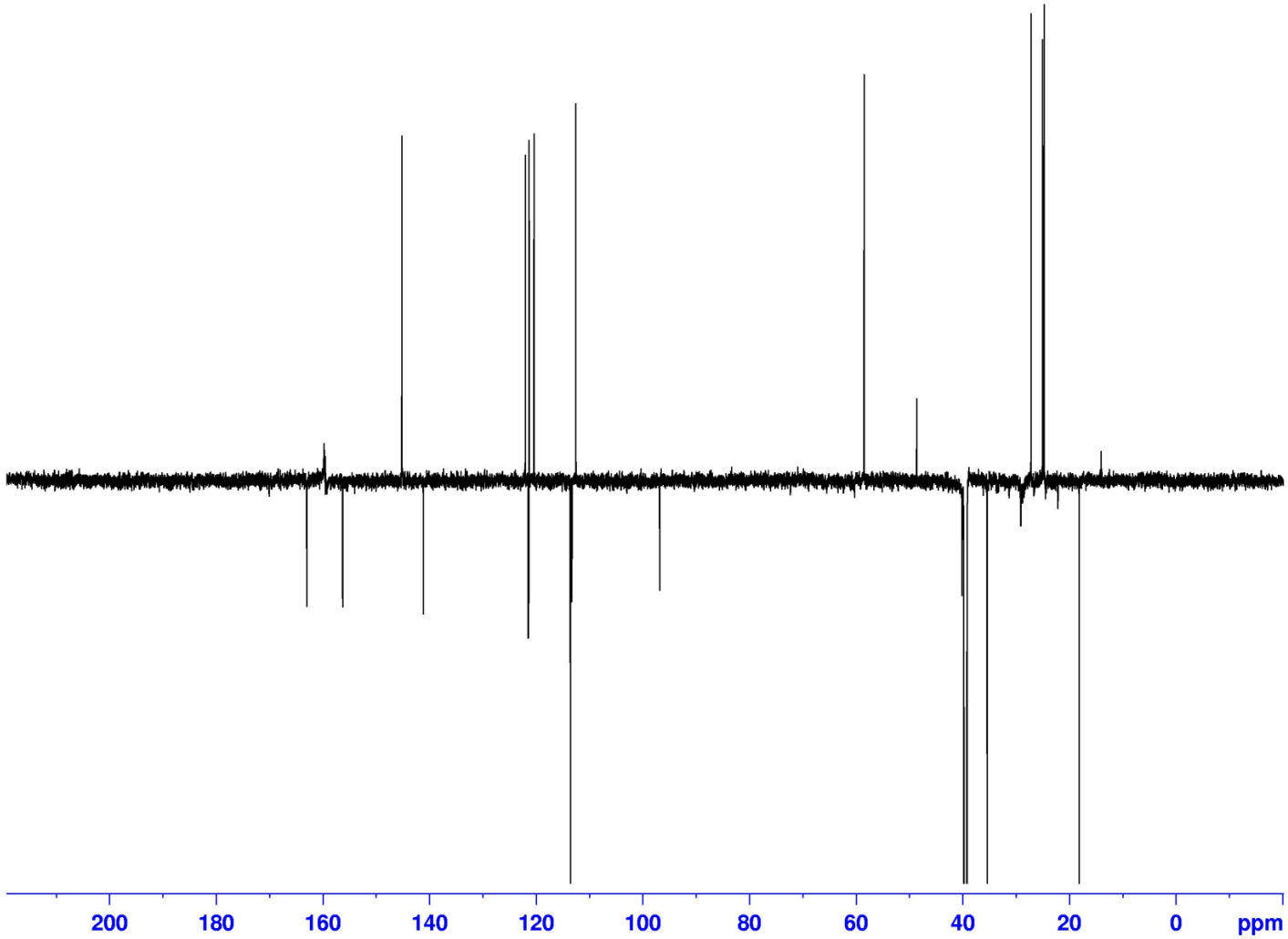

Figure 73. DEPTQ spectrum (600 MHz, DMSO-d_6) of deschloro 12-*epi*-fischerindole I nitrile (**218**)

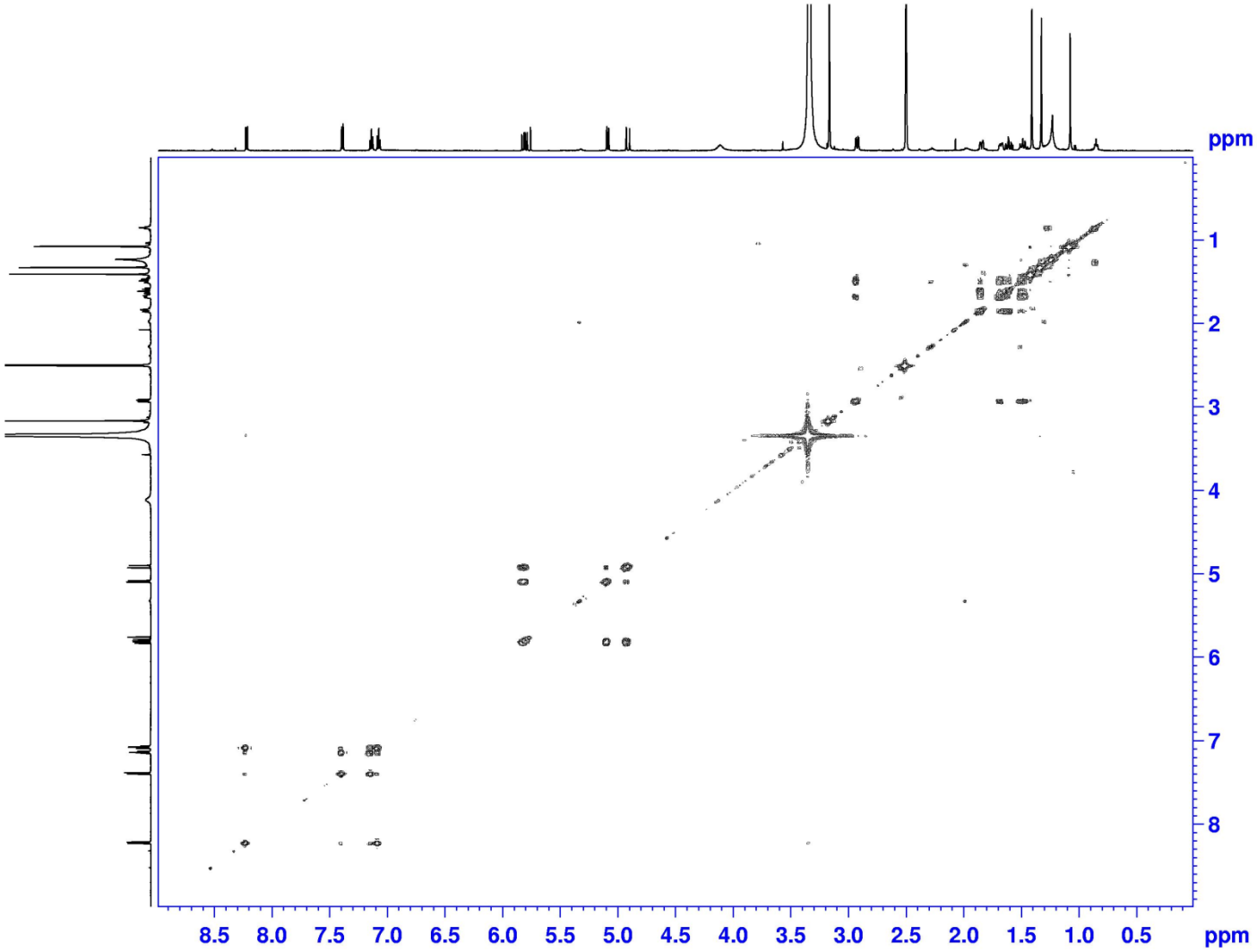

Figure 74. COSY spectrum (600 MHz, DMSO-d_6) of deschloro 12-*epi*-fischerindole I nitrile (**218**)

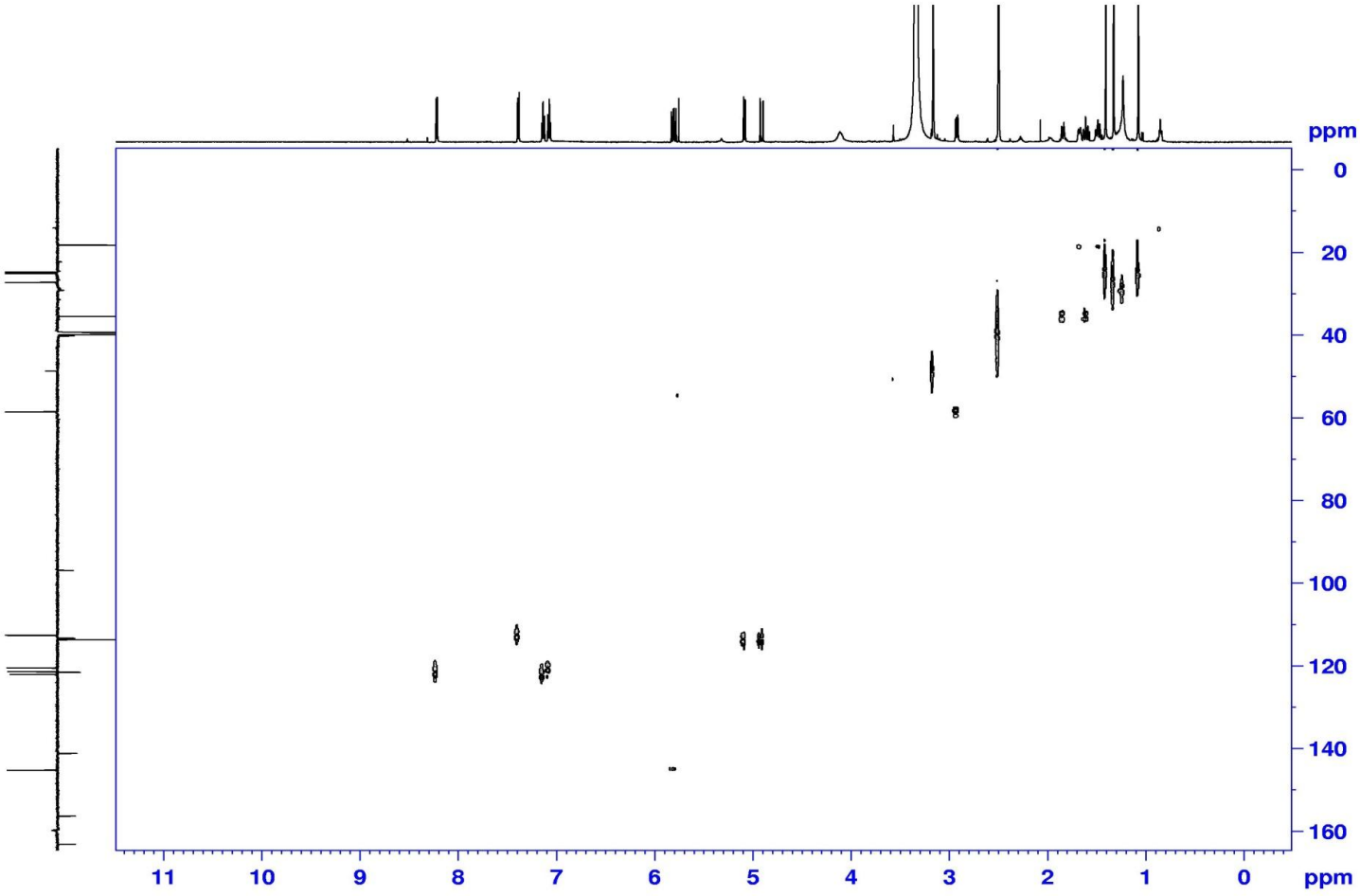

Figure 75. HSQC spectrum (600 MHz, DMSO-d_6) of deschloro 12-*epi*-fischerindole I nitrile (**218**)

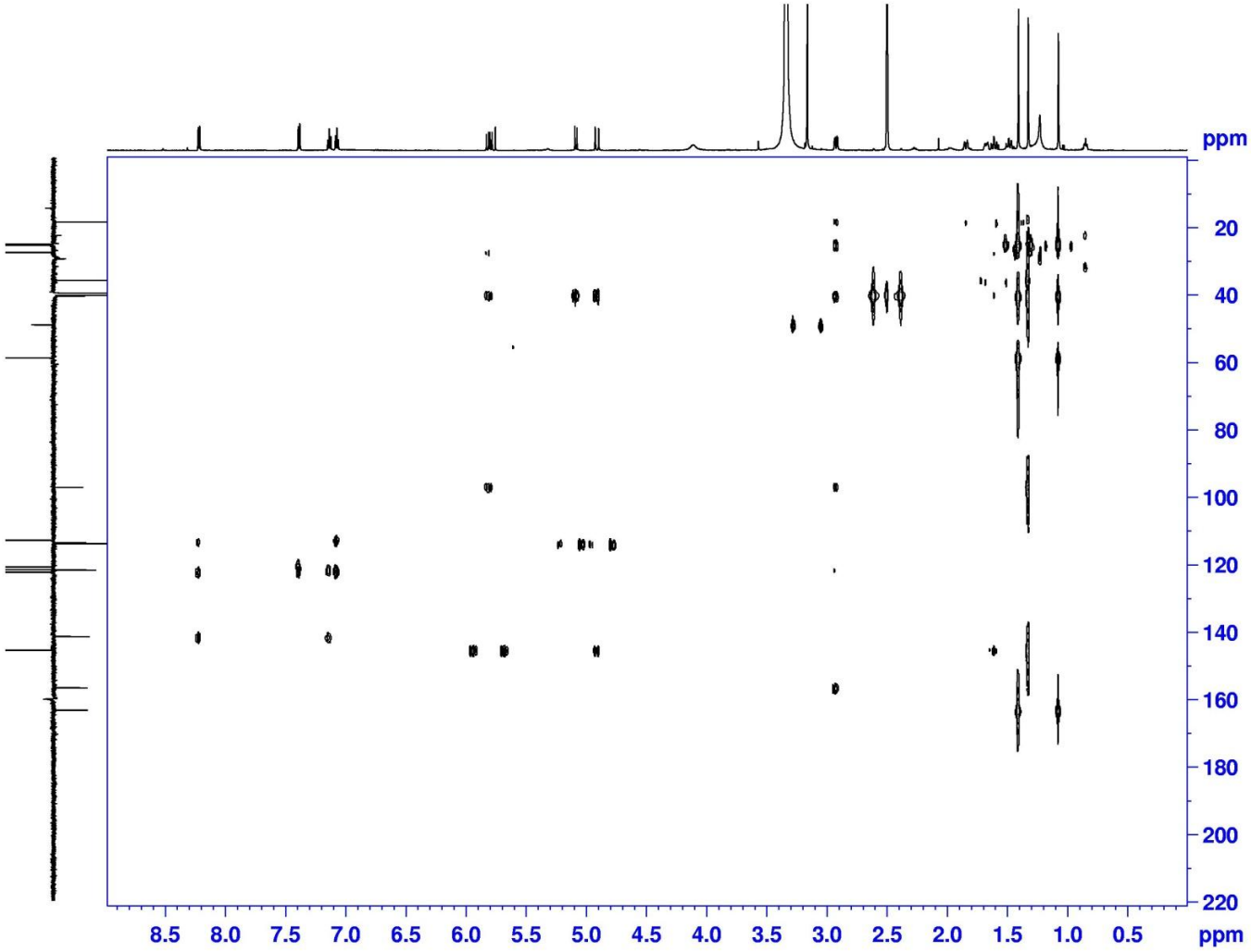

Figure 76. HMBC spectrum (600 MHz, DMSO-d_6) of deschloro 12-*epi*-fischerindole I nitrile (**218**)

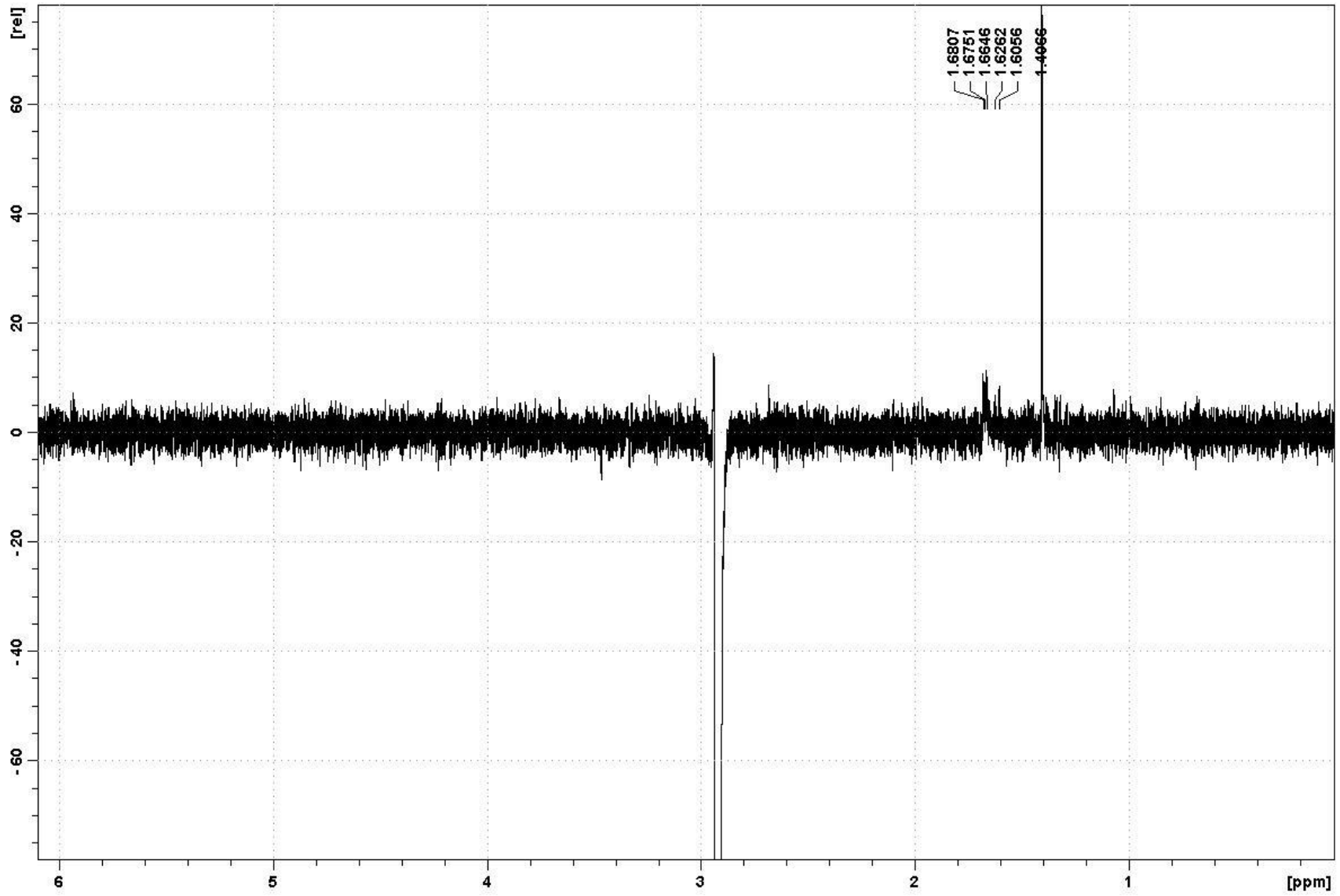

Figure 77. Selective 1D NOESY spectrum, Irradiation of H-15 (600 MHz, DMSO-d_6) of deschloro 12-*epi*-fischerindole I nitrile (**218**)

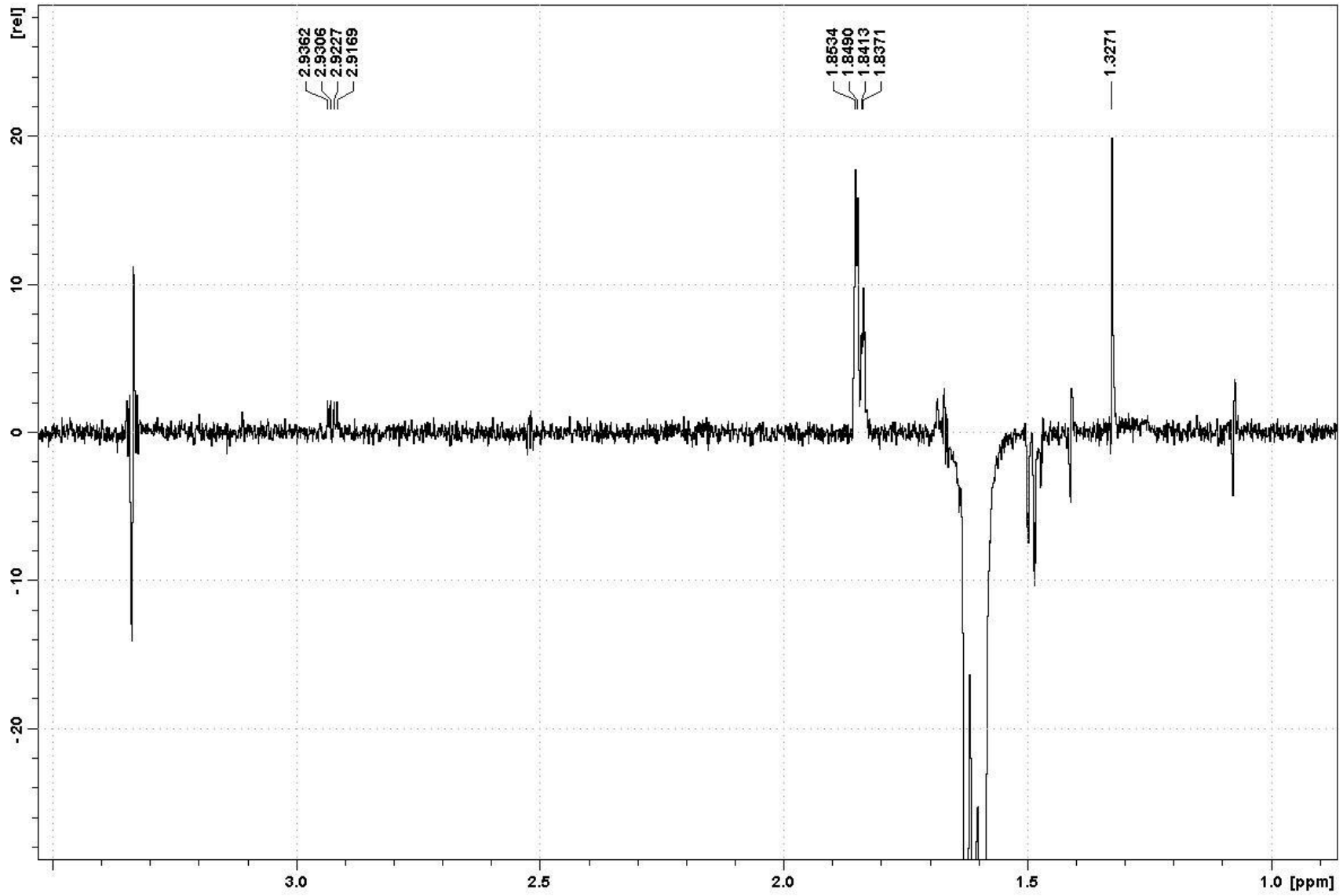

Figure 78. Selective 1D NOESY spectrum, Irradiation of H-13_{ax} (600 MHz, DMSO-d_6) of deschloro 12-*epi*-fischerindole I nitrile (**218**)

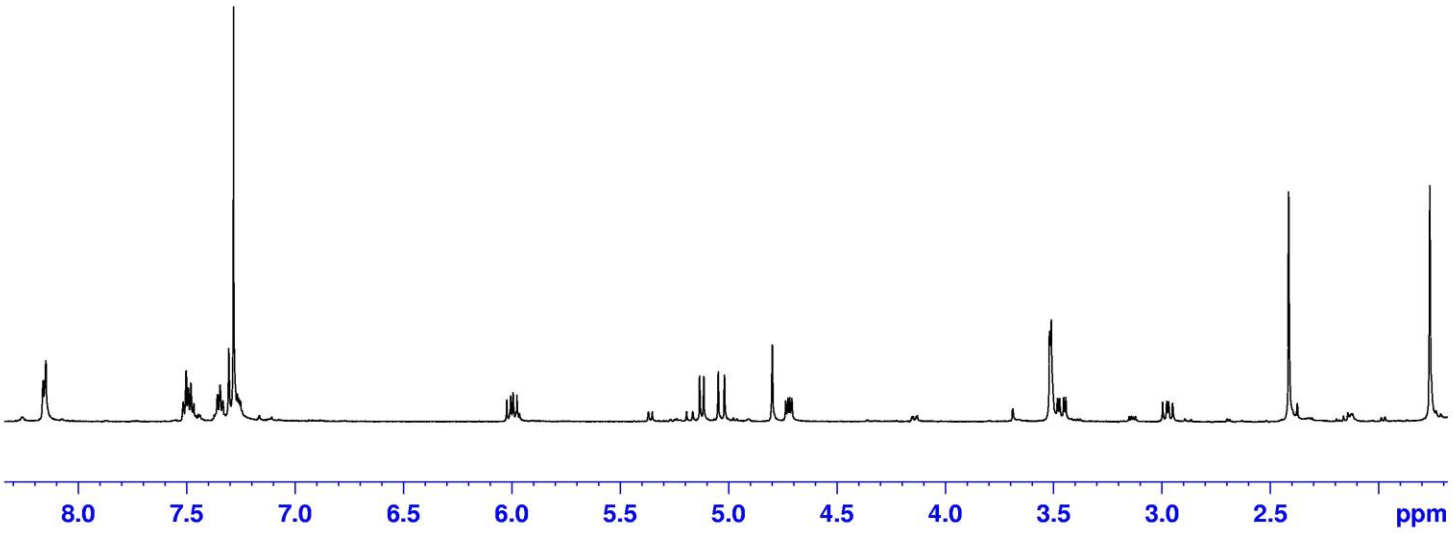

Figure 79. ^{1}H NMR spectrum (600 MHz, $CDCl_3$) of 12-*epi*-fischerindole W nitrile (**219**)

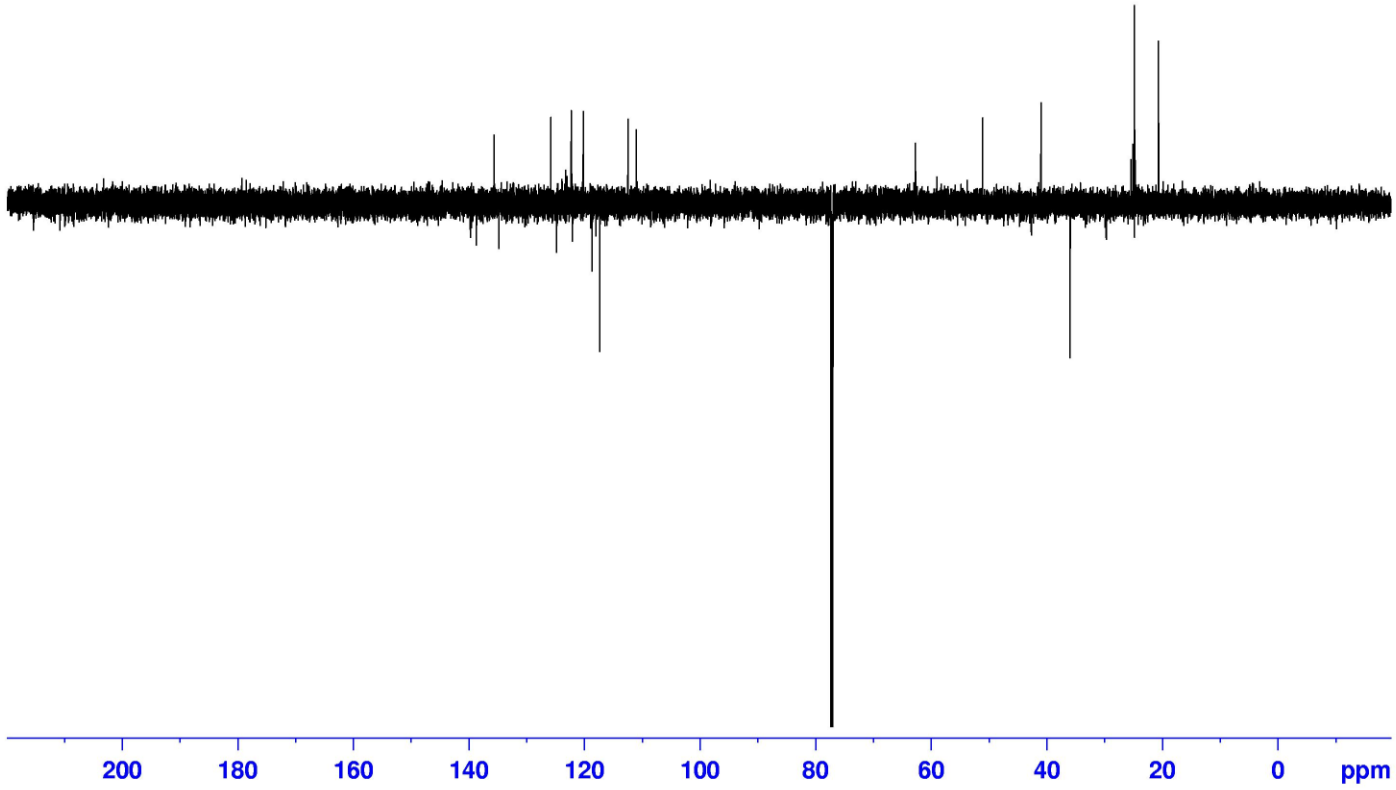

Figure 80. DEPTQ spectrum (600 MHz, $CDCl_3$) of 12-*epi*-fischerindole W nitrile (**219**)

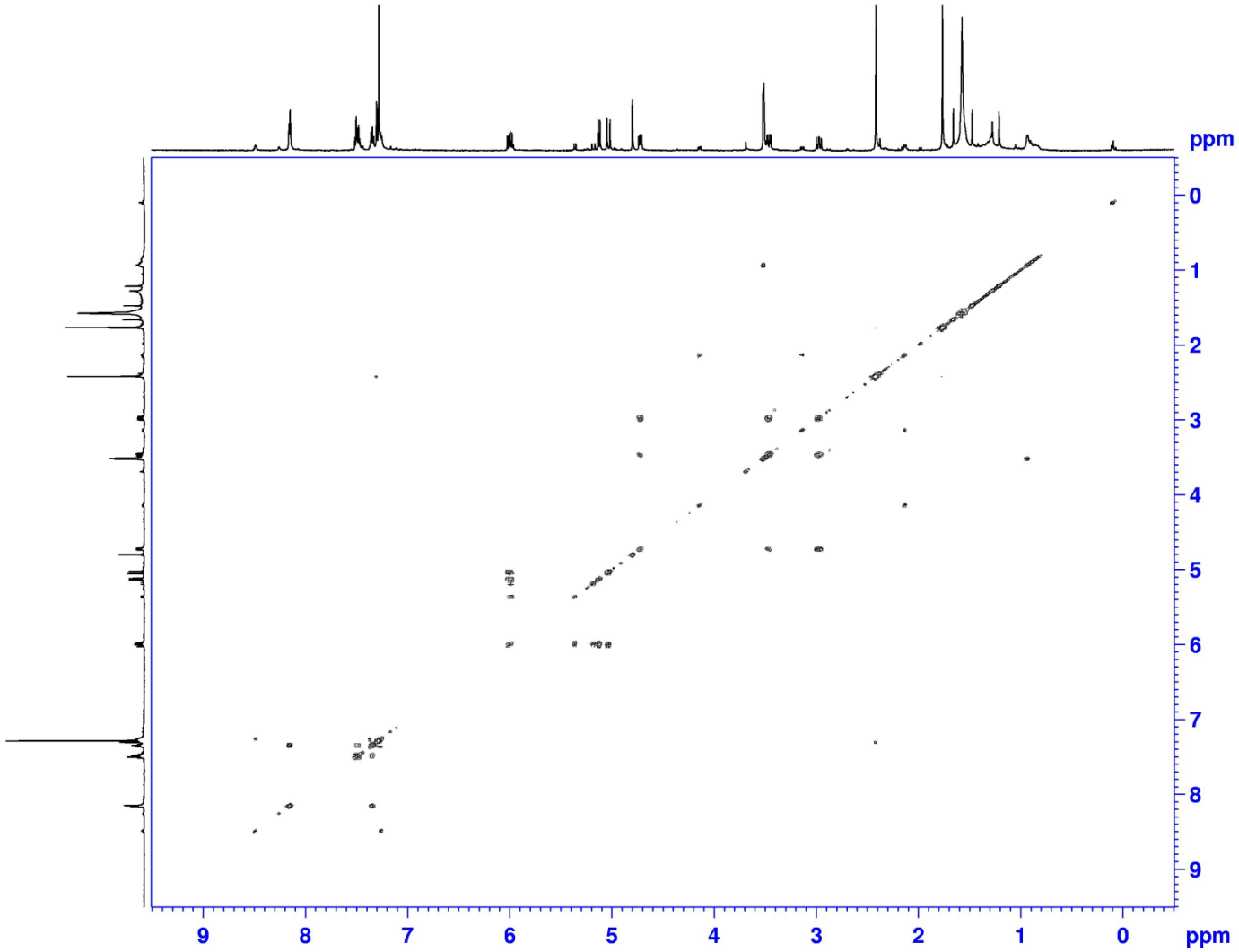

Figure 81. COSY spectrum (600 MHz, $CDCl_3$) of 12-*epi*-fischerindole W nitrile (**219**)

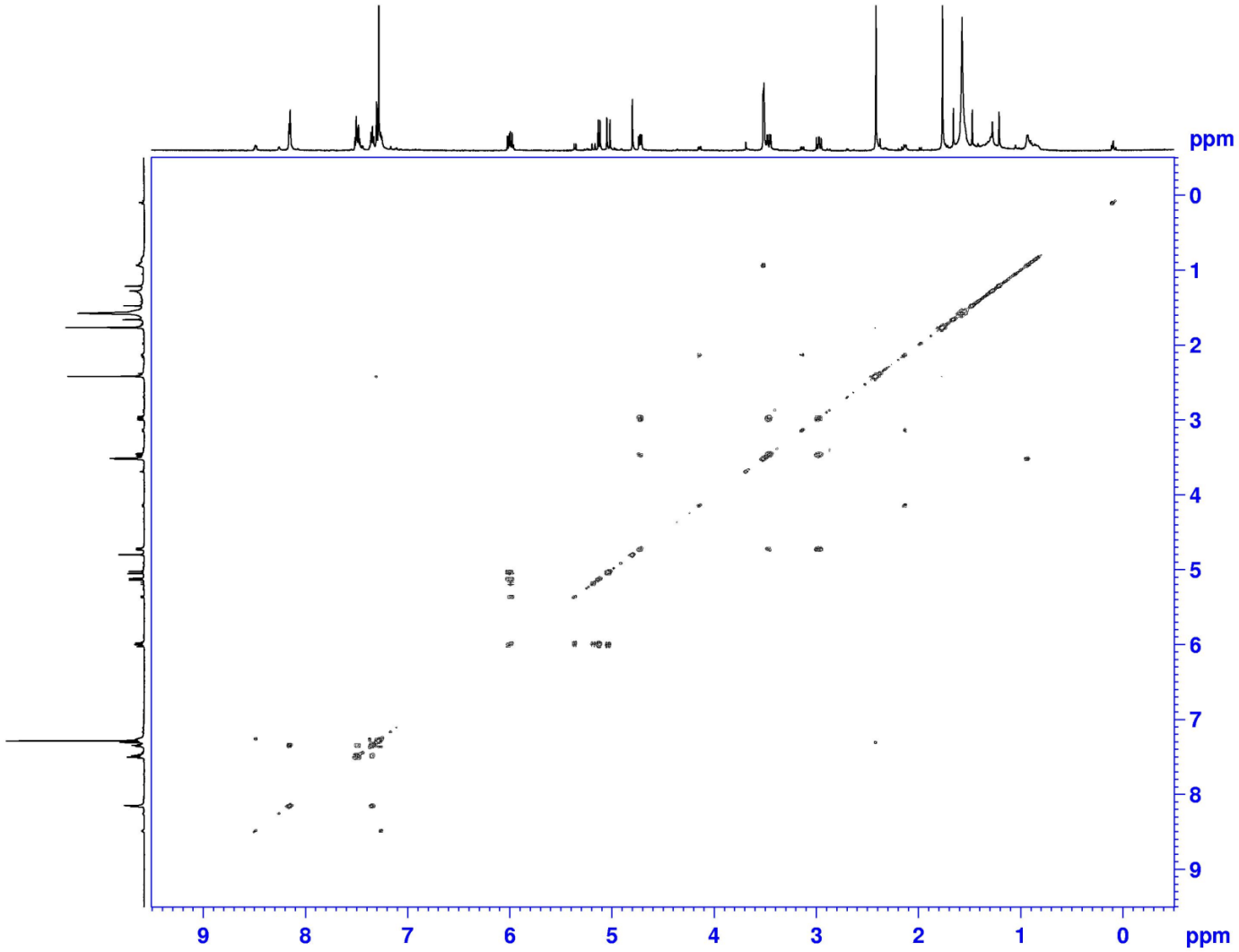

Figure 82. HSQC spectrum (600 MHz, $CDCl_3$) of 12-*epi*-fischerindole W nitrile (**219**)

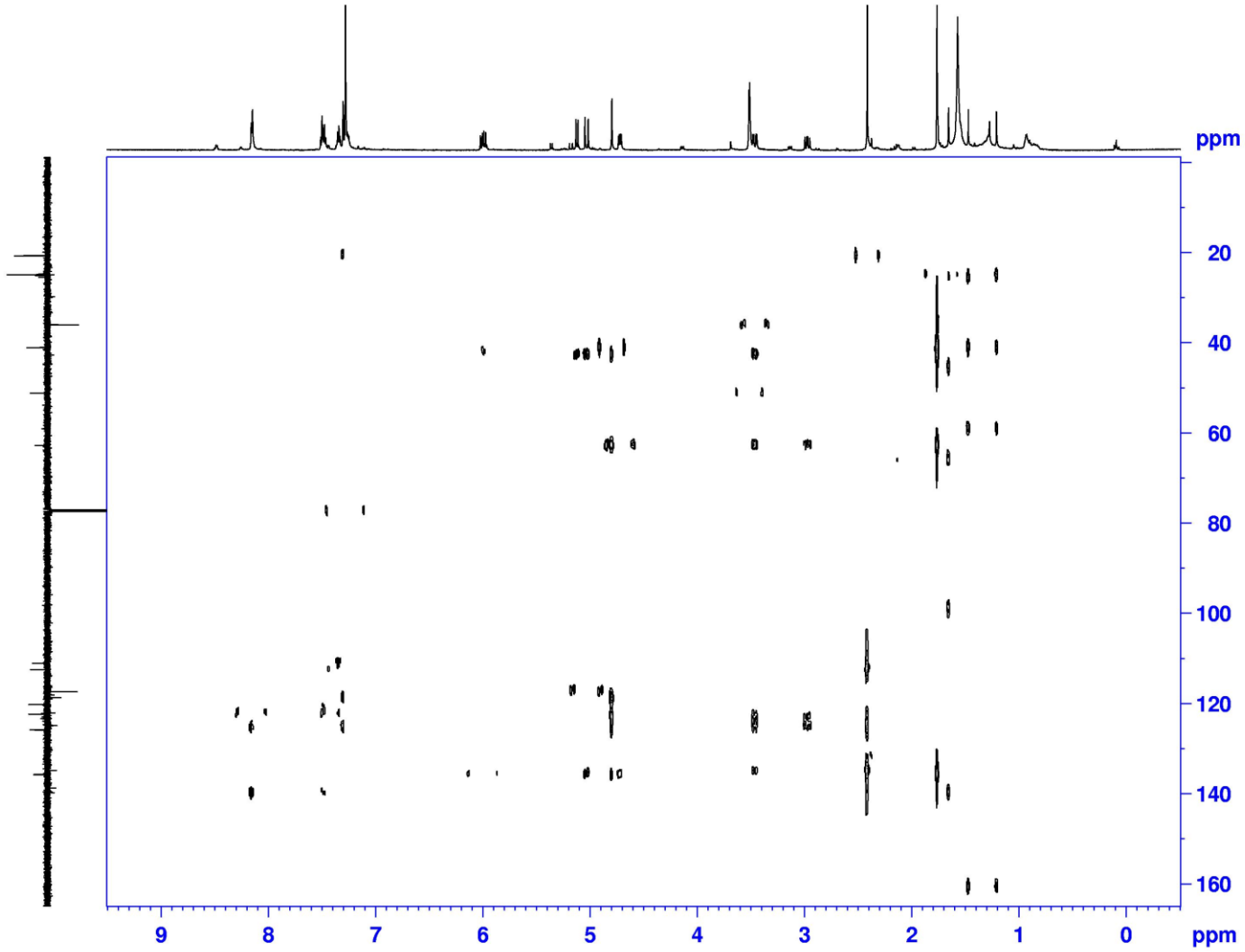

Figure 83. HMBC spectrum (600 MHz, $CDCl_3$) of 12-*epi*-fischerindole W nitrile (**219**)

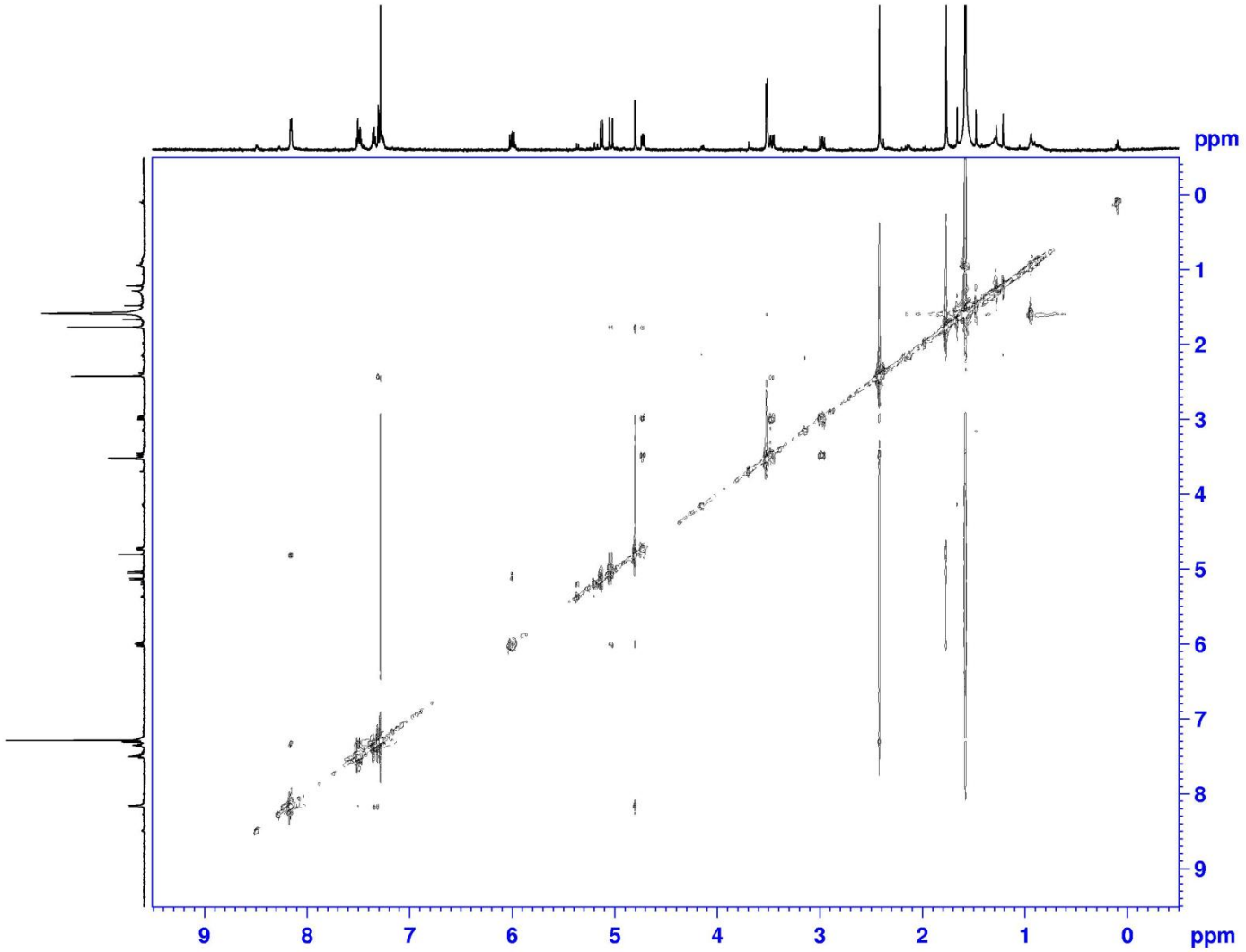

Figure 84. NOESY spectrum (600 MHz, $CDCl_3$) of 12-*epi*-fischerindole W nitrile (**219**)

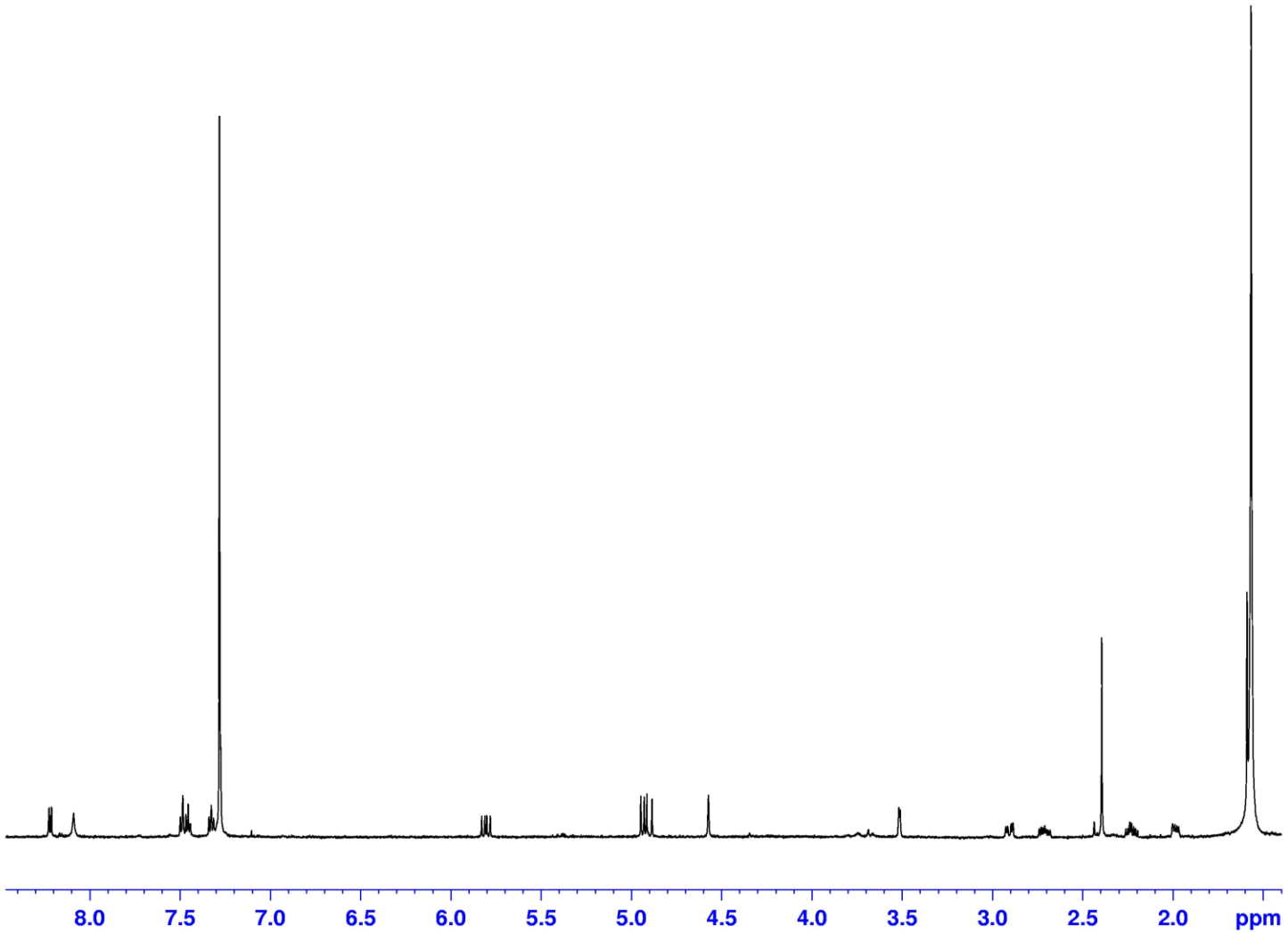

Figure 85. ^{1}H NMR spectrum (600 MHz, $CDCl_3$) of deschloro 12-*epi*-fischerindole W nitrile (**220**)

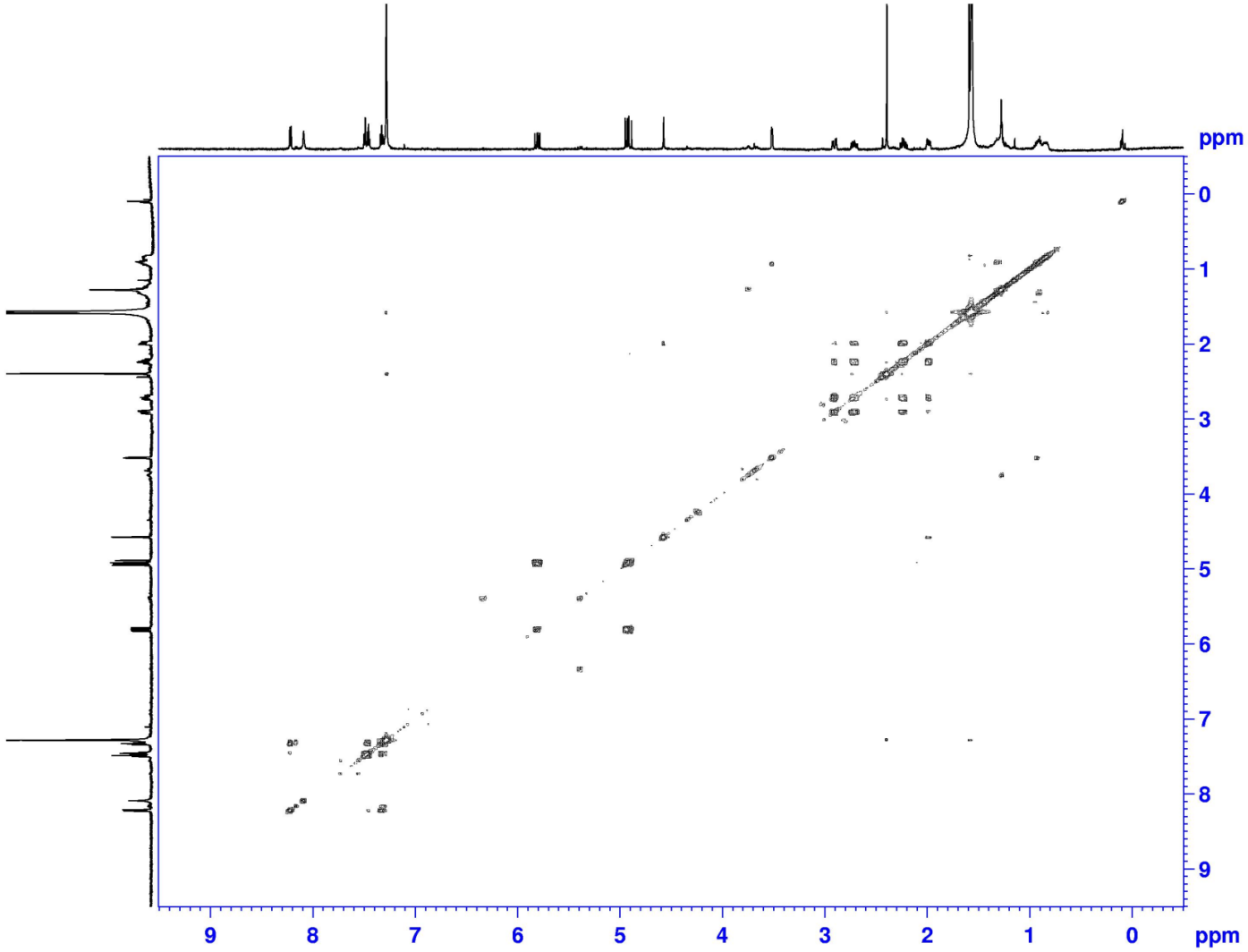

Figure 86. COSY spectrum (600 MHz, $CDCl_3$) of deschloro 12-*epi*-fischerindole W nitrile (**220**)

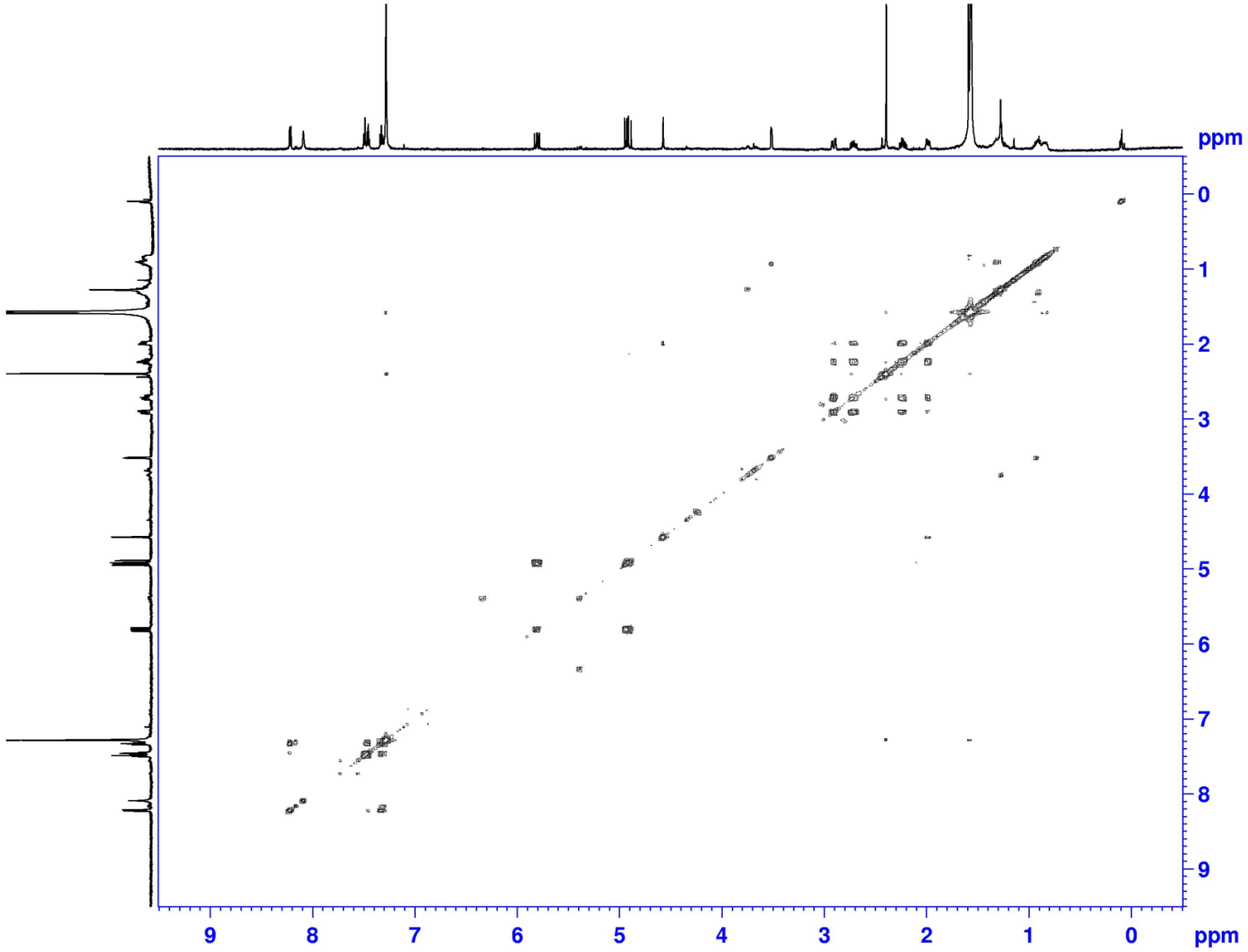

Figure 87. HSQC spectrum (600 MHz, $CDCl_3$) of deschloro 12-*epi*-fischerindole W nitrile (**220**)

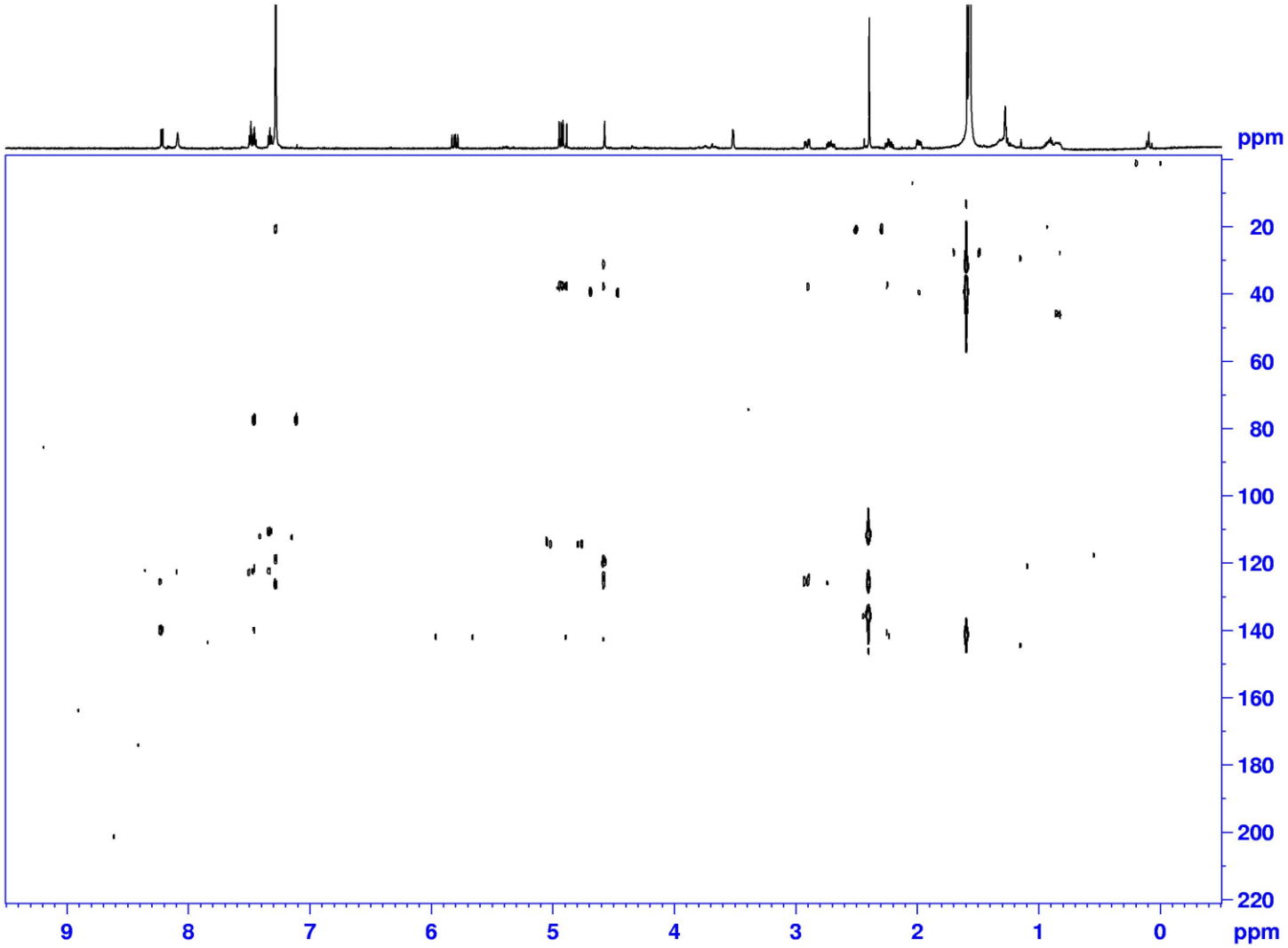

Figure 88. HMBC spectrum (600 MHz, $CDCl_3$) of deschloro 12-*epi*-fischerindole W nitrile (**220**)

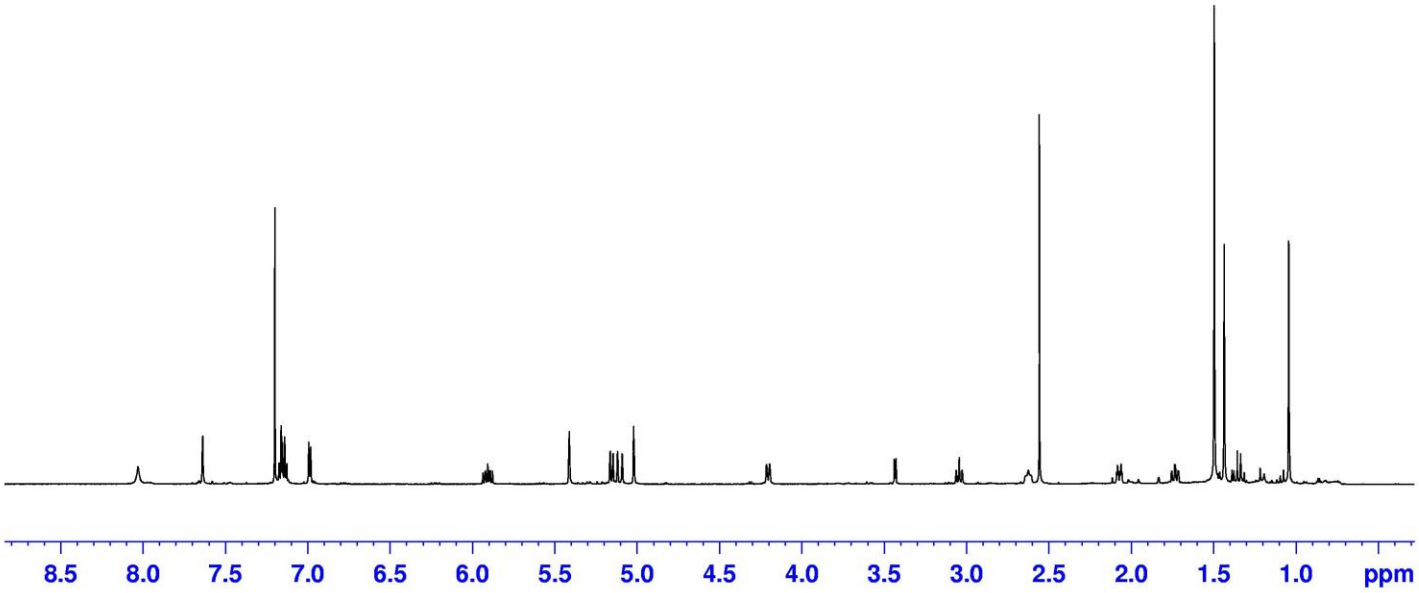

Figure 89. ^{1}H NMR spectrum (600 MHz, $CDCl_3$) of hapalindole X (**295**)

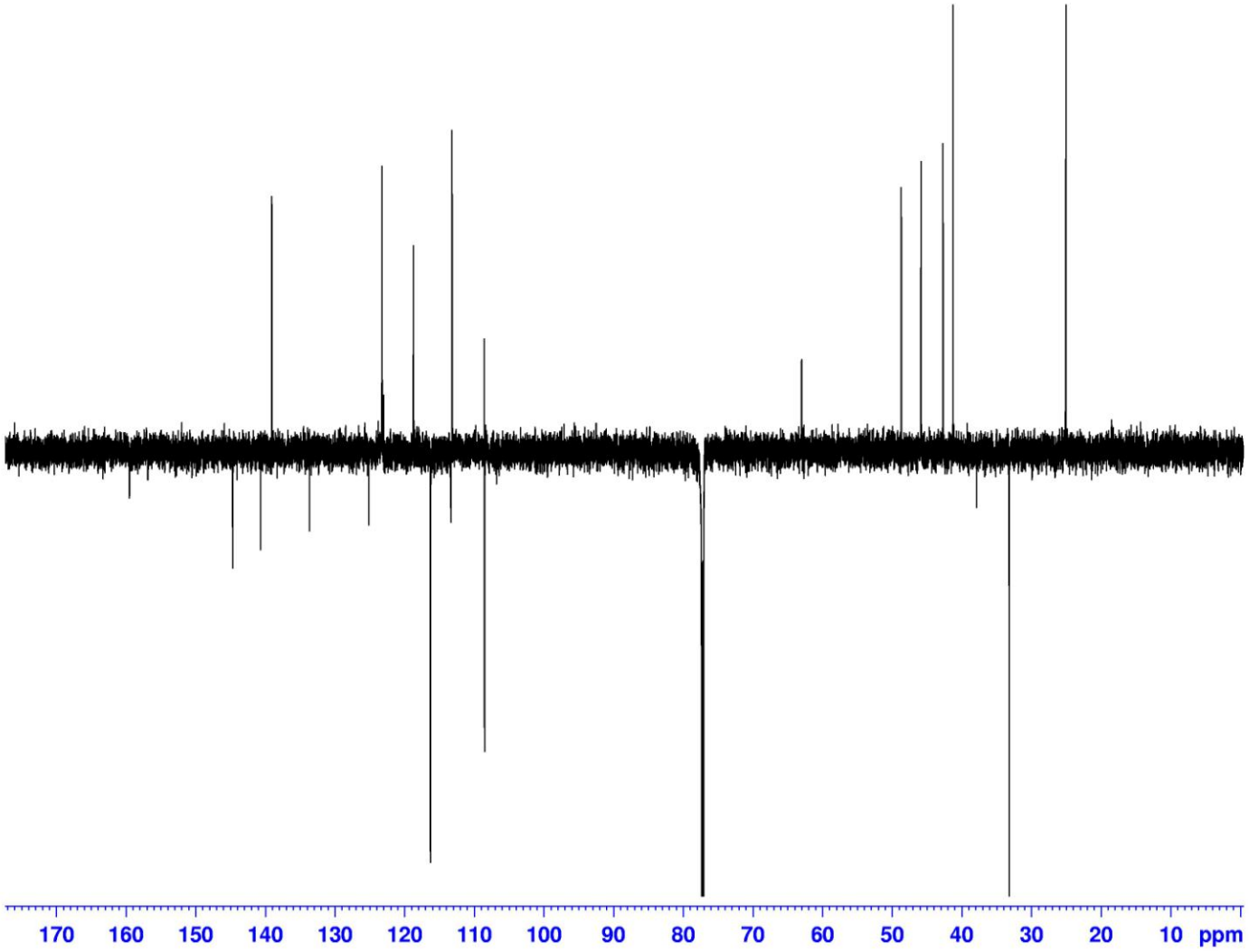

Figure 90. DEPTQ spectrum (600 MHz, $CDCl_3$) of hapalindole X (**295**)

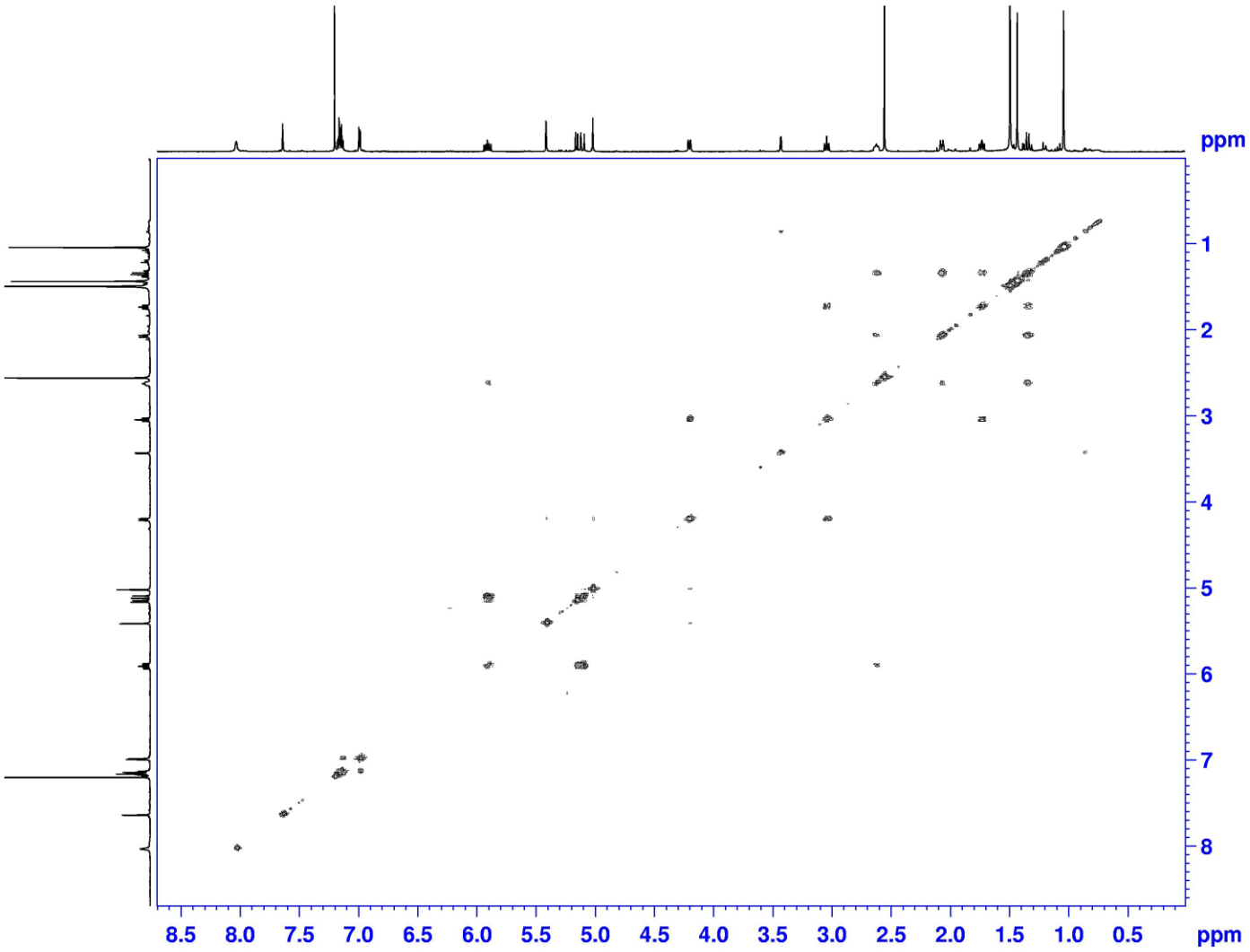

Figure 91. COSY spectrum (600 MHz, $CDCl_3$) of hapalindole X (**295**)

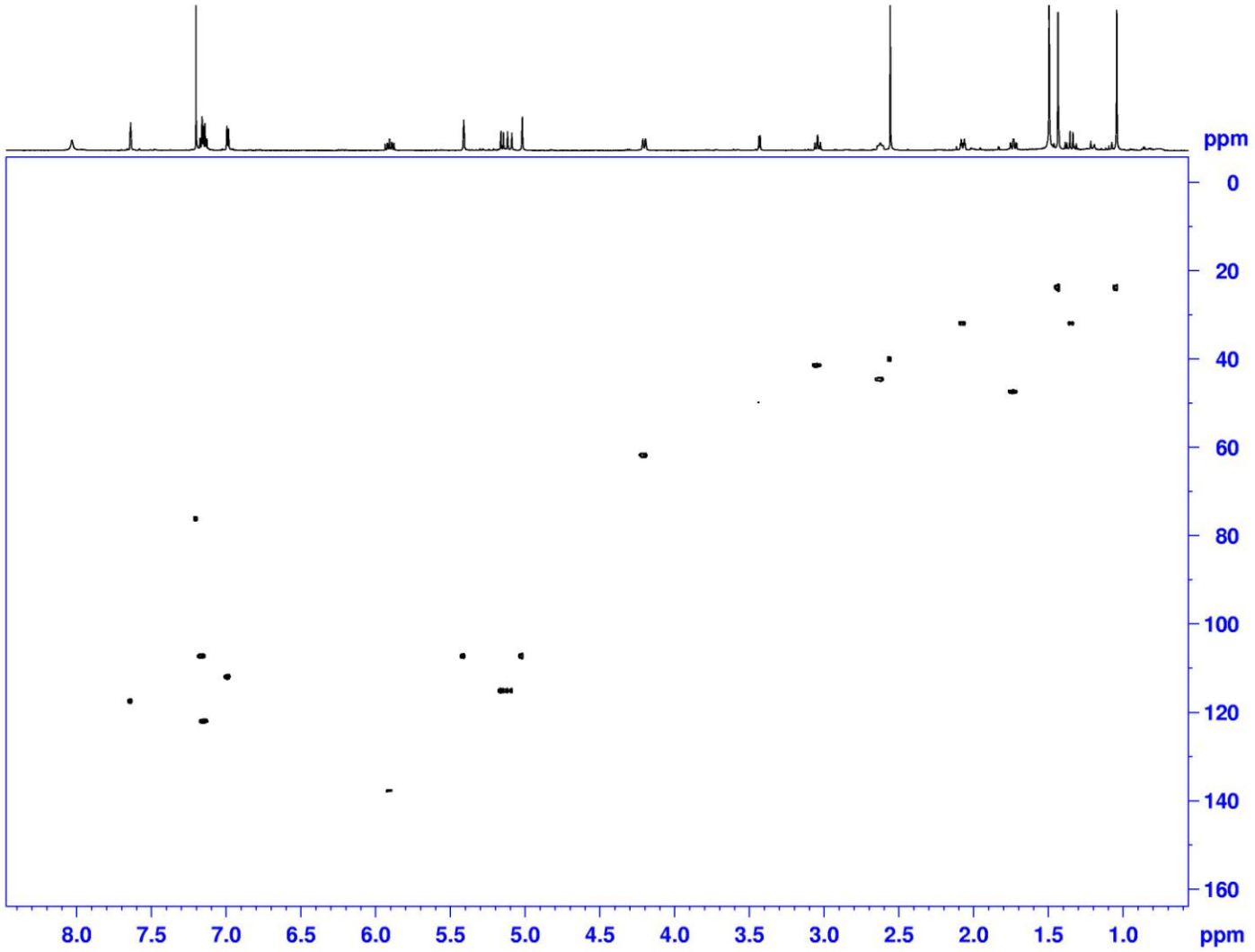

Figure 92. HSQC spectrum (600 MHz, $CDCl_3$) of hapalindole X (**295**)

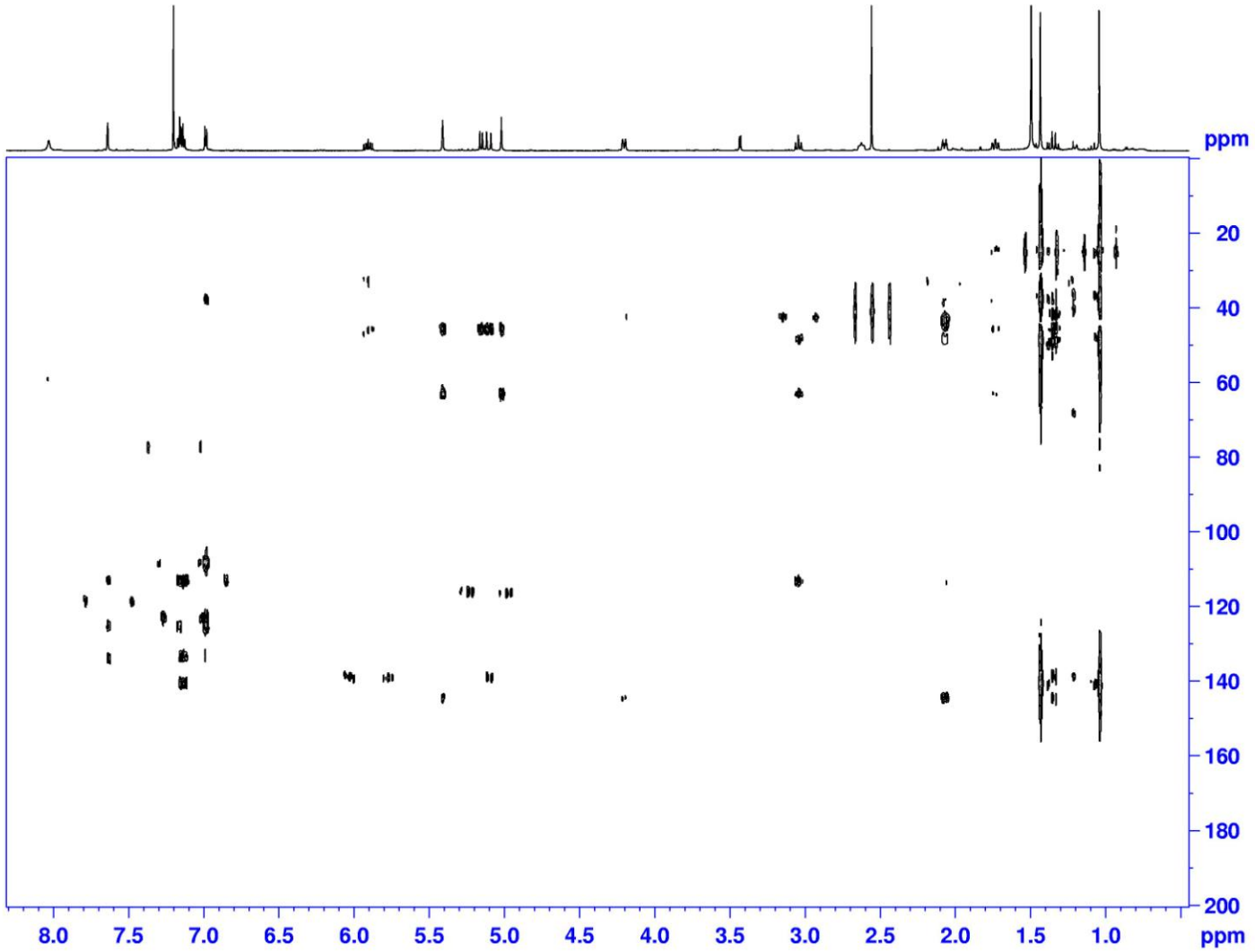

Figure 93. HMBC spectrum (600 MHz, $CDCl_3$) of hapalindole X (**295**)

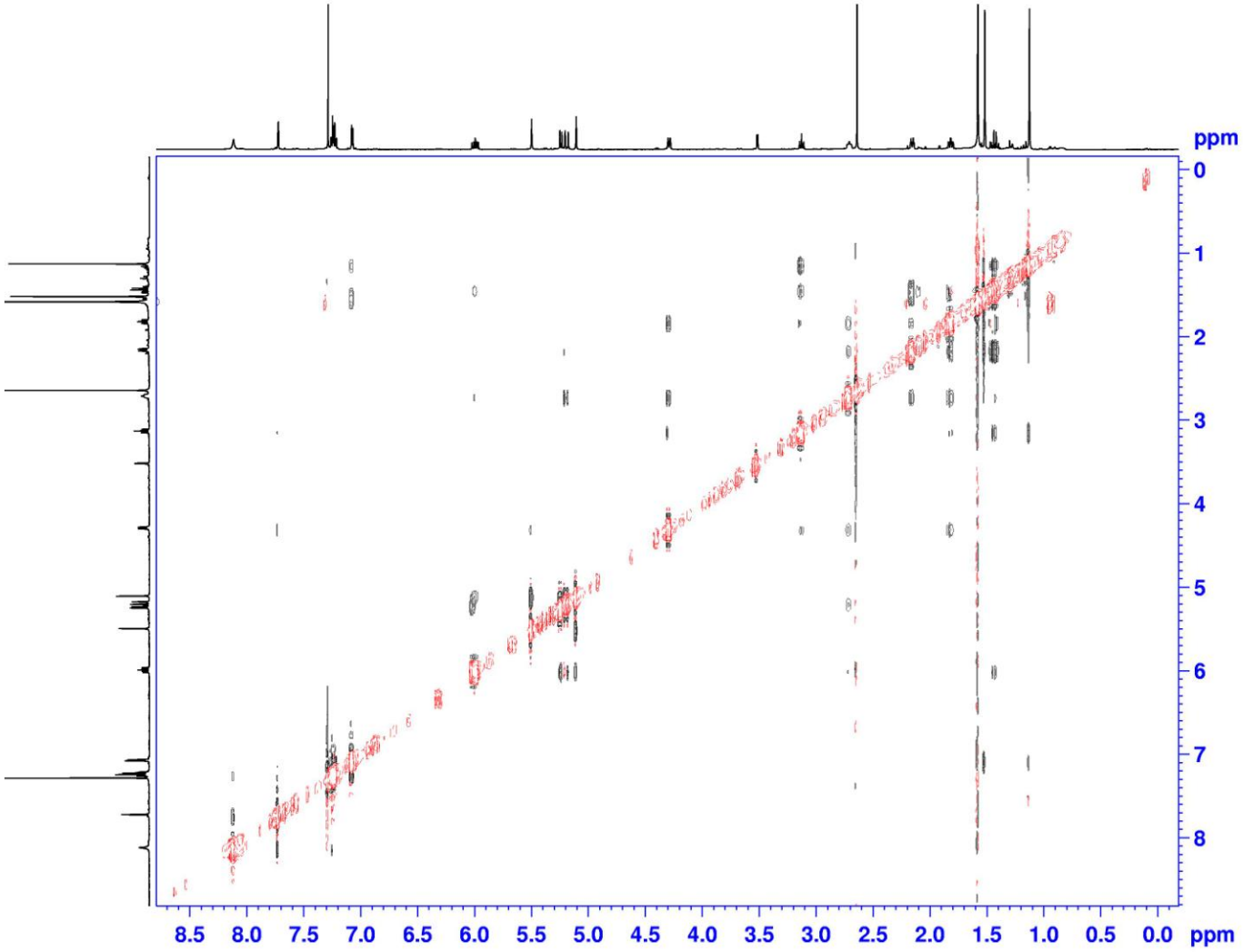

Figure 94. NOESY spectrum (600 MHz, $CDCl_3$) of hapalindole X (**295**)

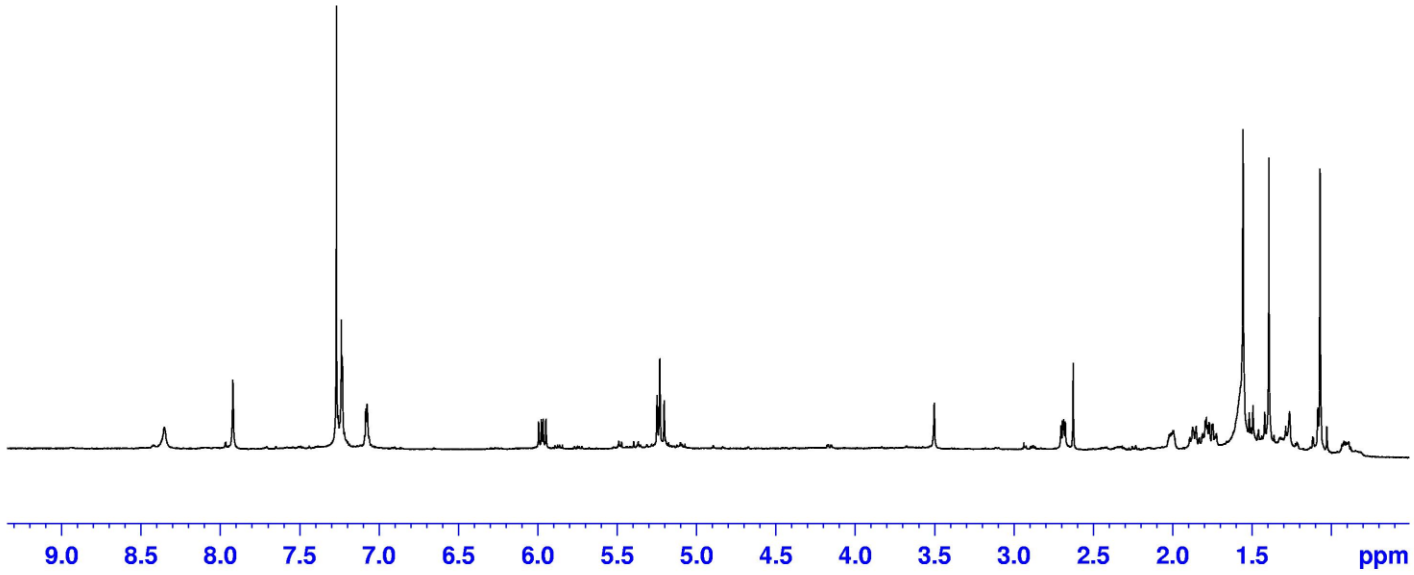

Figure 95. ^{1}H NMR spectrum (600 MHz, $CDCl_3$) of deschloro hapalindole I (**296**)

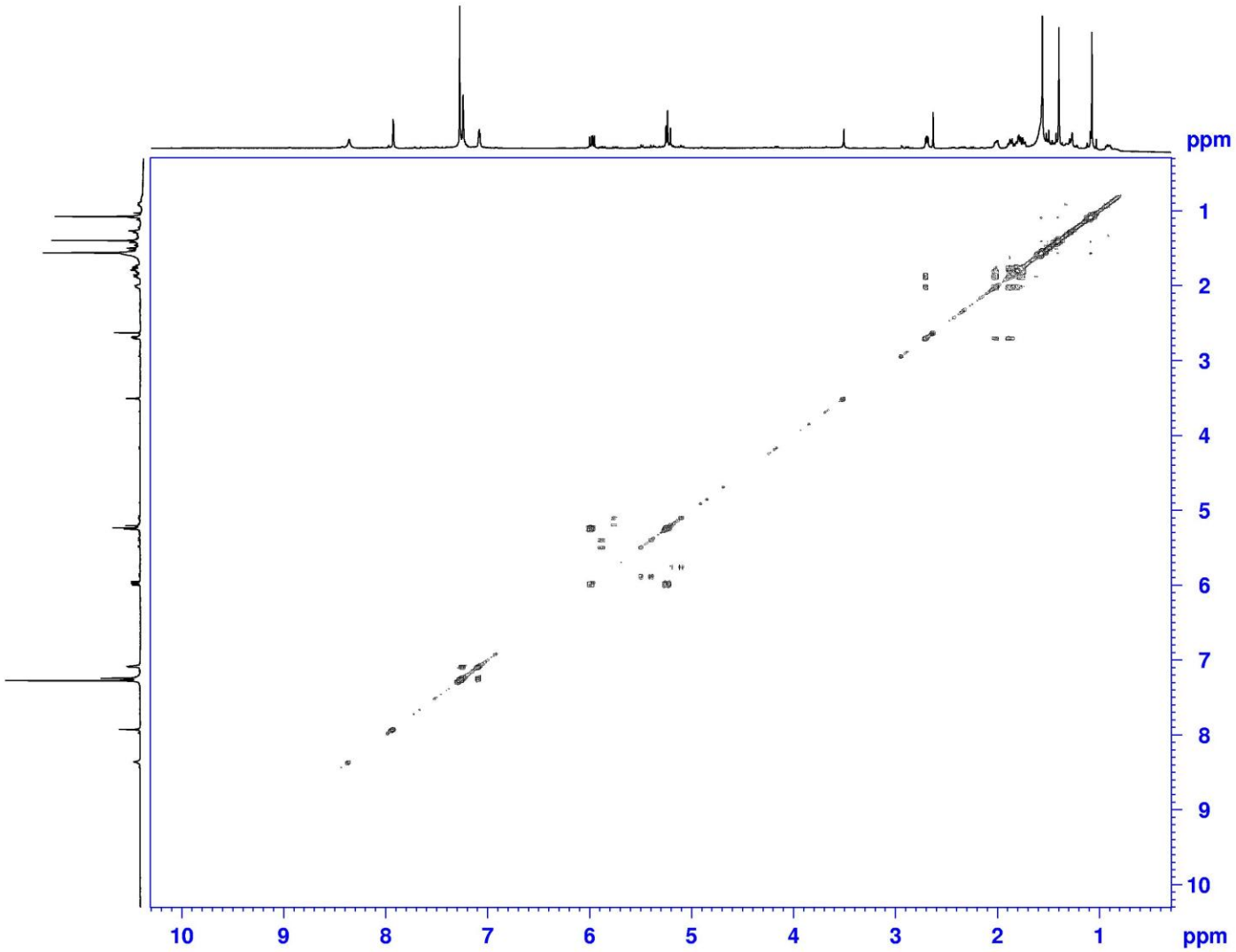

Figure 96. COSY spectrum (600 MHz, $CDCl_3$) of deschloro hapalindole I (**296**)

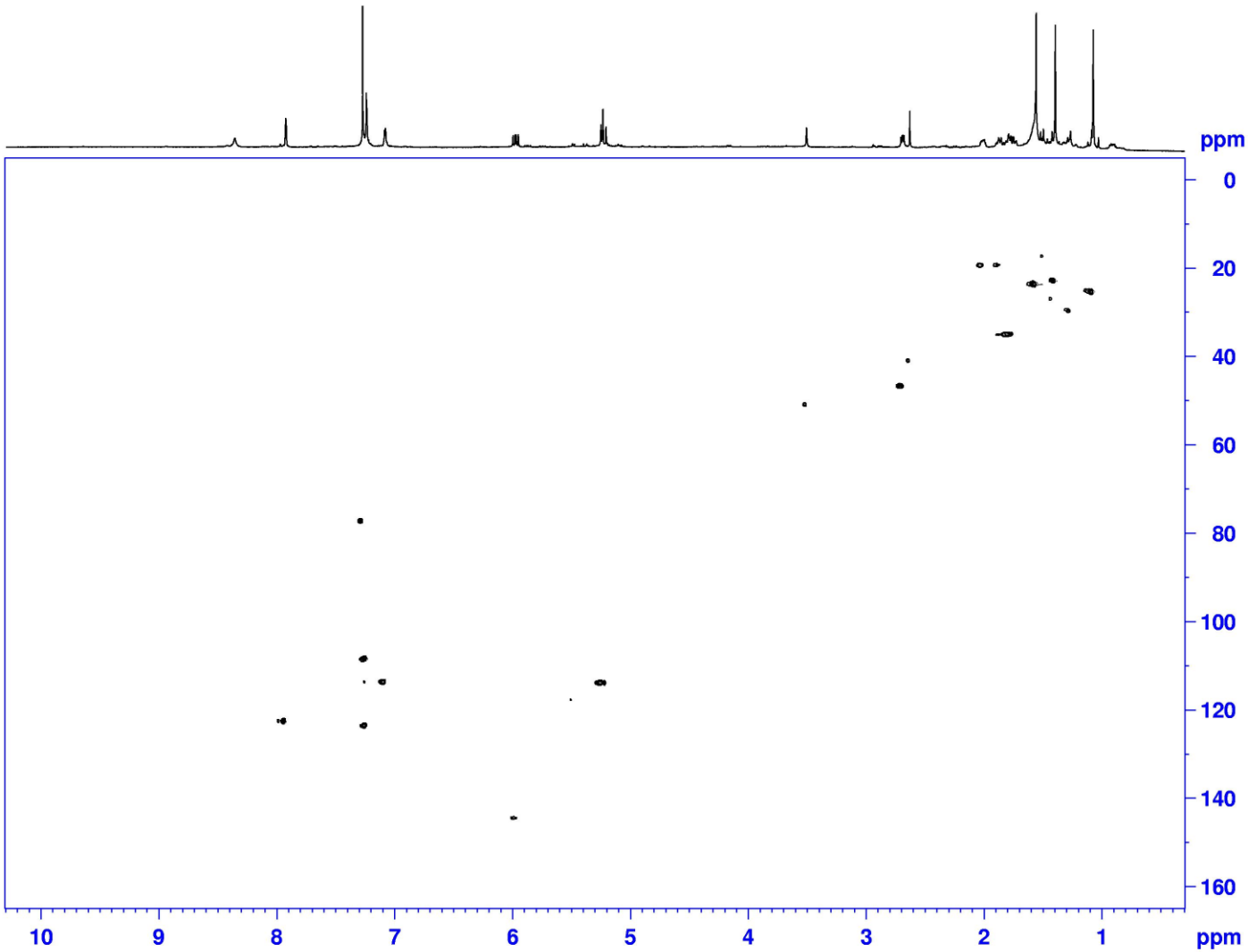

Figure 97. HSQC spectrum (600 MHz, $CDCl_3$) of deschloro hapalindole I (**296**)

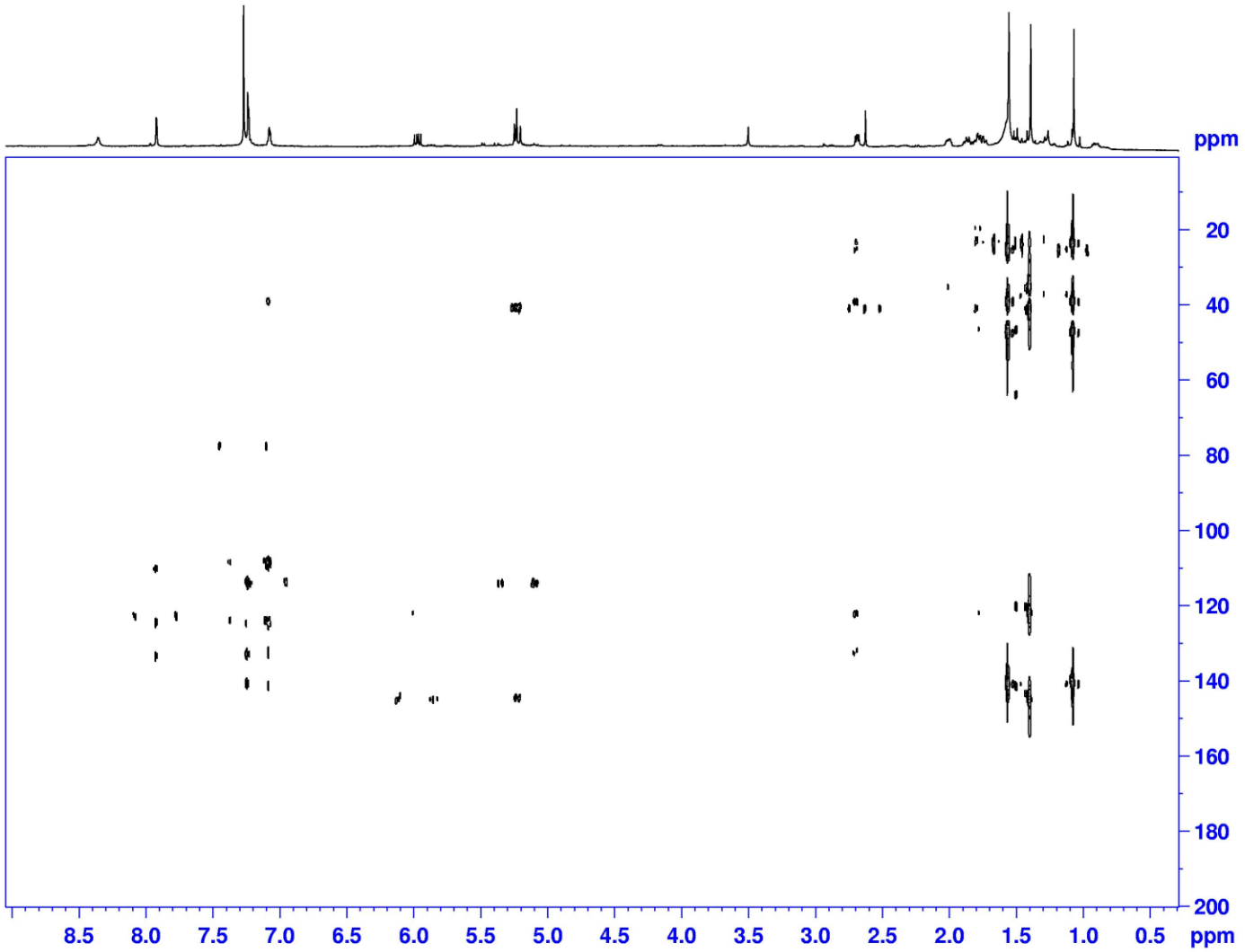

Figure 98. HMBC spectrum (600 MHz, $CDCl_3$) of deschloro hapalindole I (**296**)

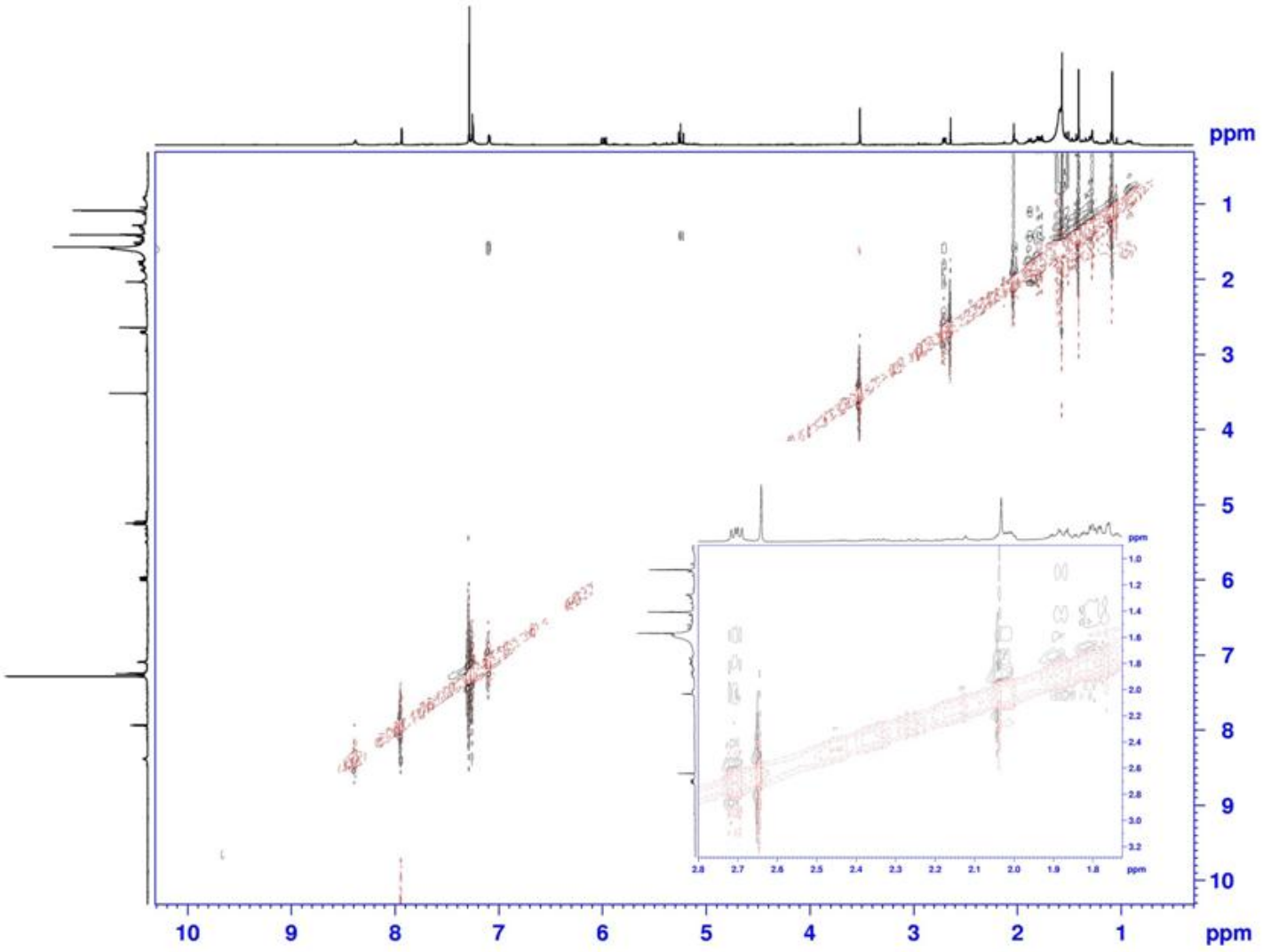

Figure 99. NOESY spectrum (600 MHz, $CDCl_3$) of deschloro hapalindole I (**296**)

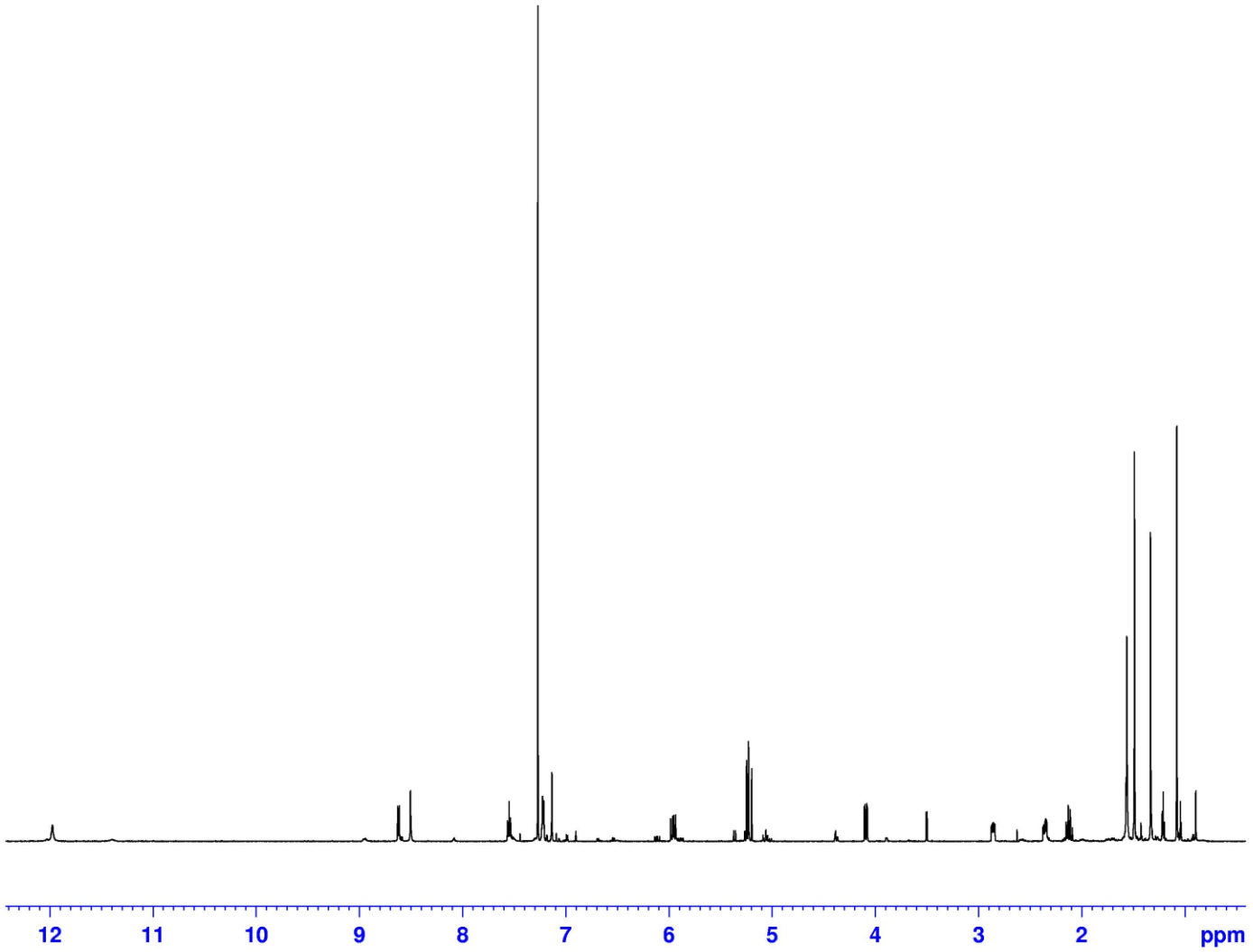

Figure 100. ^{1}H NMR spectrum (600 MHz, $CDCl_3$) of 13-hydroxy dechlorofontonamide (**297**)

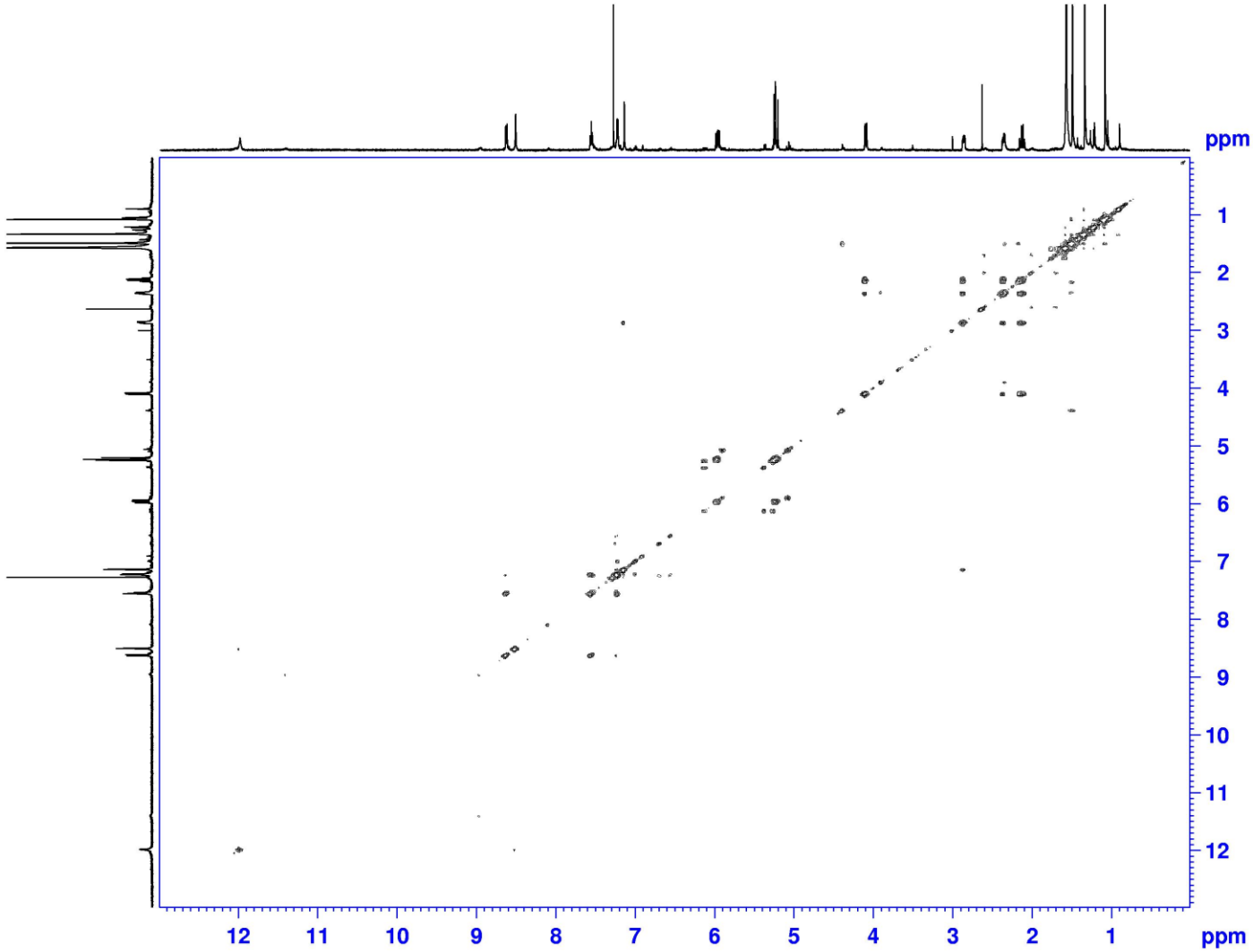

Figure 101. COSY spectrum (600 MHz, $CDCl_3$) of 13-hydroxy dechlorofontonamide (**297**)

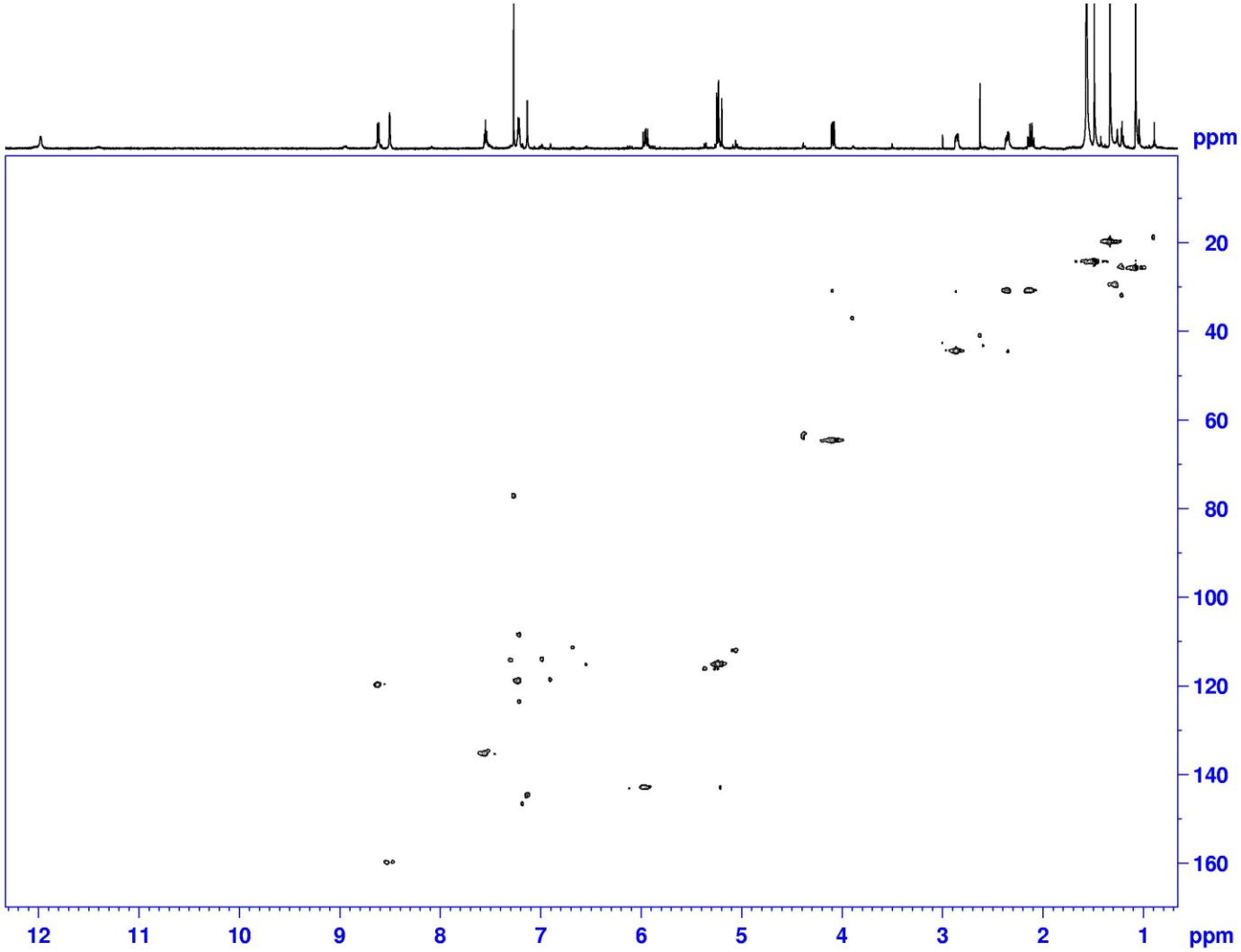

Figure 102. HSQC spectrum (600 MHz, $CDCl_3$) of 13-hydroxy dechlorofontonamide (**297**)

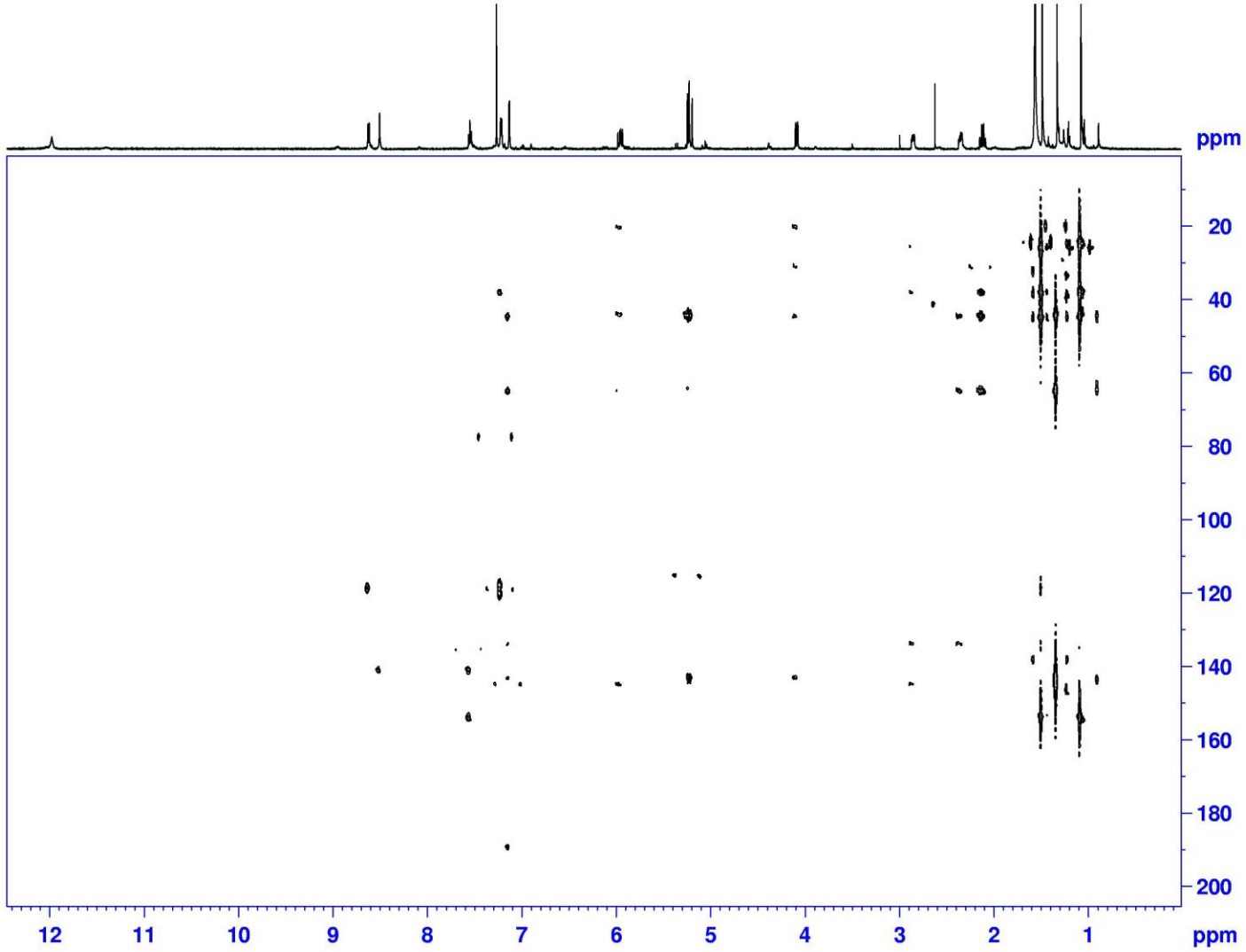

Figure 103. HMBC spectrum (600 MHz, $CDCl_3$) of 13-hydroxy dechlorofontonamide (**297**)

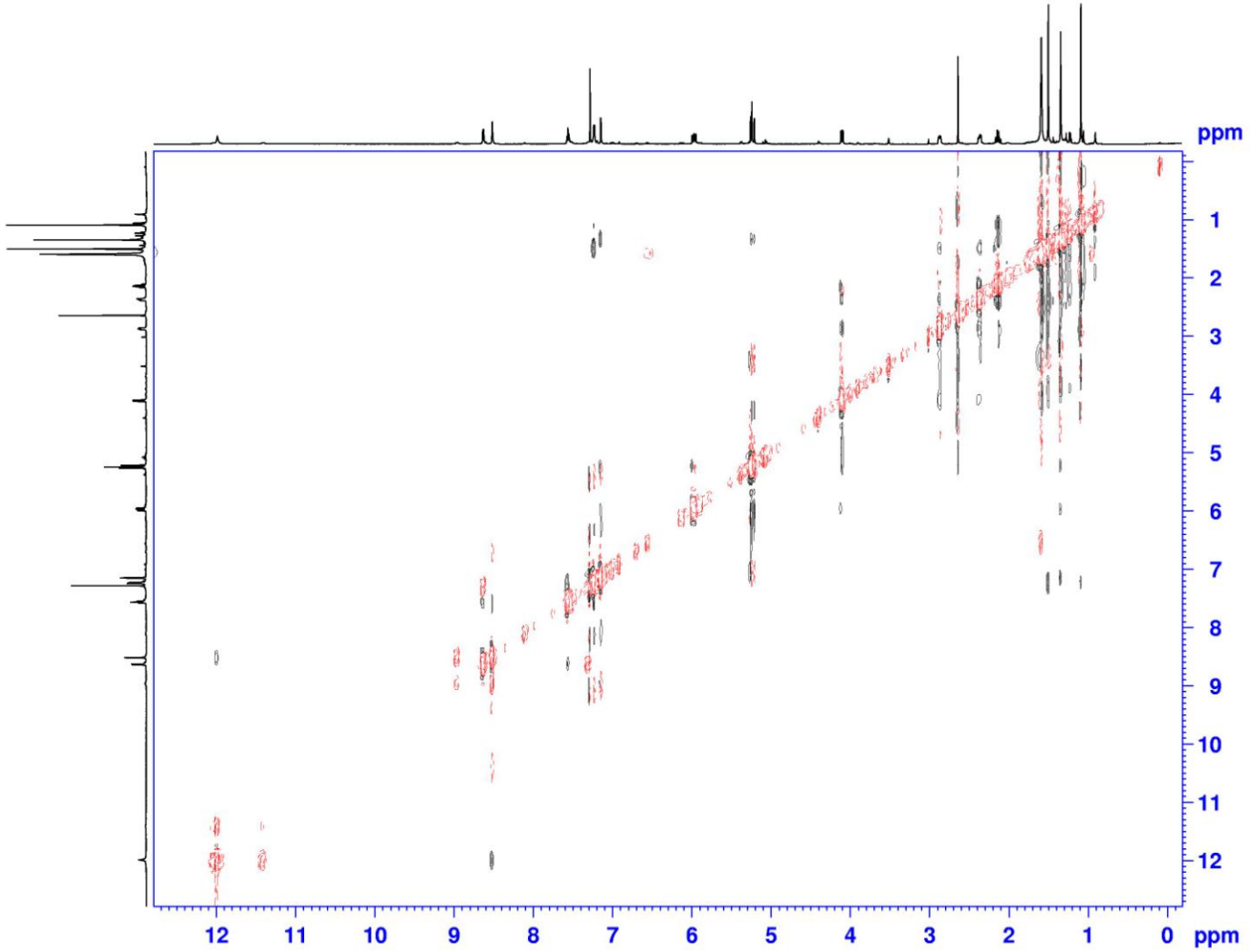

Figure 104. NOESY spectrum (600 MHz, $CDCl_3$) of 13-hydroxy dechlorofontonamide (**297**)

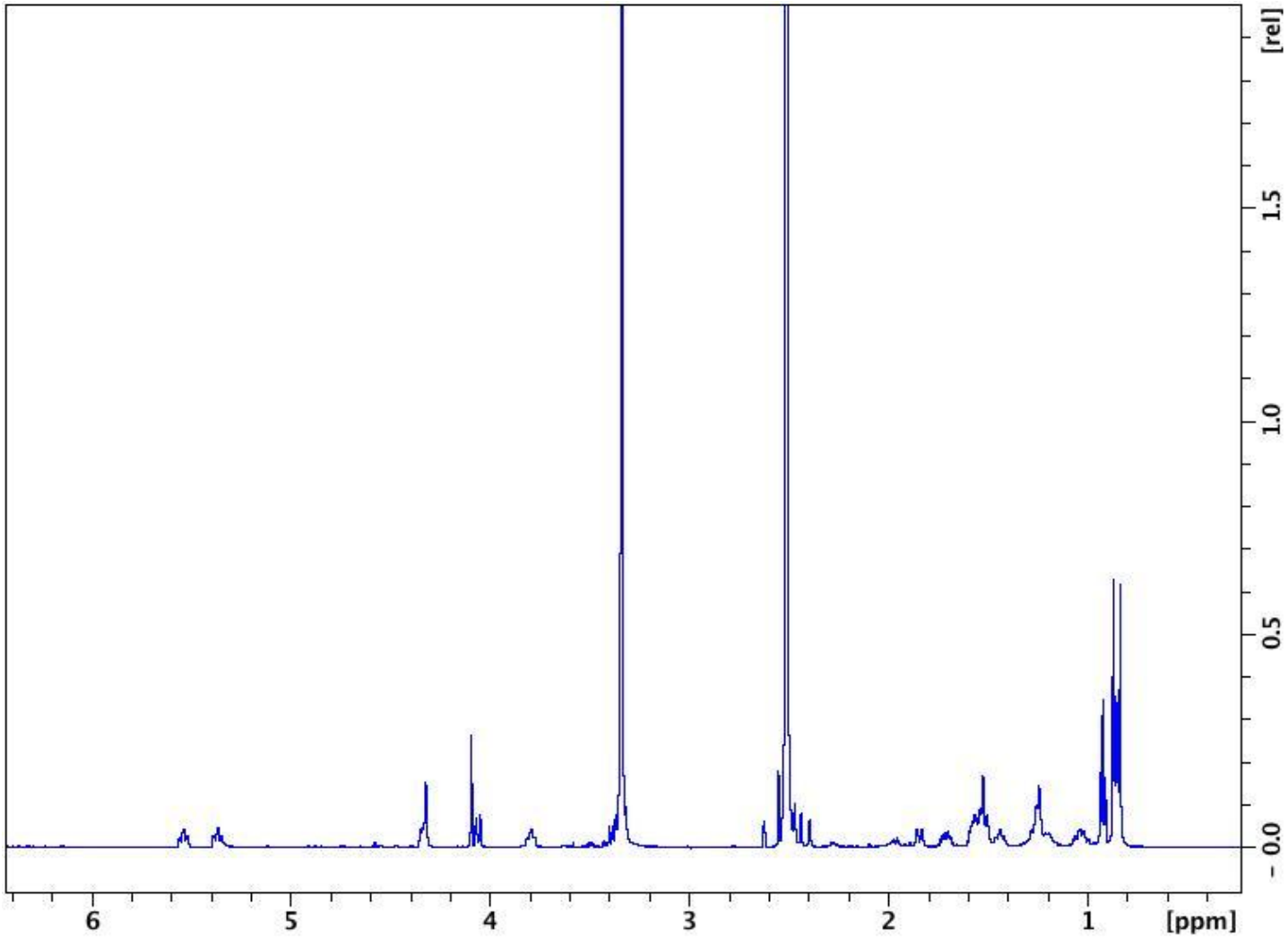

Figure 105. ^{1}H NMR spectrum (600 MHz, DMSO-d_6) of borophycin (**162**)

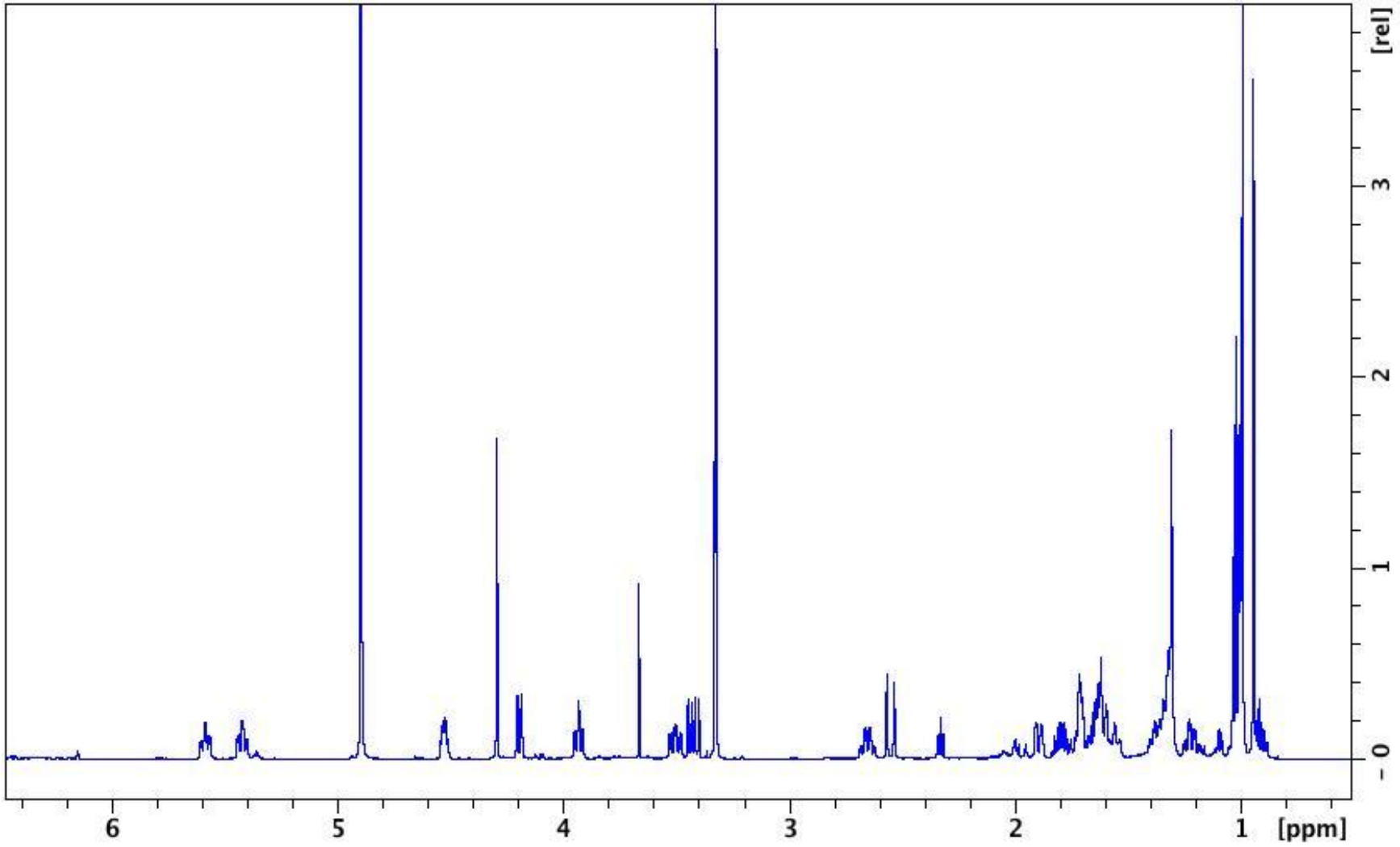

Figure 106. ^{1}H NMR spectrum (600 MHz, MeOH-d_4) of borophycin (**162**)

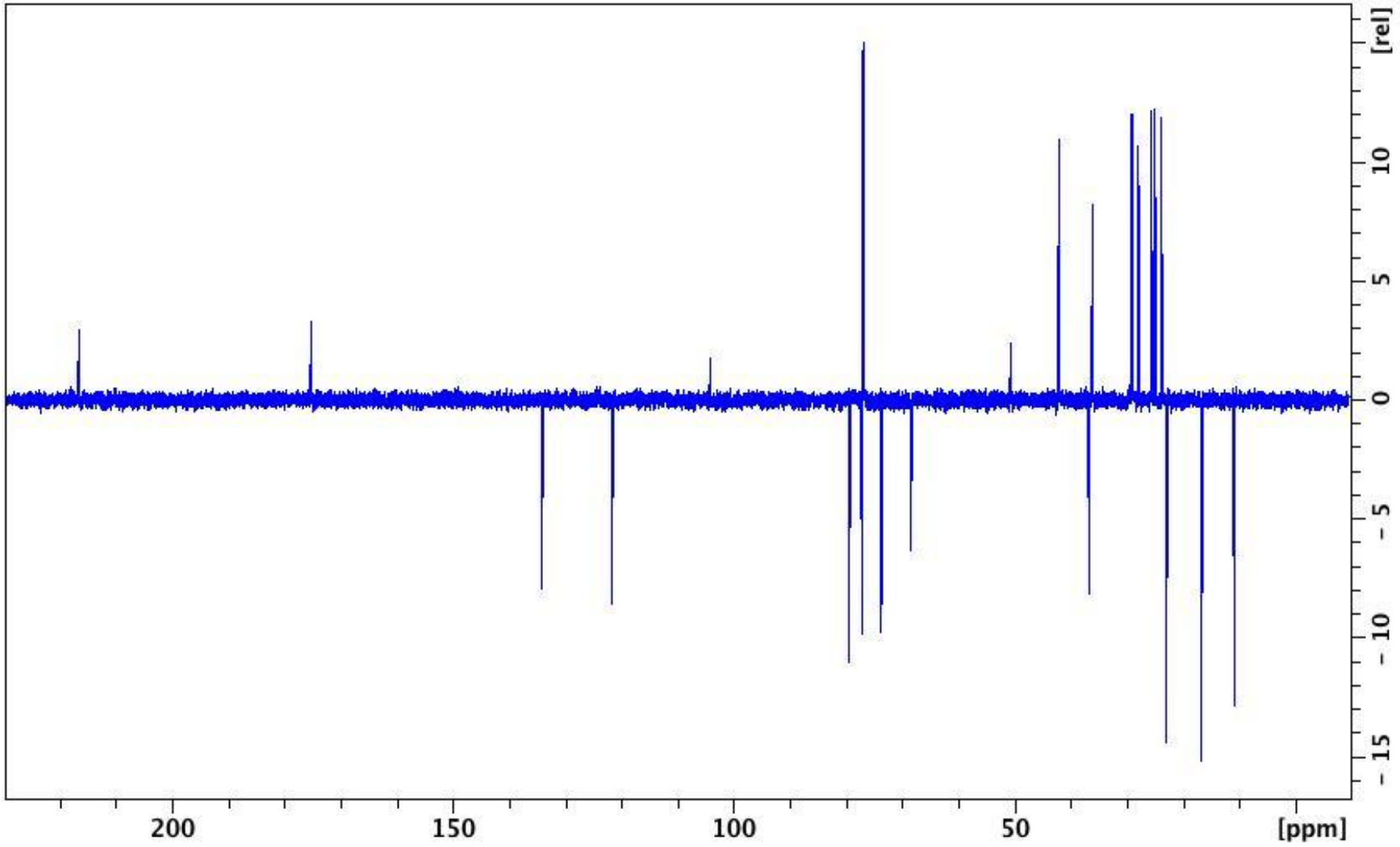

Figure 107. DEPTQ spectrum (600 MHz, DMSO-d_6) of borophycin (**162**)

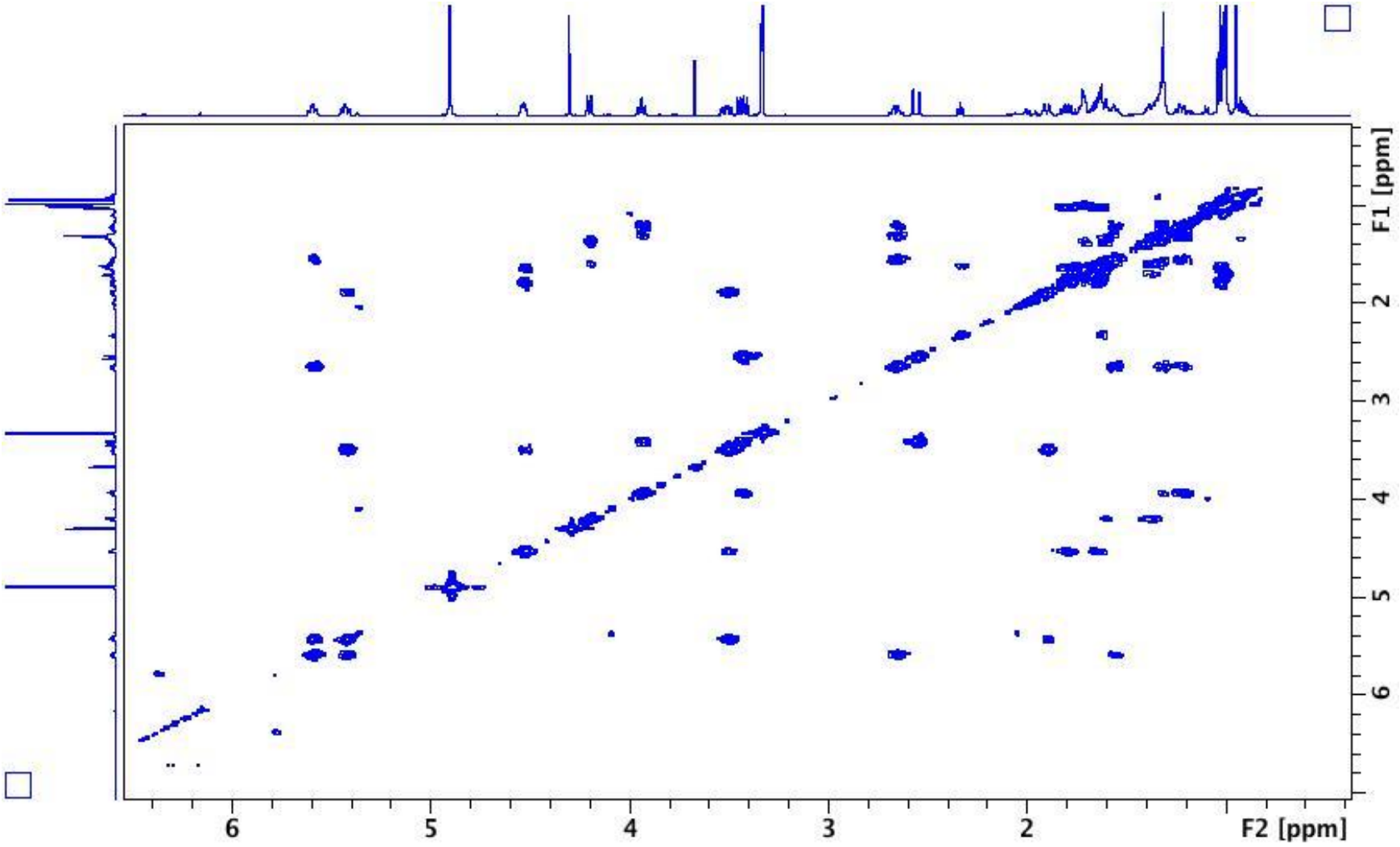

Figure 108. COSY spectrum (600 MHz, DMSO-d_6) of borophycin (**162**)

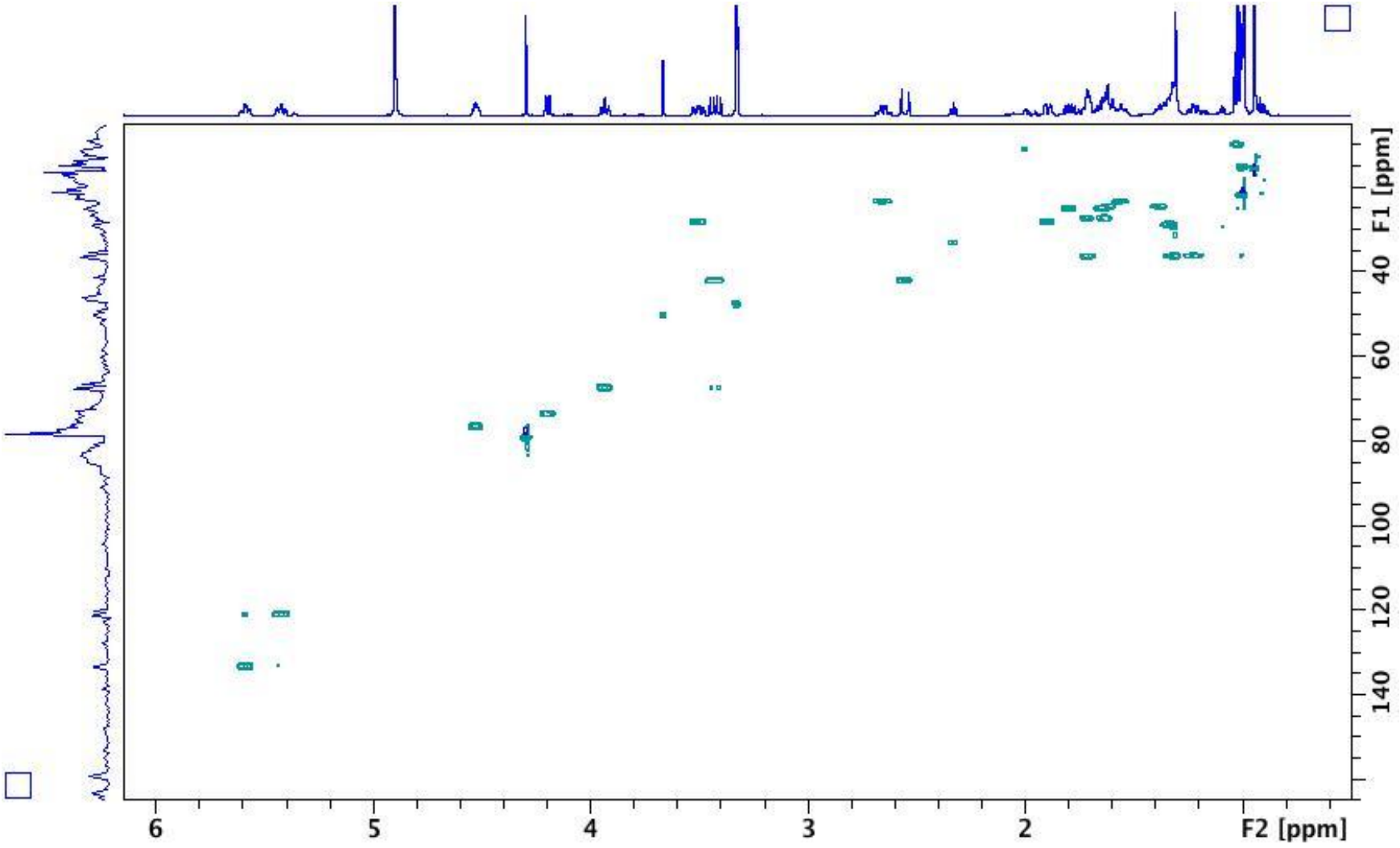

Figure 109. HSQC spectrum (600 MHz, DMSO-d_6) of borophycin (**162**)

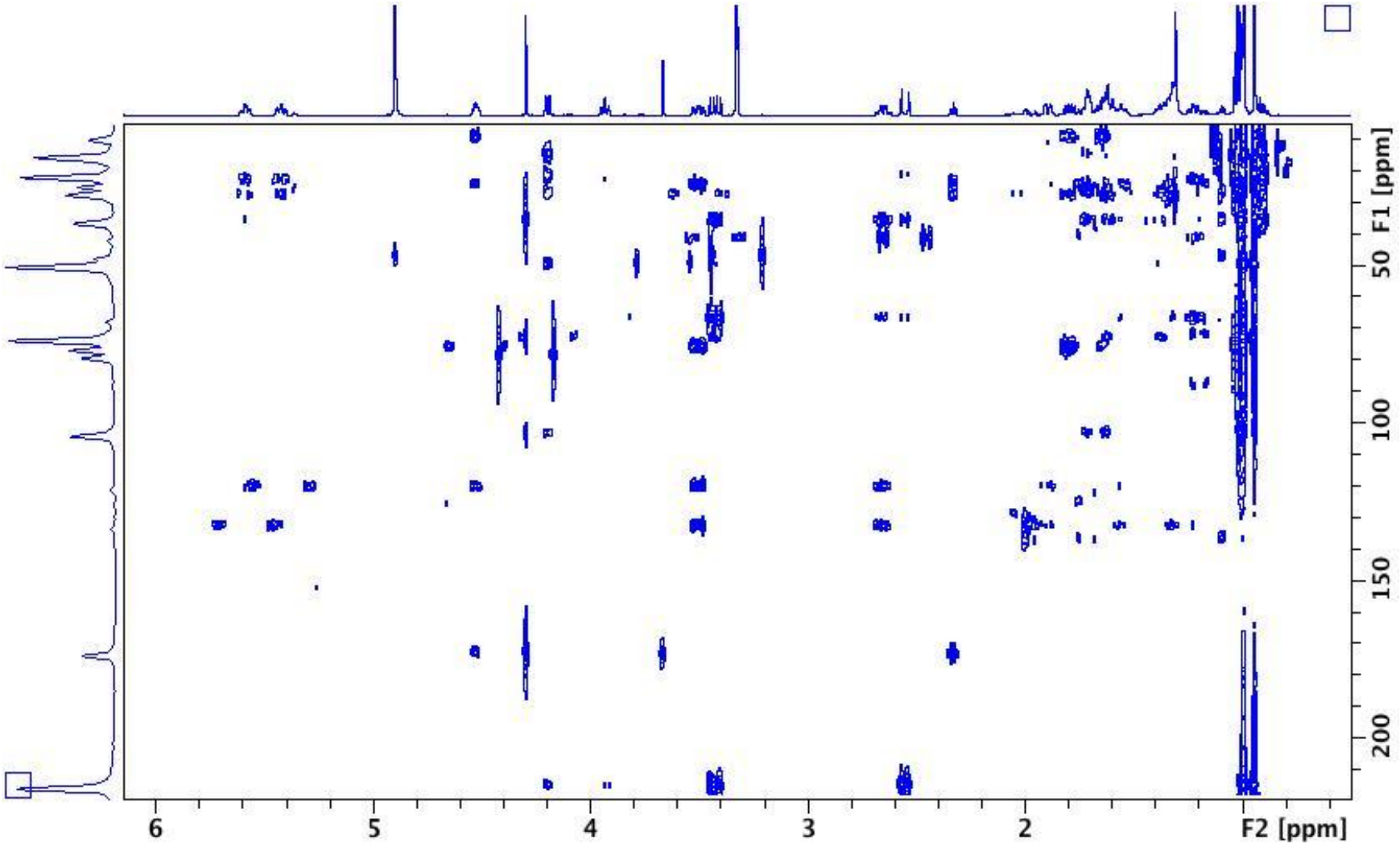

Figure 110. HMBC spectrum (600 MHz, DMSO-d_6) of borophycin (**162**)

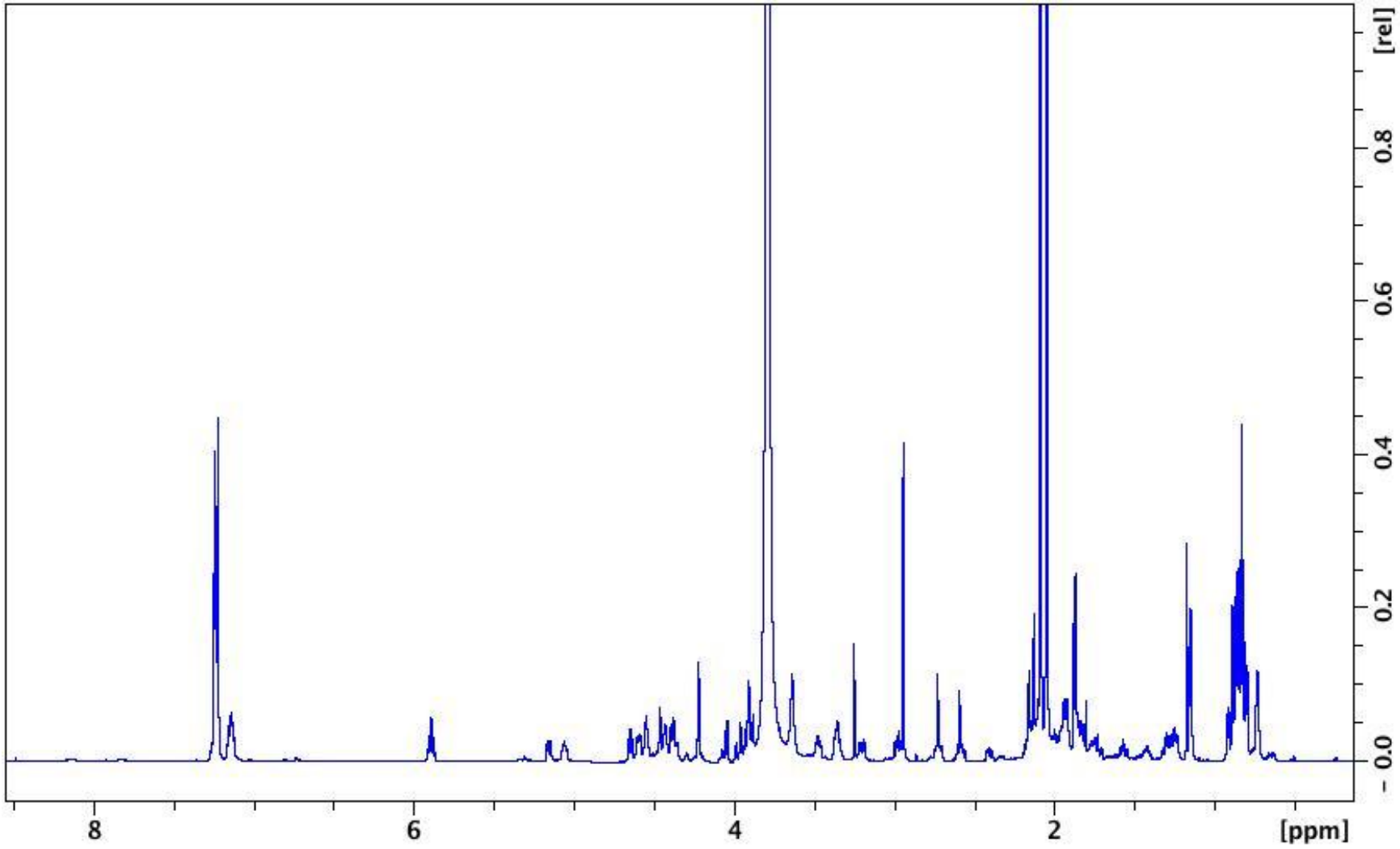

Figure 111. ^{1}H NMR spectrum (600 MHz, Acetone-d_6 and D_2O) of verdeamide A (**332**)

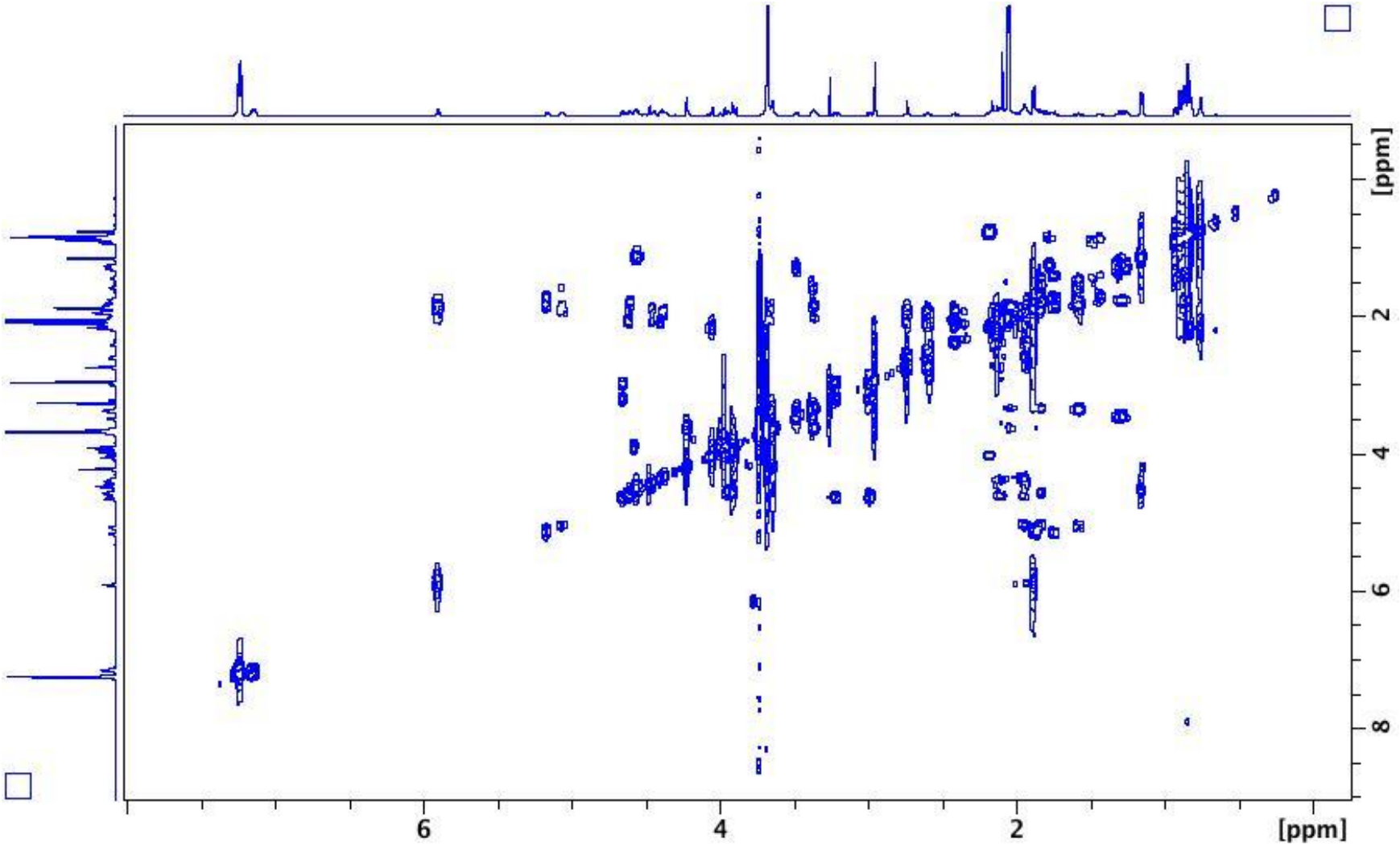

Figure 112. COSY spectrum (600 MHz, Acetone-d_6 and D_2O) of verdeamide A (**332**)

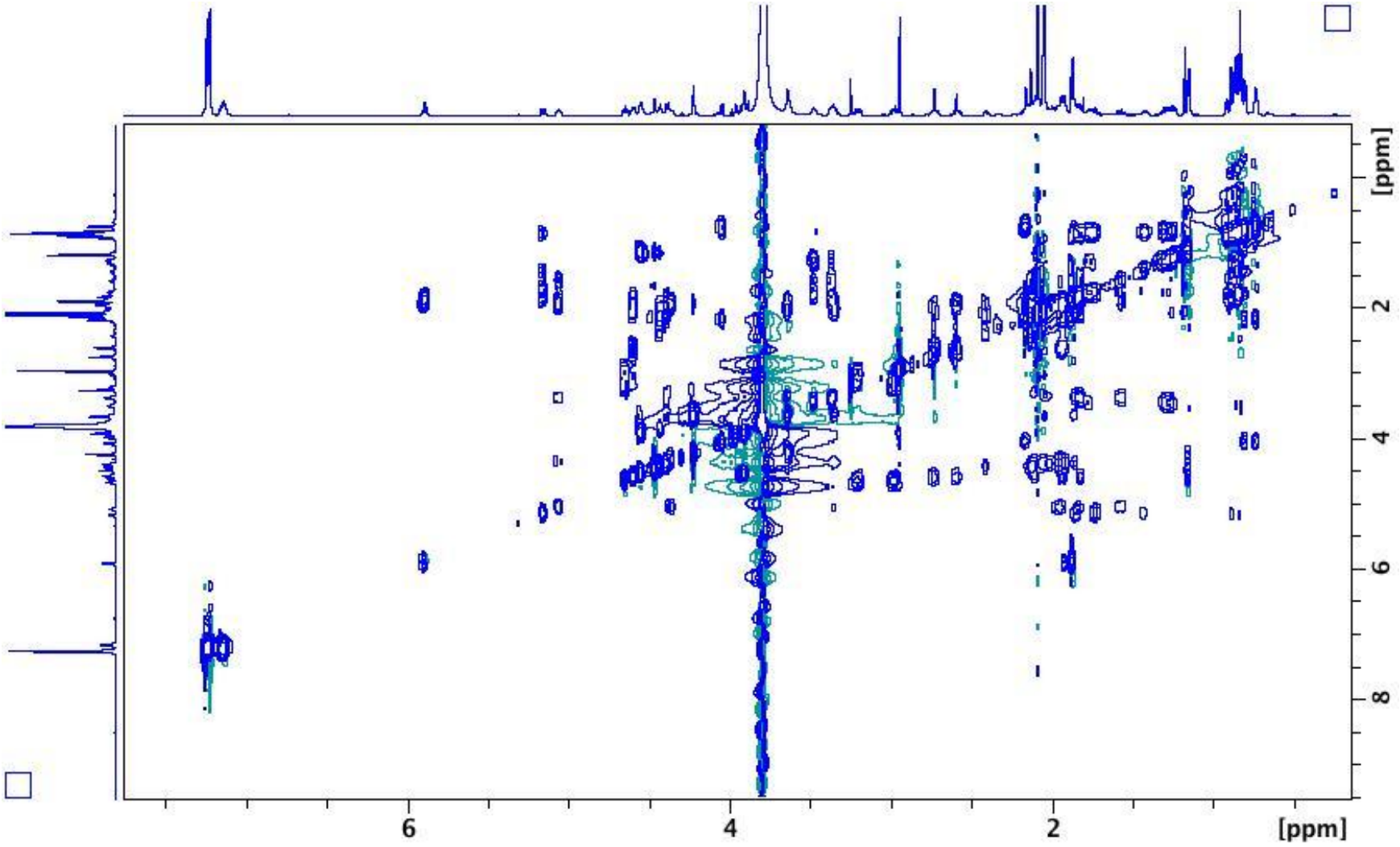

Figure 113. TOCSY spectrum (600 MHz, Acetone-d_6 and D_2O) of verdeamide A (**332**)

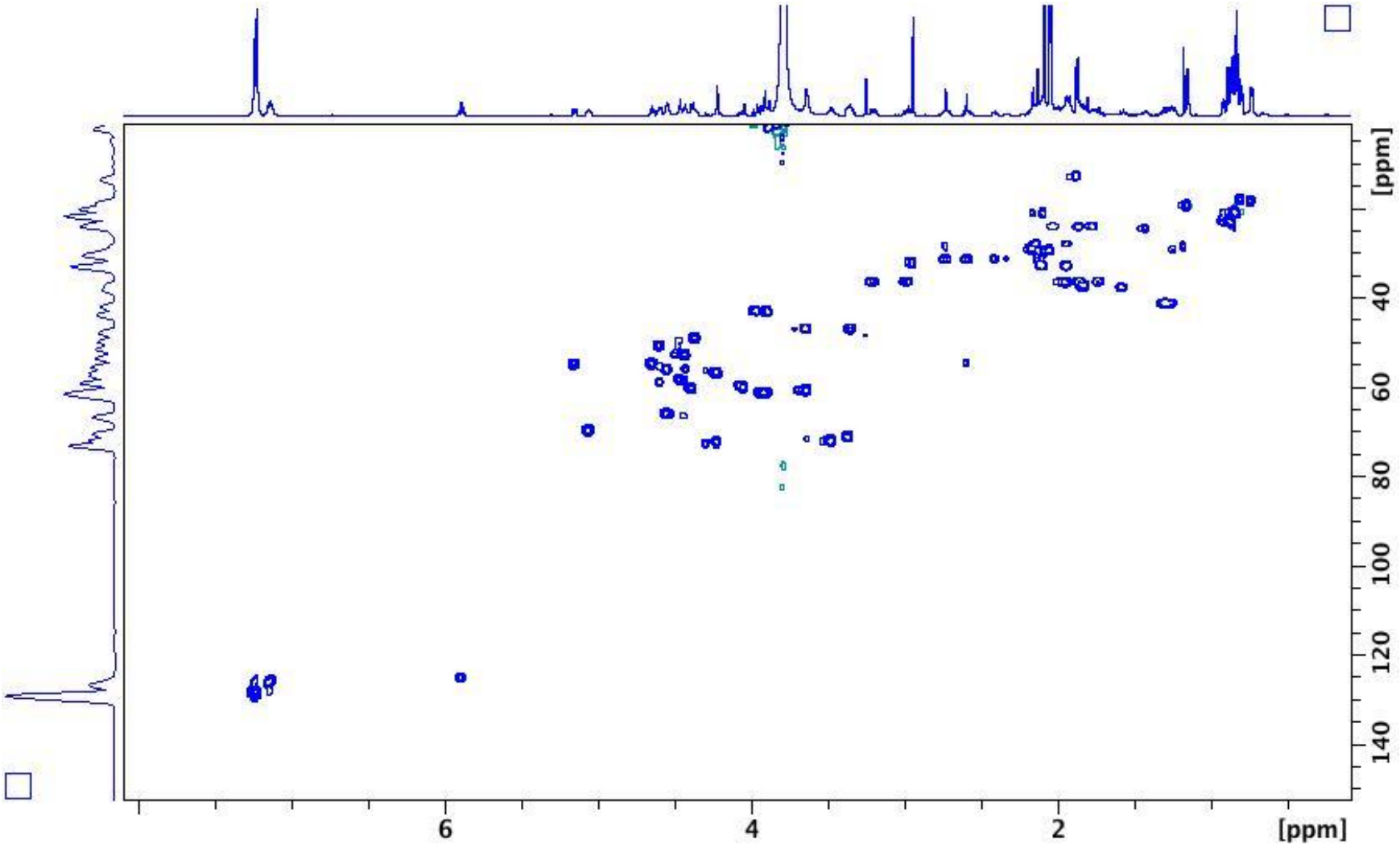

Figure 114. HSQC spectrum (600 MHz, Acetone-d_6 and D_2O) of verdeamide A (**332**)

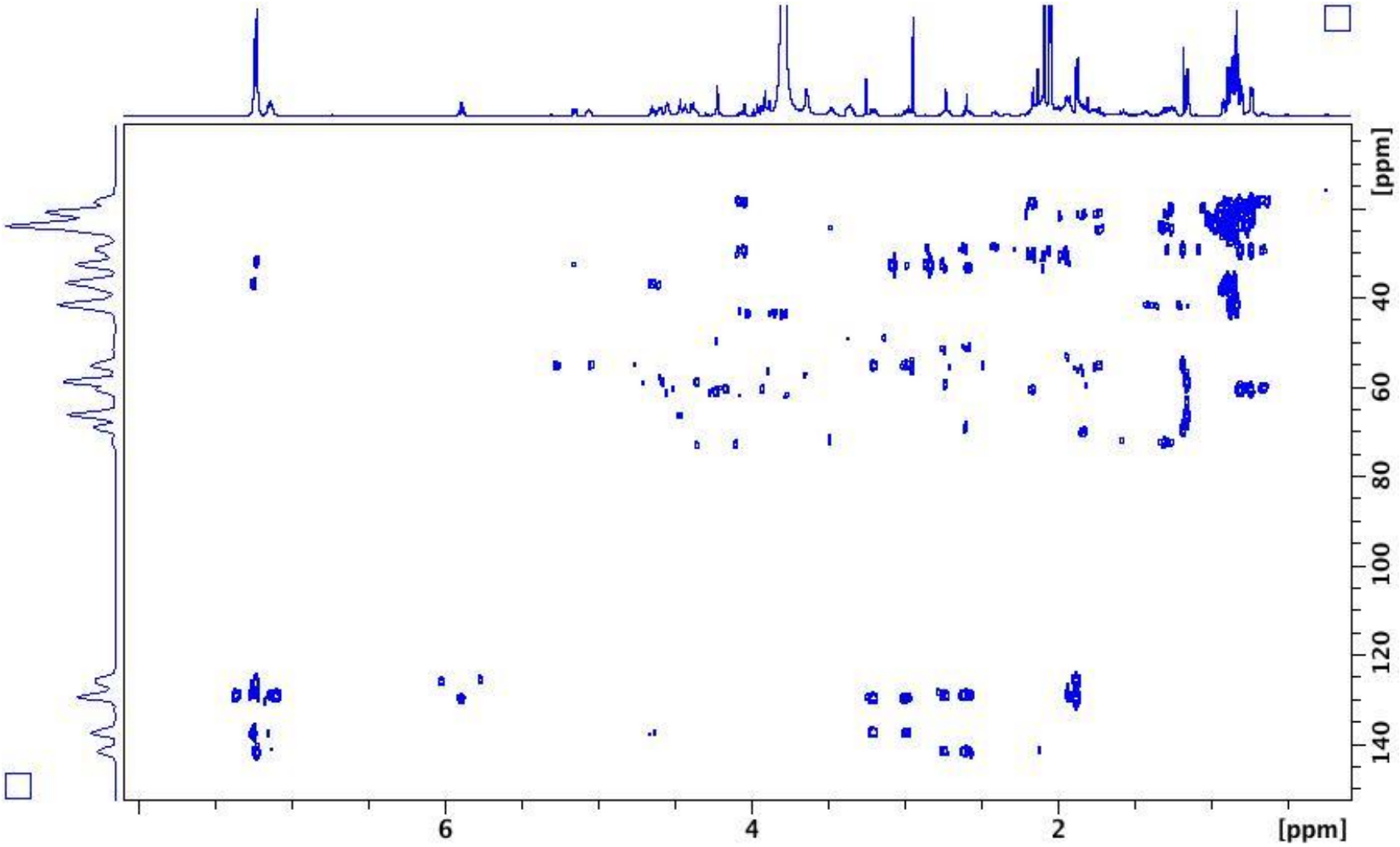

Figure 115. HMBC spectrum (600 MHz, Acetone-d_6 and D_2O) of verdeamide A (**332**)

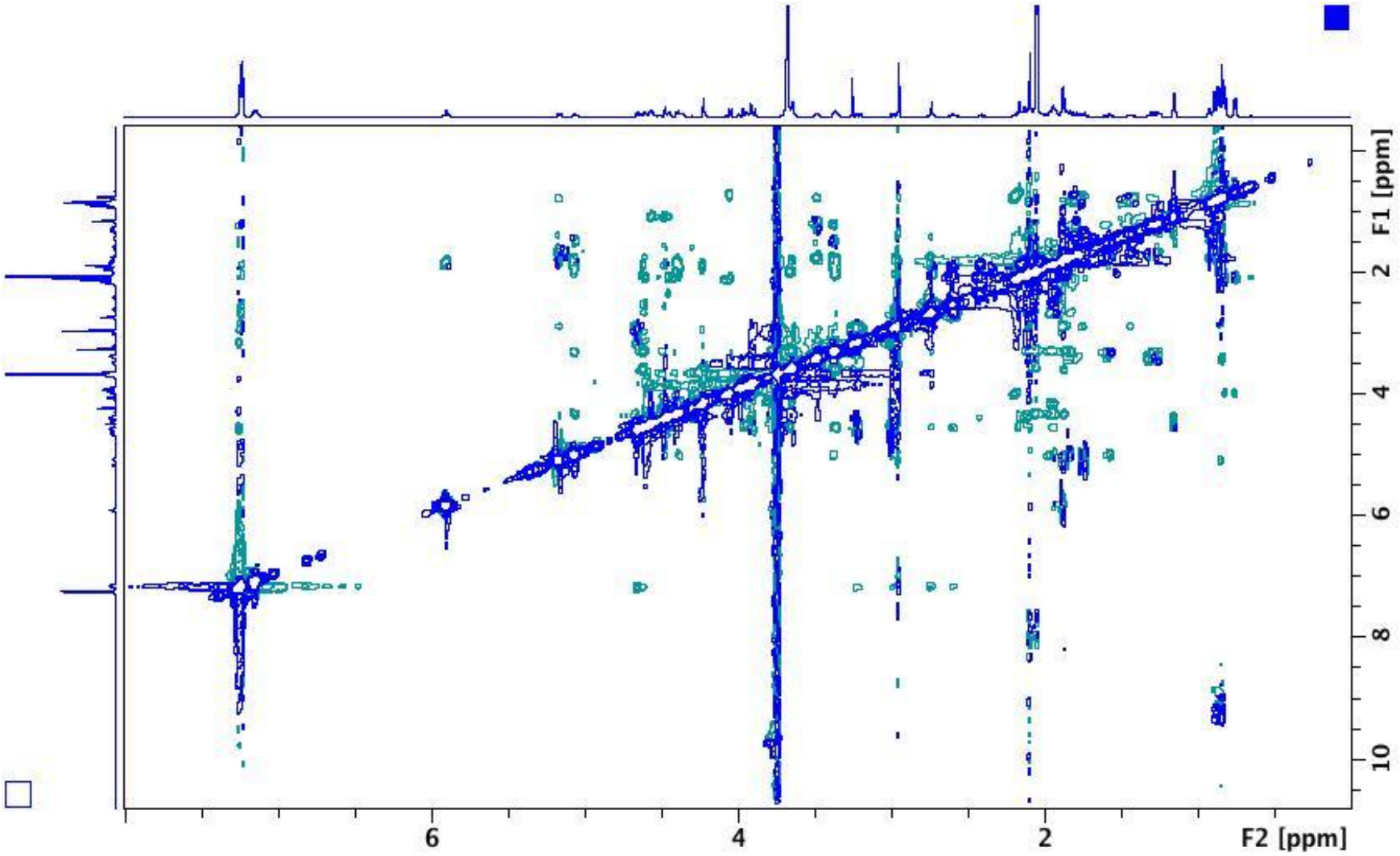

Figure 116. ROESY spectrum (600 MHz, Acetone-d_6 and D_2O) of verdeamide A (**332**)

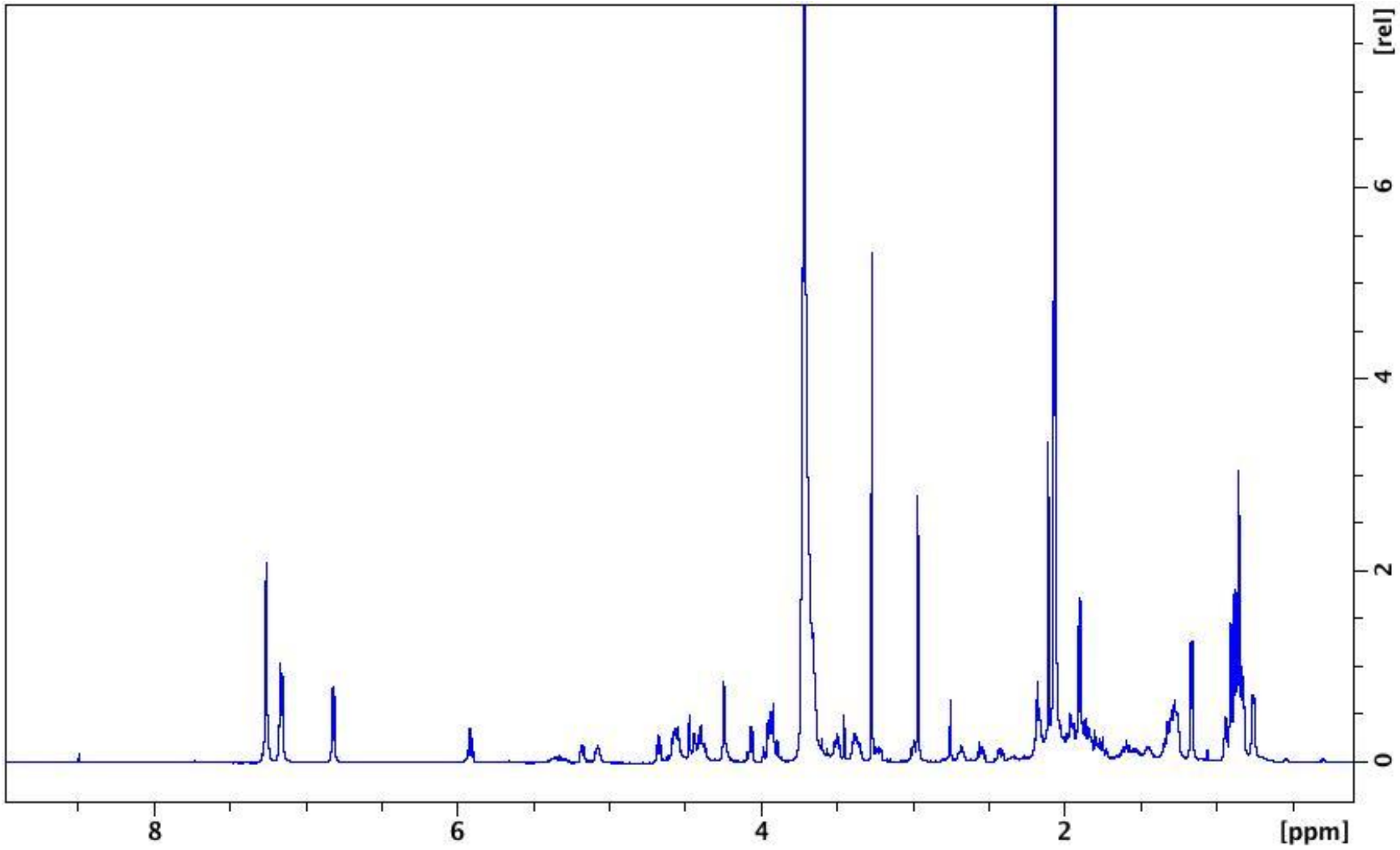

Figure 117. ^{1}H NMR spectrum (600 MHz, Acetone-d_6 and D_2O) of verdeamide B (**333**)

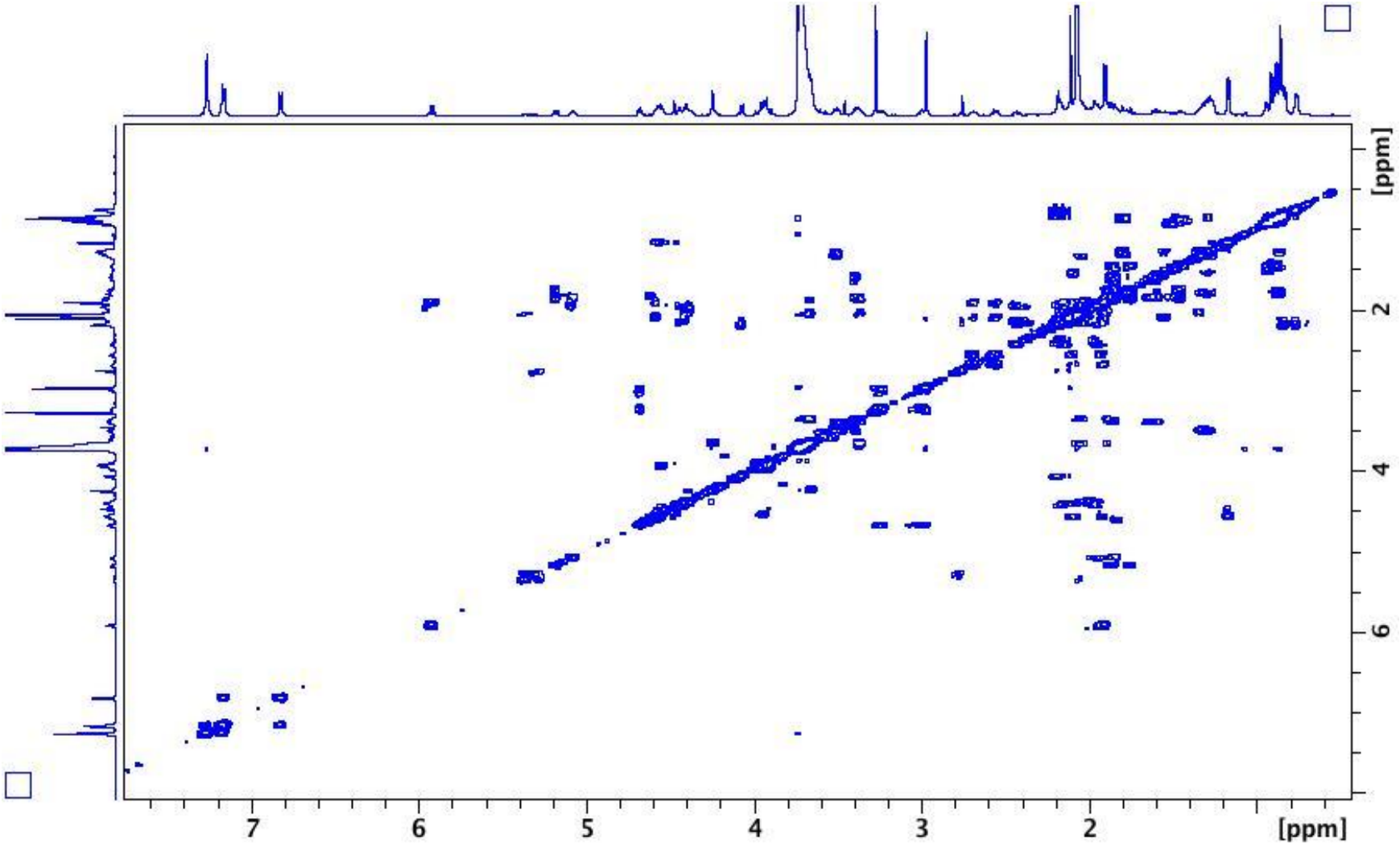

Figure 118. COSY spectrum (600 MHz, Acetone-d_6 and D_2O) of verdeamide B (**333**)

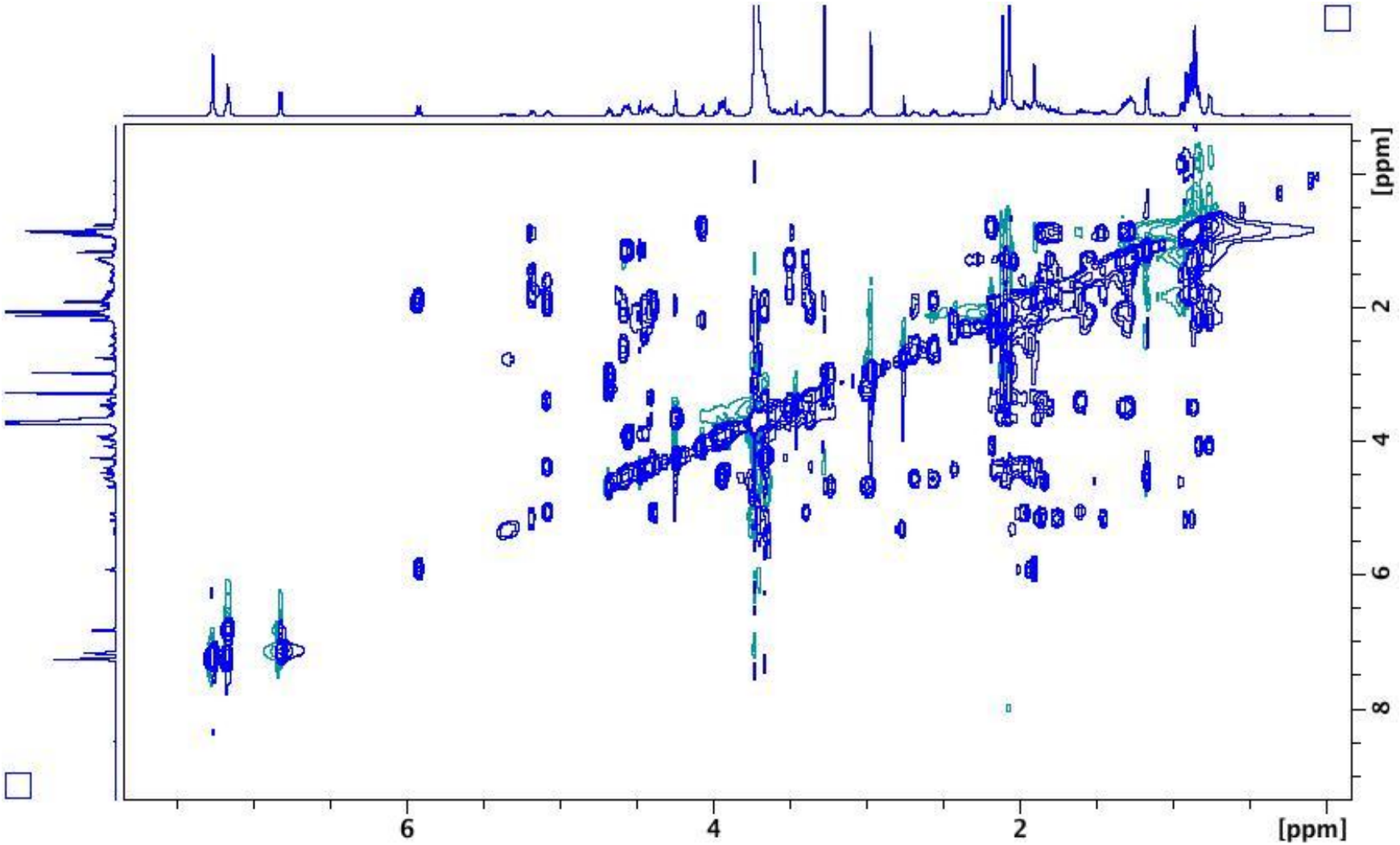

Figure 119. TOCSY spectrum (600 MHz, Acetone-d_6 and D_2O) of verdeamide B (**333**)

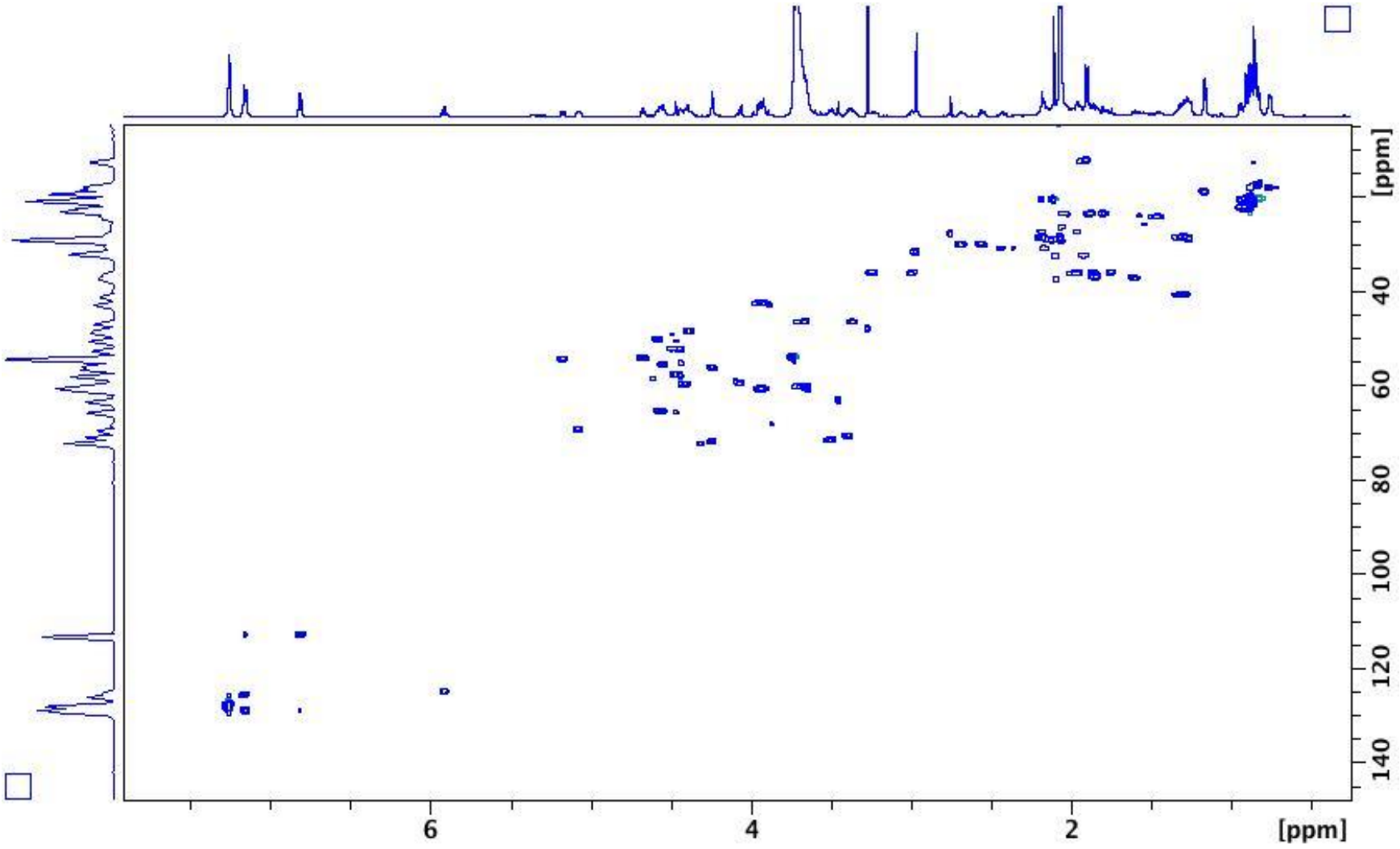

Figure 120. HSQC spectrum (600 MHz, Acetone-d_6 and D_2O) of verdeamide B (**333**)

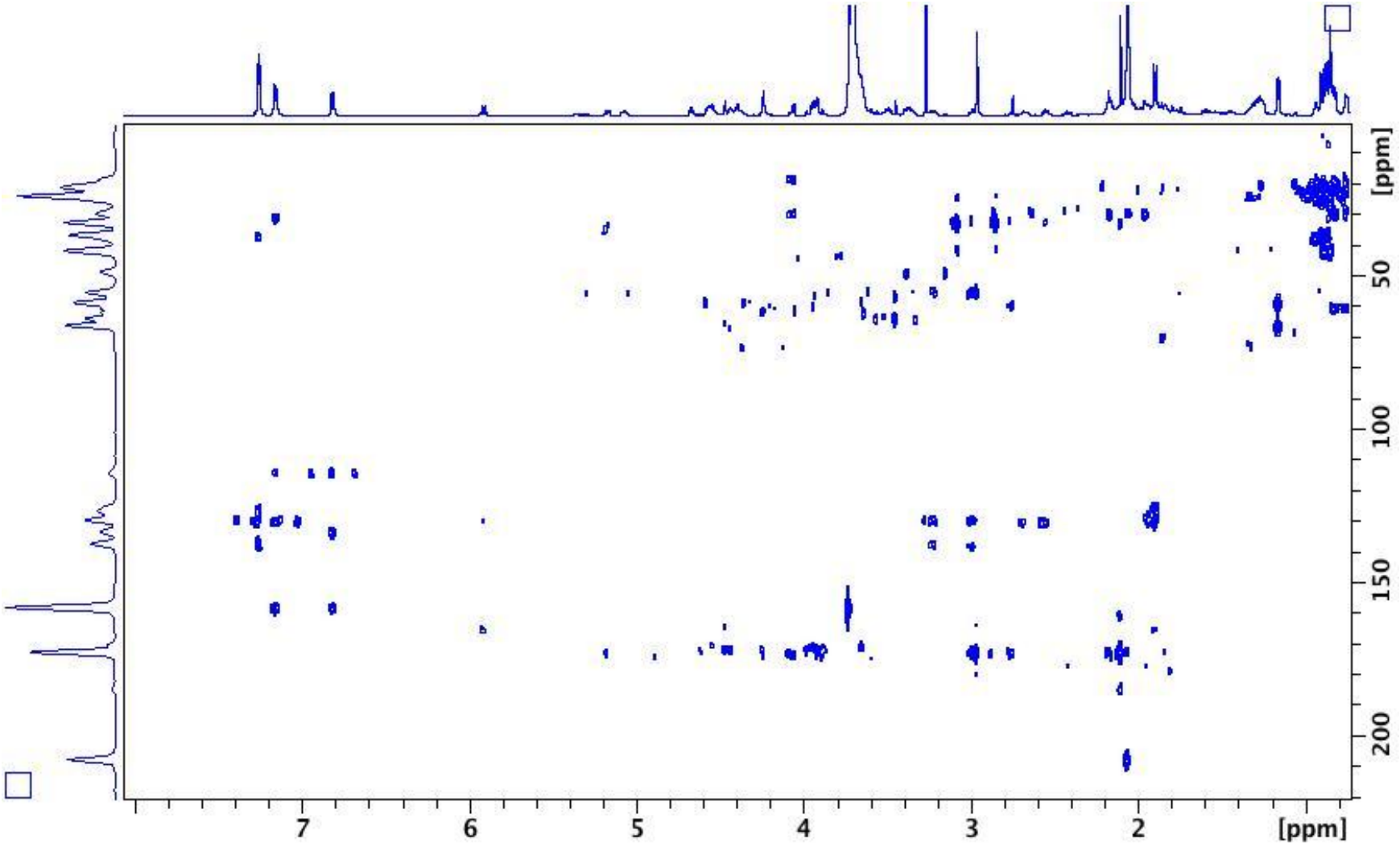

Figure 121. HMBC spectrum (600 MHz, Acetone-d_6 and D_2O) of verdeamide B (**333**)

VITA

NAME: Hyunjung Kim

EDUCATION: Ph.D. in Pharmacognosy, Department of Medicinal Chemistry and Pharmacognosy, University of Illinois at Chicago, Chicago, Illinois, 2012.

M.S. in Pharmacognosy, Chung-Ang University, South Korea, 2005.

B.S. In Horticultural Science, Chung-Ang University, South Korea, 2003.

WORK EXPERIENCE: Research Assistant, Department of Medicinal Chemistry and Pharmacognosy, College of Pharmacy, University of Illinois at Chicago, Chicago, Illinois, 2009-present.

Teaching Assistant, Department of Medicinal Chemistry and Pharmacognosy, College of Pharmacy, University of Illinois at Chicago, Chicago, Illinois, 2007-2009.

Teaching Assistant, Department of Pharmacognosy, College of Pharmacy, Chung-Ang University, 2004-2005.

Research Assistant, Department of Pharmacognosy, College of Pharmacy, Chung-Ang University, 2003-2004.

President of the Student Council, Department of Horticultural Science, College of Industrial Science, Chung-Ang University, 2002-2003.

Vice President of the Student Council, Department of Horticultural Science, College of Industrial Science, Chung-Ang University, 2001-2002.

Squad Leader, Department of Horticultural Science, College of Industrial Science, Chung-Ang University, 2000-2001.

HONORS: Poster Award
The American Society of Pharmacognosy Annual Meeting, St. Petersburg, Florida, 2010.

Graduation first in the College of Industrial Science, Chung-Ang University, 2003.

Scholarship for an hour student, Chung-Ang University, 1999-2003.

PROFESSIONAL MEMBERSHIPS: American Society of Pharmacognosy

PUBLICATIONS: Hyunjung Kim, Aleksej Krunic, Daniel Lantvit, Qi Shen, David J. Kroll, Steven M. Swanson, Jimmy Orjala. Nitrile-containing fischerindoles from the cultured cyanobacterium *Fischerella* sp. *Tetrahedron*, **2012**, 68, 3205-3209.

Hyunjung Kim, Daniel Lantvit, Chang Hwa Hwang, David J. Kroll, Steven M. Swanson, Scott G. Franzblau, Jimmy Orjala. Indole alkaloids from two cultured cyanobacteria, *Westiellopsis* sp. and *Fischerella muscicola*. *Bioorg. Med. Chem*. accepted.

Hahk-Soo Kang, Bernard D. Santarsiero, Hyunjung Kim, Aleksej Krunic, Hee-Byung Chai, A. Douglas Kinghorn, Jimmy Orjala. Merocyclophanes

A and B, antiproliferative cyclophanes from the cultured terrestrial cyanobacterium *Nostoc* sp. *Phytochemistry*, 2012

Sung Kyu Kim, Hyunjung Kim, Sun Eun Choi, Kawn Hee Park, Hyung Kyun Choi, Min Won Lee. Anti-oxidative and inhibitory activities of nitrile oxide (NO) and prostaglandin E_2 (COX-2) production of flavonoids from seeds of *Prunus tomentosa* Thunberg. *Arch. Pharm. Res.* **2008**, 31, 424-428.

Hyunjung Kim, Kwang Ho, Kim, Seung Hwan Yeom, Min Kee Kim, Jae Geul Shim, Hyun Woo Lim, Min Won Lee. New diarylheptanoid from the barks of *Alnus japonica* Steudel. *Chin. Chem. Lett.* **2005**, 10, 1337-1340.

Hyunjung Kim, Seung Hwan Yeom, Min Kee Kim, Jae Geul Shim, In Na Paek, Min Won Lee. Nitric oxide and prostaglandin E_2 synthesis inhibitory activities of diarylheptanoids from the barks of *Alnus japonica* steudel. *Arch. Pharm. Res.* **2005**, 28, 177-179.

Jae Geul Shim, Seung Hwan Yeom, Hyunjung Kim, Young Wook Choi, Do Ik Lee, Kye Yong Song, Suk Hyung Kwon, Min Won Lee. Bone loss preventing effect of Sophorae Fructus on ovariectomized rats. *Arch. Pharm. Res.* **2005**, 28, 106-110.

Hyunjung Kim, Min Kee Kim, Jae Geul Shim, Suk Hyung Kwon, Min Won Lee. Anti-oxidative phenolic compounds from Sophorae Fructus. *Nat. Prod. Sci.* **2004**, 10, 330-334.

Hyun Woo Lim, Min Kee, Kim, Hyunjung Kim, Jae Geul Shim, Hyung Kyun Choi, Min Won Lee. Quantitative determination of diarylheptanoid compounds from Korean *Alnus*. *Kor. J. Pharmacogn.* **2004**, 35, 384-387.

Seung Hwan Yeom, Min Kee Kim, Hyunjung Kim, Jae Geul Shim, Jae Hee Lee, Min Won Lee. Phenolic compounds from seeds of *Astragalus sinicus* and its antioxidative activities. *Kor. J. Pharmacogn.* **2003**, 34, 344-351.

Jae Hee Lee, Seung Hwan Yeom, Min Kee Kim, Hyunjung Kim, Jae Geul Shim, Min Won Lee. Antioxidative activities of diarylheptanoids from *Alnus japonica* and their structural relationship. *Kor. J. Pharmacogn.* **2003**, 34, 190-192.

PRESENTATIONS:

Hyunjung Kim, Aleksej Krunic, Daniel Lantvit, Steven M. Swanson, Jimmy Orjala. Nitrile-containing indole alkaloids from the cyanobacterium *Fischerella* sp. The 51th Annual Meeting of the American Society of Pharmacognosy: St. Petersburg, FL, June 2010. Poster Presentation.

Qi Shen, Hyunjung Kim, A. Douglas Kinghorn, Steven M. Swanson. Gene expression profile induced by the *Aglea* rocaglamide, silvestrol, during apoptosis of human cancer cells. The 50th Annual Meeting of the American Society of Pharmacognosy: Honolulu, HI, July 2009. Poster Presentation.

Hyunjung Kim *et al*. Nitric oxide and prostaglandin E_2 production inhibitory activities of phenolic compounds from *Sophora japonica* Linne. The Japanese Society of Pharmacognosy: Kobe, Japan, September 2004, Poster Presentation.

Hyunjung Kim *et al*. Melanogenesis inhibitory activities of phenolic compounds from *Thodiola sachalinensis* A. Bor in B16 mouse melanoma

cell. The Japanese Society of Pharmacognosy: Kobe, Japan, September 2004, Poster Presentation.

Poster Presentation at The Korean Society of Pharmacognosy: South Korea, 2003-2005.

- Development of evaluation method from herbal cosmetics containing phenolic compounds
- Anti-oxidative and nitric oxide inhibitory activities of phenolic compounds from the seeds of *Prunus tomentosa* Thunberg
- Anti-oxidative effects of flavonoids from the leaves of *Ulmus davidiana* Planchon var. *japonica* Nakal
- PGE_2 production inhibitory activities of flavonoids from the seeds of *Astragalus sinicus* Linne

Poster Presentation at The Pharmaceutical Society of Korea: South Korea, 2003-2005.

- Study on staminal activities of the extracts of watermelon and octacosanol
- Anti-oxidative phenolic compounds from the fruits of *Actinidia arguta*
- Anti-oxidative, nitric oxide and prostaglandin E_2 production inhibitory activities of phenolic compounds from the seeds of *Prunus tomentosa* Thunberg
- Anti-oxidative and nitric oxide production inhitory effects of extract and fractions from the barks of *Actinidia arguta*
- Anti-oxidative phenolic compounds from the seeds of *Prunus tomentosa* Thunberg
- Bone loss preventing effect of Sophorae Fructus in ovariectomized rats
- Tyrosinase and melanin production inhibitory activities of phenolic compounds from bark of *Ulmus macrocarpa*
- Anti-hyperlipidemic effect of isoflavone extract from Sophorae Fructus on hyperlipidemic rat induced by high fat-rich diet
- Nitric oxide production inhibitory and anti-oxidative activities of phenolic compounds from the barks of *Ulmus davidiana*
- Nitric oxide and PGE_2 production inhibitory activities of phenolic compounds from *Sophora japonica* Linne
- Anti-inflammatory activity of flavonoids from the seeds of *Astragalus sinicus* Linne
- Anti-inflammatory activities of diarylheptanoid from the bark of *Alnus japonica* Steudel
- Flavonoids from the seeds of *Astragalus sinicus* Linne